Observational Cosmology

Ramon Miquel
ICREA / IFAE Barcelona

TAE, Benasque (Spain), September 25-26, 2014

Outline (I)

- Preliminaries
- The Cosmic Microwave Background

  Intro

  Origin

  The temperature fluctuations

  Cosmological parameters from the CMB

  Polarization

Outline (II)

- Dark Energy

Discovery: Type-Ia SNe

Growth of structure: the large-scale structure of the Universe

Baryon accoustic oscillations (BAO)

Galaxy clusters

Weak gravitational lensing

Current status

Outline (III)

- Current and Future Galaxy Surveys

The Dark Energy Survey (DES)

The PAU Survey at the WHT

The Dark Energy Spectroscopic Instrument (DESI)

Preliminaries

Robertson-Walker Metric

- Cosmological Principle: we assume the universe is homogeneous and isotropic at all times (at least at large scales)

- Then the curvature has to be constant everywhere, either positive, negative or zero (flat space).

- This leads to the Robertson-Walker metric for the universe:

$$ds^2 = dt^2 - a^2(t)\left[dr^2 + S_\kappa^2(r)\left(d\theta^2 + \sin^2\theta d\phi^2\right)\right]$$

with three options:

$$S_{+1}(r) = R\sin(r/R)$$ positive curvature

$$S_0(r) = r$$ flat

$$S_{-1}(r) = R\sinh(r/R)$$ negative curvature

a : scale factor of the universe (dimensionless)

R : radius of curvature (constant)

t : proper time

r : co-moving distance

Friedmann-Lemaître Equations

Introducing the Robertson-Walker metric into Einstein's field equations of GR we can easily obtain the Friedmann-Lemaître equations:

$$\frac{\ddot{a}}{a} = -\frac{4\pi G}{3}(\rho + 3p)$$

$$\left(\frac{\dot{a}}{a}\right)^2 = \frac{8\pi G}{3}\rho - \frac{\kappa}{R^2 a^2}$$

G: Newton's constant

ρ: energy density

p : pressure

Since *a*, p and ρ all depend on *t*, to solve for *a(t)* we have to specify an equation of state p = $p(\rho)$ for each component of the universe:

- matter (baryonic or dark): $p = 0$, so $w = p/\rho = 0$
- radiation: $p = \rho / 3$, so $w = 1/3$
- cosmological constant: $p = -\rho$, so $w = -1$
- general dark energy: $w = w(t) < -1/3$, for acceleration to take place.

Friedmann-Lemaître Equations

Assuming for simplicity a flat universe, the Friedmann-Lemaître equations can be used to obtain:

$$\frac{d\rho}{da} = -3\,(1+w)\,\frac{\rho}{a}$$

so, for w = const, one has

$$\rho = \rho_0\, a^{-3(1+w)}$$

where 0 means now, and $a_0 = 1$

Defining now $H = \dot{a}/a$ and $\rho_c = 3H_0^2/8\pi G$, one can cast the second Friedmann-Lemaître equation as:

$$H^2(a) = H^2_0 \;[\wedge_M\, a^{-3} + \wedge_R\, a^{-4} + \wedge_{DE}\, a^{-3(1+w)}]$$

matter radiation dark energy

$\wedge_i = \rangle^0{}_i / \rangle_c$ (density now). We assume flat universe, constant w

It is easy to see that $\wedge_M + \wedge_R + \wedge_{DE} = 1 + | \;/ R^2H^2_0 = 1$ (flat)

Measuring the history of the expansion rate, $H(a)$, we can learn about the universe constituents: $\wedge_M$, $\wedge_{DE}$, w, etc.

The Cosmological Redshift

Because of the expansion of the universe, the light from a distant source is observed on Earth redder than was emitted:

$z = (\lambda_o - \lambda_e) / \lambda_e > 0$ is the redshift of the source.

The redshift z can be easily related to the scale factor $a(t_e)$. Imagine two wave-fronts emitted at times t_e and $t_e+\lambda_e/c$. Since light travels in geodesics ($ds^2=0$), we have:

$$\int_{t_e}^{t_0} \frac{dt}{a(t)} = \int_0^r dr = r \quad \text{and} \quad \int_{t_e+\lambda_e/c}^{t_0+\lambda_0/c} \frac{dt}{a(t)} = \int_0^r dr = r \quad \text{so that}$$

$$\int_{t_e}^{t_0} \frac{dt}{a(t)} = \int_{t_e+\lambda_e/c}^{t_0+\lambda_0/c} \frac{dt}{a(t)} \quad \text{or} \quad \int_{t_e}^{t_e+\lambda_e/c} \frac{dt}{a(t)} = \int_{t_0}^{t_0+\lambda_0/c} \frac{dt}{a(t)}$$

Since the expansion is very slow compared to the frequency of light,

$$\frac{\lambda_e}{a(t_e)} = \frac{\lambda_o}{a(t_0)} \quad \text{or} \quad \boxed{a(t_e) = 1/(1+z)}$$

Measuring Redshifts

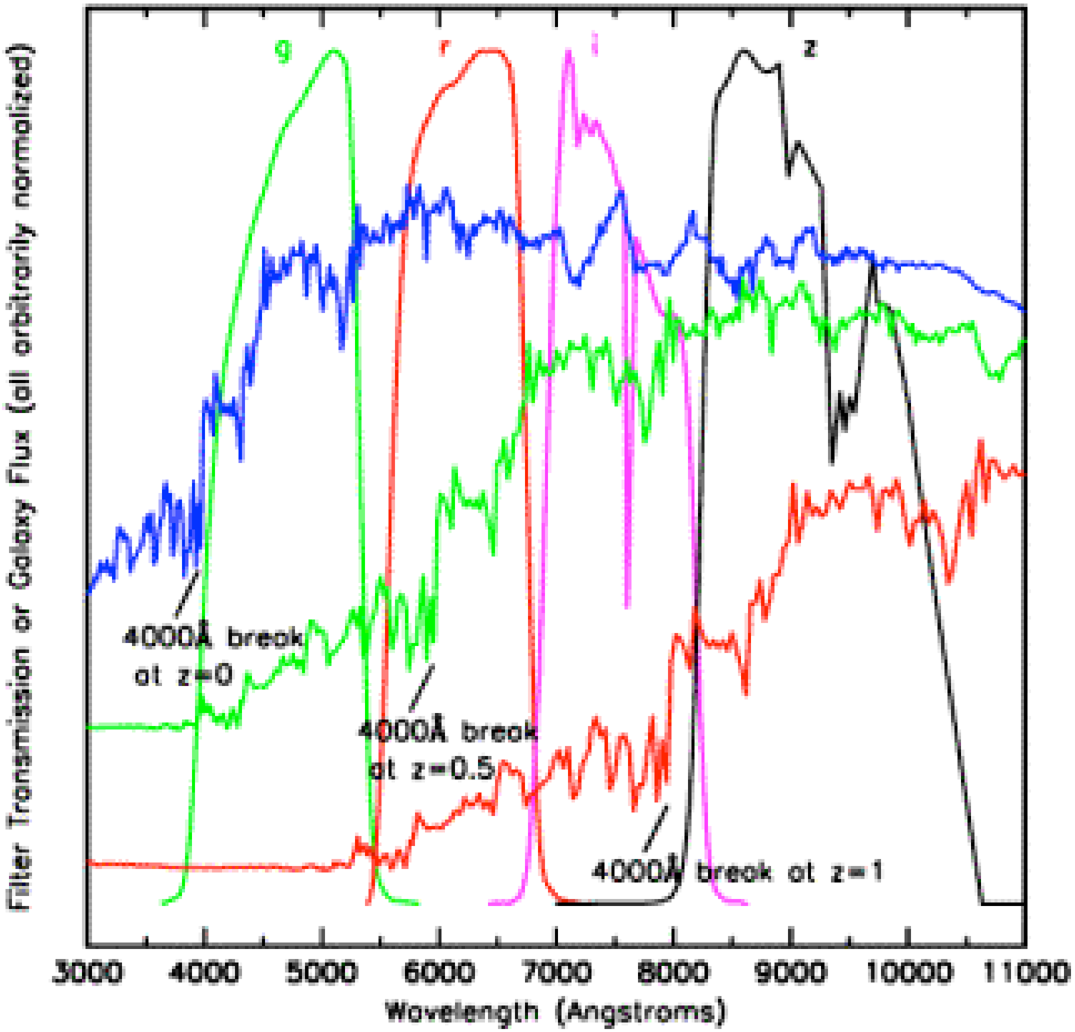

Distances

The co-moving distance between a source at z and us can be computed as:

$$r(z) = \int_0^r dr = \int_{t_e}^{t_0} \frac{dt}{a(t)} = \int_{a_e}^{1} \frac{da}{a\dot{a}} = \int_0^z \frac{dz'}{H(z')}$$

so, it gives us integrals of $1/H(z)$.

Several distances can be measured observationally:

- Luminosity distance: if we have a “standard candle” with luminosity L, we define d_L such that the measured flux is √ $= L / 4$□d_L^2. It is easy to see that $d_L(z) = S_|\,(r(z))\,(1+z) = r(z)\,(1+z)$ (flat).

- Angular distance: if we have a “standard ruler” with length l, we define d_A such that the measured angle subtended by l is ⊗ $=$ l $/ d_A$. It is easy to see that $d_A(z) = S_|\,(r(z)) / (1+z) = r(z) / (1+z)$ (flat).

So by having a collection of either standard candles or standard rulers at

Particle Horizon

- The most distant object we can see is one for which the light emitted at $t = 0$ is just now reaching us at $t = t_0$. The co-moving distance to this object is called the particle ho

$$d_{\rm hor}(t_0) = c\int_0^{t_0} \frac{dt}{a(t)}$$

- The integral is dominated by what happens at early times. Since the early universe was radiation-dominated, $H = \dot{a} / a \sim a^{-2}$, from which $a \sim t^{1/2}$, the integral converges, and the proper horizon distance becomes $a(t_0)d_{\rm hor}(t_0) \sim 2c\, t_0 \sim c / H(t_0)$.

CMB

The Cosmic Microwave Background Radiation

- The early Universe had two main components:
  - A plasma of protons and electrons interacting through photons
  - Dark matter

- Throughout the expansion, the Universe cooled down.

- About 380 000 years after the Big Bang, the temperature dropped enough (to ~ 3000 K) to allow for protons and electrons to combine into neutral hydrogen atoms.

- The Universe became transparent to light: Cosmic Microwave Bkgd.

- The CMB light allows us to know how the Universe was only 380 000 years after the Big Bang. This epoch corresponds to z ~ 1100.

- Before it reached 380 000 years of age, the Universe was opaque and, hence, we can't observe it directly.

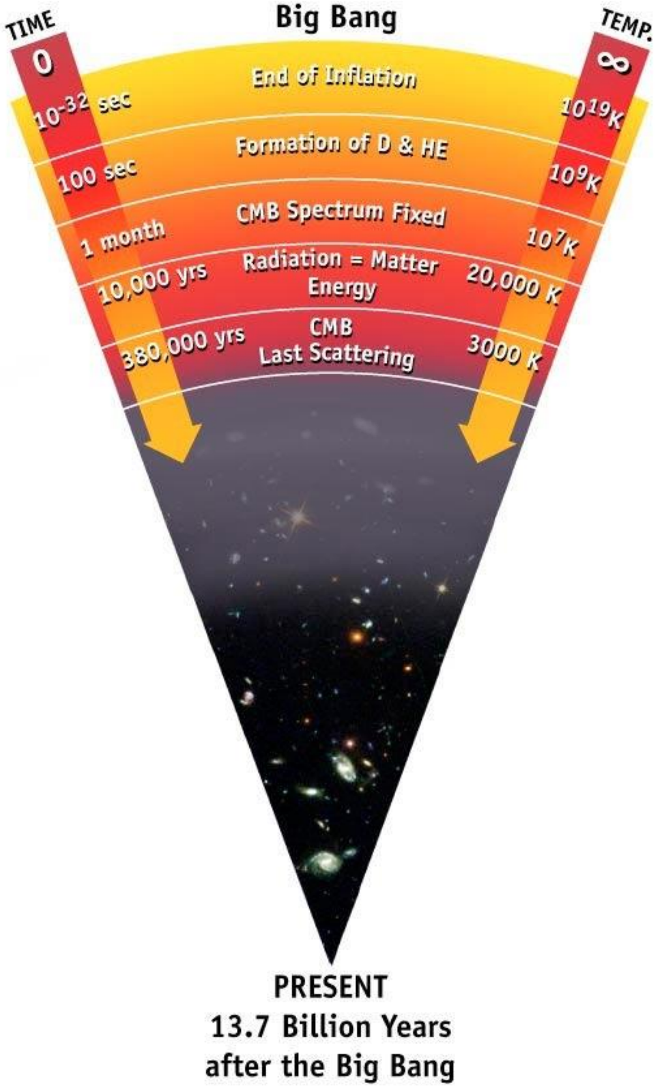

The cosmic microwave background Radiation's "surface of last scatter" is analogous to the light coming through the clouds to our eye on a cloudy day.

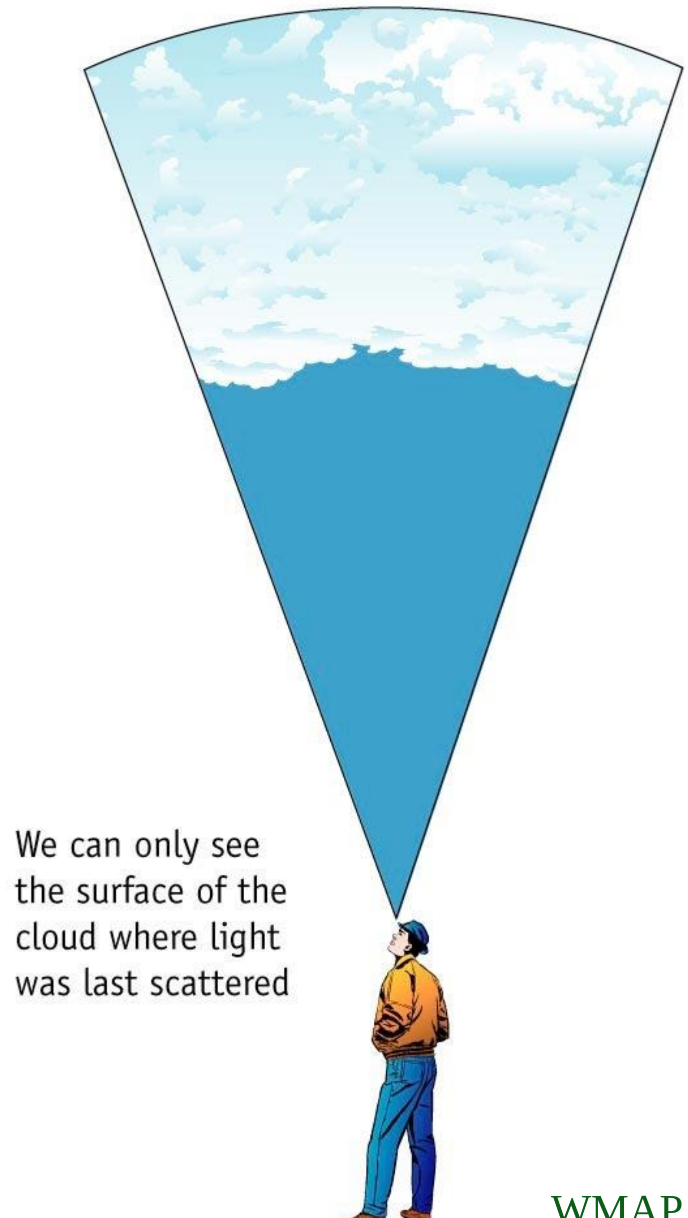

WMAP web page

History of the Universe

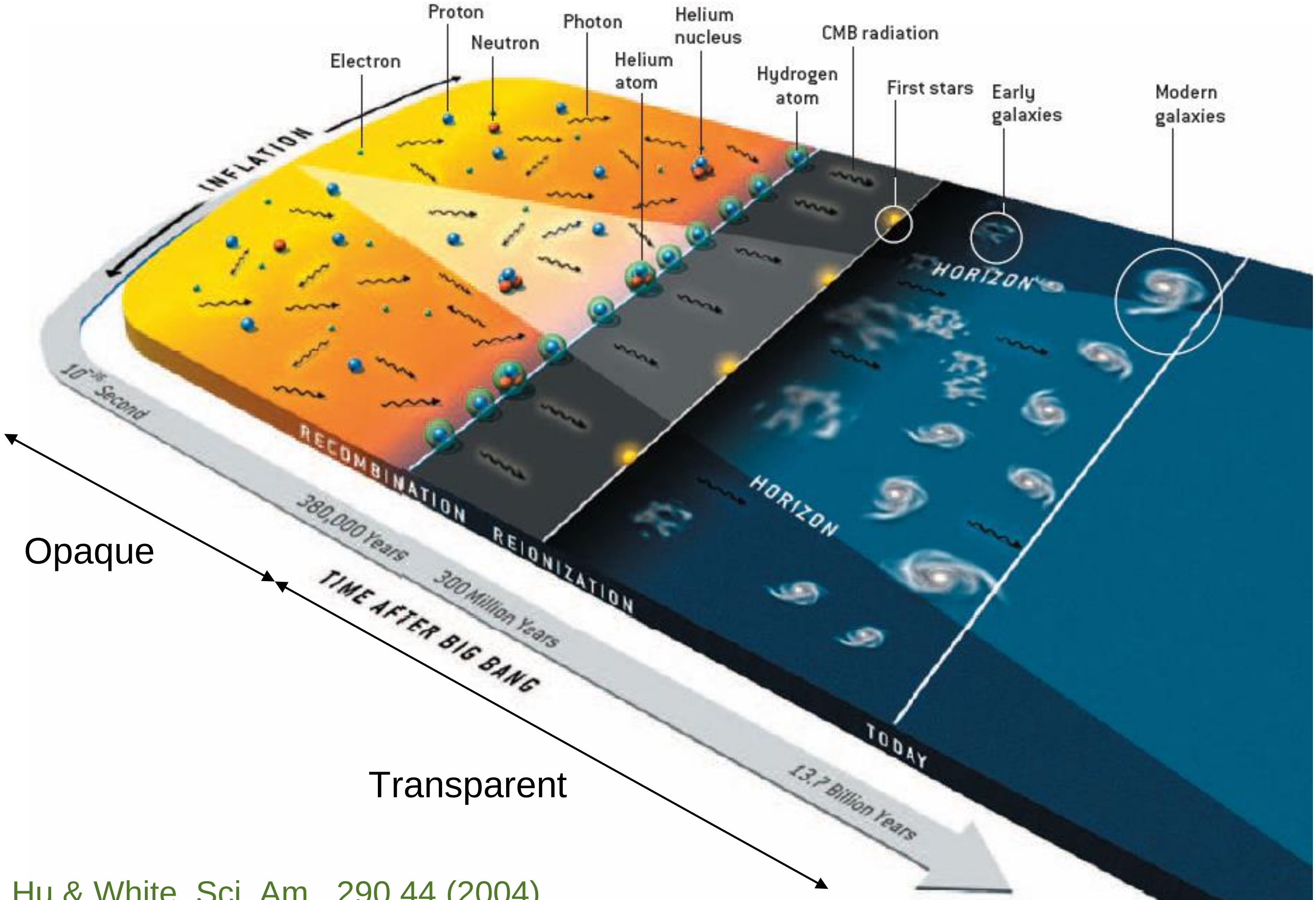

Opaque

Transparent

Hu & White, Sci. Am., 290 44 (2004)

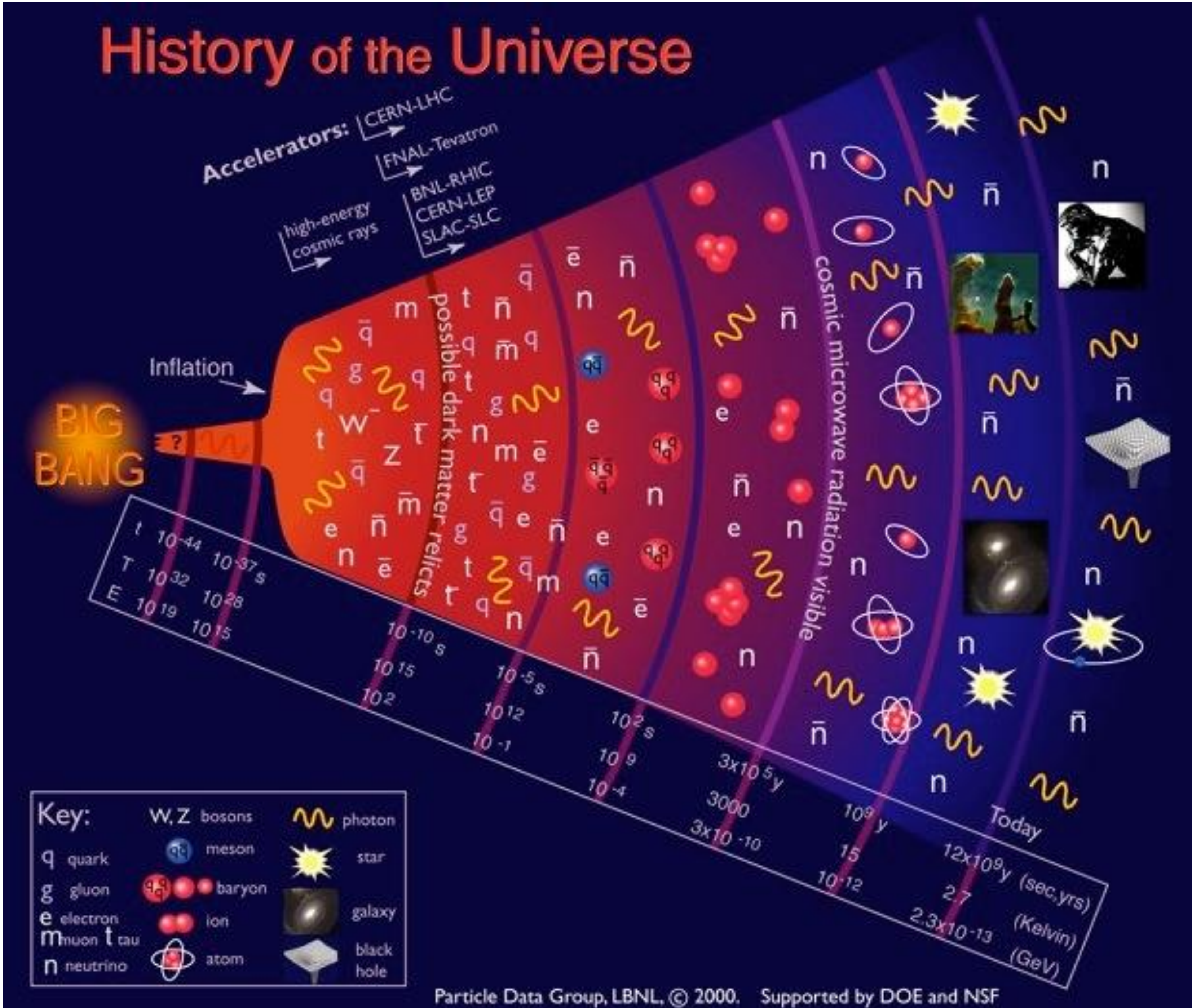
History of the Universe
Accelerators:
CERN-LHC
FNAL-Tevatron
BNL-RHIC
CERN-LEP
SLAC-SLC
high-energy cosmic rays
Inflation
BIG BANG
possible dark matter relicts
cosmic microwave radiation visible
t 10^-44 10^-37 s
T 10^32 10^28
E 10^19 10^15
10^-10 s
10^15
10^2
10^-5 s
10^12
10^-1
10^2 s
10^9
10^-4
3x10^5 y
3000
3x10^-10
10^9 y
15
10^-12
Today
12x10^9 y (sec, yrs)
2.7 (Kelvin)
2.3x10^-13 (GeV)
Key:
q quark
g gluon
e electron
m muon t tau
n neutrino
W, Z bosons
meson
baryon
ion
atom
photon
star
galaxy
black hole
Particle Data Group, LBNL, © 2000. Supported by DOE and NSF

History of the Universe

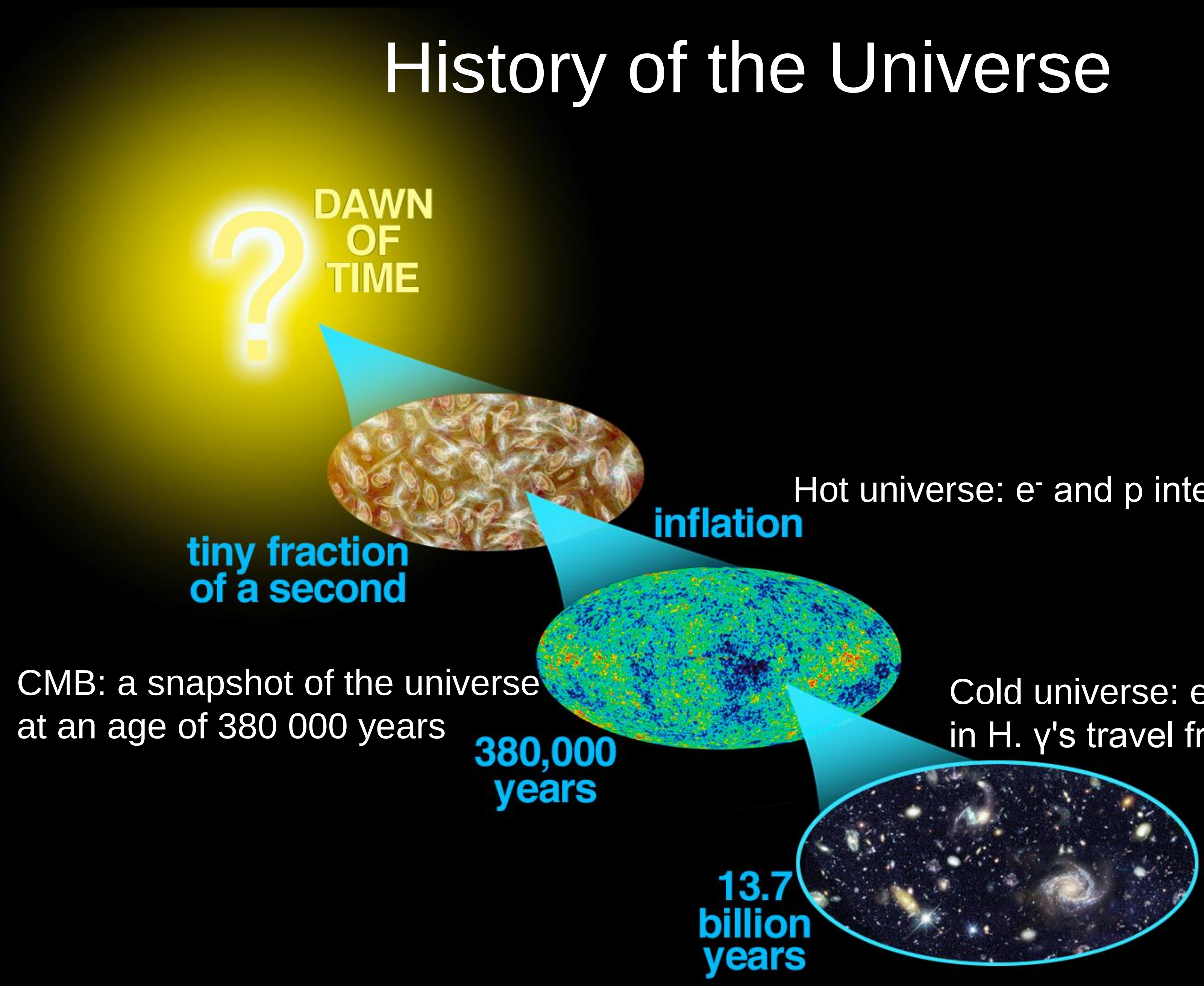

Hot universe: e^- and p interact through γ

CMB: a snapshot of the universe at an age of 380 000 years

Cold universe: e^- and p bound in H. γ's travel freely

1965 Penzias and Wilson

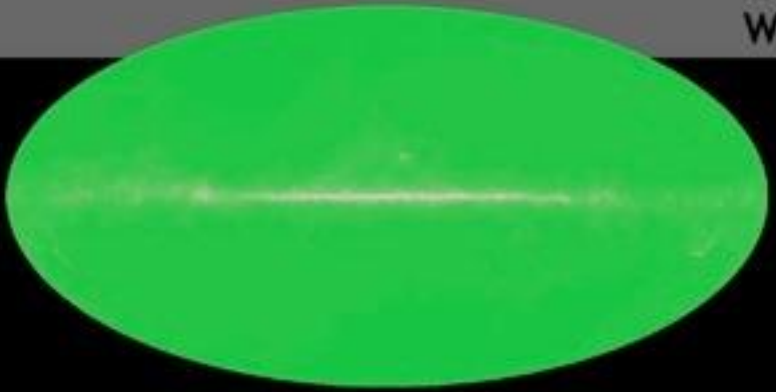

1992 COBE

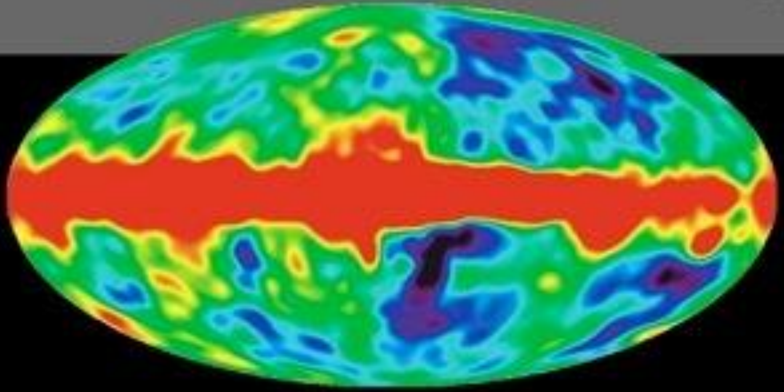

2003 WMAP

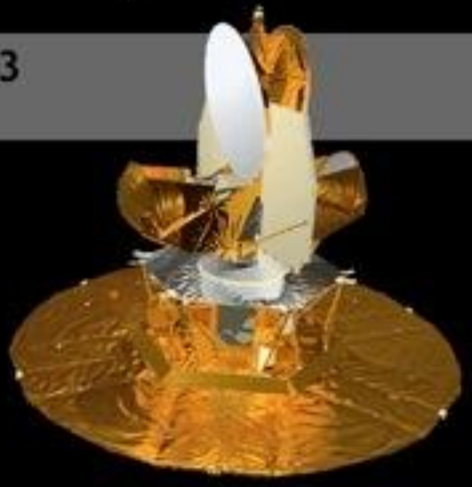

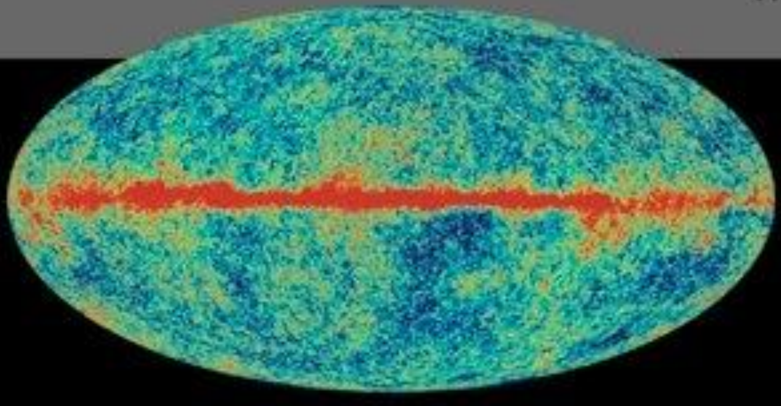

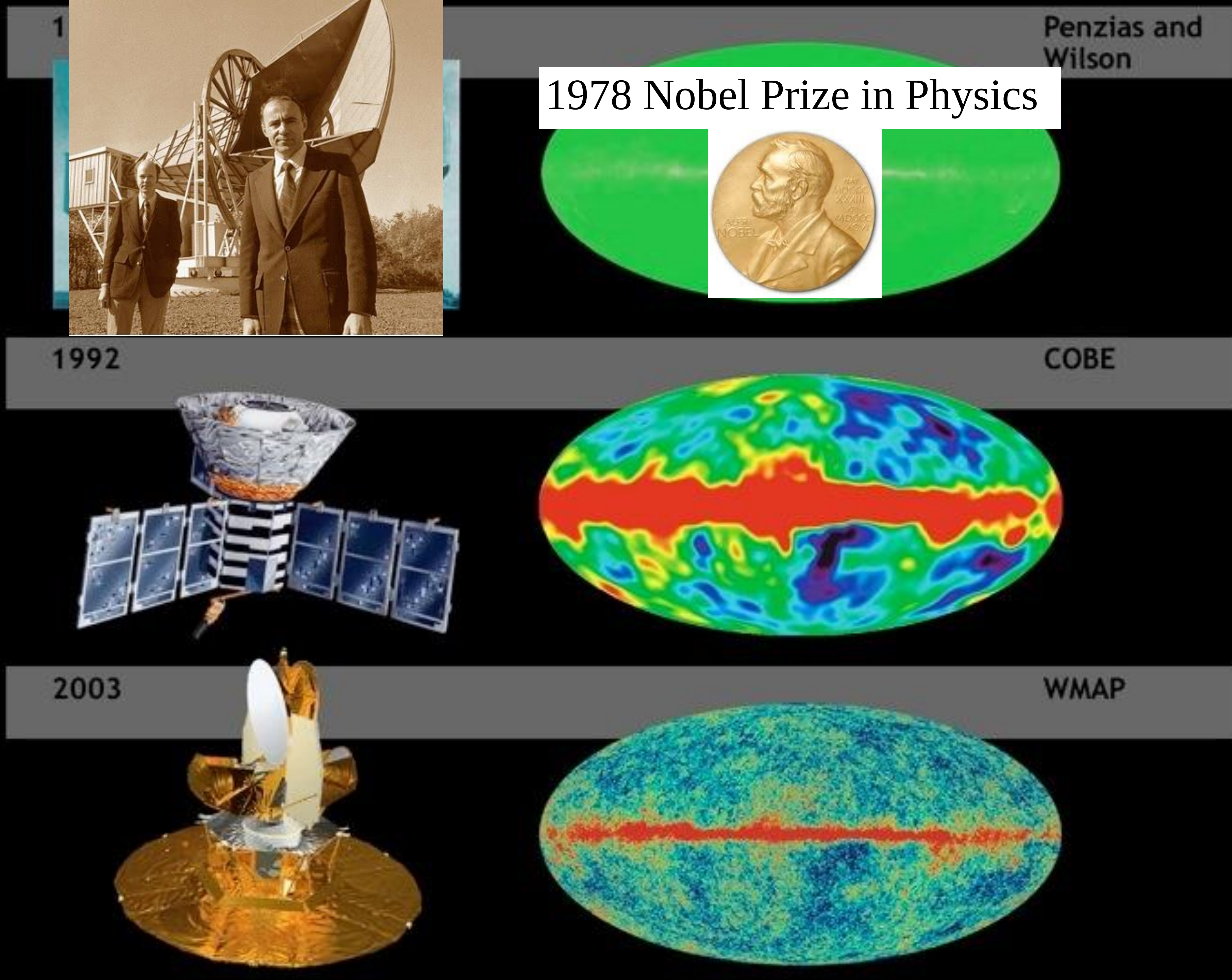
Penzias and Wilson
1978 Nobel Prize in Physics
1992
COBE
2003
WMAP

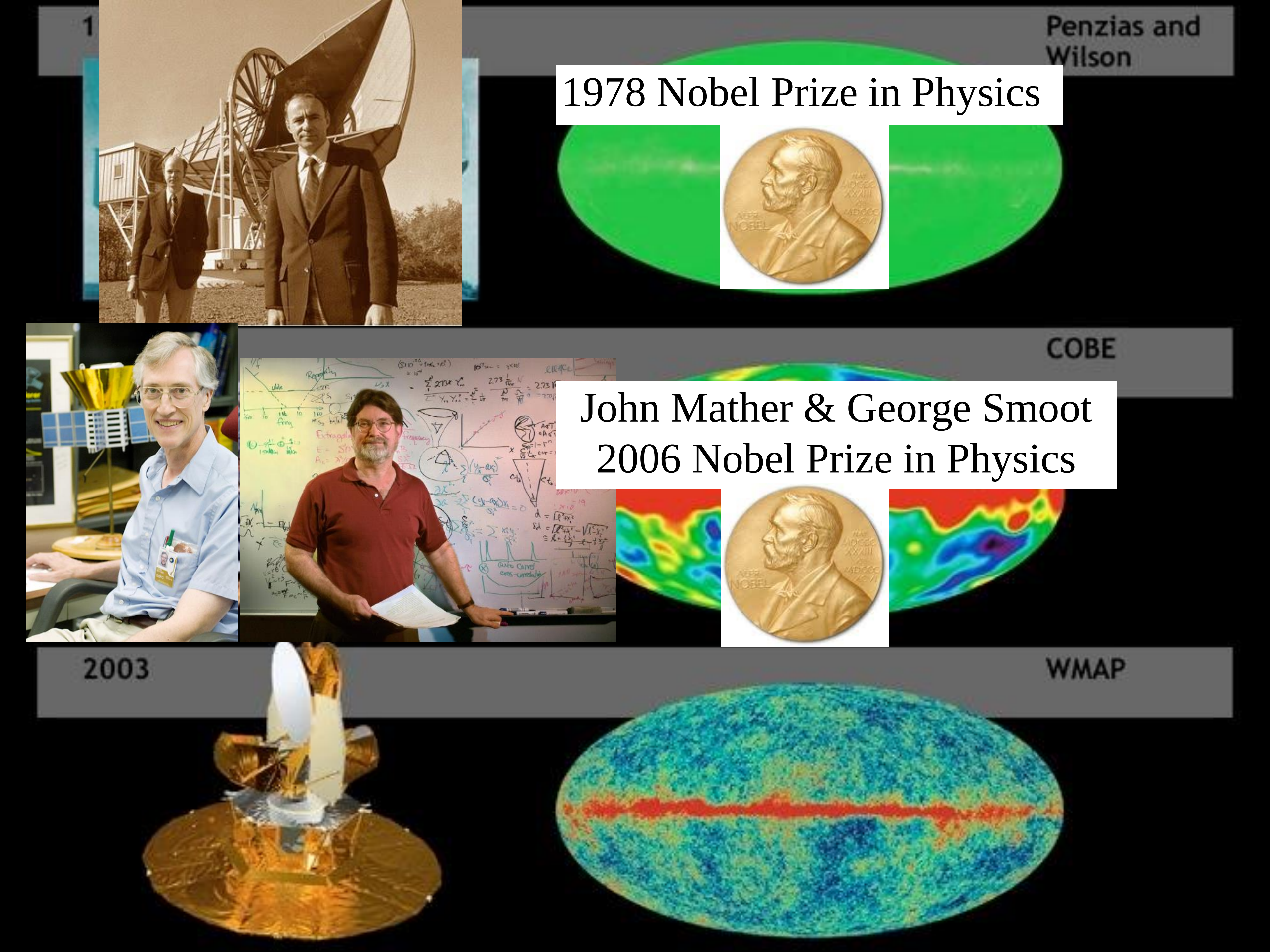
1
Penzias and Wilson
1978 Nobel Prize in Physics
COBE
John Mather & George Smoot
2006 Nobel Prize in Physics
2003
WMAP

Planck (2013)

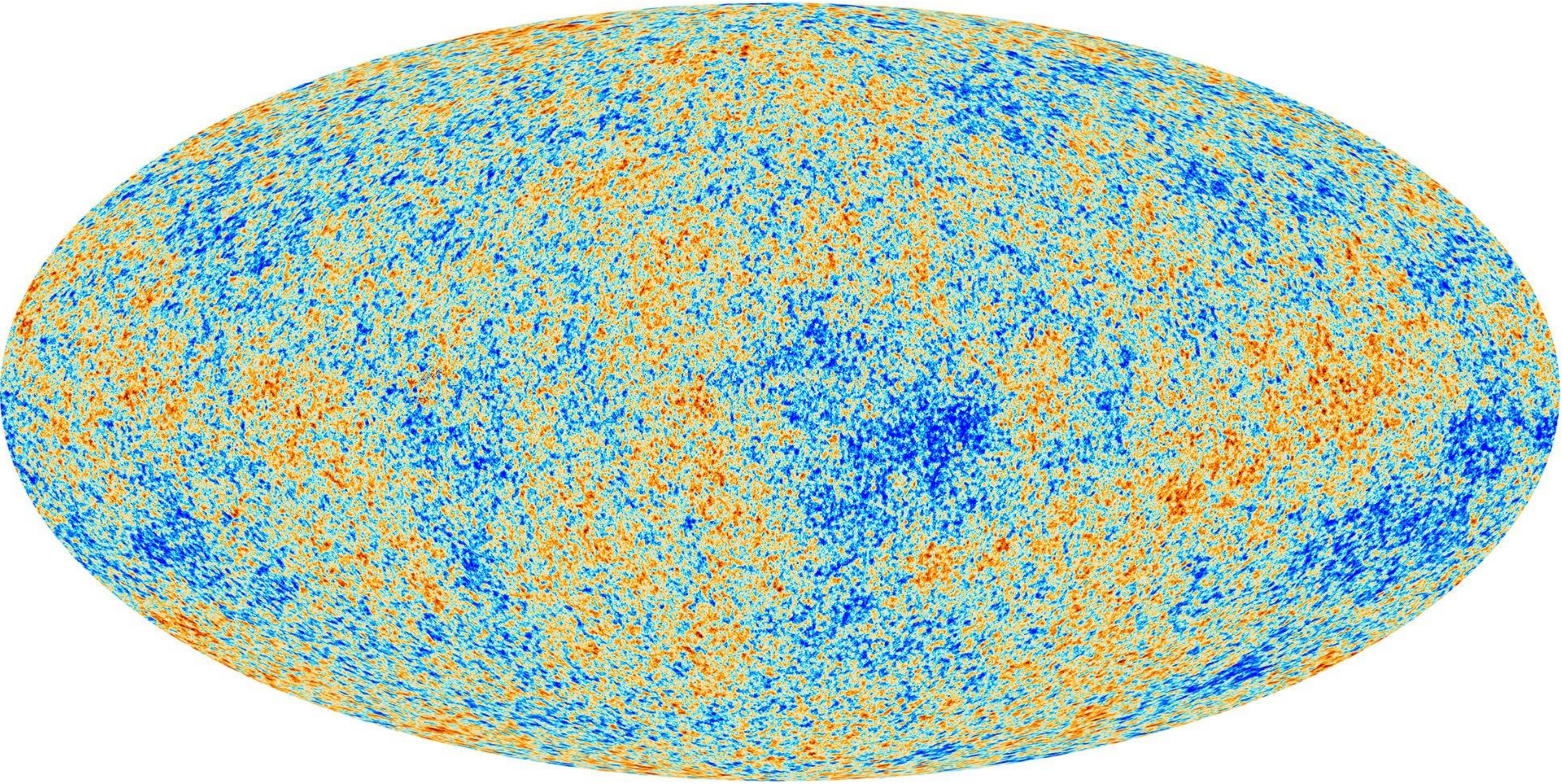

$$\frac{\delta\rho}{\rho} \sim 10^{-5} \xrightarrow[\text{gravitation}]{} \frac{\delta\rho}{\rho} \gg 1$$

CMB Results

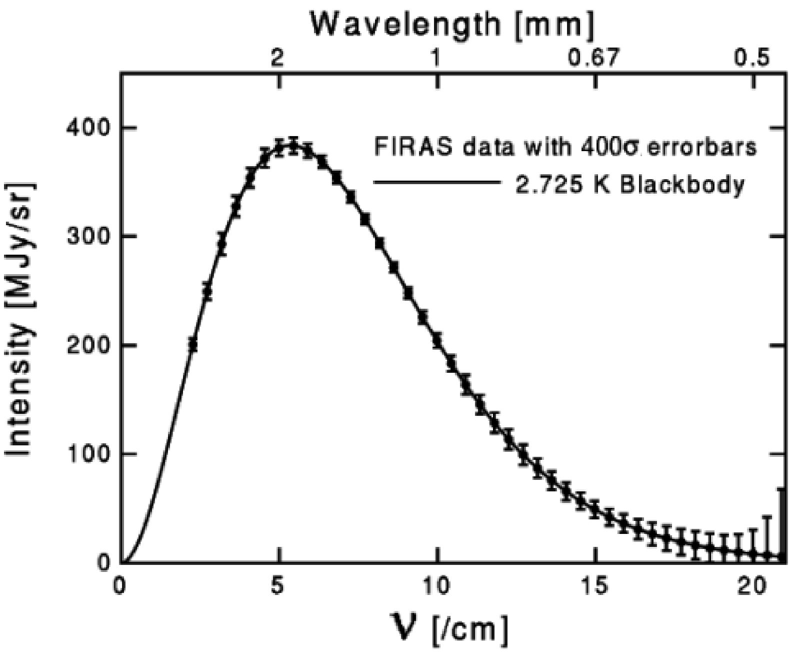

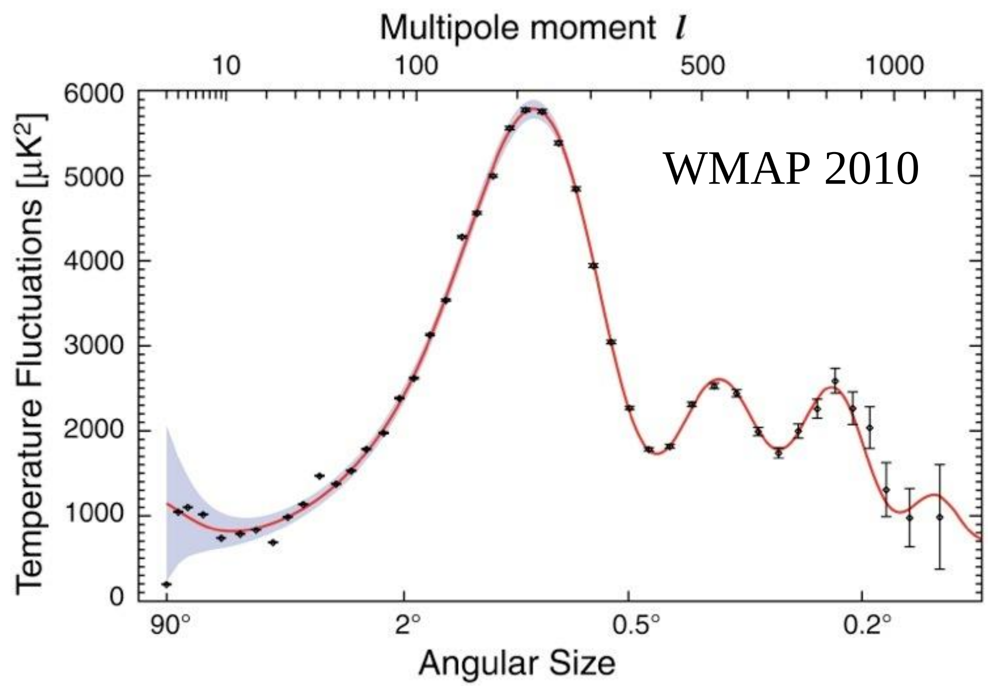

- The spectrum corresponds to a black body with temperature
T = 2.725 K ~ 3000 K / (1+1100)
There are about 410 CMB photons per cm^3

- Very uniform: thermal contact
→ Big Bang

- Temperature, and hence density, fluctuations tell us how galaxies were formed

- The angle where we find the maximum of the fluctuations tells us that the Universe is flat

What's the Origin of the Fluctuations?

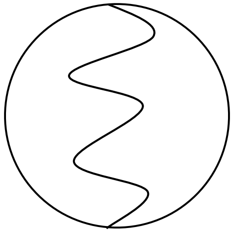

Quantum Mechanical
microscopic fluctuations

Inflation
makes them $>10^{30}$ times bigger

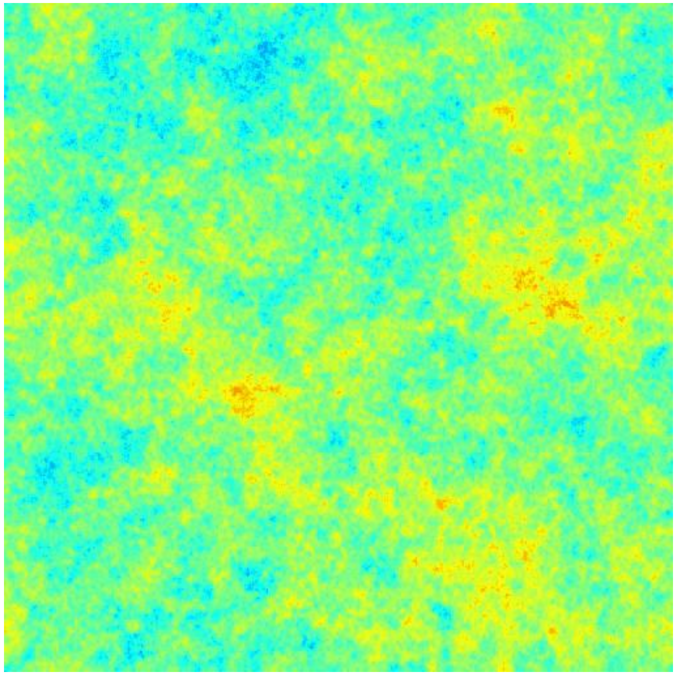

After inflation
Huge size, amplitude $\sim 10^{-5}$

Predicting the CMB Phenomenology

Ingredients:

- Thomson scattering for $e^- \gamma$ collisions
- Physics of recombination $e^- + p \leftrightharpoons H + \gamma$
- General Relativity
- Boltzmann equation

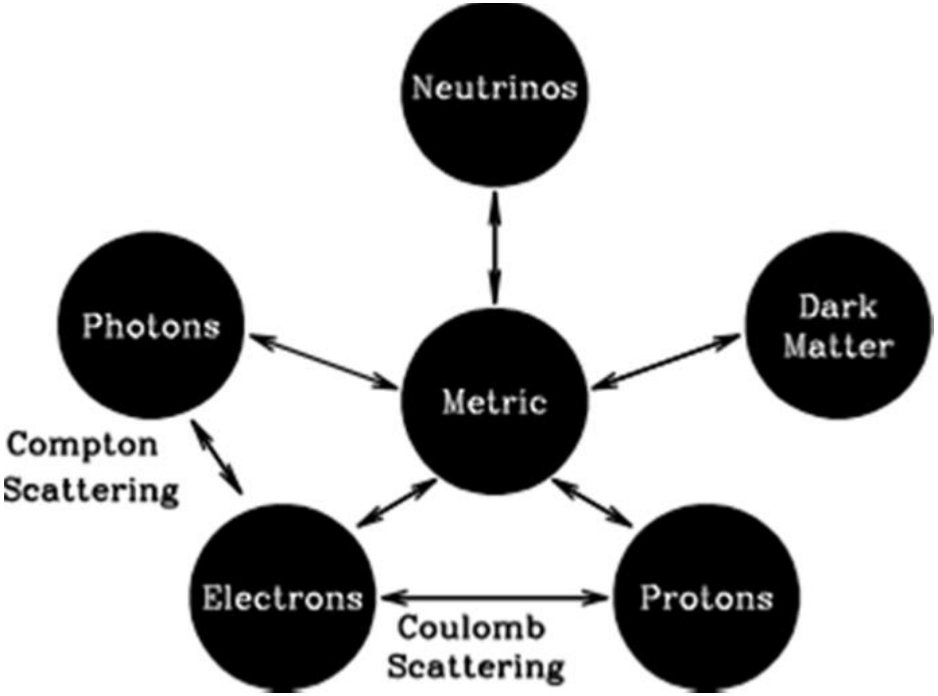

(Re-)Combination (I)

- Why did recombination happen at T ~ 3000 K, when the binding energy of H is 13.6 eV / k_B ~ 1.6 × 10^5 K?
- The photon energy distribution follows a black-body (Planck) spectrum:

$$u_{\rm PL}(\nu) = \frac{8\pi h}{c^3} \frac{\nu^3}{\exp\left(\frac{h\nu}{kT}\right) - 1}$$

- Peak of the energy distribution ~ mean energy ~ 2.7 k_BT ~ 0.7 eV, but with long exponential tail: one in 30 × 10^9 has E > 30 k_BT ~ 8 eV, and there are ~10^9 photons per electron (and proton).
- Let's define the recombination time as the time at which

$$X \equiv n_p / (n_p+n_H) = n_e / (n_p+n_H) = 0.5$$

n_p: number density of ionized protons
n_e: number density of ionized electrons (= n_p)
n_H: number density of neutral H atoms

(Re-)Combination (II)

- Because $e^- + p \leftrightharpoons H + \gamma$ is in equilibrium and e^-, p and H are non-relativistic, their number densities are given by ($x = e^-$, p, H)

$$n_x = g_x \left(\frac{m_x kT}{2\pi\hbar^2}\right)^{3/2} \exp\left(-\frac{m_x c^2}{kT}\right)$$

Maxwell-Boltzmann

$g_x = 2$ (e^-, p), 4 (H)

- Therefore, we can write:

$$\frac{n_{\rm H}}{n_p n_e} = \frac{g_{\rm H}}{g_p g_e}\left(\frac{m_{\rm H}}{m_p m_e}\right)^{3/2}\left(\frac{kT}{2\pi\hbar^2}\right)^{-3/2}\exp\left(\frac{[m_p + m_e - m_{\rm H}]c^2}{kT}\right)$$

- Which can be simplified to

$$\frac{1-X}{X} = n_p\left(\frac{m_e kT}{2\pi\hbar^2}\right)^{-3/2}\exp\left(\frac{Q}{kT}\right)$$

$Q = 13.6$ eV

- And now we can introduce $\eta \equiv n_{baryon} / n_\gamma = n_p / (X n_\gamma)$ and compute n_γ by integrating the number density of photons ($u_{PL}(\nu) / h\nu$):

$$n_\gamma = \frac{2.404}{\pi^2}\left(\frac{kT}{\hbar c}\right)^3 = 0.243\left(\frac{kT}{\hbar c}\right)^3$$

(Re-)Combination (III)

- Finally, we get the Saha equation for *X*:

$$\frac{1-X}{X^2} = 3.84\eta \left(\frac{kT}{m_e c^2}\right)^{3/2} \exp\left(\frac{Q}{kT}\right)$$

with $\eta \sim 5.5 \times 10^{-10}$

- From where we can solve for *X* as a function of T, or z (T = 2.725 K × (1+z))

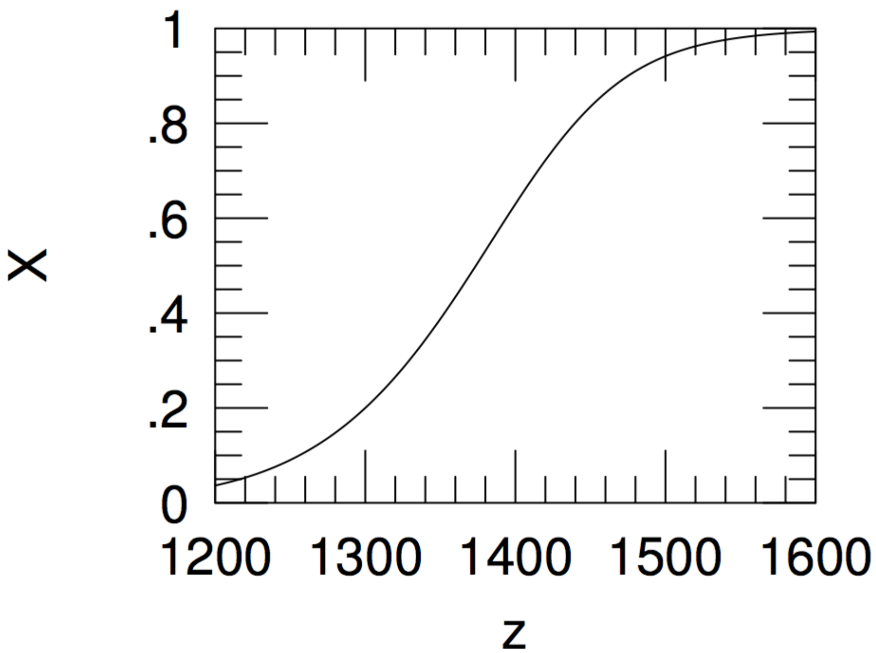

$X = 0.5 \Rightarrow k_B T_{rec} = 0.323$ eV = Q / 42

$T_{rec} = 3740$ K

$z_{rec} = 1370$

$t_{rec} = 240\,000$ years

Why not z ~ 1100?

(Re-)Combination (IV): Decoupling

- The photon decoupling occurs when the rate of photon scattering, Γ, falls below the expansion rate, H. We have

$$\Gamma = \frac{c}{\lambda} = n_e \sigma_e c \quad \text{with} \quad \lambda = \frac{1}{n_e \sigma_e}$$

the photon mean free path

$\sigma_e \sim 6.65 \times 10^{-29}\ \mathrm{m}^2$ (Thomson)

- When the hydrogen is partially ionized, we have

$$\Gamma(z) = n_e(z)\sigma_e c = X(z)(1+z)^3 n_{\mathrm{bary},0}\sigma_e c = 4.4 \times 10^{-21}\,\mathrm{s}^{-1} X(z)(1+z)^3$$ (assuming $\Omega_{\mathrm{baryons},0} = 0.04$)

- The expansion rate in the matter dominated era is given by

$$H = H_0 \sqrt{\Omega_{m,0}\,(1+z)^3} = 1.24 \times 10^{18} s^{-1}\,(1+z)^{3/2}$$ (assuming $\Omega_{\mathrm{m},0} = 0.3$)

- Therefore, imposing Γ = H, we have

$$1 + z_{dec} = 43.0\ X(z_{dec})^{-2/3} \implies z_{dec} = 1120$$

- The small discrepancy is due to non-equilibrium effects…

(Re-)Combination (V): Last Scattering Surface

- The number of collisions that a photon has experimented between a time *t* and now, t_0, is given by the optical depth τ :

$$\tau(t) = \int_t^{t_0} \Gamma(t) dt$$

- The time of last scattering is given by $\tau = 1$. Changing variables from *t* to *z*,

$$\tau(z) = \int_0^z \frac{\Gamma(z)}{H(z)} \frac{dz}{1+z} = 0.0035 \int_0^z X(z)(1+z)^{1/2} dz$$

- From which imposing $\tau = 1$, we get z_{ls} ~1100.
- In reality, the LSS is a thin layer with a width Δz ~200 (non-equilibrium…)
- So in summary

z_{rec} ~ 1370, T_{rec} ~ 3740 K, t_{rec} ~ 240 000 years

z_{dec} ~ z_{ls} ~ 1100, T_{ls} ~ 3000 K, t_{ls} ~ 350 000 years

Perturbations: Statistical Analysis

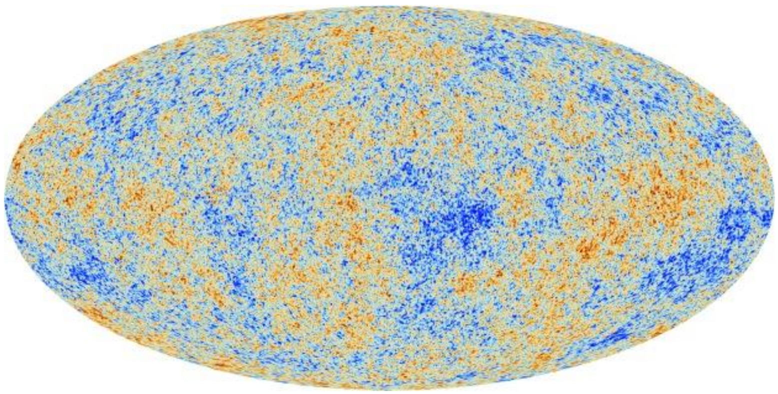

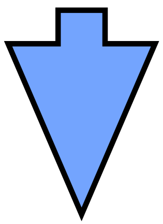

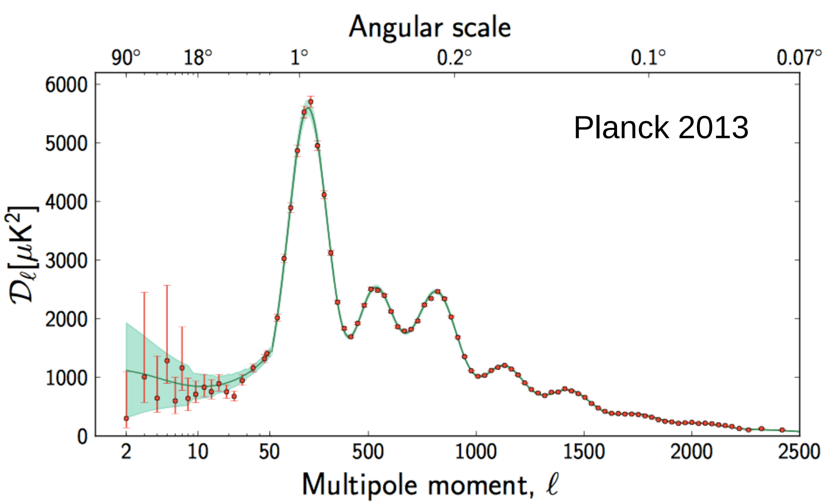

- Interested in temperature fluctuations, $\delta T = T(\theta,\Phi) - 2.725$ K
- Since the measurement is on a sphere, use spherical harmonics:

$$\frac{\delta T}{T}(\theta,\phi) = \sum_{l=0}^{\infty}\sum_{m=-l}^{l} a_{lm} Y_{lm}(\theta,\phi)$$

- Then, measure angular correlations:

$$\begin{aligned} C(\theta) &= \left\langle \frac{\delta T}{T}(\hat{n})\frac{\delta T}{T}(\hat{n}')\right\rangle_{\hat{n}\cdot\hat{n}'=\cos\theta} \\ &= \frac{1}{4\pi}\sum_{l=0}^{\infty}(2l+1)C_l P_l(\cos\theta) \\ &\sim \int_0^{\infty}\frac{dl}{l}\frac{l(2l+1)C_l}{4\pi}P_l(\cos\theta) \end{aligned}$$

- Results given in $D_l = l(l+1)\, C_l / 2\pi$ as a function of $l \sim 180^o / \theta$

Three Different Regimes

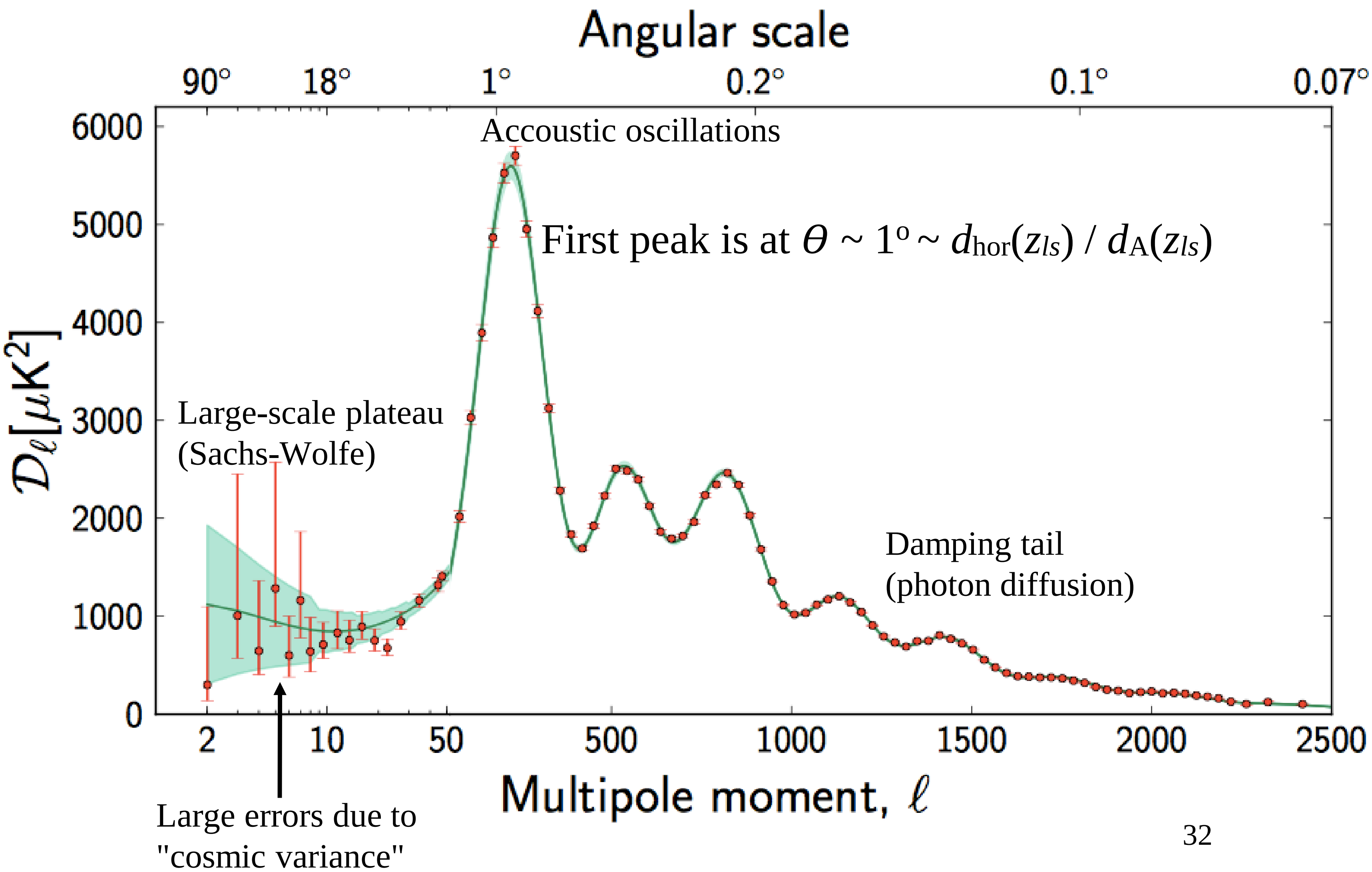

Three Different Regimes

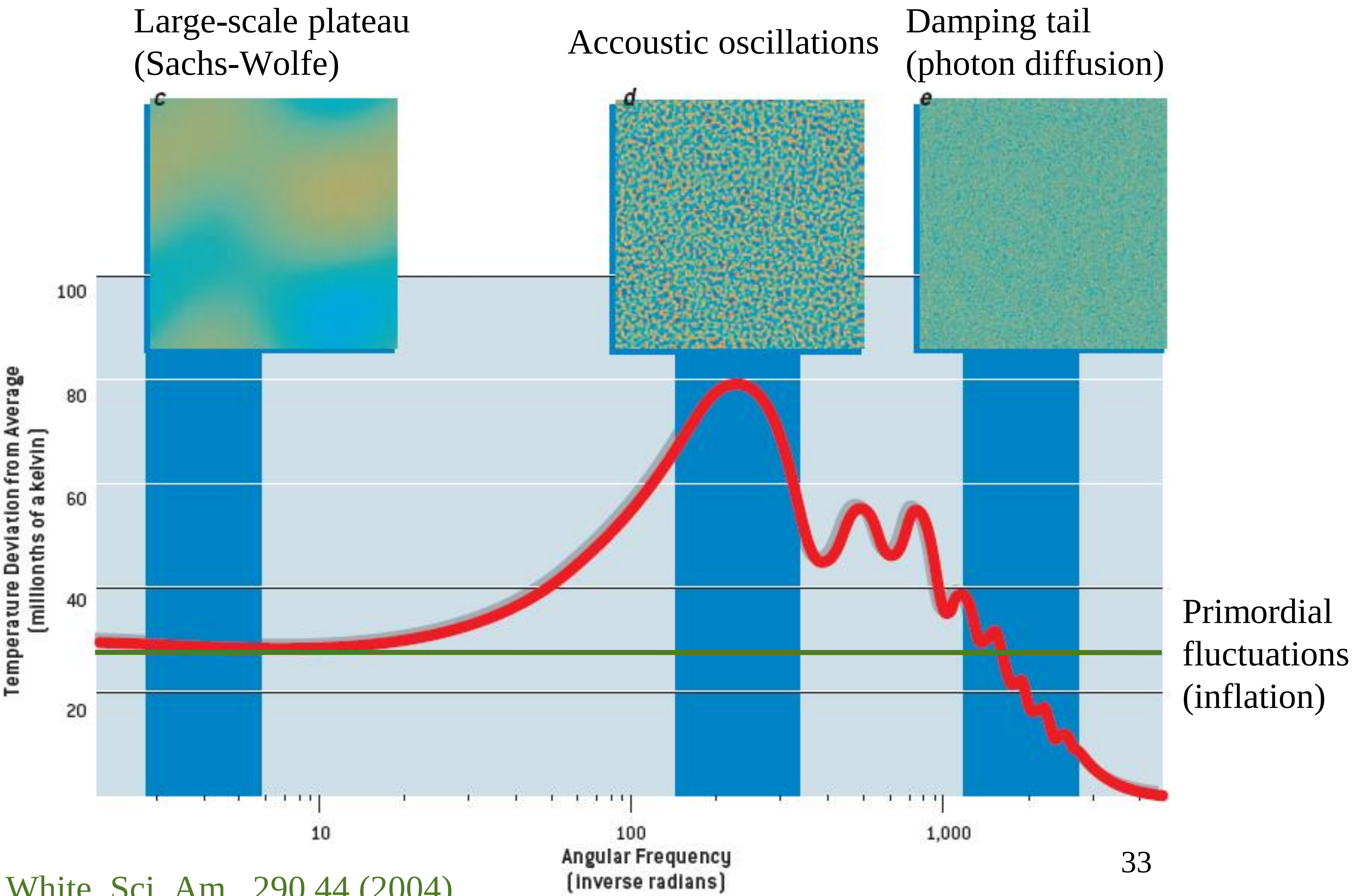

Hu & White, Sci. Am., 290 44 (2004)

Large-Scale Plateau

- Matter density at LSS is not homogeneous:

$$\varepsilon(\vec{r}) = \bar{\varepsilon} + \delta\varepsilon(\vec{r}) \longrightarrow \nabla^2(\delta\Phi) = \frac{4\pi G}{c^2}\delta\varepsilon \longrightarrow \frac{\delta T}{T} = \frac{1}{3}\frac{\delta\Phi}{c^2}$$

Sachs-Wolfe

- When a photon is at a minimum of the gravitational potential at the LSS: redshift

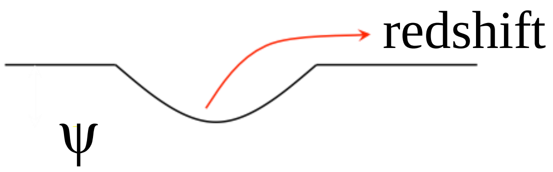

- When a photon is at a maximum of the gravitational potential at the LSS: blueshift

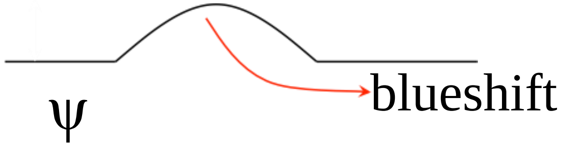

- The temperature fluctuations at large θ tell us about the gravitational potential fluctuations at the LSS

Accoustic Oscillations

- The photon-baryon plasma will fall into the gravitation potential wells created by the inhomogeneities in the distribution of the (dominant) dark matter.
- Being compressed there, pressure will increase ($w = p / \rho \sim 1/3$) and the fluid will expand outwards, until pressure decreases and gravity pulls the fluid back into the well
- These are pressure (sound) waves with $c_s \sim c\,(dp / d\rho)^{1/2} = c / \sqrt{3}$.

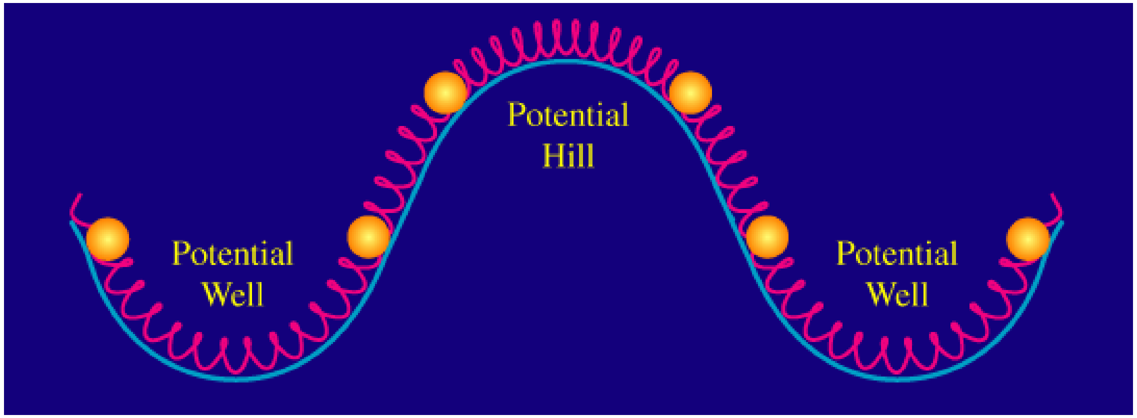

W. Hu

Analogy: Bouncing Balls

- Let’s drop a series of balls from different heights and wait 10 seconds.
- Balls dropped from low heights bounce a large number of times.
- Balls dropped from high enough don’t even reach the ground in 10 s.
- There is a certain height from which the ball just touches the ground after those 10 s.

Analogy: Bouncing Balls

- Bouncing balls
- 10 seconds
- Bounces
- Height of the ball that just reaches the ground
- Balls dropped from higher heights don't bounce

- Photon-baryon plasma oscillating
- Age of the Universe at the last scattering surface
- Accoustic peaks in CMB
- Position of first peak: sound horizon at the last scattering surface: $\theta \sim c_s/c \times d_{\mathrm{hor}}(z_{ls})\ /\ d_A(z_{ls}) \lesssim 1^o$

(This corresponds to maximal compression: maximal temperature)

- No acoustic oscillations at scales $\theta \gtrsim 1^o$ (only Sachs-Wolfe effect)

Three Different Regimes

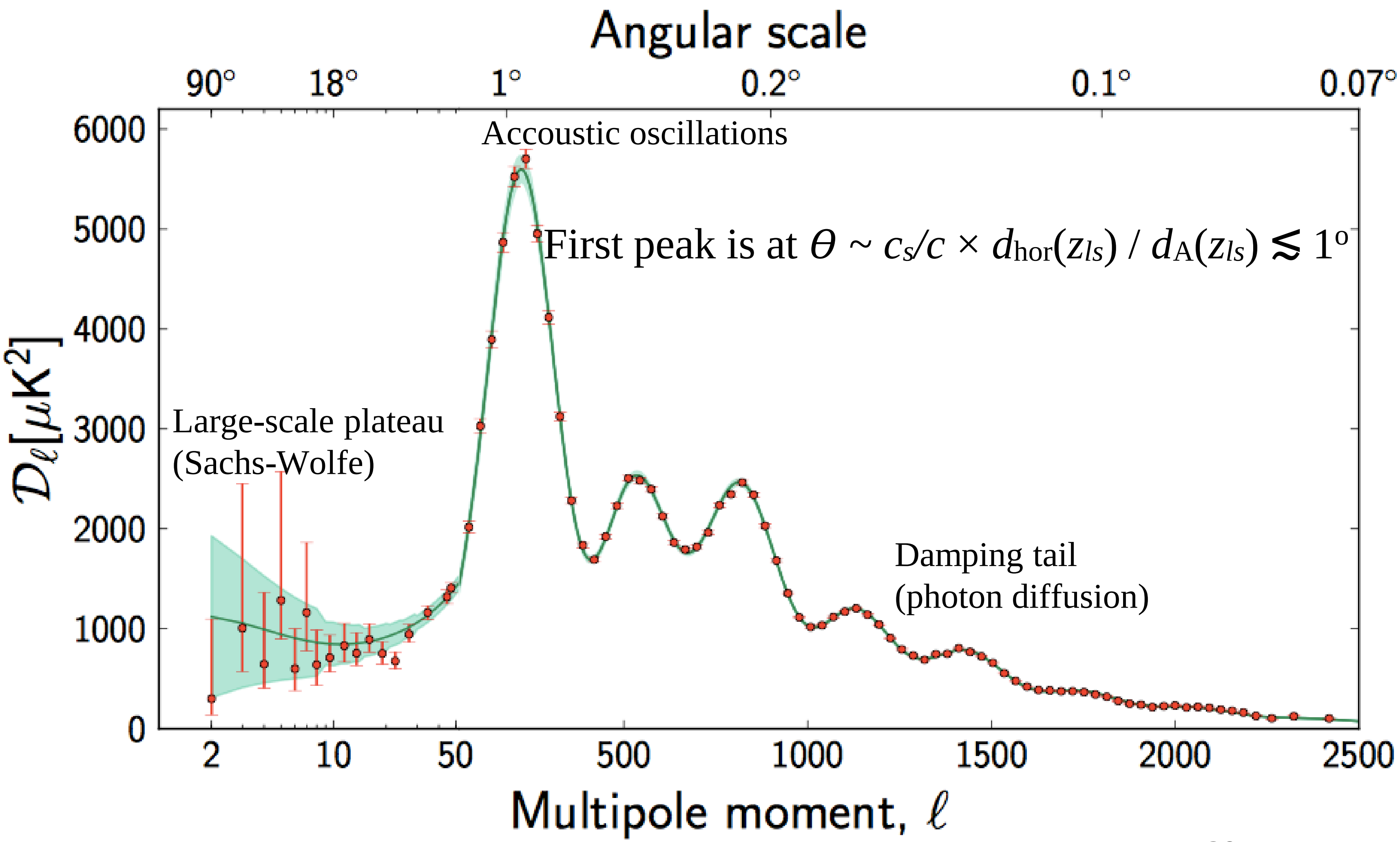

Structure of Peaks

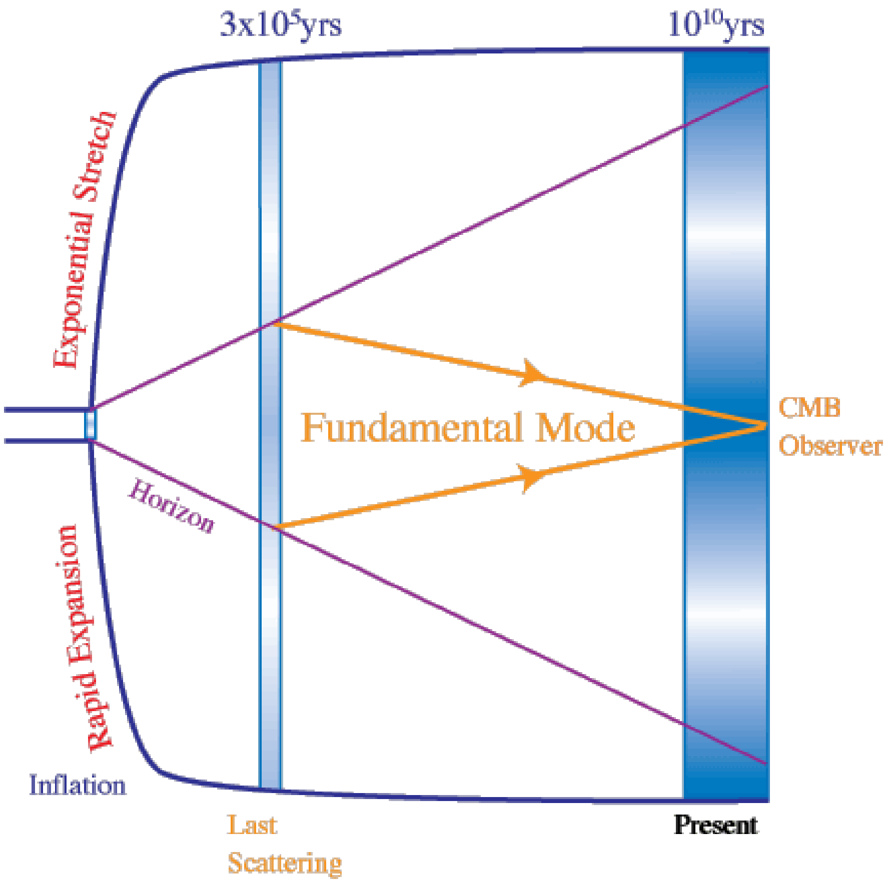

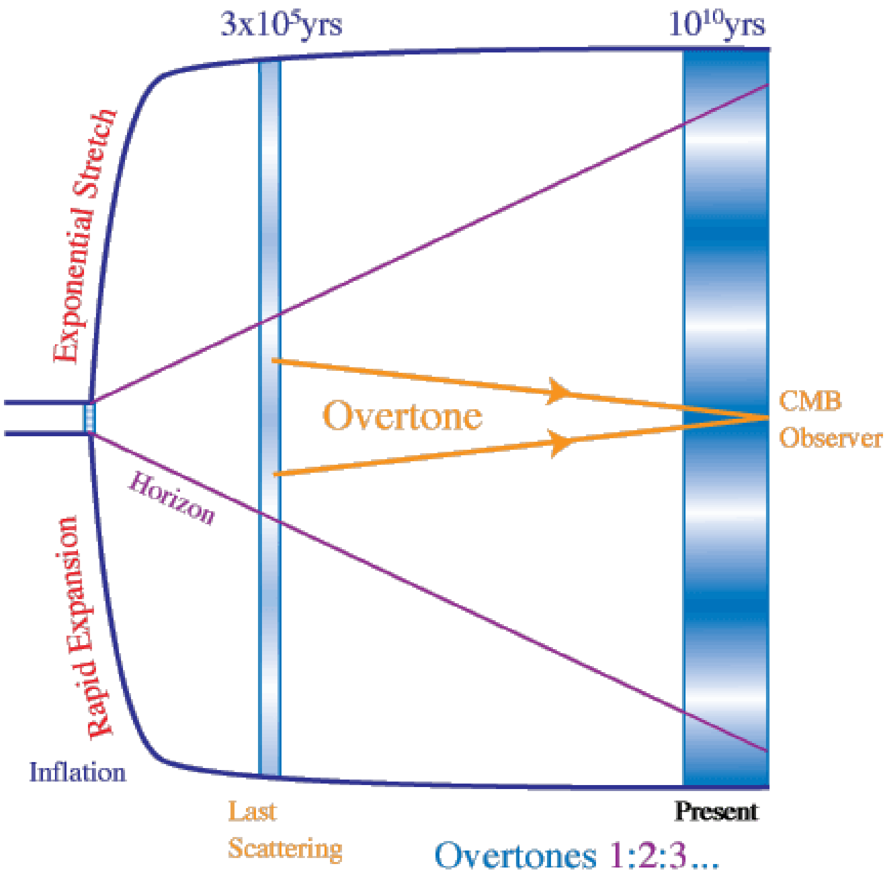

The Universe Is Flat

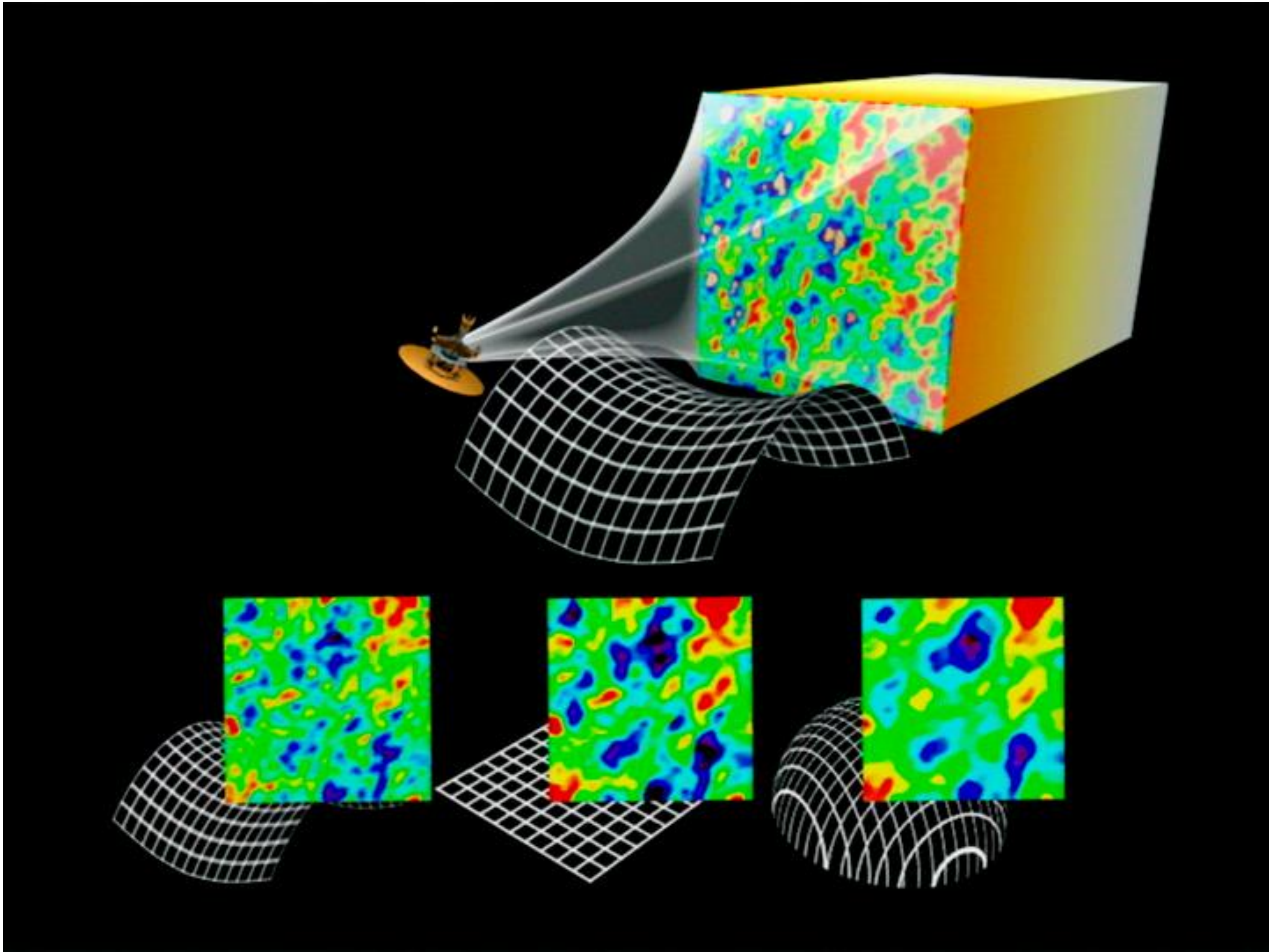

The Universe Is Flat

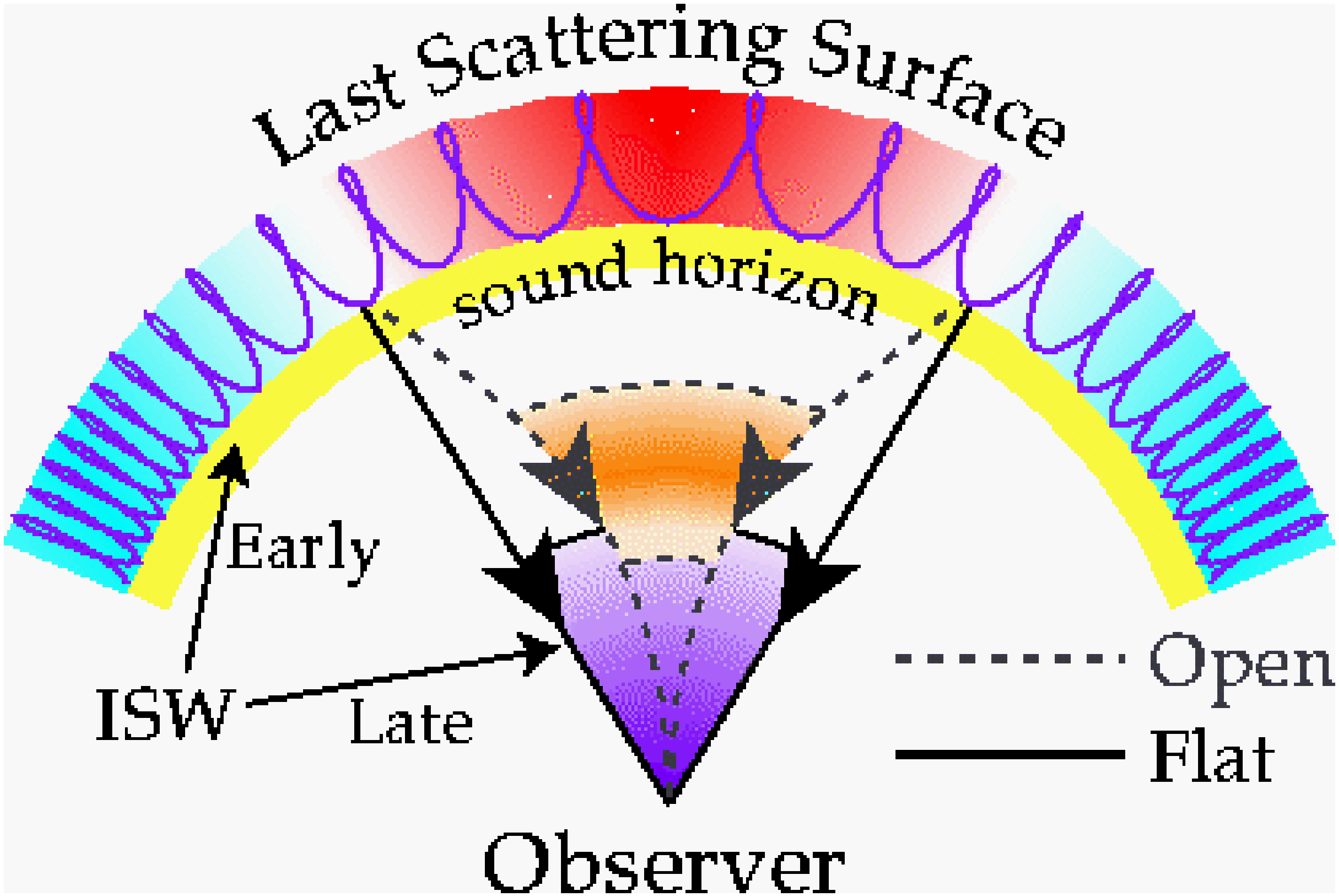

Diffusion Tail (Silk Damping)

- At small enough scales, photon random walk collisions erase the signature of acoustic oscillations
- Recall that mean free path was $\lambda = \frac{1}{n_e \sigma_e}$. The scale of diffusion due to random walk is $\lambda_d = \sqrt{N}\lambda$, where *N* is the number of collisions since the Bing Bang: $N \sim 2c/H/\lambda$, so that

$$\lambda_d^c \sim (1+z)\sqrt{2c\lambda/H}$$ (co-moving)

- And, therefore, the damping should start at angular scales

$$\theta \sim \lambda_d^c(z_{ls})/d_A(z_{ls}) \sim 0.1^\circ$$

$$l \sim 180^\circ/\theta \sim 1800$$

Three Different Regimes

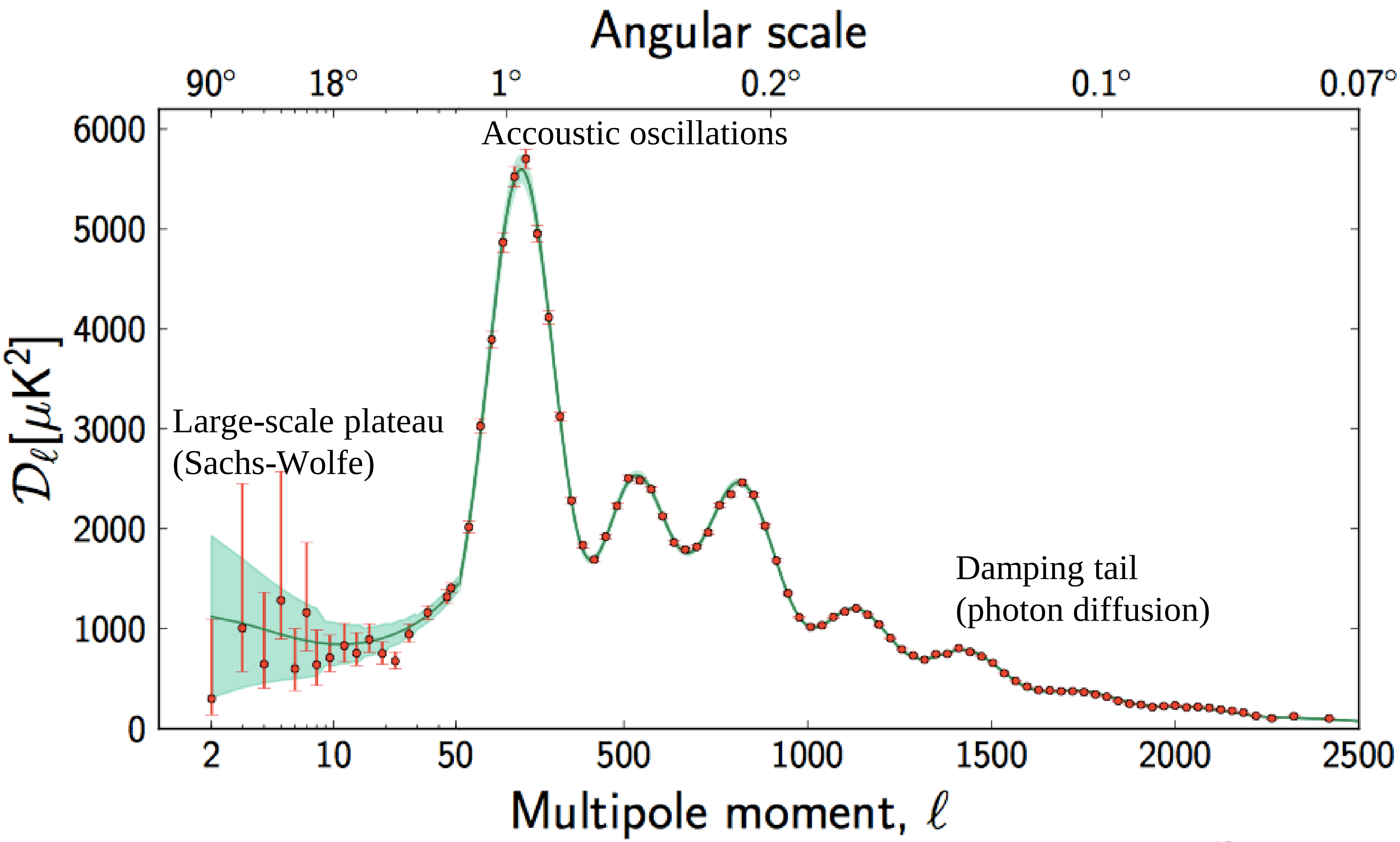

What Can We Learn from the CMB?

Ω_k : Curvature affects the relationship between sound horizon at last scattering surface and current angular scale: position of peaks

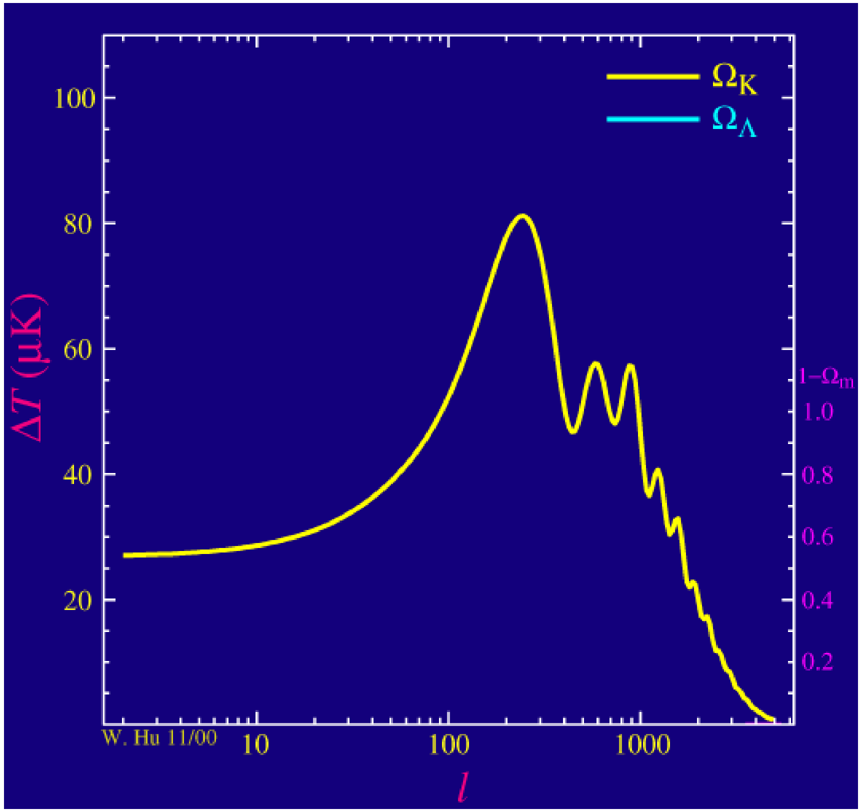

What Can We Learn from the CMB?

Ω_b : Larger baryon density enhances odd-numbered peaks (compression), and decreases even-numbered peaks (expansion)

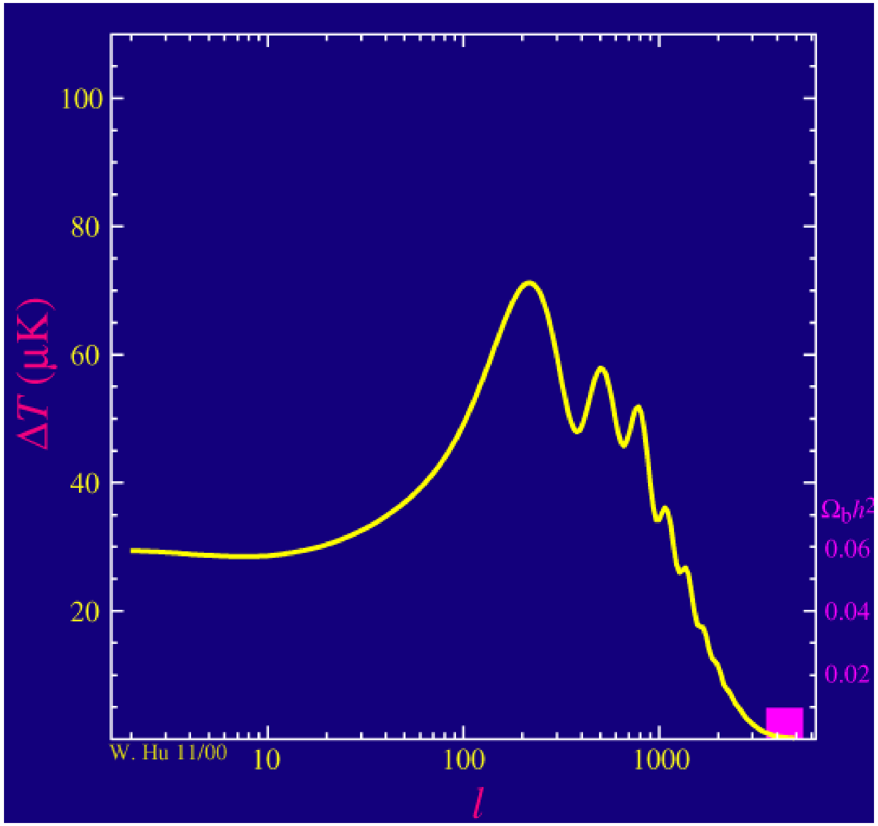

What Can We Learn from the CMB?

Ω_m : The 3rd and higher peaks are sensitive to the ratio between the matter and radiation energy densities

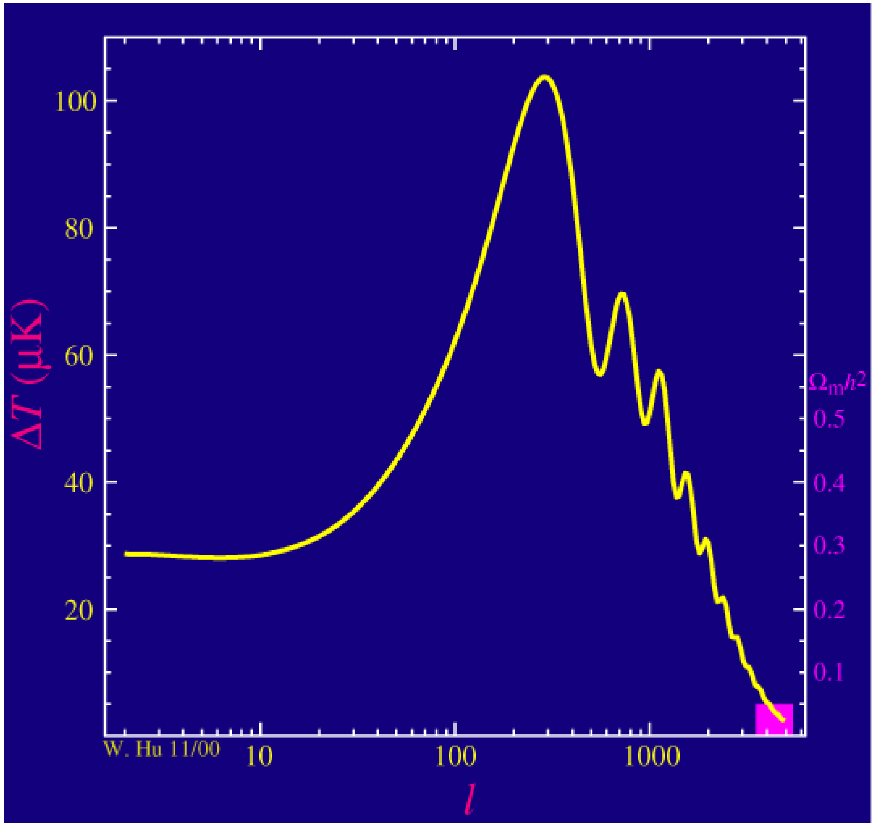

What Can We Learn from the CMB?

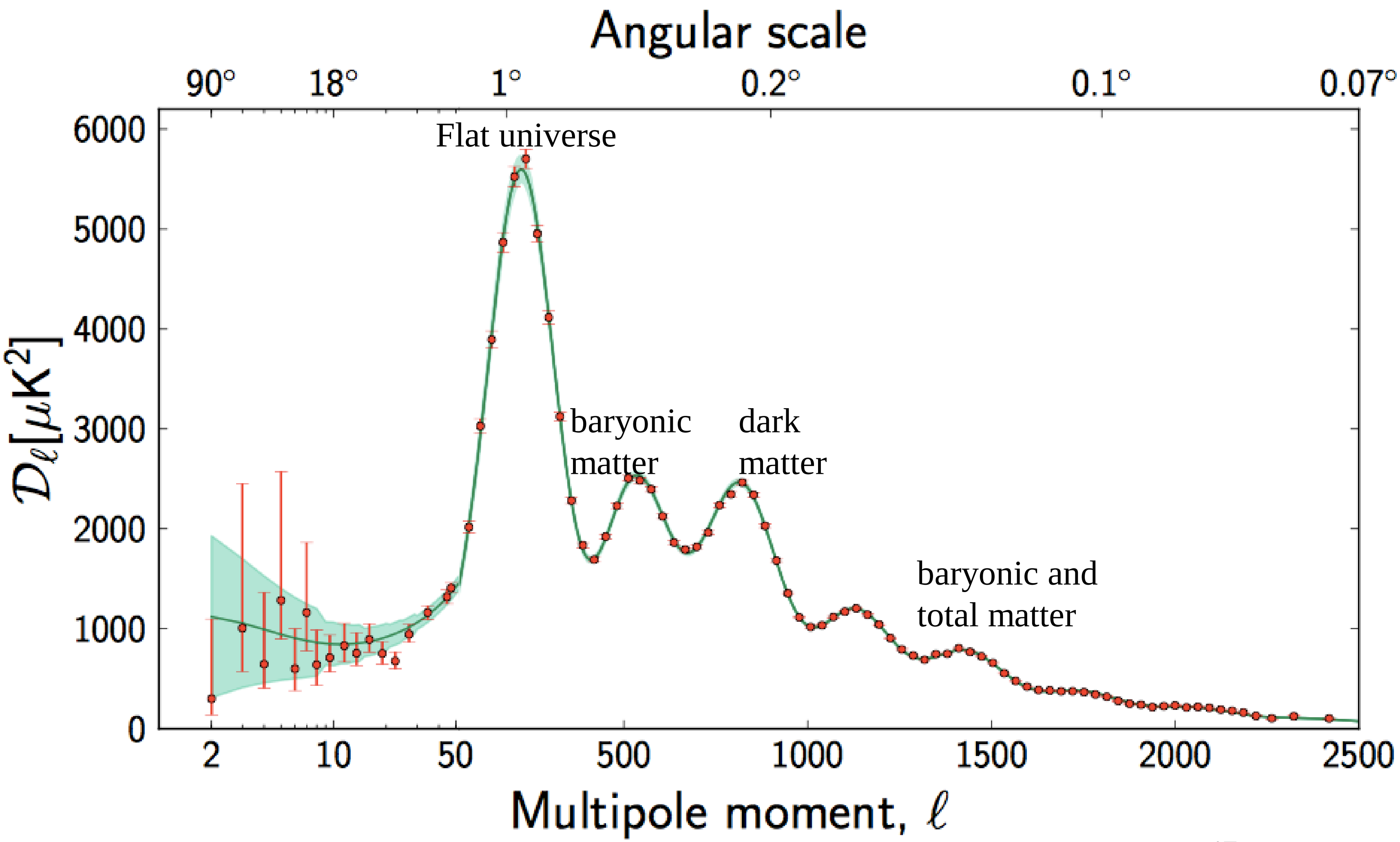

What Can We Learn from the CMB?

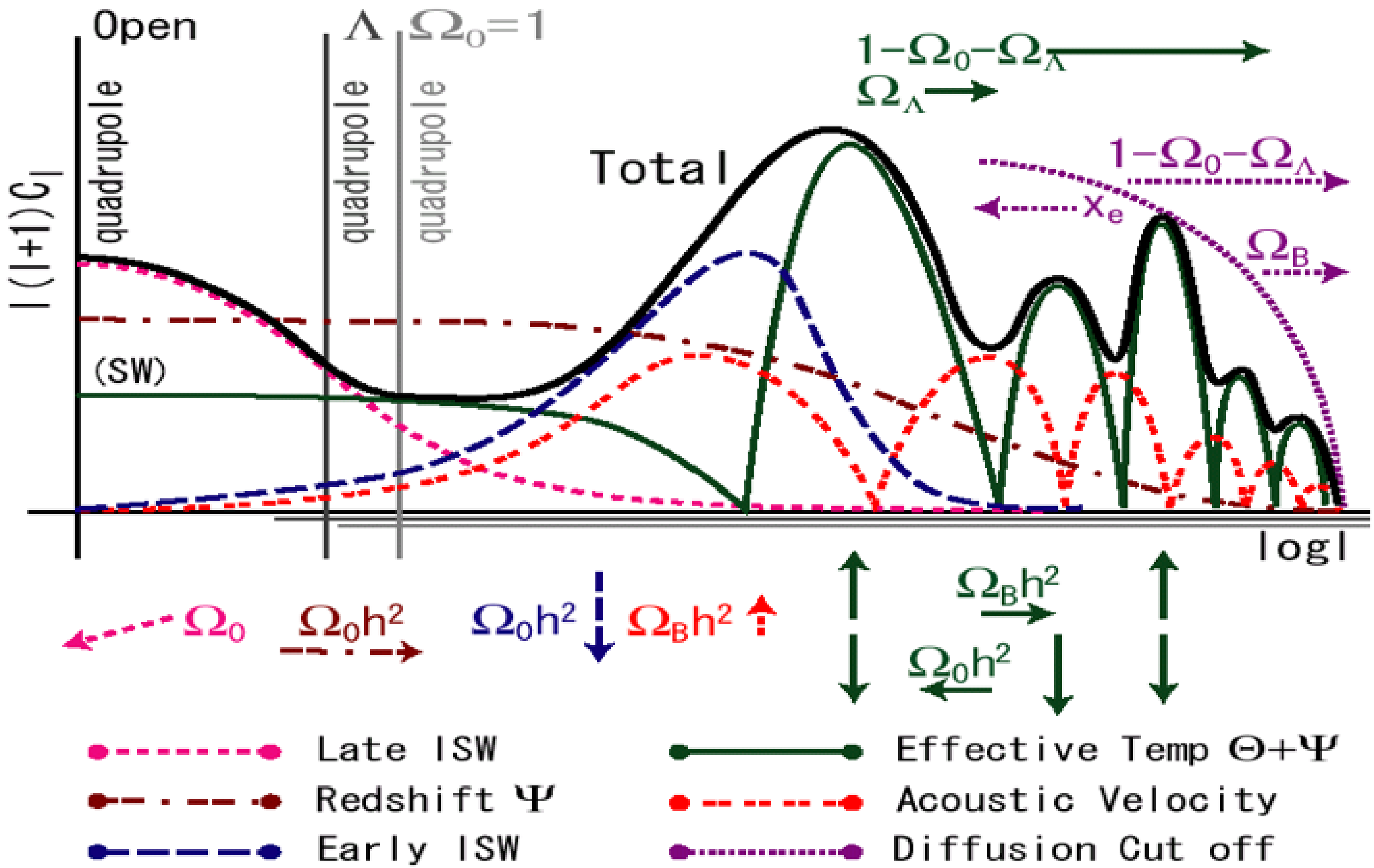

Planck Results

Parameter	*Planck* Best fit	*Planck* 68% limits	*Planck*+lensing Best fit	*Planck*+lensing 68% limits	*Planck*+WP Best fit	*Planck*+WP 68% limits
$\Omega_b h^2$	0.022068	0.02207 ± 0.00033	0.022242	0.02217 ± 0.00033	0.022032	0.02205 ± 0.00028
$\Omega_c h^2$	0.12029	0.1196 ± 0.0031	0.11805	0.1186 ± 0.0031	0.12038	0.1199 ± 0.0027
$100\theta_{MC}$	1.04122	1.04132 ± 0.00068	1.04150	1.04141 ± 0.00067	1.04119	1.04131 ± 0.00063
τ	0.0925	0.097 ± 0.038	0.0949	0.089 ± 0.032	0.0925	$0.089^{+0.012}_{-0.014}$
n_s	0.9624	0.9616 ± 0.0094	0.9675	0.9635 ± 0.0094	0.9619	0.9603 ± 0.0073
$\ln(10^{10} A_s)$	3.098	3.103 ± 0.072	3.098	3.085 ± 0.057	3.0980	$3.089^{+0.024}_{-0.027}$
Ω_Λ	0.6825	0.686 ± 0.020	0.6964	0.693 ± 0.019	0.6817	$0.685^{+0.018}_{-0.016}$
Ω_m	0.3175	0.314 ± 0.020	0.3036	0.307 ± 0.019	0.3183	$0.315^{+0.016}_{-0.018}$
σ_8	0.8344	0.834 ± 0.027	0.8285	0.823 ± 0.018	0.8347	0.829 ± 0.012
z_{re}	11.35	$11.4^{+4.0}_{-2.8}$	11.45	$10.8^{+3.1}_{-2.5}$	11.37	11.1 ± 1.1
H_0	67.11	67.4 ± 1.4	68.14	67.9 ± 1.5	67.04	67.3 ± 1.2
$10^9 A_s$	2.215	2.23 ± 0.16	2.215	$2.19^{+0.12}_{-0.14}$	2.215	$2.196^{+0.051}_{-0.060}$
$\Omega_m h^2$	0.14300	0.1423 ± 0.0029	0.14094	0.1414 ± 0.0029	0.14305	0.1426 ± 0.0025
$\Omega_m h^3$	0.09597	0.09590 ± 0.00059	0.09603	0.09593 ± 0.00058	0.09591	0.09589 ± 0.00057
Y_P	0.247710	0.24771 ± 0.00014	0.247785	0.24775 ± 0.00014	0.247695	0.24770 ± 0.00012
Age/Gyr	13.819	13.813 ± 0.058	13.784	13.796 ± 0.058	13.8242	13.817 ± 0.048
z_*	1090.43	1090.37 ± 0.65	1090.01	1090.16 ± 0.65	1090.48	1090.43 ± 0.54
r_*	144.58	144.75 ± 0.66	145.02	144.96 ± 0.66	144.58	144.71 ± 0.60
$100\theta_*$	1.04139	1.04148 ± 0.00066	1.04164	1.04156 ± 0.00066	1.04136	1.04147 ± 0.00062
z_{drag}	1059.32	1059.29 ± 0.65	1059.59	1059.43 ± 0.64	1059.25	1059.25 ± 0.58
r_{drag}	147.34	147.53 ± 0.64	147.74	147.70 ± 0.63	147.36	147.49 ± 0.59
k_D	0.14026	0.14007 ± 0.00064	0.13998	0.13996 ± 0.00062	0.14022	0.14009 ± 0.00063
$100\theta_D$	0.161332	0.16137 ± 0.00037	0.161196	0.16129 ± 0.00036	0.161375	0.16140 ± 0.00034
z_{eq}	3402	3386 ± 69	3352	3362 ± 69	3403	3391 ± 60
$100\theta_{eq}$	0.8128	0.816 ± 0.013	0.8224	0.821 ± 0.013	0.8125	0.815 ± 0.011
$r_{drag}/D_V(0.57)$	0.07130	0.0716 ± 0.0011	0.07207	0.0719 ± 0.0011	0.07126	0.07147 ± 0.00091

CMB Polarization (I)

Polarization of the CMB comes from Thomson scattering of photons off electrons

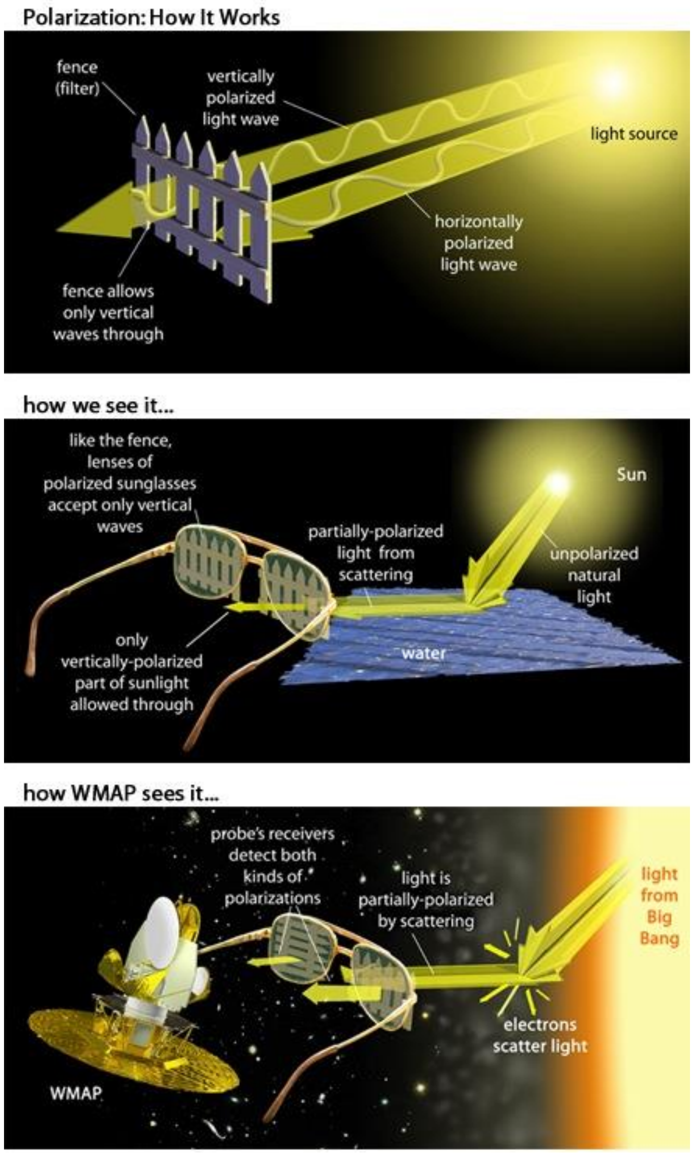

Wayne Hu's CMB tutorials:

http://background.uchicago.edu/index.html

CMB Polarization (II)

- CMB polarization also necessitates a quadrupole anisotropy in the CMB

photon from the left

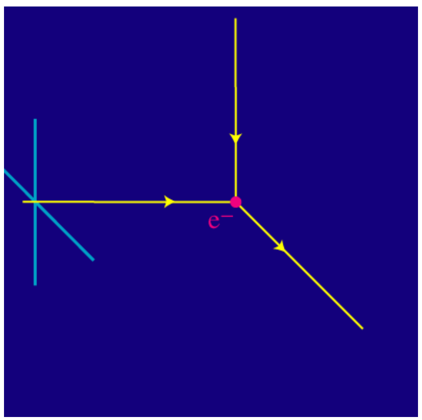

photon from the left +
photon from the top

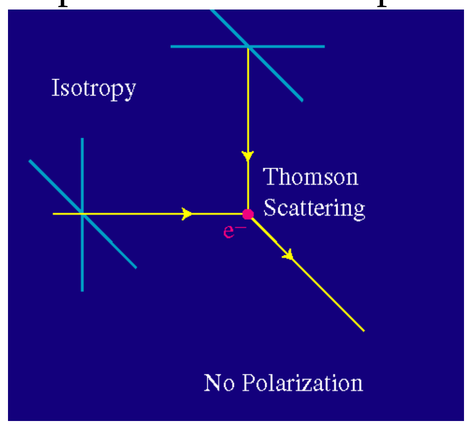

photon from the left +
photon from the top
with quadrupole anisotropy

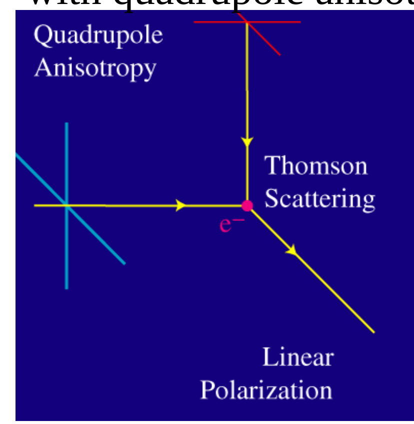

- The direction of polarization corresponds to the direction of the anisotropy
- Sources of quadrupole anisotropy: density perturbations (scalar), vorticity (vector, negligible), gravitational waves (tensor, inflation)

CMB Polarization (III)

Scalar fields only generate E modes, while tensor fields generate both E and B modes

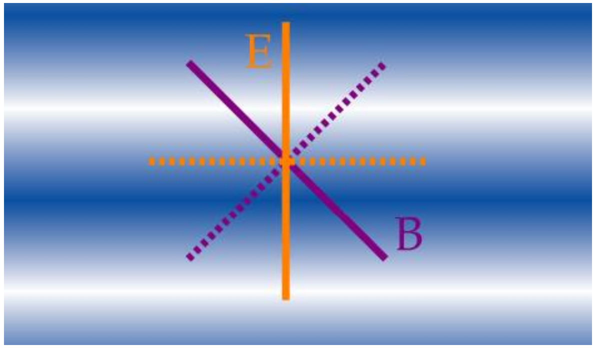

E: parallel or perpendicular

B: 45 degrees

E mode

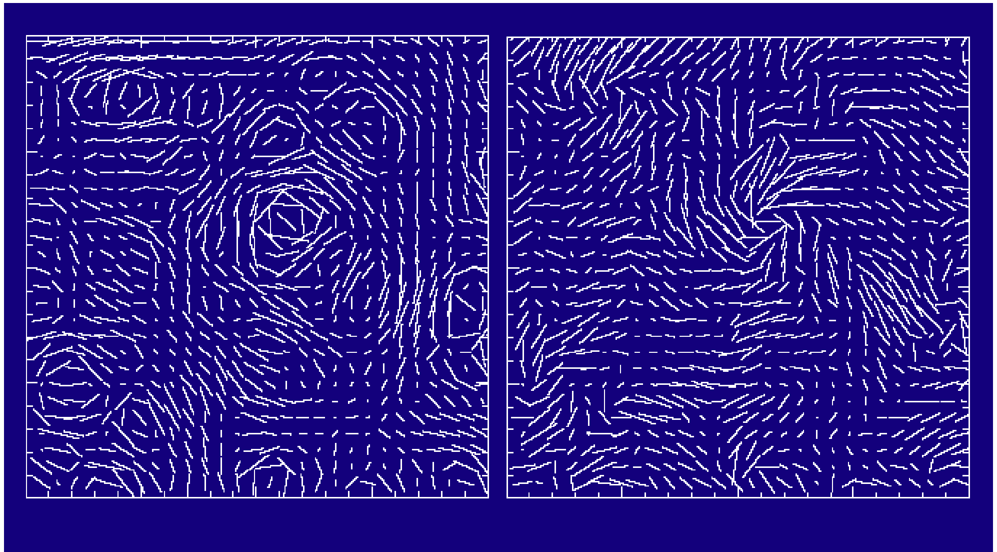

B mode

All Fluctuations if Only Gravitational Waves

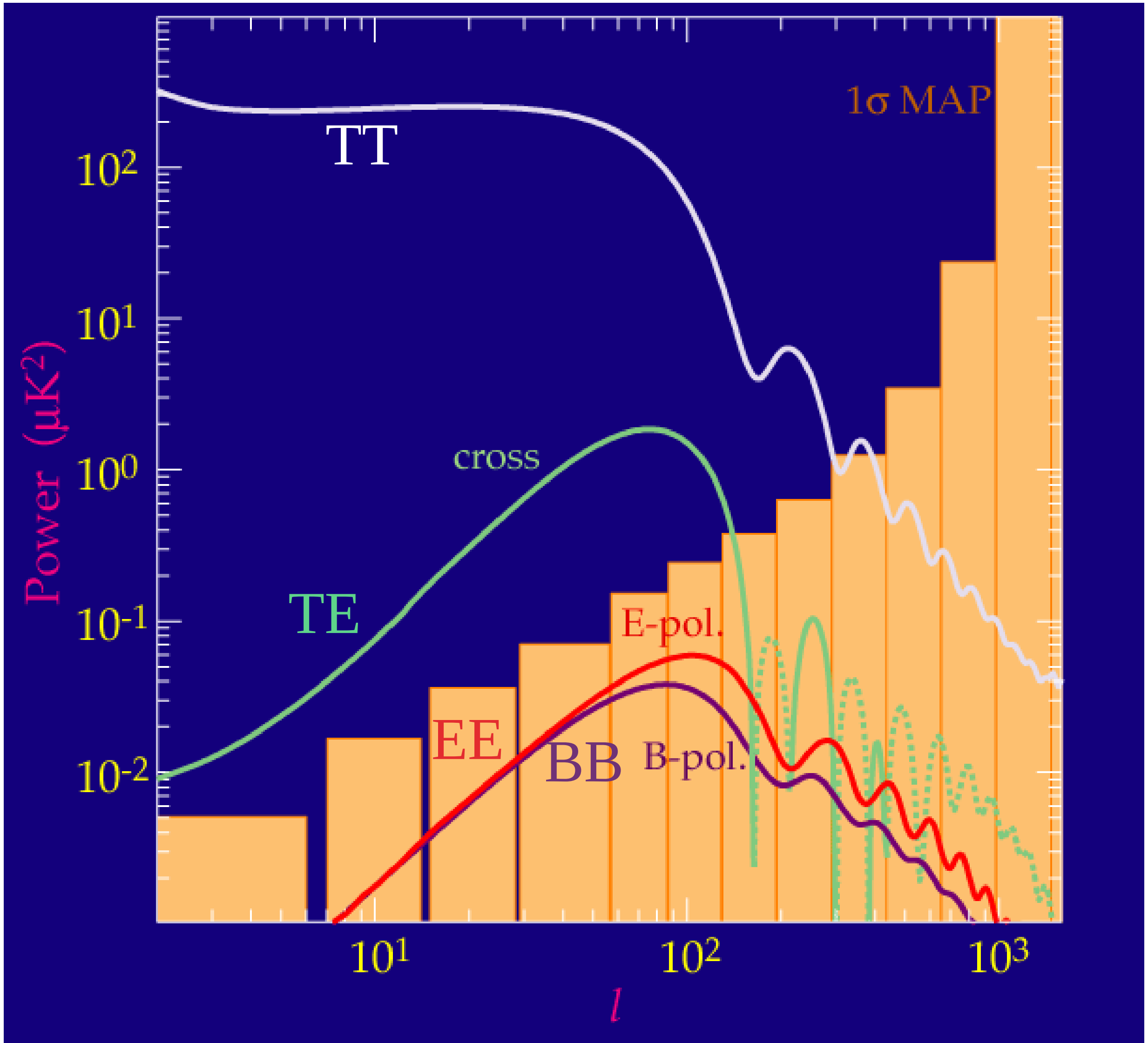

All Fluctuations as a Function of $r = T / S$

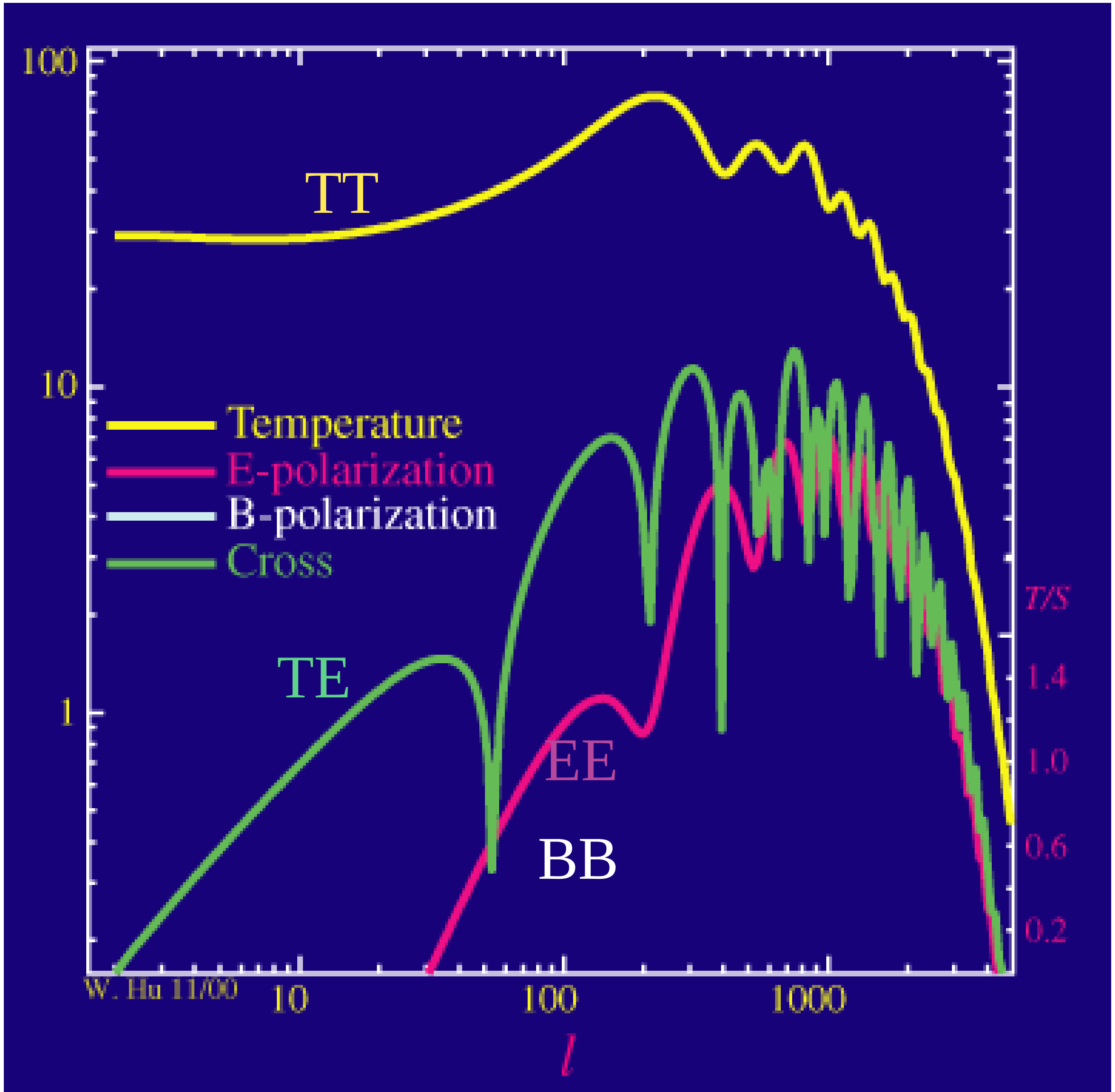

BICEP II Results (2014)

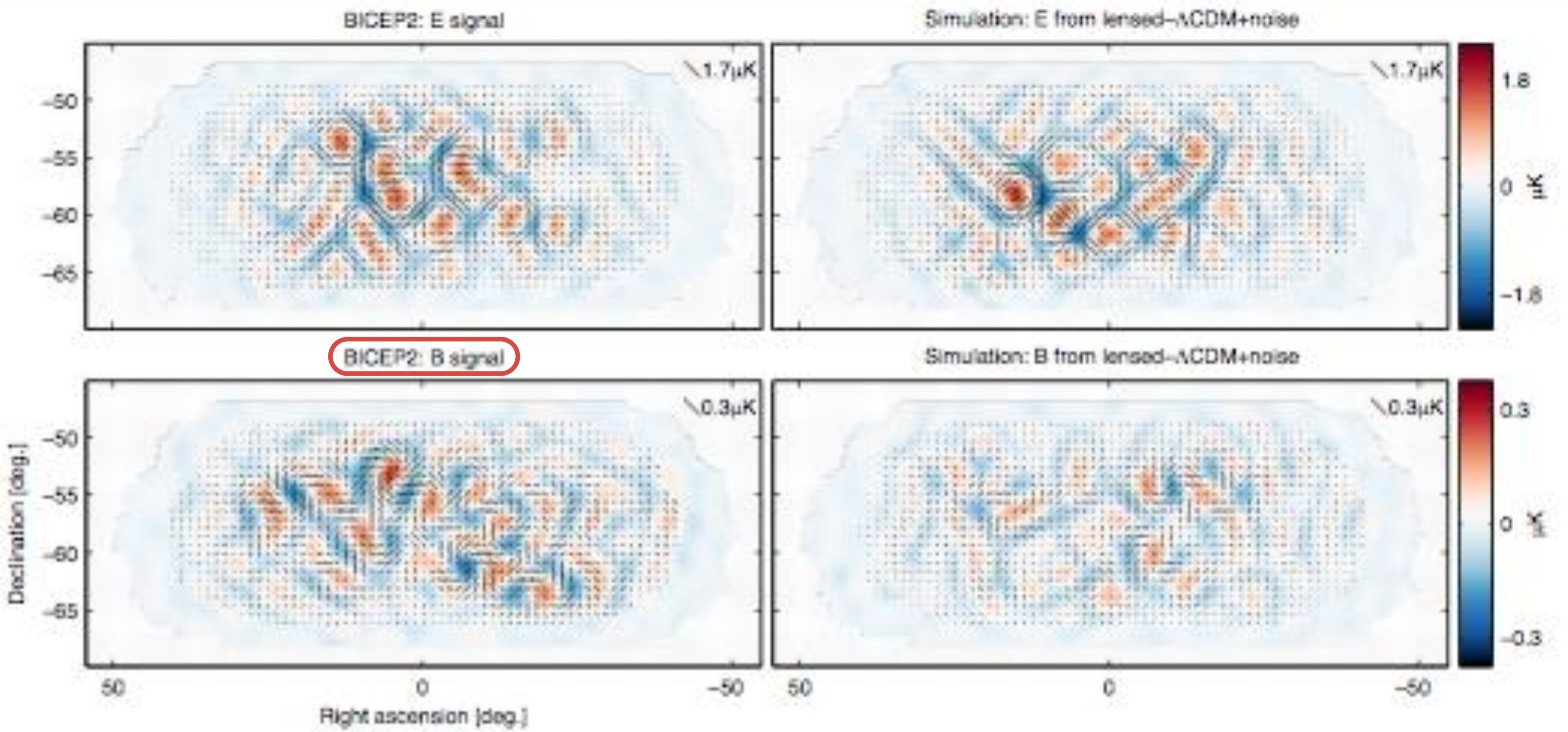

BICEP II Results (2014)

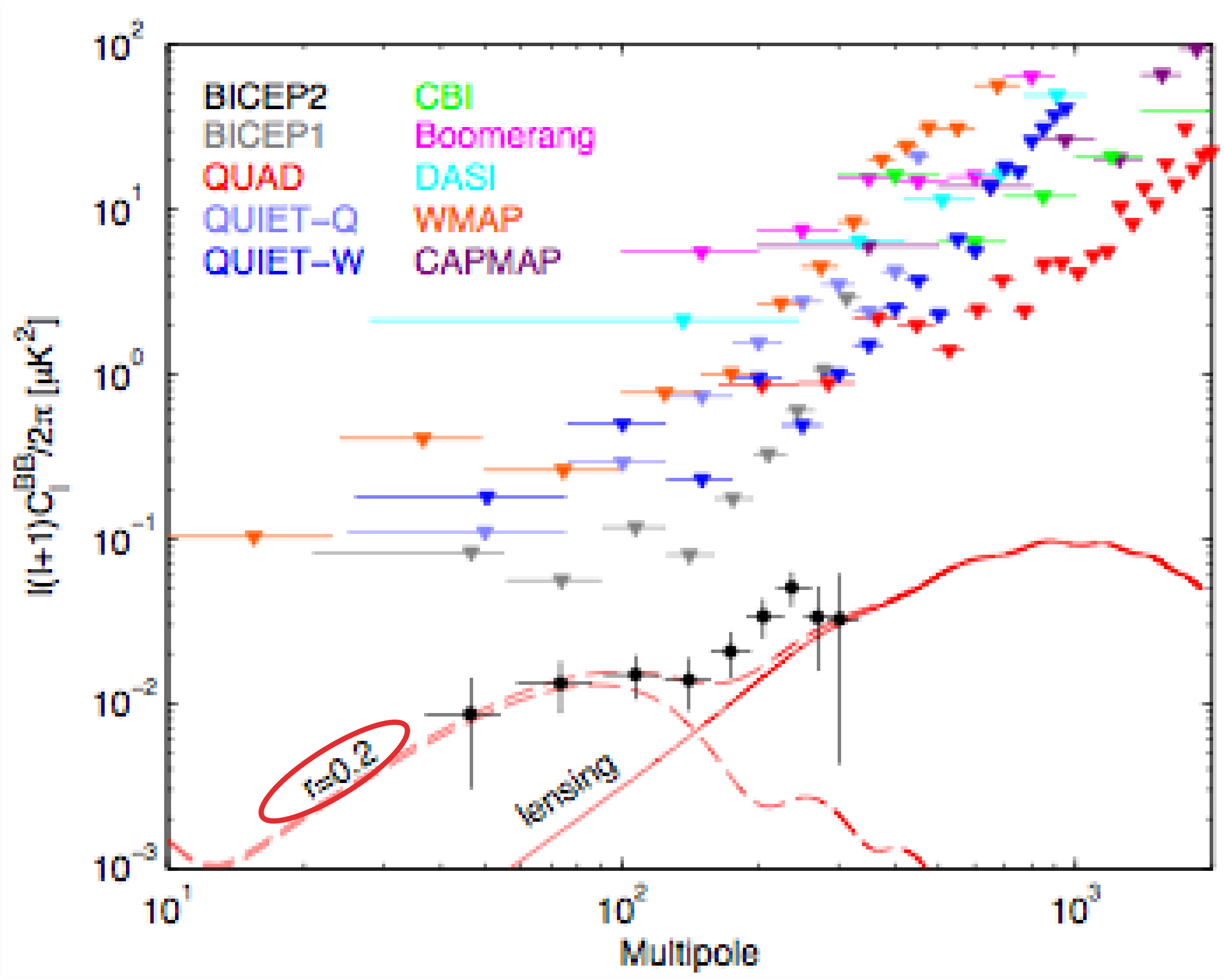

Discovery of primordial gravitational waves? If so, "smoking gun" of inflation

BUT

Planck Results (Sep 22, 2014)

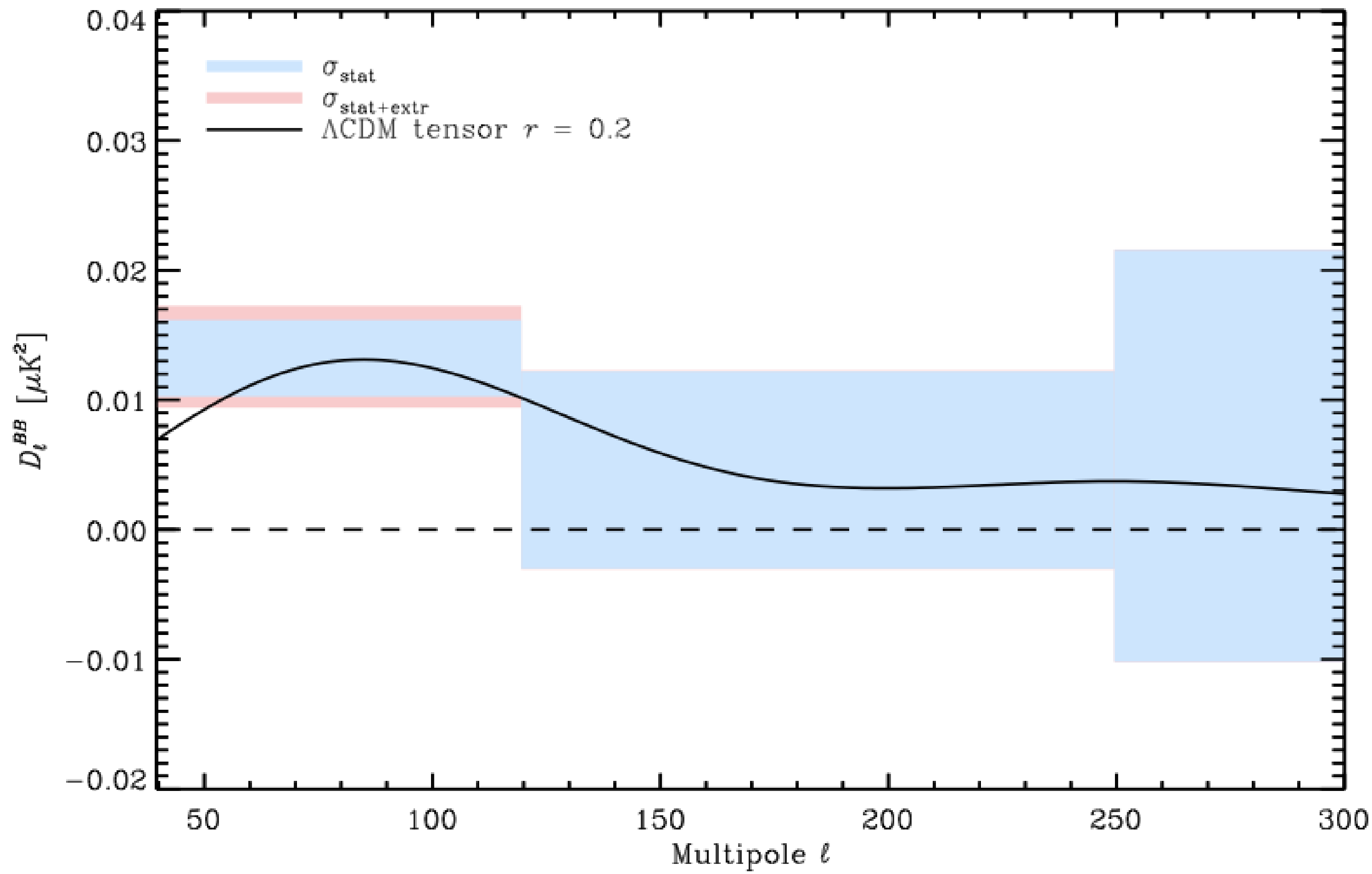

The BB power spectrum of dust in the BICEP2 field looks very similar to the claimed signal

Dark Energy

What Do We Mean by Dark Energy?

- In 1998 two teams of astronomers and physicists studying type-Ia supernovae found that the expansion rate of the universe is increasing with time: accelerated expansion

  Perlmutter et al. 1999 7677 citations Riess et al. 1998 7508 citations

- Gravity tends to slow down the expansion
- Whatever mechanism causes the acceleration, we call it "dark energy":
  - Einstein's cosmological constant?
  - Some dynamical field ("quintessence") not unlike the Higgs field?
  - Modifications to General Relativity?
  - …

The New Standard Model

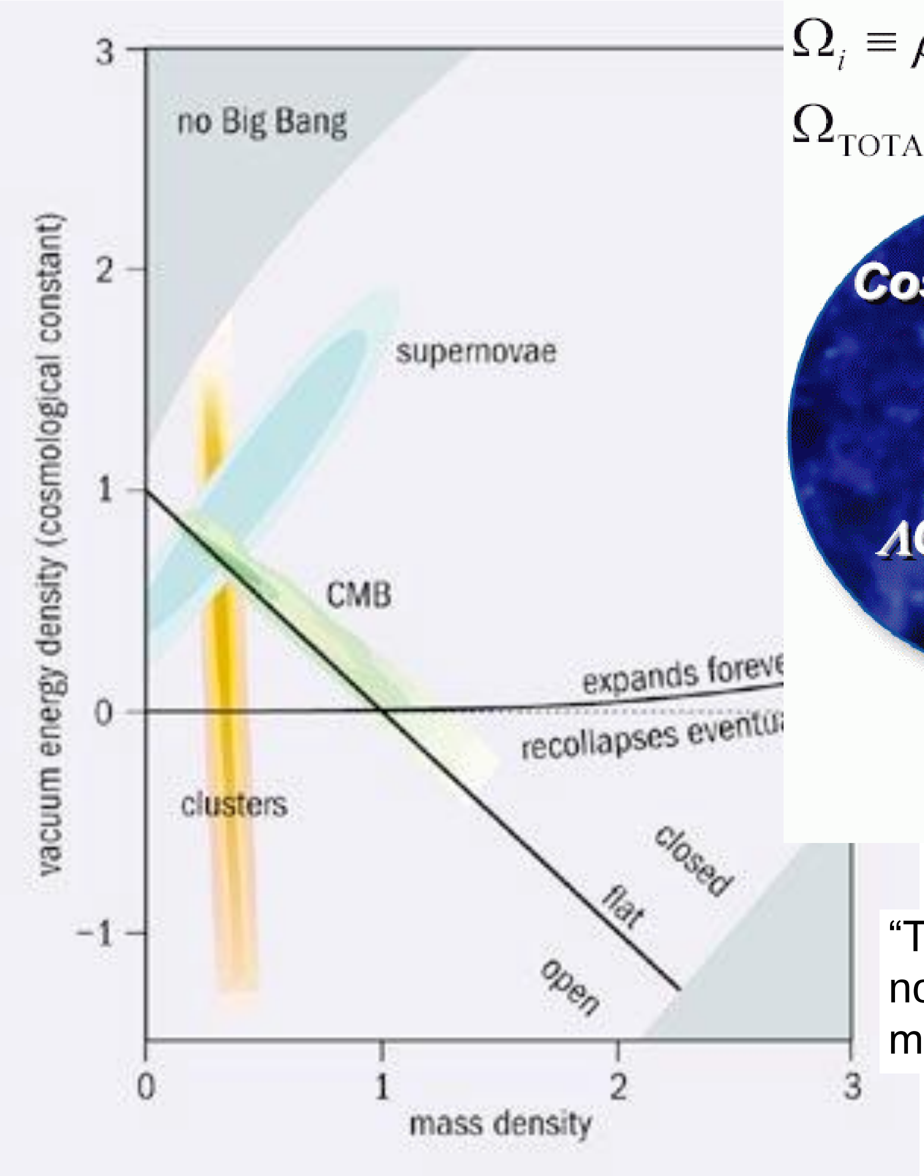

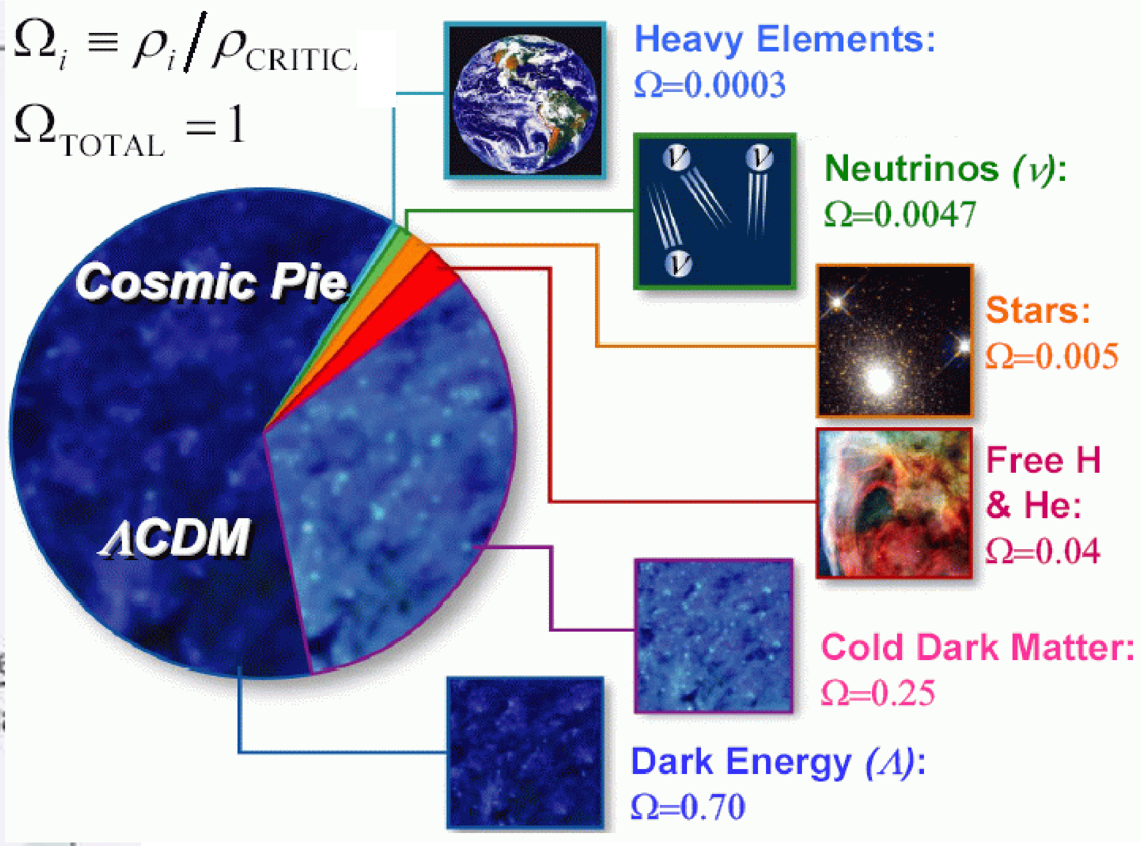

"The last Copernican revolution. (...) Not only we are not at the center of the universe, we are not even made of the stuff most of the universe is made of."
B. Sadoulet

Friedmann-Lemaître Equations

Assuming for simplicity a flat universe, the Friedmann-Lemaître equations can be used to obtain:

$$\frac{d\rho}{da} = -3\,(1+w)\,\frac{\rho}{a}$$

so, for w = const, one has

$$\rho = \rho_0\, a^{-3(1+w)}$$

where 0 means now, and $a_0 = 1$

Defining now $H = \dot{a}/a$ and $\rho_c = 3H_0^2/8\pi G$, one can cast the second Friedmann-Lemaître equation as:

$$H^2(a) = H^2_0\ [\wedge_M\, a^{-3} + \wedge_R\, a^{-4} + \wedge_{DE}\, a^{-3(1+w)}]$$

matter radiation dark energy

$\wedge_i = \rangle^0{}_i / \rangle_c$ (density now). We assume flat universe, constant w

It is easy to see that $\wedge_M + \wedge_R + \wedge_{DE} = 1 + | \ / R^2 H^2_0 = 1$ (flat)

Measuring the history of the expansion rate, $H(a)$, we can learn about the universe constituents: $\wedge_M$, $\wedge_{DE}$, w, etc.

Friedmann-Lemaître Equations

Assuming for simplicity a flat universe, the Friedmann-Lemaître equations can be used to obtain:

$$\frac{d\rho}{da} = -3\,(1+w)\,\frac{\rho}{a}$$ so, for w = const, one has

$$\rho = \rho_0\, a^{-3(1+w)}$$ where 0 means now, and $a_0 = 1$

Defining now $H = \dot{a}/a$ and $\rho_c = 3H_0^2/8\pi G$, one can cast the second Friedmann-Lemaître equation as:

$$H^2(a) = H^2_0\ [\wedge_M\, a^{-3} + \wedge_R\, a^{-4} + (1-\wedge_M-\wedge_R)\, a^{-3(1+w)}]$$

now

matter radiation dark energy

$\wedge_i = \rangle\, ^0{}_i / \rangle\, _c$ (density now). We assume flat universe, constant w

It is easy to see that $\wedge_M + \wedge_R + \wedge_{DE} = 1 + | \ / R^2 H^2_0 = 1$ (flat)

Measuring the history of the expansion rate, $H(a)$, we can learn about the universe constituents: $\wedge_M$, $\wedge_{DE}$, w, etc.

Distances

The co-moving distance between a source at *z* and us can be computed as:

$$r(z) = \int_0^r dr = \int_{t_e}^{t_0} \frac{dt}{a(t)} = \int_{a_e}^{1} \frac{da}{a\dot{a}} = \int_0^z \frac{dz'}{H(z')}$$

so, it gives us integrals of $1/H(z)$.

Several distances can be measured observationally:

– Luminosity distance: if we have a "standard candle" with luminosity *L*, we define d_L such that the measured flux is √ = L / 4□d_L^2. It is easy to see that $d_L(z) = S_|$ $(r(z))$ $(1+z) = r(z)$ $(1+z)$ (flat).

– Angular distance: if we have a "standard ruler" with length l, we define d_A such that the measured angle subtended by l is ⊗⟨ = l / d_A. It is easy to see that $d_A(z) = S_|$ $(r(z))$ / $(1+z) = r(z)$ / $(1+z)$ (flat).

So by having a collection of either standard candles or standard rulers at different known redshifts, we will have many integrals of $1/H(z)$, from where one can reconstruct $H(z)$ and, hence, $\wedge_M$,$\wedge_{DE}$,*w*, etc.

Probes of Dark Energy

- Geometric tests

Standard Candles	Type-Ia SNe	Luminosity distance	$d_L(z) = r(z)\,(1+z)$
Standard Rulers	BAO	Angular distance	$d_A(z) = r(z) \,/\, (1+z)$
Standard Population	Clusters	Volume Element	$\mathrm{d}V \,/\, \mathrm{d}z\mathrm{d}\wedge = r^2(z) \,/\, H(z)$

- Tests based on growth of structure

The rate of the growth of structure in the universe depends on the expansion:

Weak Lensing, Clusters
(also probe geometry)

$$\ddot{\delta} + 2H\dot{\delta} - \frac{3}{2}\Omega_m H^2 \delta = 0$$

$$\delta = \frac{\rho_m - \bar{\rho}_m}{\rho_m}$$

Probing Dark Energy with Type-Ia SNe

- Standard candles provide a measurement of the luminosity distance as a function of redshift:

$$\phi = L / 4\pi d_L^2$$

$$d_L(z) = (1+z) \times r(z)$$

$$r(z) = \int_0^z \frac{dz'}{H(z')}$$

(geometric test of dark energy)

ϕ : flux

L : intrinsic luminosity

d_L : luminosity distance

$r(z)$: co-moving distance

- Astronomers measure the apparent magnitude and redshift:

$$\boxed{m(z) = -2.5\log_{10}(\phi/\phi_0) = \mathcal{M} + 5\log_{10}[H_0 d_L(z)]}$$

$$\mathcal{M} \equiv M + 25 - 5\log_{10}[H_0 / 100 \mathrm{km\,s^{-1} Mpc^{-1}}]$$

- M is the (assumed unknown) absolute magnitude of a type-Ia SN.
- $H_0\, d_L$ does NOT depend on H_0

Type-Ia Supernovae (I)

- Defined empirically as supernovae without Hydrogen but with Silicon in spectrum.
- Progenitor understood as a white dwarf accreting material from a binary companion.
- As the white dwarf approaches Chandrasekhar mass, a thermonuclear runaway is triggered.
- A naturally triggered and standard bomb.

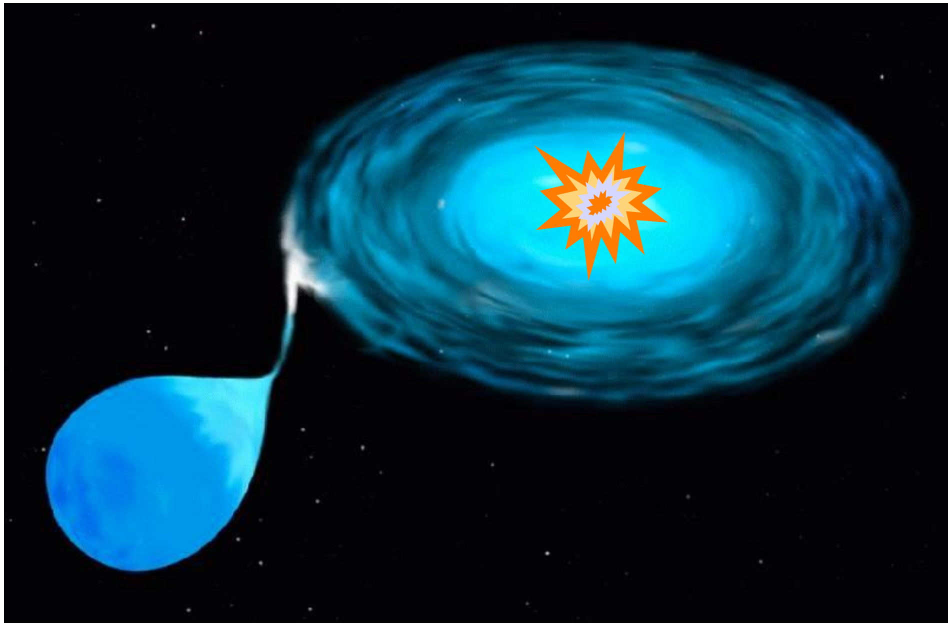

Type-Ia Supernovae (II)

- General properties:
  - Homogeneous class of events: luminosity, color, spectrum at maximum light. Only small (correlated) variations
  - Rise time: ~ 15 – 20 days
  - Decay time: ~ 2 months
  - Bright: M_B ~ –19.5 at peak

- No hydrogen in the spectra:
  - Early spectra: Si, Ca, Mg, ...(absorption)
  - Late spectra: Fe, Ni,…(emission)

- SN Ia found in all types of galaxies, including ellipticals
  - Progenitor systems must have long lifetimes

Discovering Supernovae

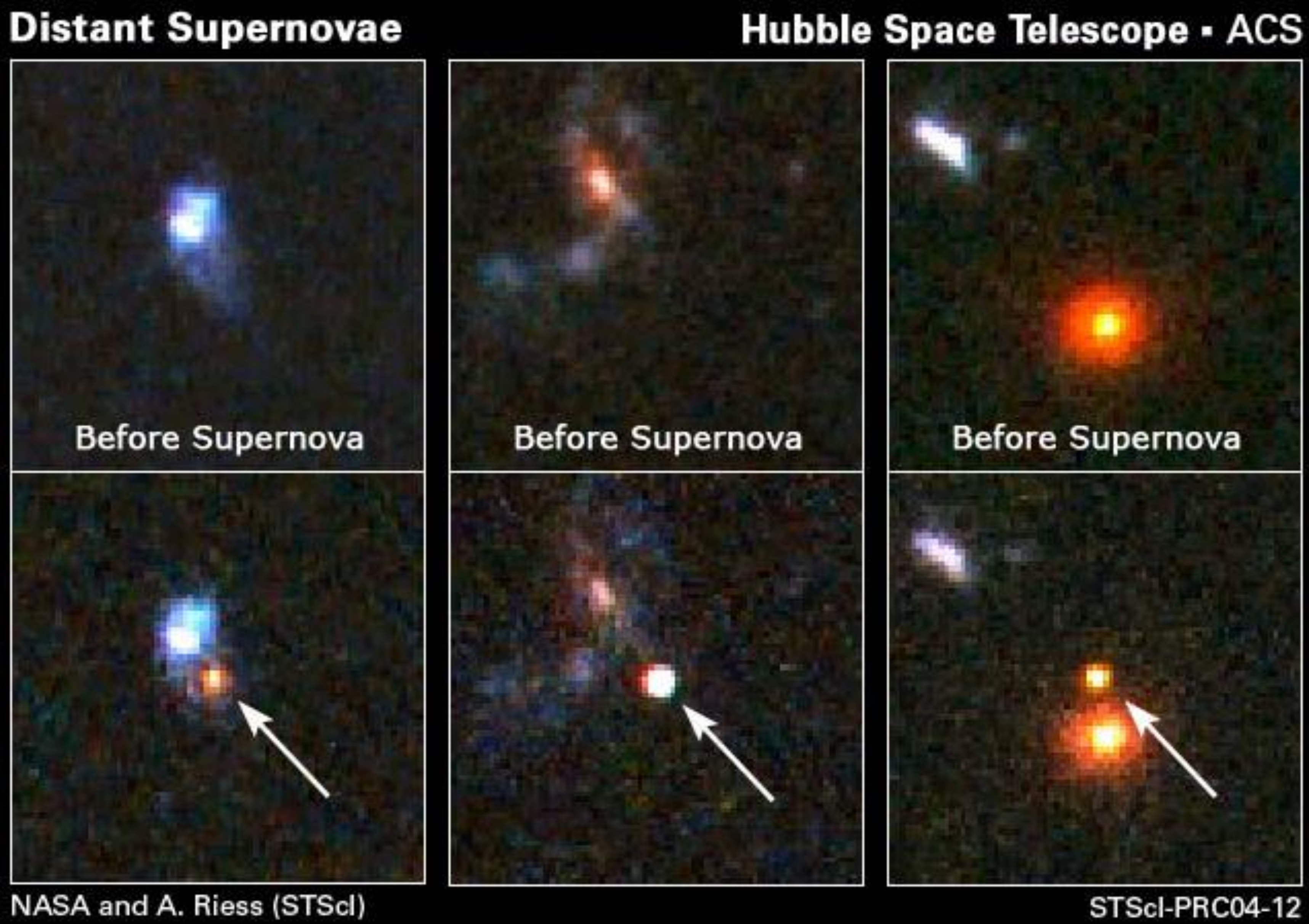

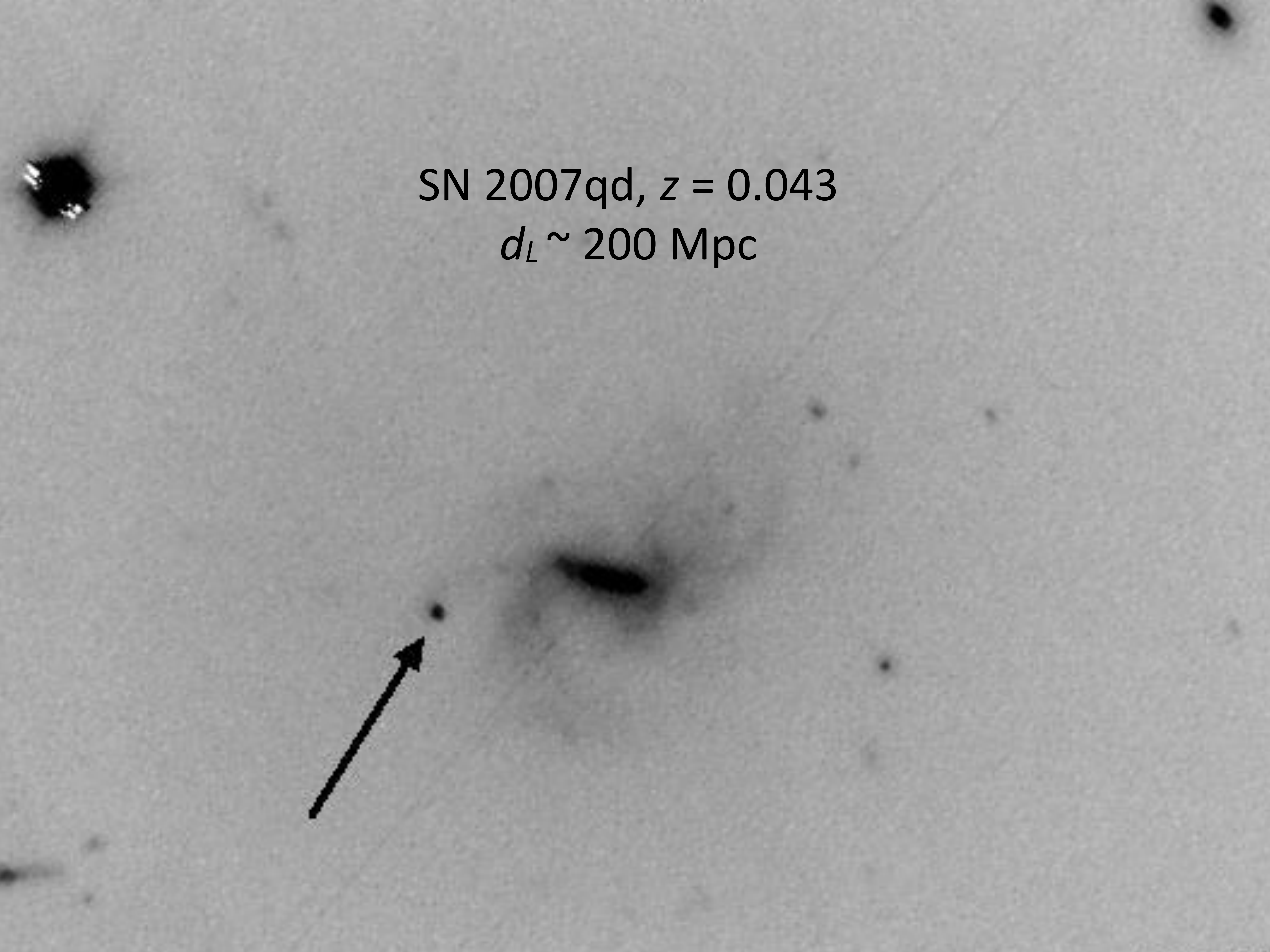
SN 2007qd, z = 0.043
d_L ~ 200 Mpc

Are Type-Ia SNe Standard Candles?

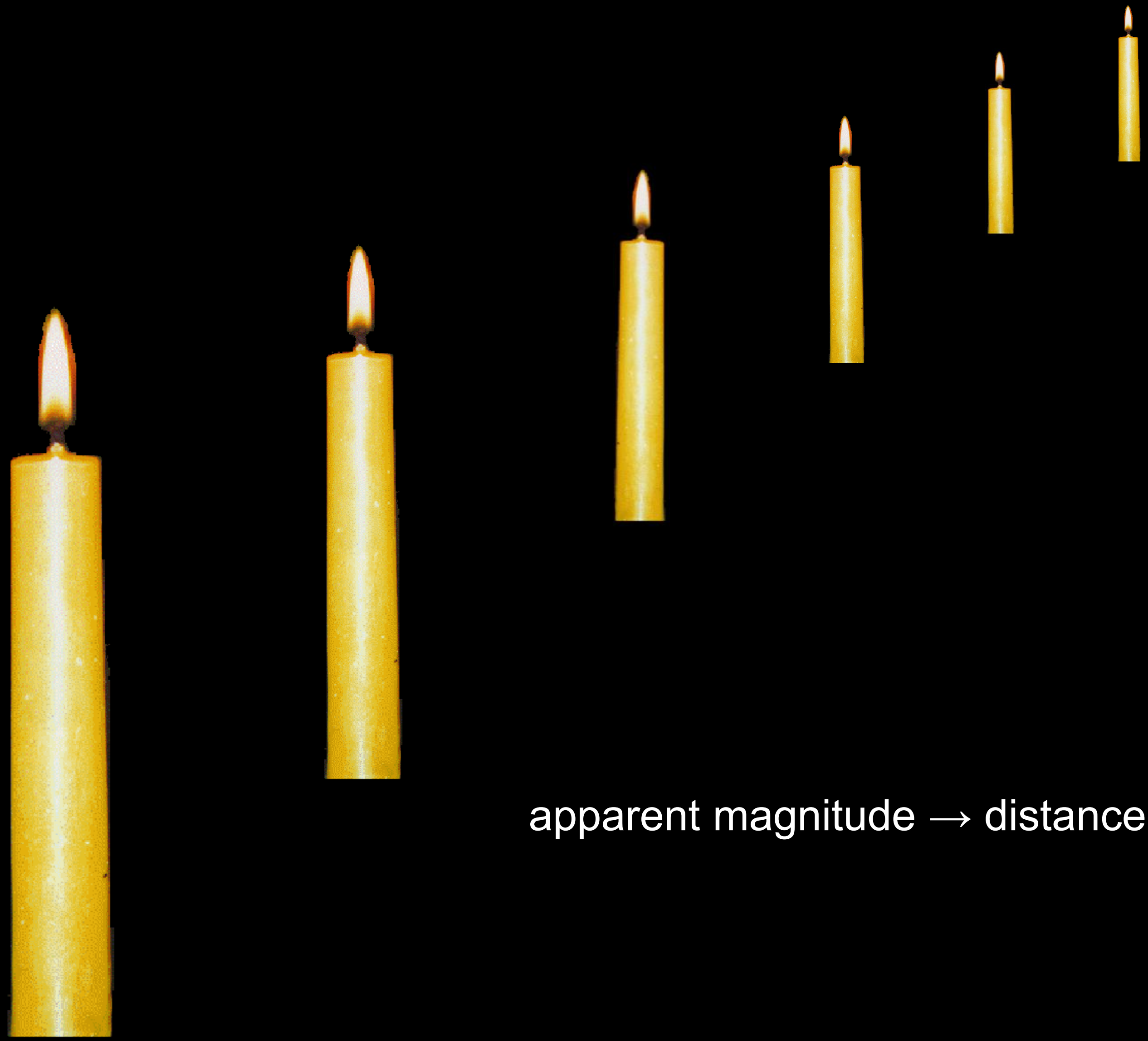

apparent magnitude → distance → time

Type-Ia SNe as Standardizable Candles

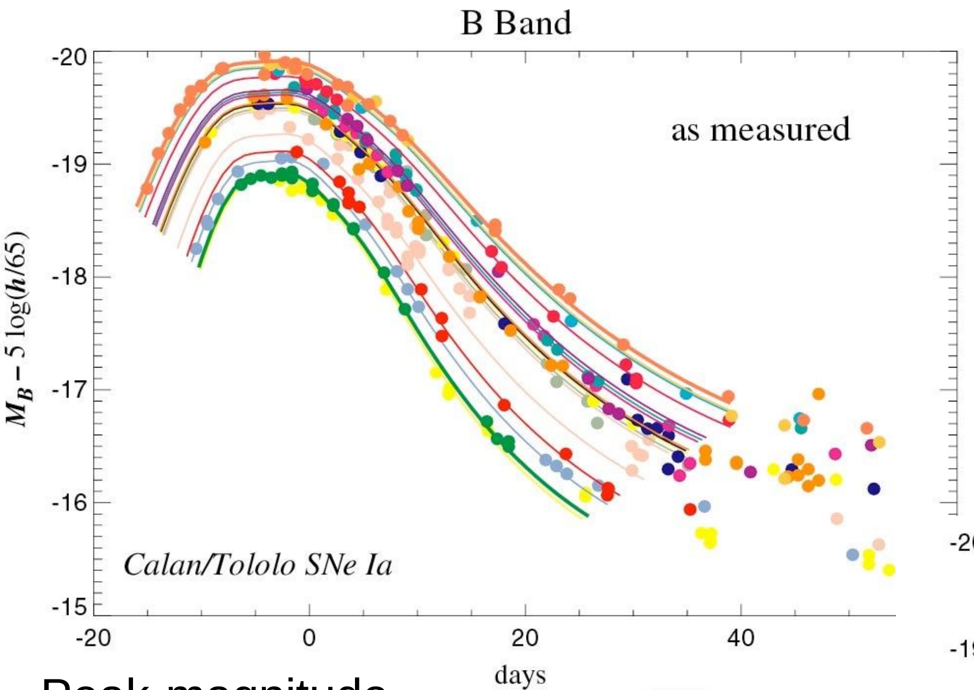

- Nearby (z < 0.1) supernovae used to study SNe light curves
- Brightness not quite standard
- Intrinsically brighter SNe last longer
- Correction needed

Peak-magnitude dispersion of 0.25 – 0.30 mag

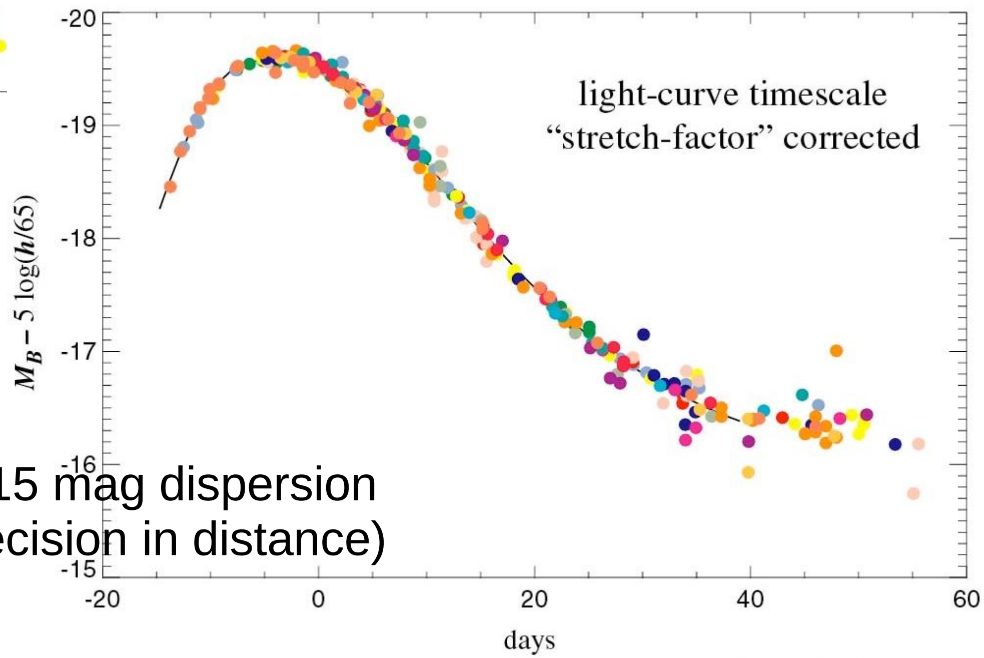

- After correction, standard candles in optical region (at least).

~ 0.10 – 0.15 mag dispersion (5 – 7% precision in distance)

Kim, *et al.* (1997)

SNLS Light Curves After Stretch Correction

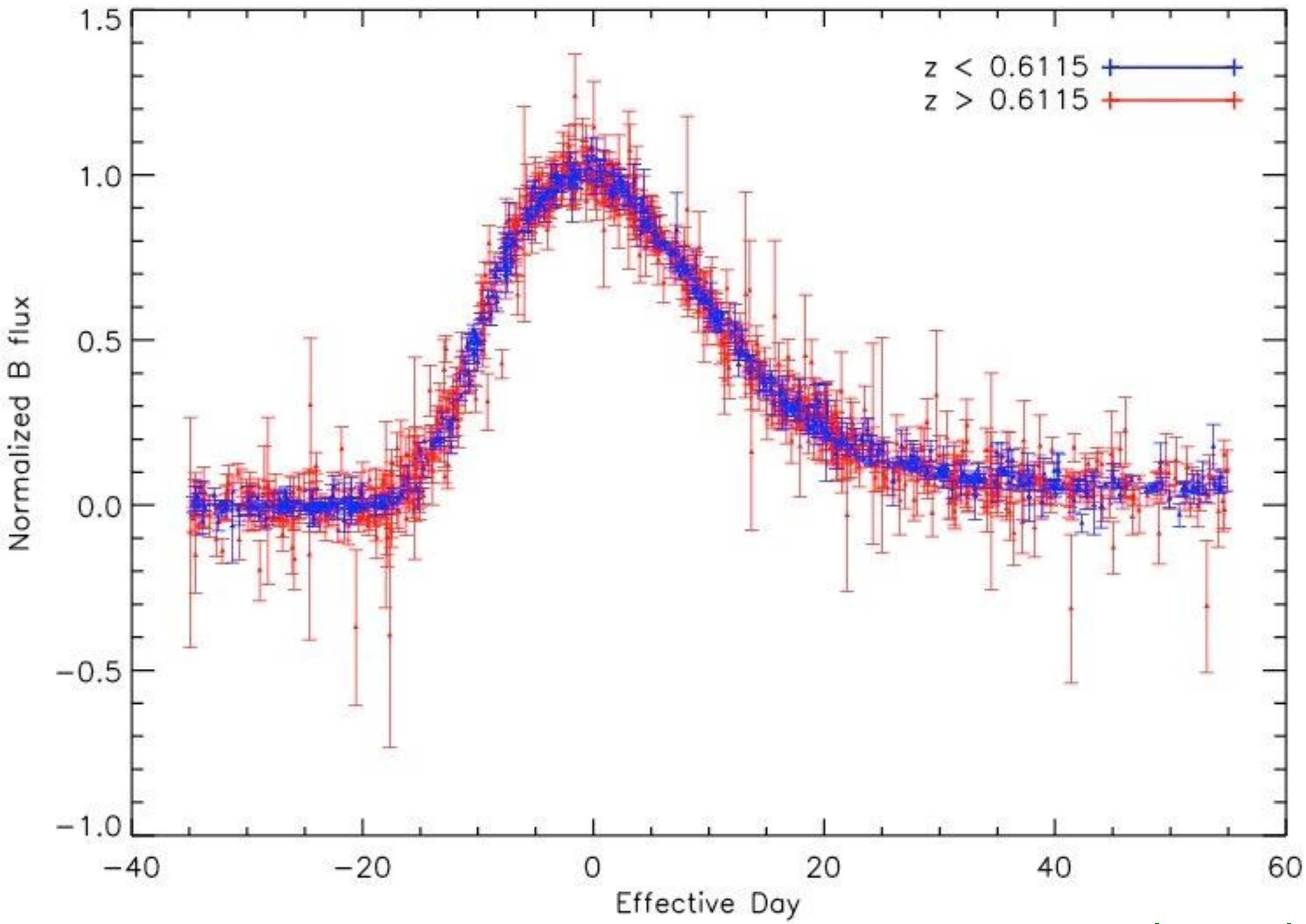

Conley et al. 2006

Type-Ia SN Spectral Features

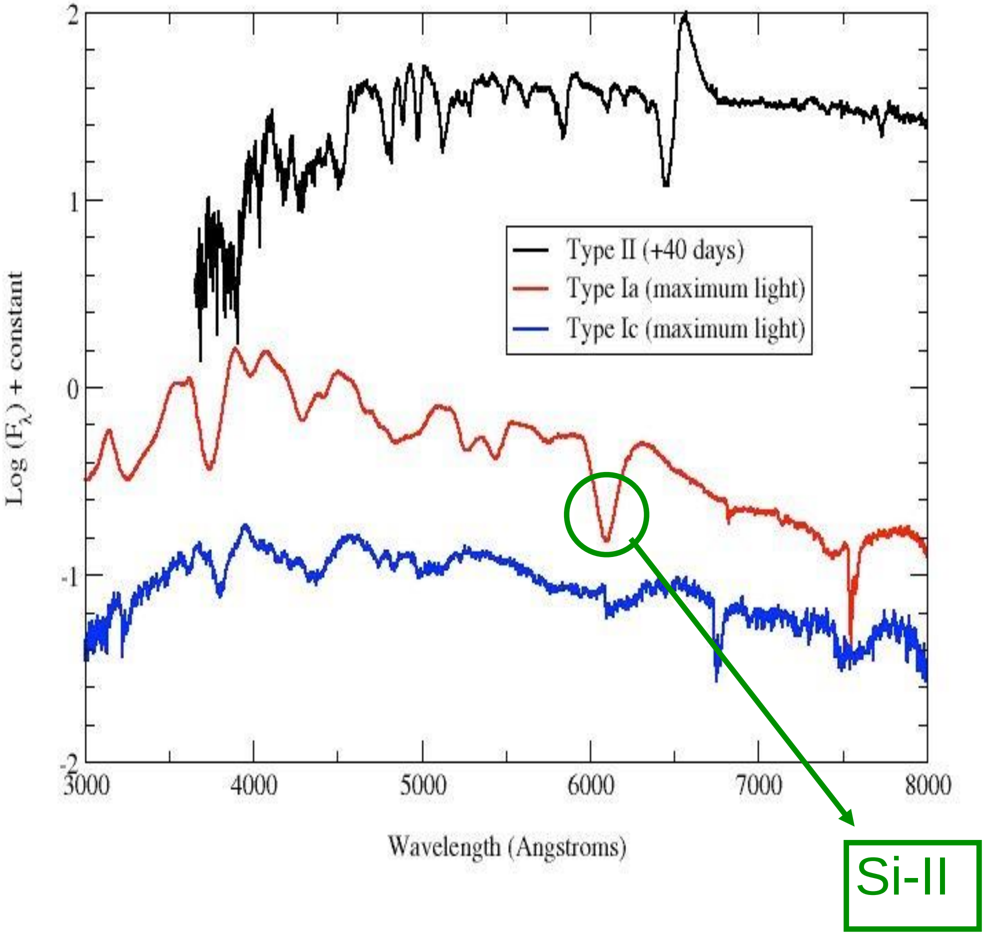

- **Spectra at near maximum light are used to determine type of SN (Si-II feature)**
- **And to measure the redshift, z, by observing the shift in the spectrum**

SN Analysis

Light Curves

Images

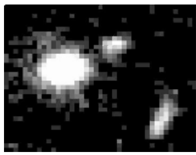

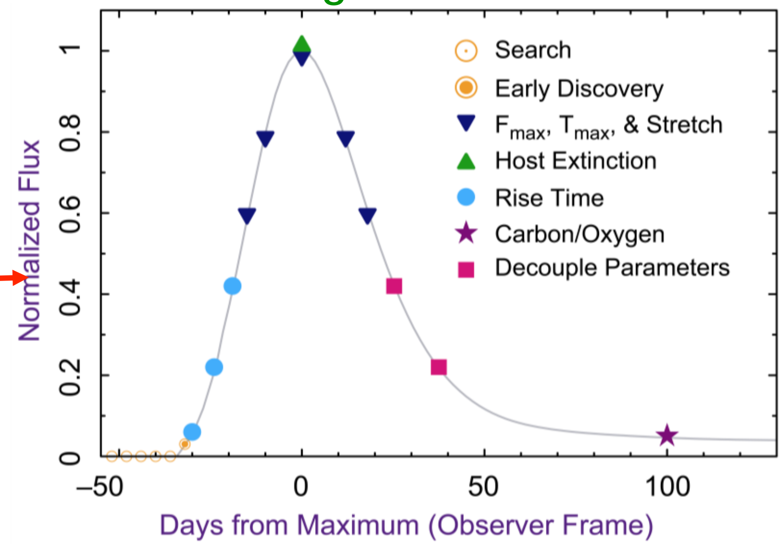

Redshift & spectral properties

Λ_M and w

Spectra

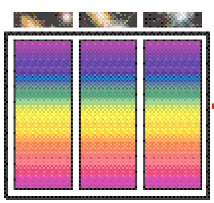

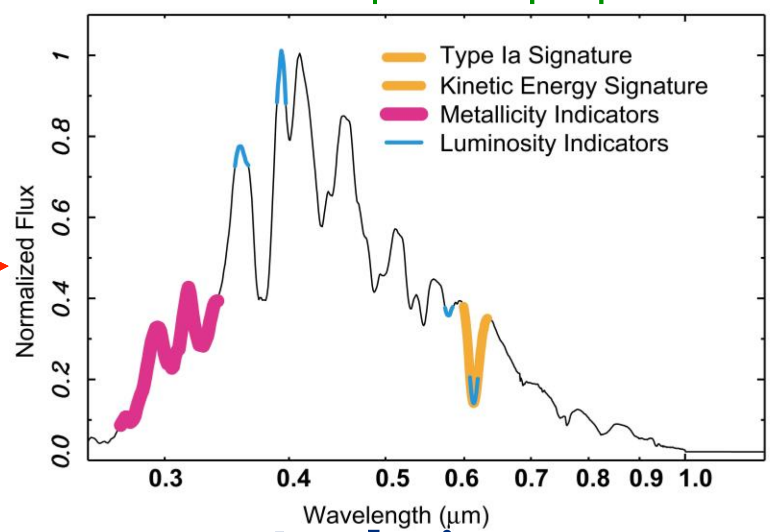

Data → **Analysis** → **Science**

Hubble Diagram

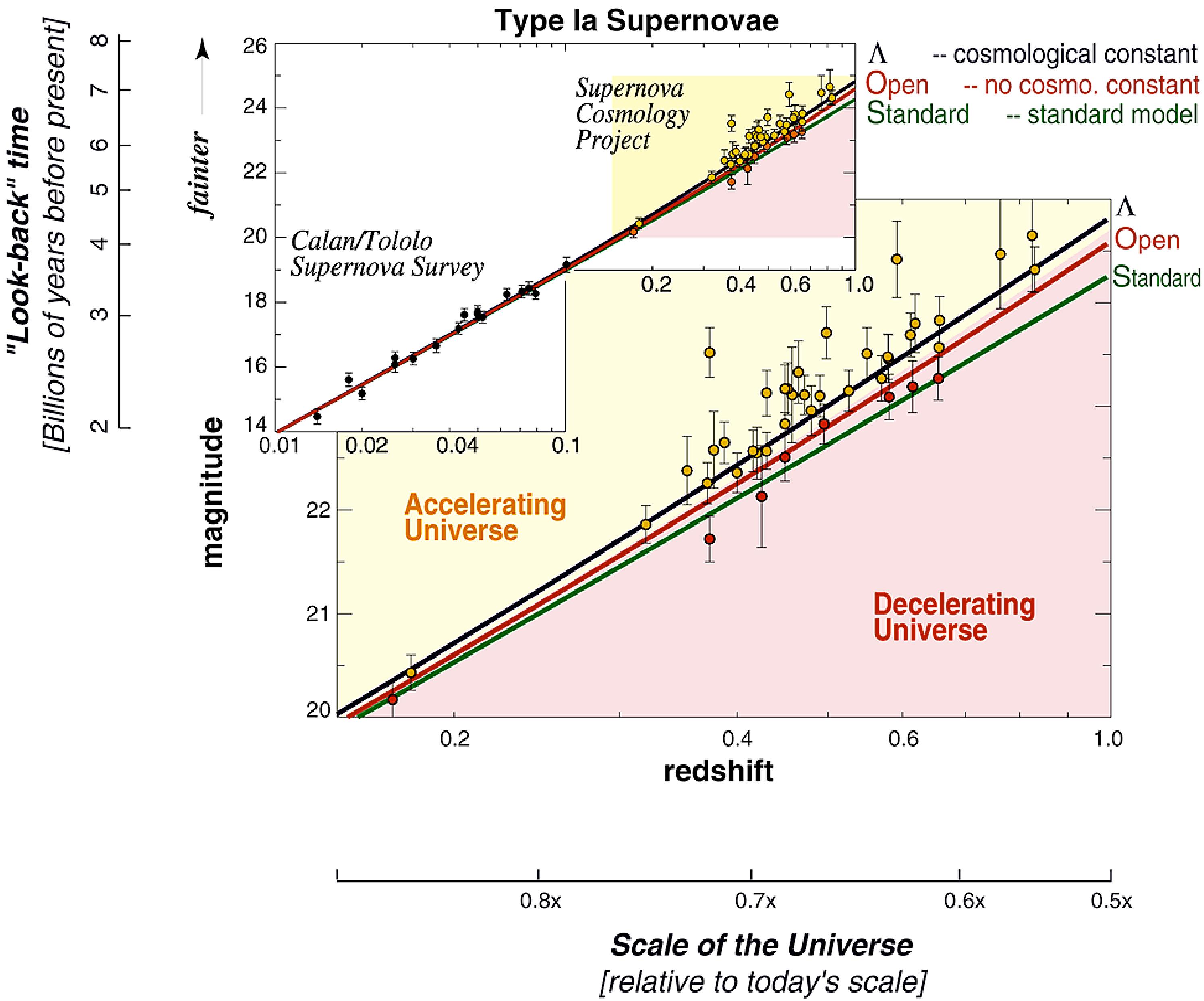

Hubble Diagram

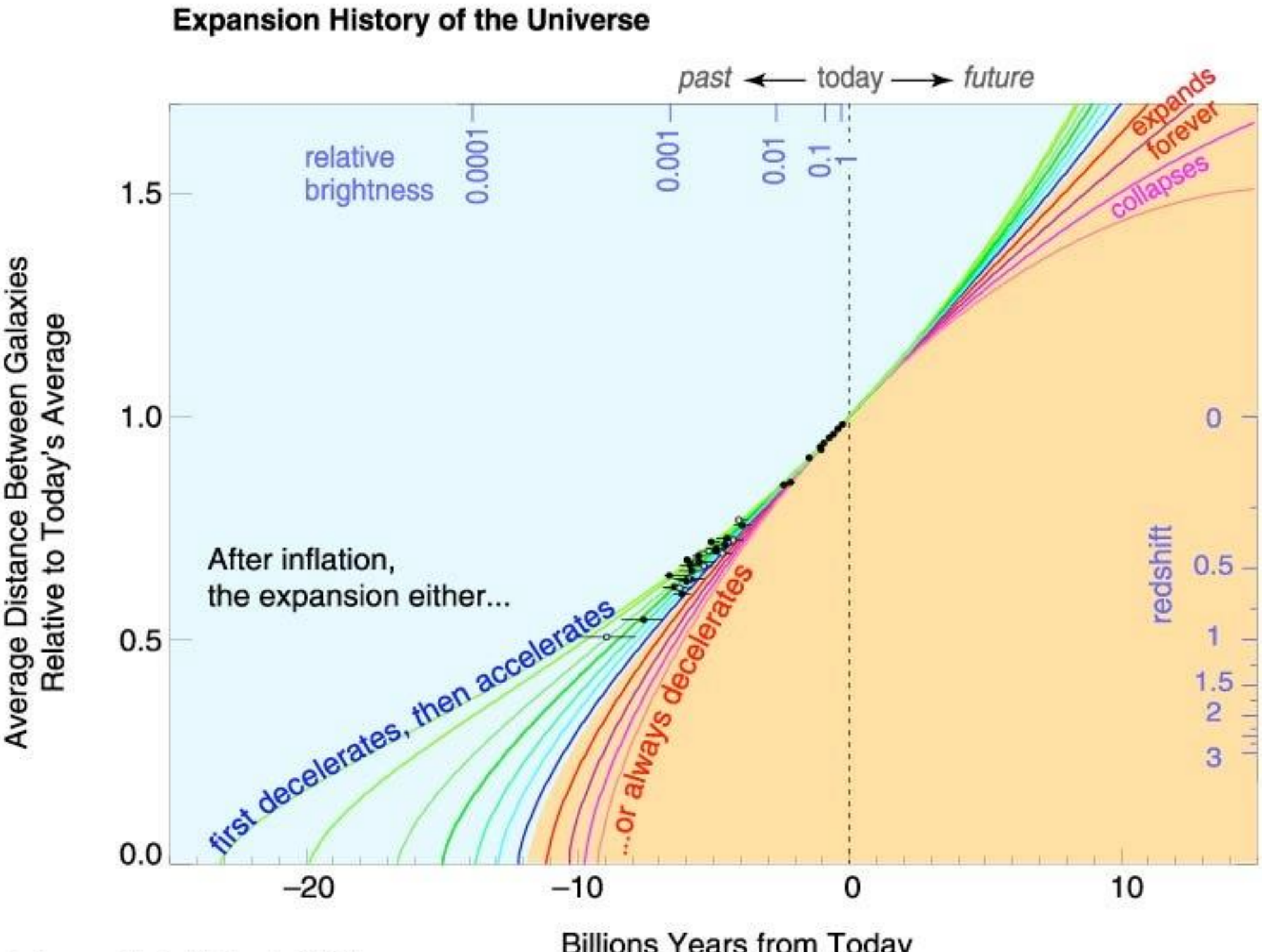

Perlmutter, Physics Today, April 2003

Discovery of Acceleration

Supernova Cosmology Project
Perlmutter *et al.* (1999)

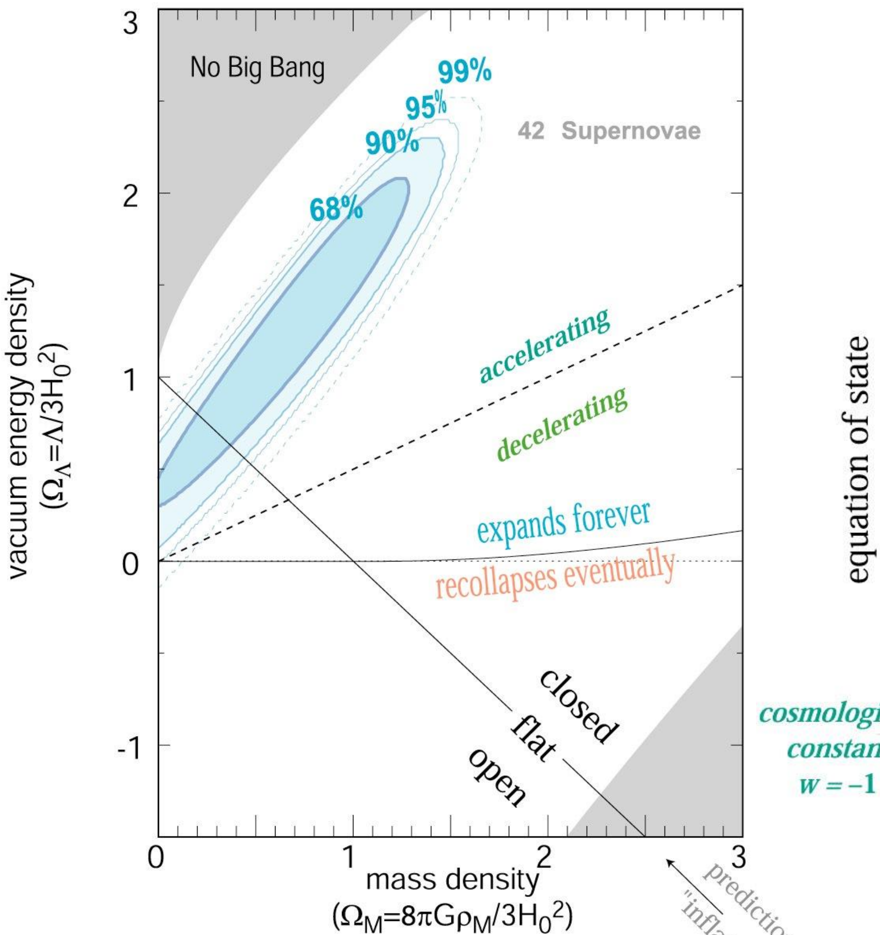

Two groups results agree:
c.f. Riess *et al.* (1998)

Supernova Cosmology Project
Perlmutter *et al.* (1999)

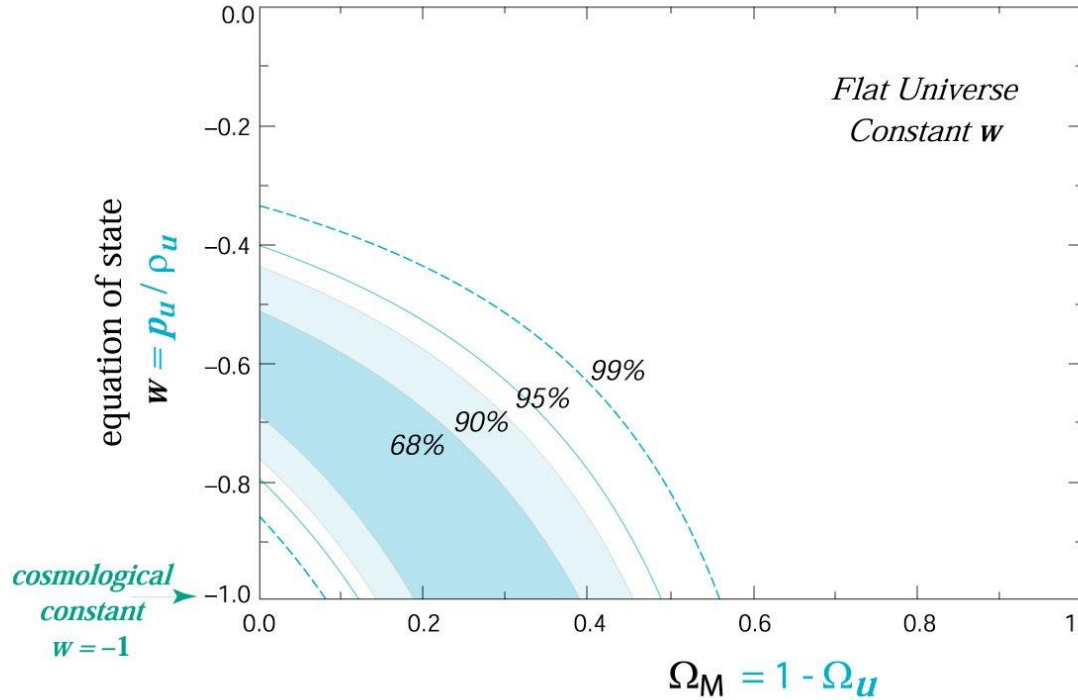

Systematic Errors

- Statistical error is dominated by intrinsic SN peak magnitude dispersion $\int_{\text{int}}$ = 0.10–0.15

- Many systematic errors will be totally correlated for SNe at similar redshifts
  - Current and near-future surveys will have *O*(100) SNe for ⊗z = 0.1 redshift bin.

  - Therefore, systematic errors of order $\int_{\text{int}}/\sqrt{N_{SN}}$ = 0.01–0.02 will already become important or even dominant.

Sources of Systematic Errors

Error Source	Control
Host-galaxy dust extinction*	Wavelength-dependent absorption identified with *high S/N multi-band photometry*.
Supernova evolution*	Supernova sub-classified with *high S/N light curves and peak-brightness spectrum*.
Flux calibration error*	Program to construct a set of *1% error flux standard stars.*
Malmquist bias	Supernova discovered early with *high S/N multi-band photometry*.
K-corrections*	Construction of a *library of supernova spectra*.
Gravitational lensing	Measure the average flux for a *large number of supernovae in each redshift bin*.
Non-Type-Ia contamination	Classification of each event with a *peak-brightness spectrum*.

Kim, Linder, Miquel, Mostek, MNRAS 347 (2004) 909

Extinction by Dust

Dust in the path between the SN and the telescope attenuates the amount of light measured

- **Milky Way dust is well measured and understood**
  6956 citations
  (Schlegel, Finkbeiner & Davis 1998)
- Host galaxy extinction leads to reddening of supernova colors:

$$A_V = R_V \cdot E(B\text{-}V)$$

A_V : increase in magnitude in V band
$E(B\text{-}V)$: excess in $B\text{-}V$ color over expected
R_V ≈ 3.1 in nearby galaxies

- **In another band *j*, the extinction is** (Cardelli, Clayton & Mathis 1989) 3709 citations

known

$$m_j \to m_j + A_V \cdot \left(a(\lambda_j) + \frac{b(\lambda_j)}{R_V} \right) = m_j + E(B-V) \cdot (R_V \cdot a(\lambda_j) + b(\lambda_j))$$

(≈ 0-0.10)

What is the value of R_V in distant galaxies?

Dust Biases

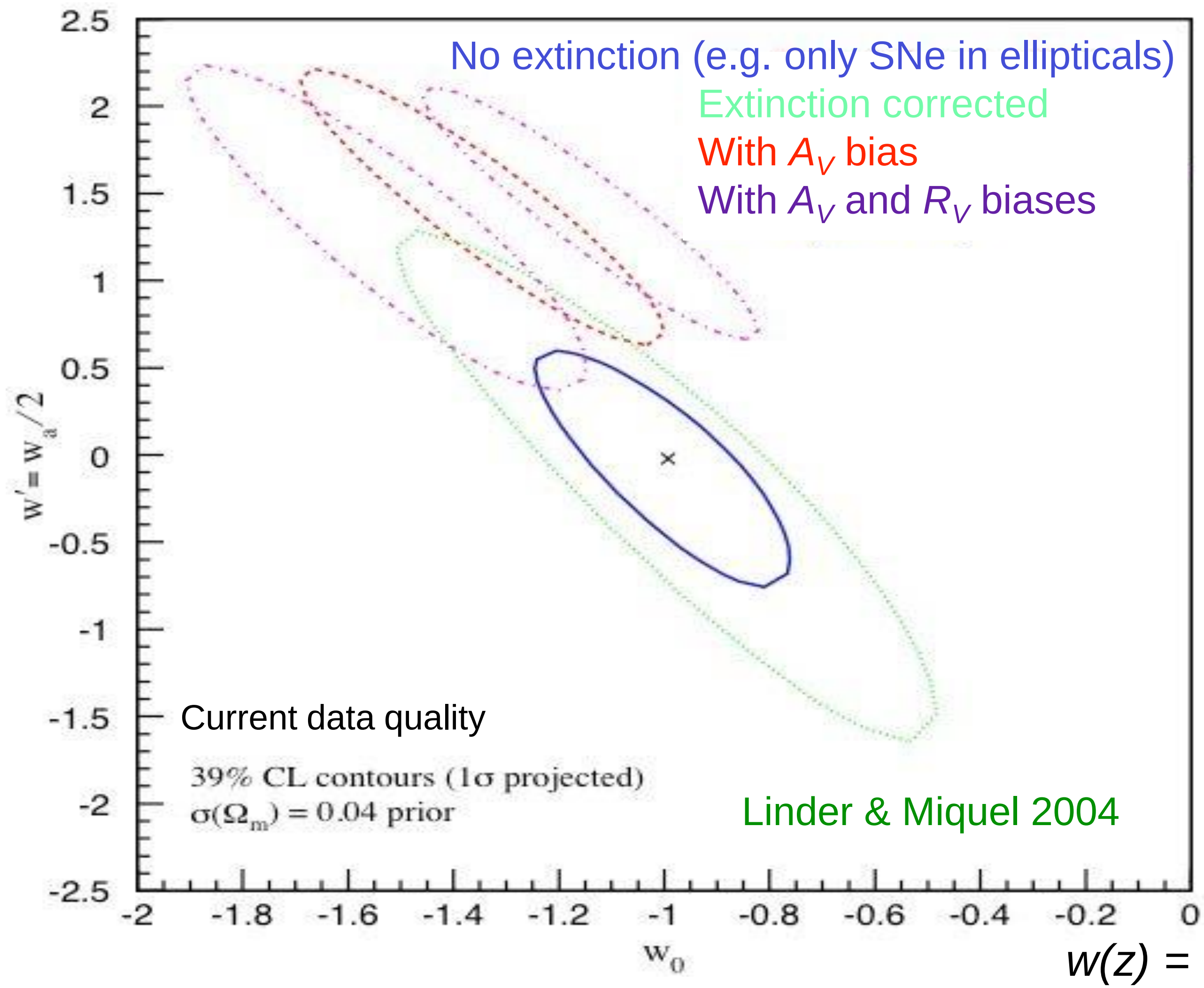

$w(z) = w_0 + (1\text{-}a)\, w_a$

Near-Optical Bands

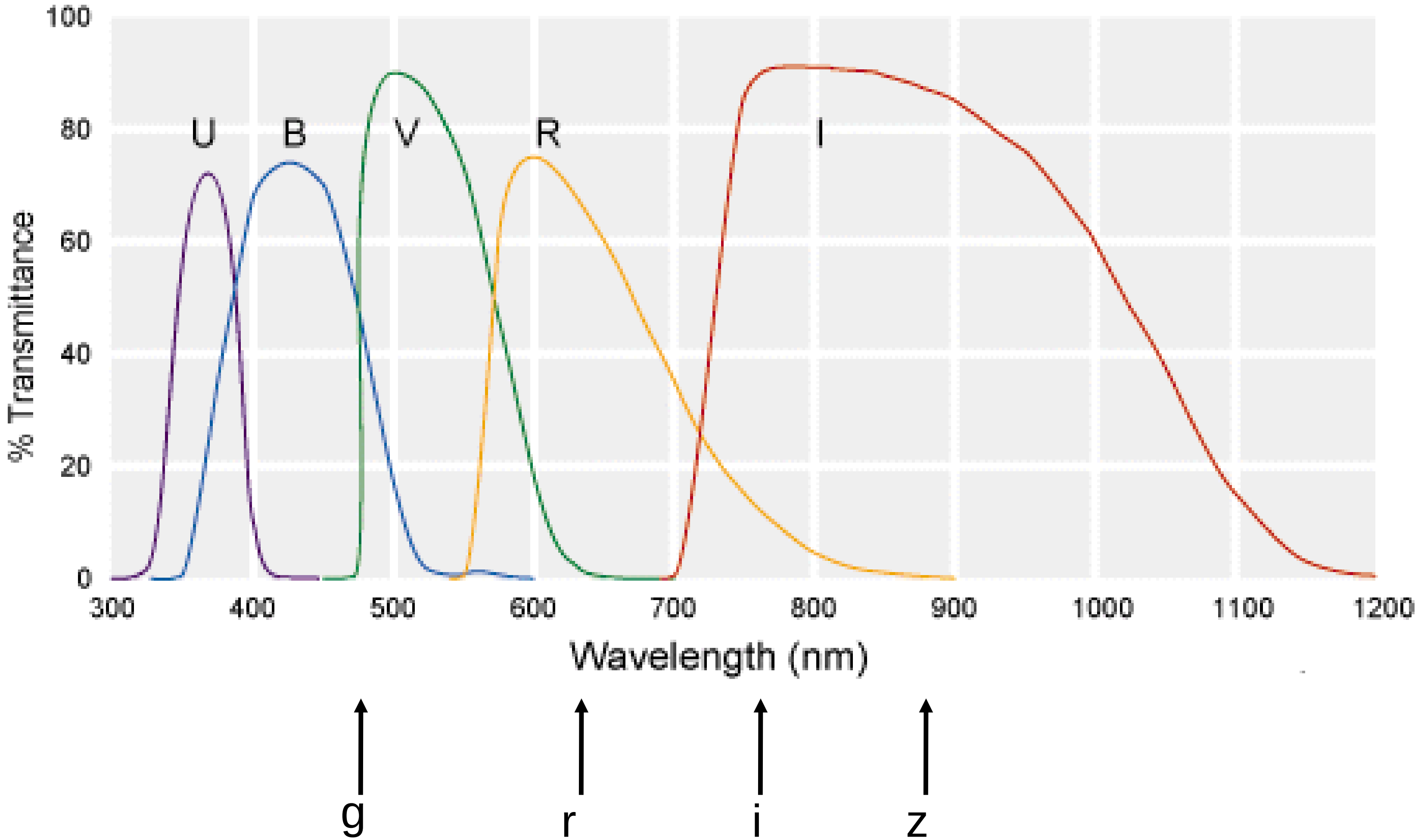

Near-Optical Bands

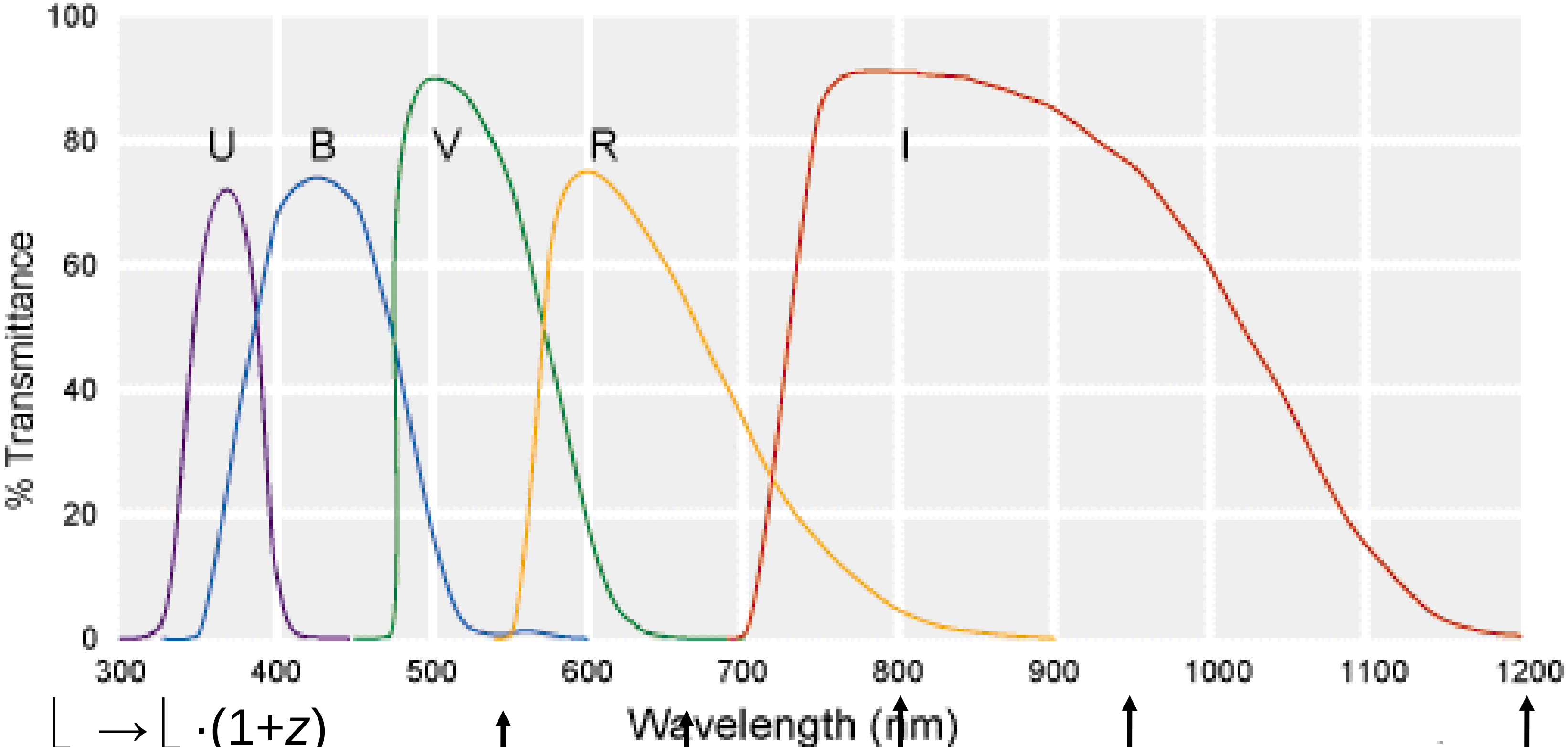

$\lambda \rightarrow \lambda \cdot (1+z)$

z = 0.5 U B V R I

z = 1.0 U B V R

K-corrections

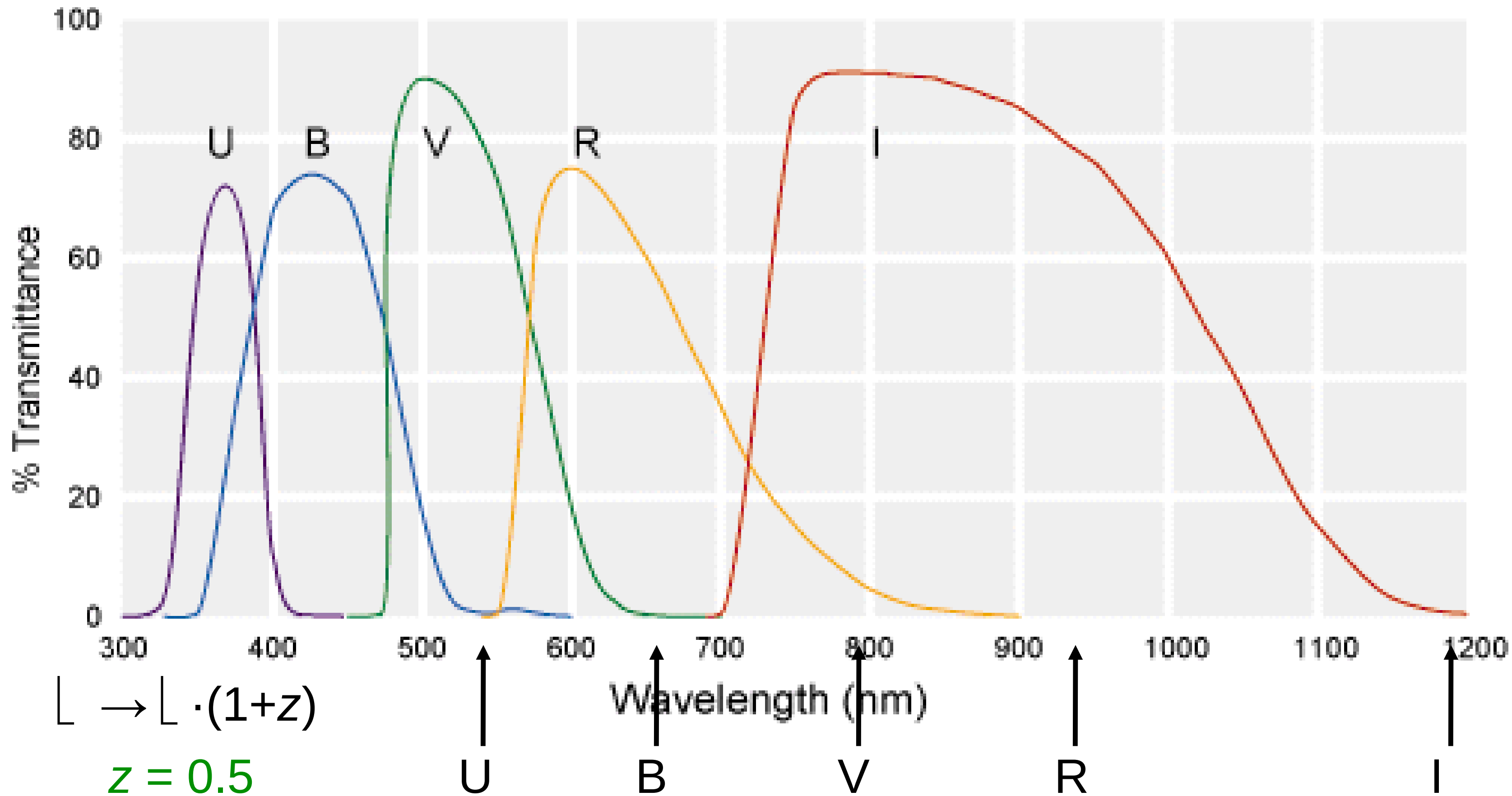

- At high z, one needs to relate measured fluxes in, say, R, I, z filters with fluxes in SN rest frame B, V, R bands.

$$K_{BR} = -2.5\log_{10}\left(\frac{\int d\lambda \phi_0(\lambda) T_B(\lambda)}{\int d\lambda \phi_0(\lambda) T_R(\lambda)}\right) + 2.5\log_{10}\left(\frac{\int d\lambda \phi_{SN}(\lambda) T_B(\lambda)}{\int d\lambda' \phi_{SN}(\lambda') T_R(\lambda'(1+z))}\right) \approx O(0.5 \text{ mag})$$

- Good empirical model for SN spectrum from B to z is needed.

Calibration

- Calibration ≡ determining the "zero-points" $)_{0,j}$ of each filter *j*
- Overall normalization is irrelevant
- Relative filter-to-filter normalization is crucial (K-corrections, dust-extinction corrections)

Standard procedure uses well-understood stars to get $\int_{cal} = 0.01$ at best

Alternative procedure using also SN data themselves achieves a large degree of self-calibration (Kim & Miquel 2006)

Example for SNF + "SNAP" (300 + 2000 SNe up to z = 1.7)

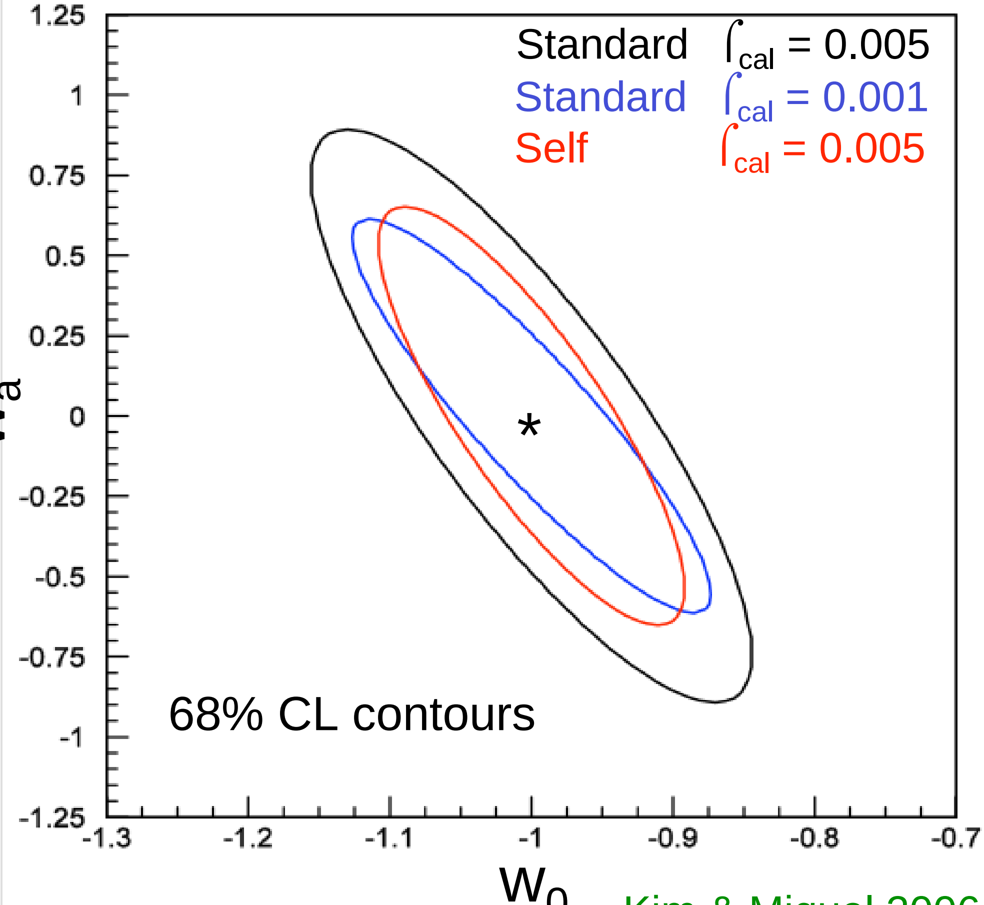

Kim & Miquel 2006

Current Cosmological Results from SNe

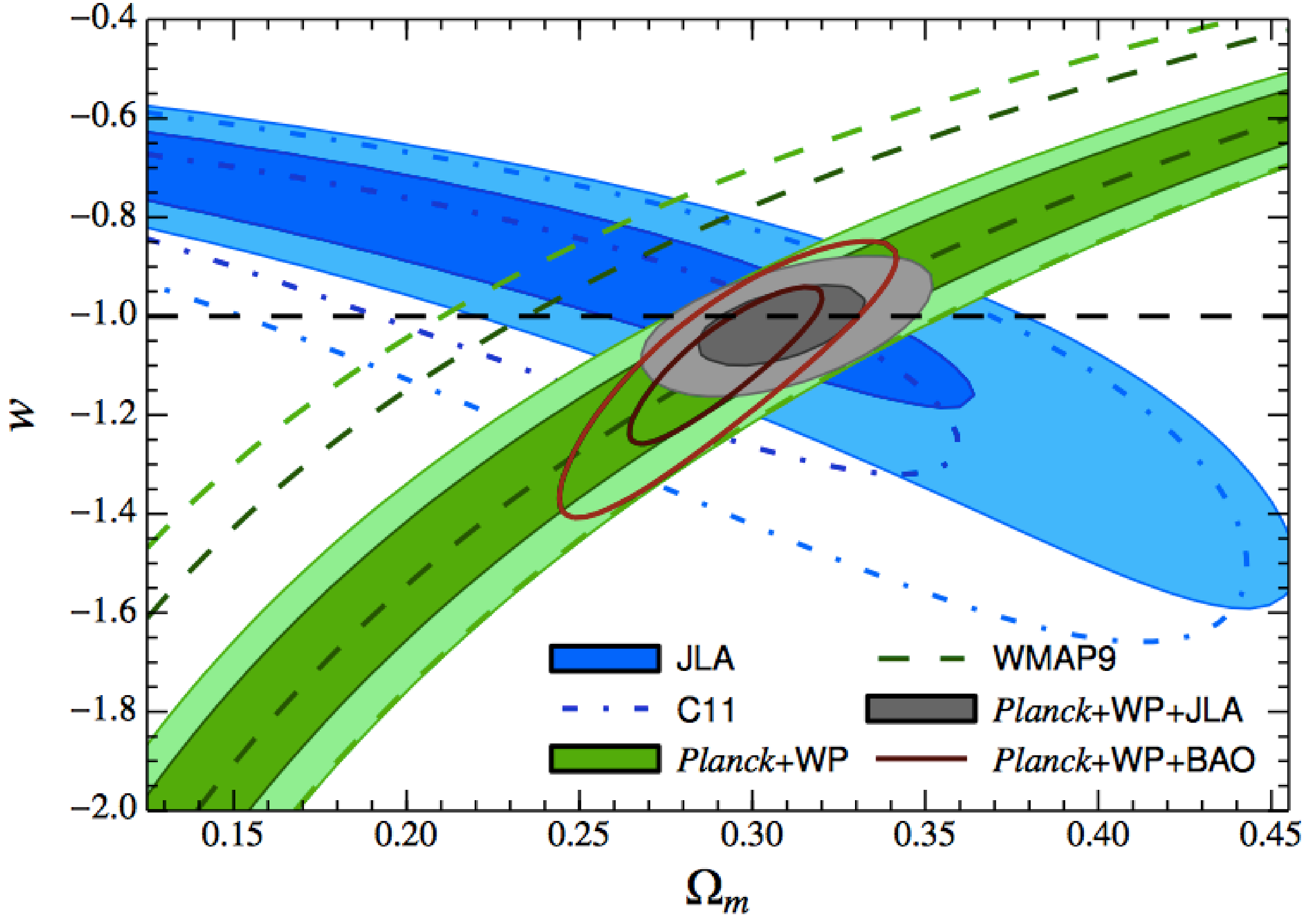

Betoule et al. (SNLS+SDSS-II/SNe), 2014

Summary: Type-Ia Supernovae

- Type-Ia SNe provided the "smoking gun" for acceleration.
- Mature technique still being perfected.
- Control of systematic errors key to future improvements.
- Vigorous current and future program:
  - Low-z from ground: SNF, SDSS-II/SNe, CfA, Carnegie…
  - Medium- to high-z from ground: SNLS, DES, Pan-STARRS, LSST
  - High-z from space: HST, Euclid

Expect more insight on the nature of Dark Energy from type-Ia SNe studies

Large-Scale Structure of the Universe

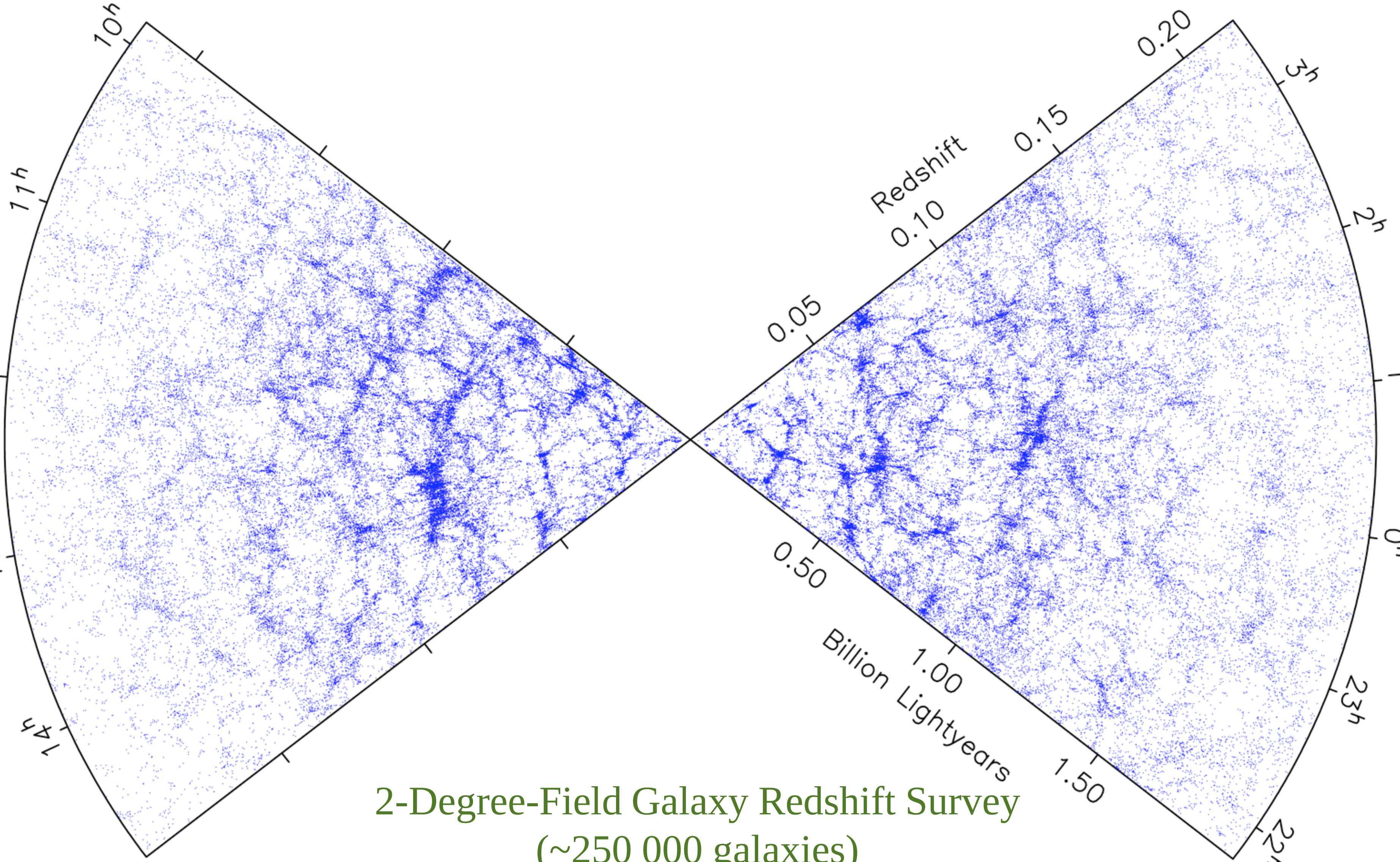

2-Degree-Field Galaxy Redshift Survey
(~250 000 galaxies)

Growth of Structure in the Universe

- Consider a sphere of radius *R* and mass *M*, and add to it a small amount of mass so that $\rho = \bar{\rho}(1+\delta(t))$.
- Then the gravitational acceleration at the edge of the sphere is

$$\ddot{R} = -\frac{GM}{R^2} = -\frac{4\pi}{3} G\bar{\rho}R(1+\delta(t))$$

- Mass conservation throughout the expansion implies that $R(t) \propto \bar{\rho}(t)^{-1/3}\,[1+\delta(t)]^{-1/3}$. Since $\rho(t) = \rho_0 / a^3$, then $R(t) \propto a(t)\,[1+\delta(t)]^{-1/3}$
- Differentiating two times with respect to *t* yields

$$\frac{\ddot{R}}{R} \approx \frac{\ddot{a}}{a} - \frac{\ddot{\delta}}{3} - \frac{2}{3}\frac{\dot{a}}{a}\dot{\delta} \qquad (\delta \ll 1)$$

- Combining the two equations, we get $-\tfrac{4}{3}\pi G\bar{\rho} - \tfrac{4}{3}\pi G\bar{\rho}\delta = \frac{\ddot{a}}{a} - \tfrac{1}{3}\ddot{\delta} - \tfrac{2}{3}\dot{\delta}\frac{\dot{a}}{a}$. And subtracting the equation for $\delta = 0$, we finally get

$$\ddot{\delta} + 2H\dot{\delta} - \tfrac{3}{2}\Omega_m H^2 \delta = 0 \quad \text{with} \quad \Omega_m = \frac{8\pi G\bar{\rho}}{3H^2}$$

Radiation Dominated

$$\ddot{\delta} + 2H\dot{\delta} - \tfrac{3}{2}\Omega_m H^2 \delta = 0$$

- $H = 1/(2t)$ and $\Omega_m \ll 1$, so $\ddot{\delta} + \frac{1}{t}\dot{\delta} \approx 0$
- The solution is $\delta(t) = C_1 + C_2 \ln t$
- Overdensities grow only logarithmically with time. ✗

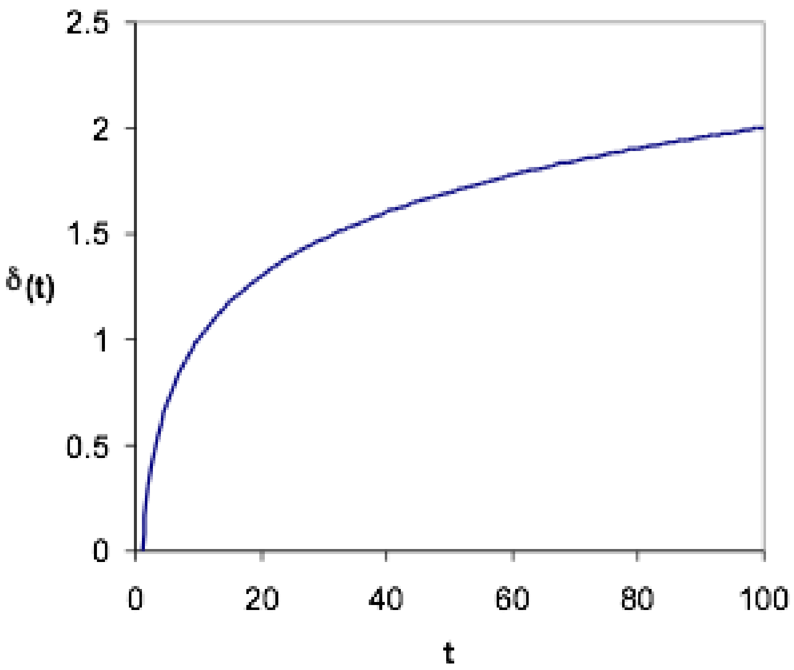

Cosmological Constant Dominated

$$\ddot{\delta} + 2H\dot{\delta} - \tfrac{3}{2}\Omega_m H^2 \delta = 0$$

- $H = H_\Lambda$ and $\Omega_m \ll 1$, so $\ddot{\delta} + 2H_\Lambda \dot{\delta} \approx 0$
- Solution: $\delta(t) = C_1 + C_2 \exp(-2H_\Lambda t)$
- Overdensities decrease with time. ✗

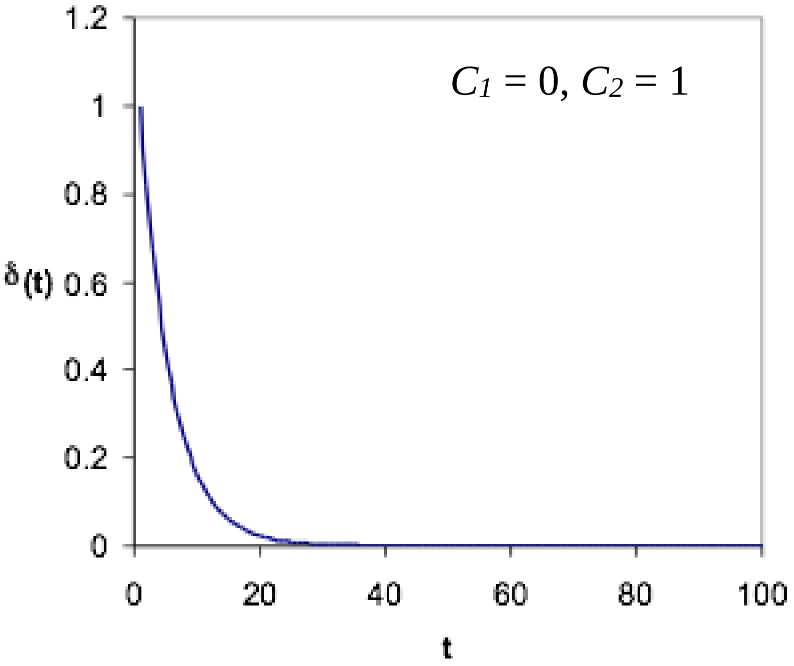

Matter Dominated

$$\ddot{\delta} + 2H\dot{\delta} - \tfrac{3}{2}\Omega_m H^2 \delta = 0$$

- $H = 2/(3t)$ and, for $\Omega_m \sim 1$, we have

$$\ddot{\delta} + \frac{4}{3t}\dot{\delta} - \frac{2}{3t^2}\delta \approx 0$$

- Solution: $\delta(t) = C_1\, t^{-1} + C_2\, t^{2/3}$
- Overdensities grow with time as $\delta(t) \propto t^{2/3} \propto a(t)$ ✔
- Structure formation is only possible in the matter dominated era

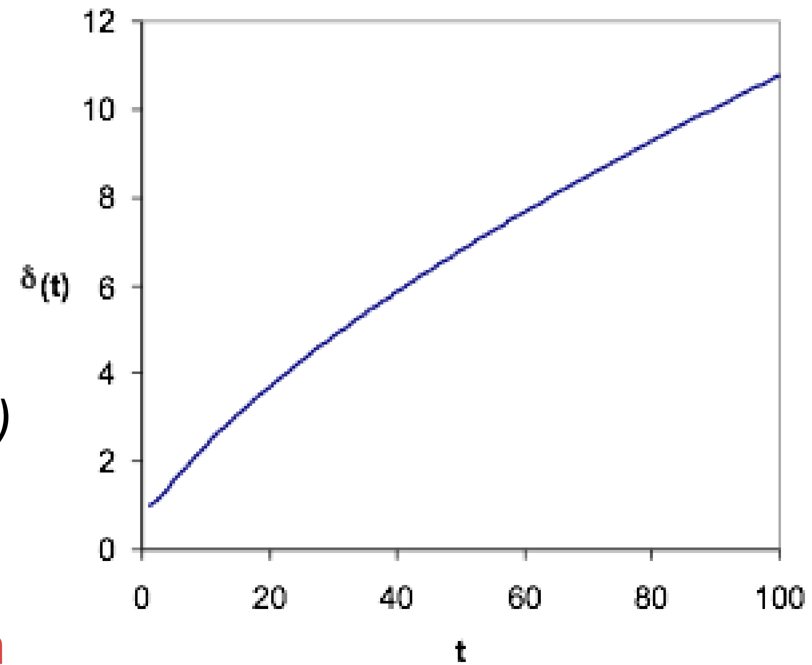

The Jeans Length (1)

- Forgetting the expansion for a moment, we have $\ddot{\delta} = 4\pi G\bar{\rho}\delta$ which implies an exponential growth of the perturbation with $t_{col} \sim \sqrt{4\pi G\bar{\rho}}$
- Astrophysical objects are stabilized against collapse by pressure gradients, which travel at the speed of sound $c_s = c\,(dp\,/\,d\rho)^{1/2} = c\,w^{1/2}$
- If the density perturbation occupies a region of size R, pressure gradients need $t_{pre} \sim R\,/\,c\,w^{1/2}$ to stabilize it. If $t_{pre} > t_{col} \rightarrow$ collapse
- So collapse occurs when $R \gtrsim c(w/G\bar{\rho})^{1/2} \sim w^{1/2}c/H$
- Being more precise, collapse occurs when the characteristic size of an object is larger than the Jeans length: $\lambda_J = 2\pi\,(2/3)^{1/2}\,w^{1/2}\,c\,/\,H$

The Jeans Length (2)

- Collapse occurs when the characteristic size of an object is larger than the Jeans length: $\lambda_J = 2\pi\,(2/3)^{1/2}\,w^{1/2}\,c\,/\,H$
- Prior to decoupling, $w_{gas} \sim 1/3$ and we get $\lambda_J \sim 3c\,/\,H(z_{dec})$. Larger than the horizon! ✗
- Right after decoupling, $w_{baryon} \sim (k_B T\,/\,mc^2) \sim 2.3\times10^{-10}$, so $\lambda_J \sim 15$ pc, which now is ~15 pc × $(1+z_{dec}) \sim 16$ kpc, the size of a dwarf galaxy. ✓
- However, this growth is too slow to produce the structures we see. ✗

Dark Matter

- Dark matter is not coupled to photons. Therefore, its *w* is always very small.

- Density fluctuations in dark matter can start growing from the start of the matter-dominated era (z_{rm} ~ 3300).

- At the time of decoupling, the baryons fell in the pre-existing gravitational wells of dark-matter and the baryon perturbations grew from there.

- This explains the observed structure.

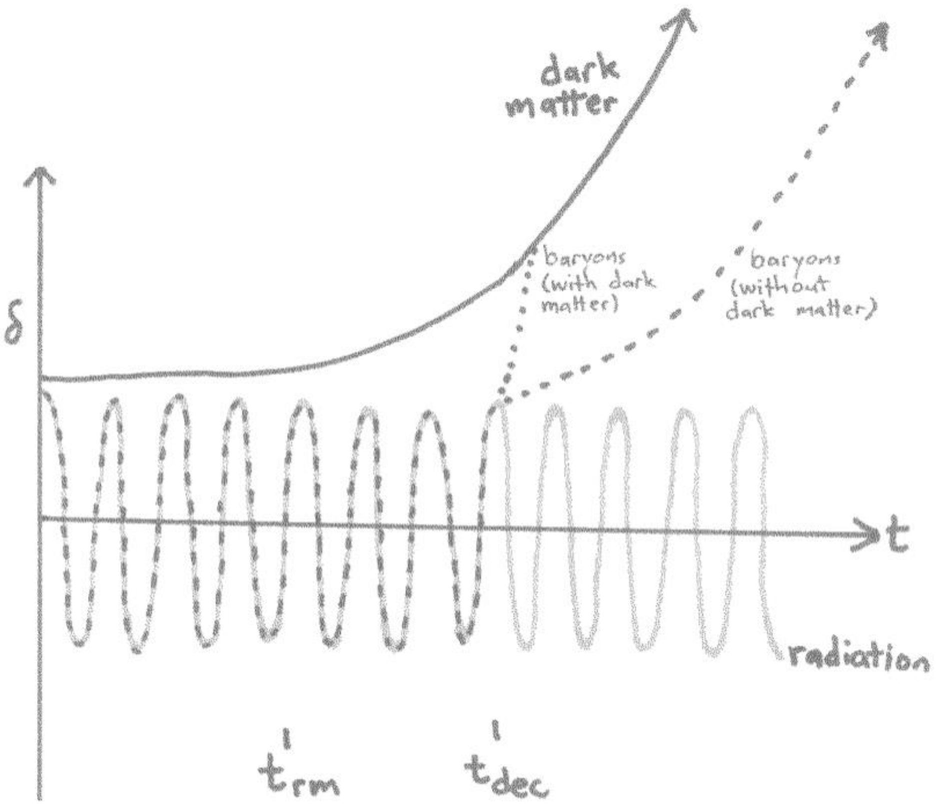

Analysis of Galaxy Maps

- Galaxy surveys provide galaxy maps.
- Similarly to the CMB, we want to study the statistical properties of the **density** fluctuations
- Since the maps are in 3D, we use Fourier transforms and the power spectrum:

$$\delta(\mathbf{r}) = \frac{V}{(2\pi)^3} \int \delta_{\mathbf{k}} e^{-i\mathbf{k}\cdot\mathbf{r}}\, d^3\mathbf{k}$$

$$P(k) = \left\langle \left|\delta_{\mathbf{k}}\right|^2 \right\rangle$$

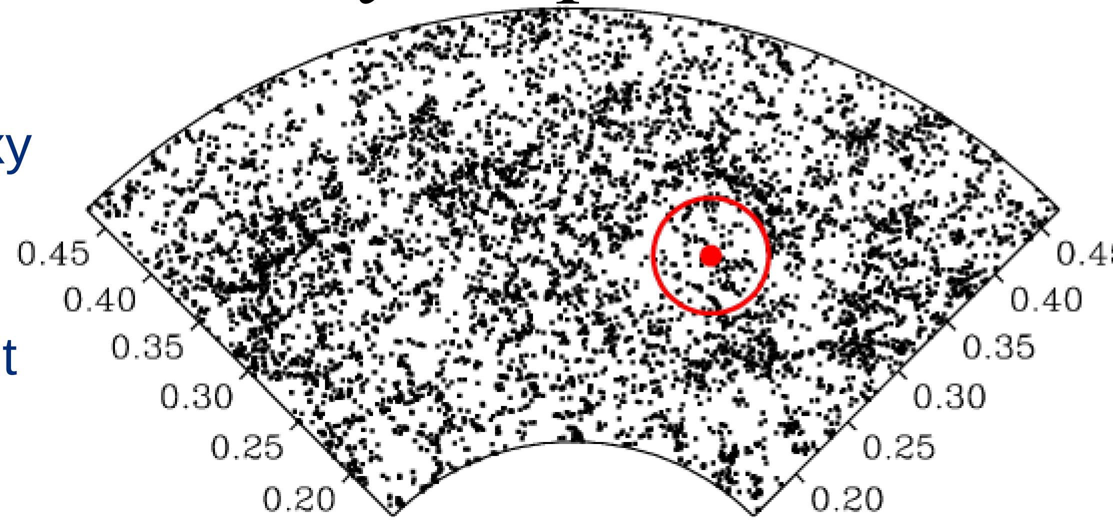

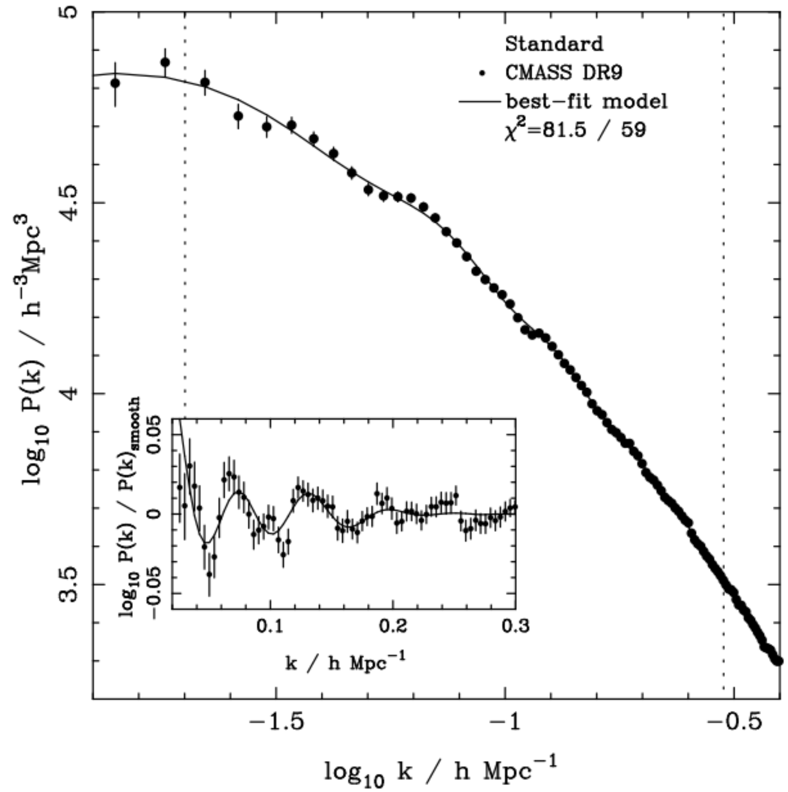

Baryon Acoustic Oscillations

- At z>>1000 the universe was made of dark matter (DM), neutrinos and a highly-coupled relativistic photon-“baryon” (nucleons and electrons) gas.

- Any initial over-density (in DM, neutrinos and gas) creates an overpressure that launches a spherical pressure (sound) wave in the gas.

- This wave travels outwards at the speed of sound in the gas, $c_s = c / \sqrt{3}$

- At z ~ 1100 (t ~ 350 000 yr), temperature drops enough (T ~ 3000 K) for protons and electrons to combine into neutral hydrogen atoms. Pressure-providing photons decouple and free-stream to us (CMB).

- Sound speed of baryons plummets. Wave stalls at a radius of ~150 Mpc = 500 million light-yr, the co-moving sound horizon at recombination.

- Over-density in shell (gas) and in the original center (DM) both seed the formation of galaxies.

- Preferred separation of galaxies is 150 Mpc → standard ruler

Acoustic Wave

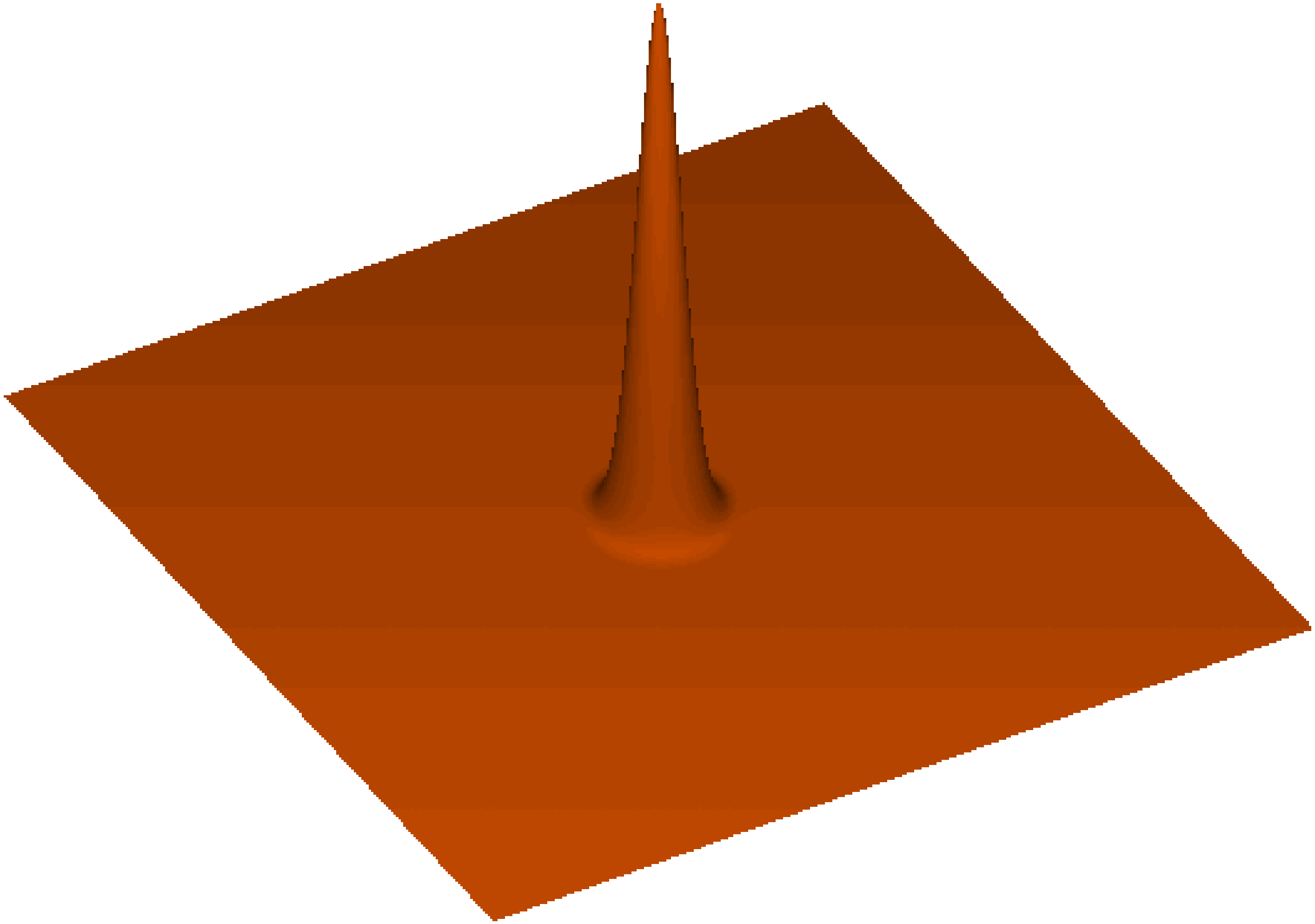

Acoustic Wave

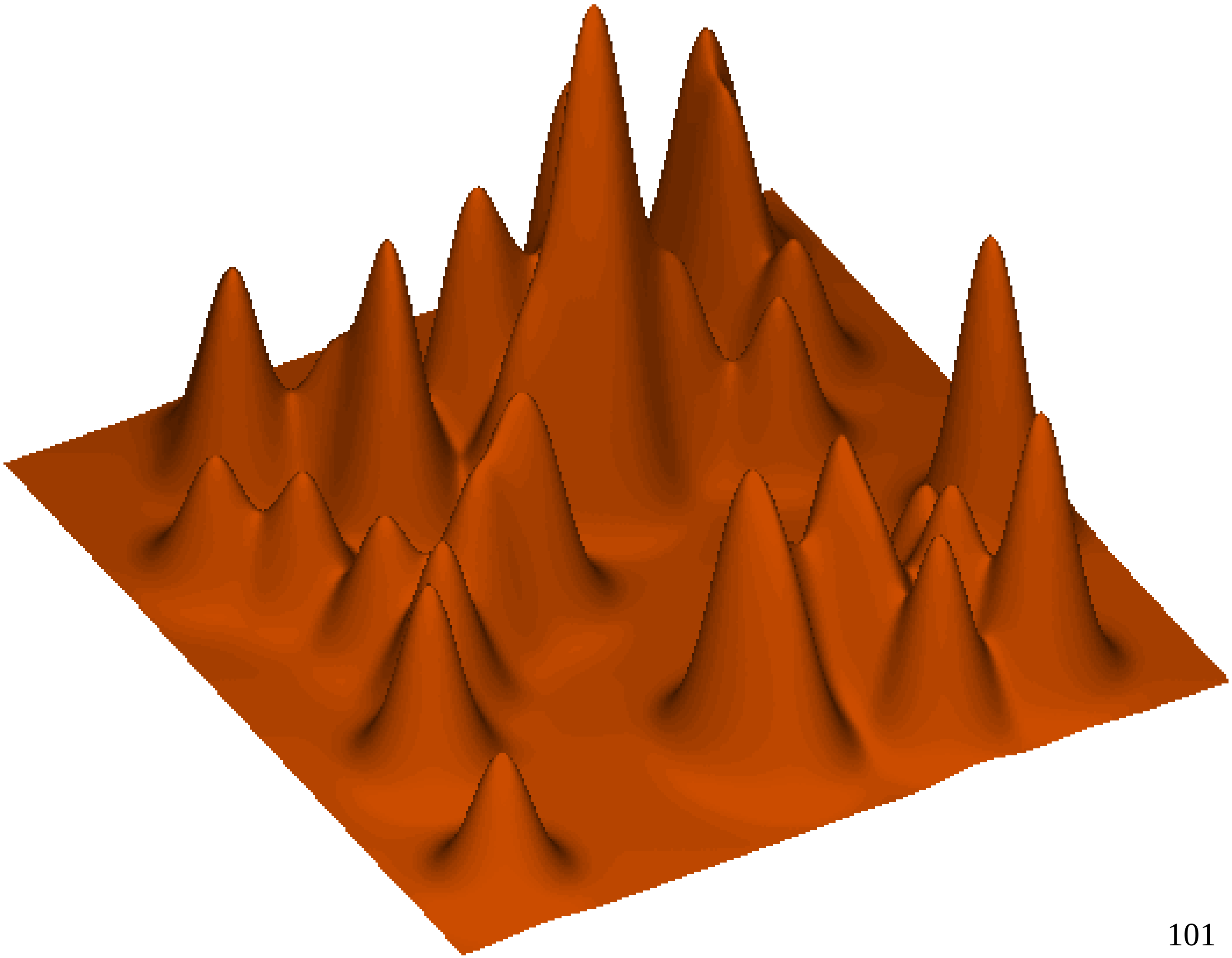

Propagation of Density Perturbations

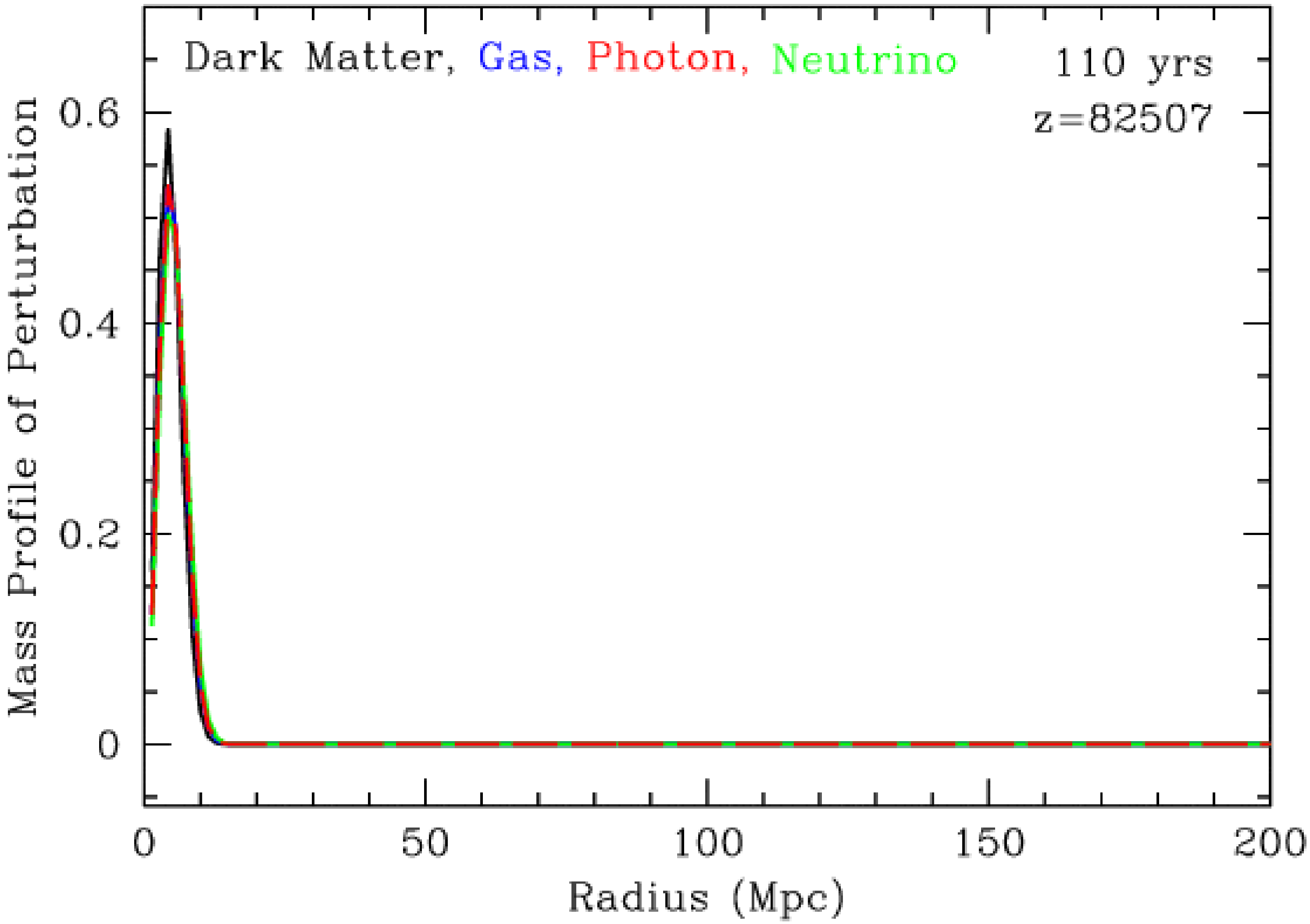

D. Eisenstein, http://scholar.harvard.edu/files/deisenstein/files/acoustic_anim.gif

Final Density Profile

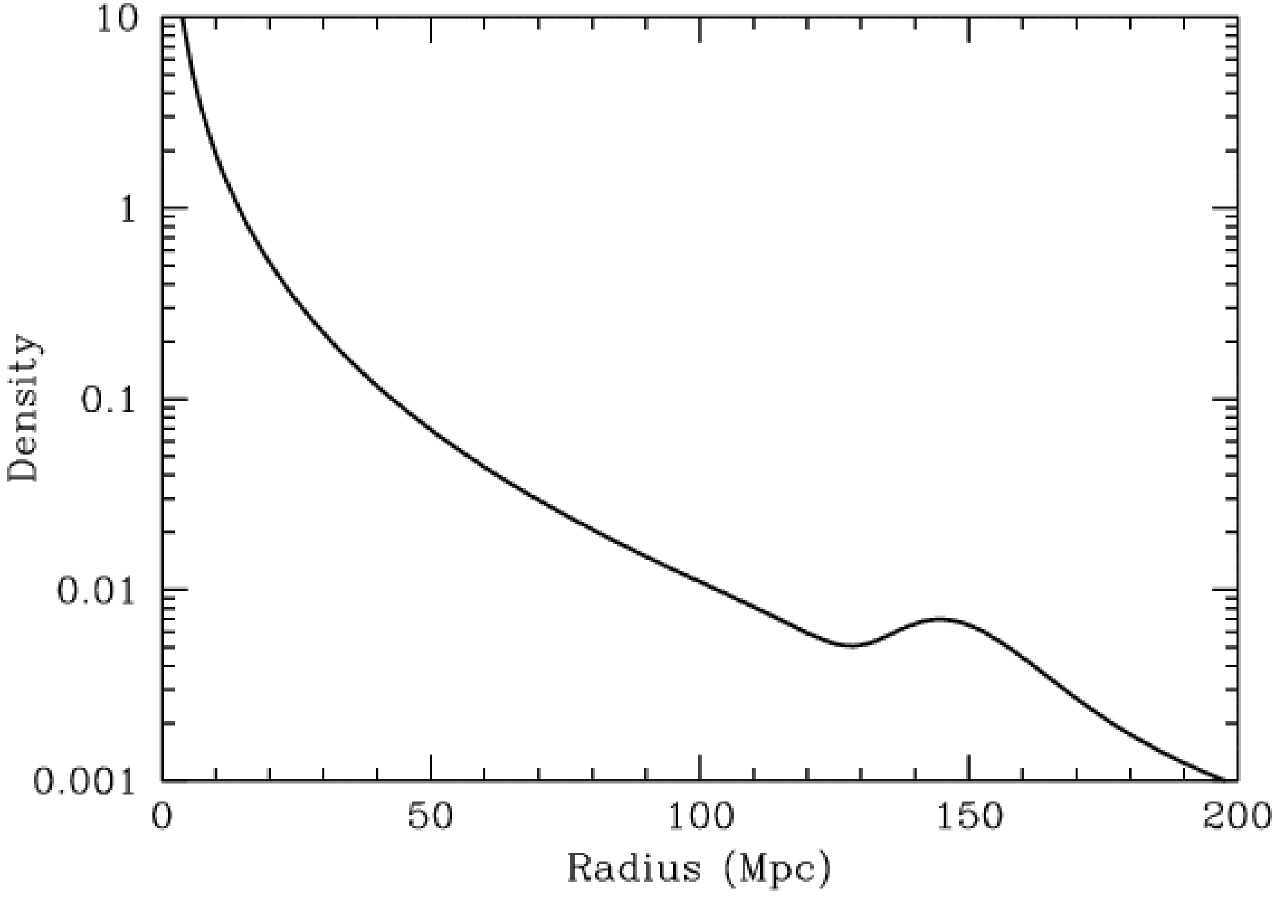

Galaxy-Galaxy Correlation Function

Based on 55000 “luminous red galaxies” from the SDSS spectroscopic galaxy survey

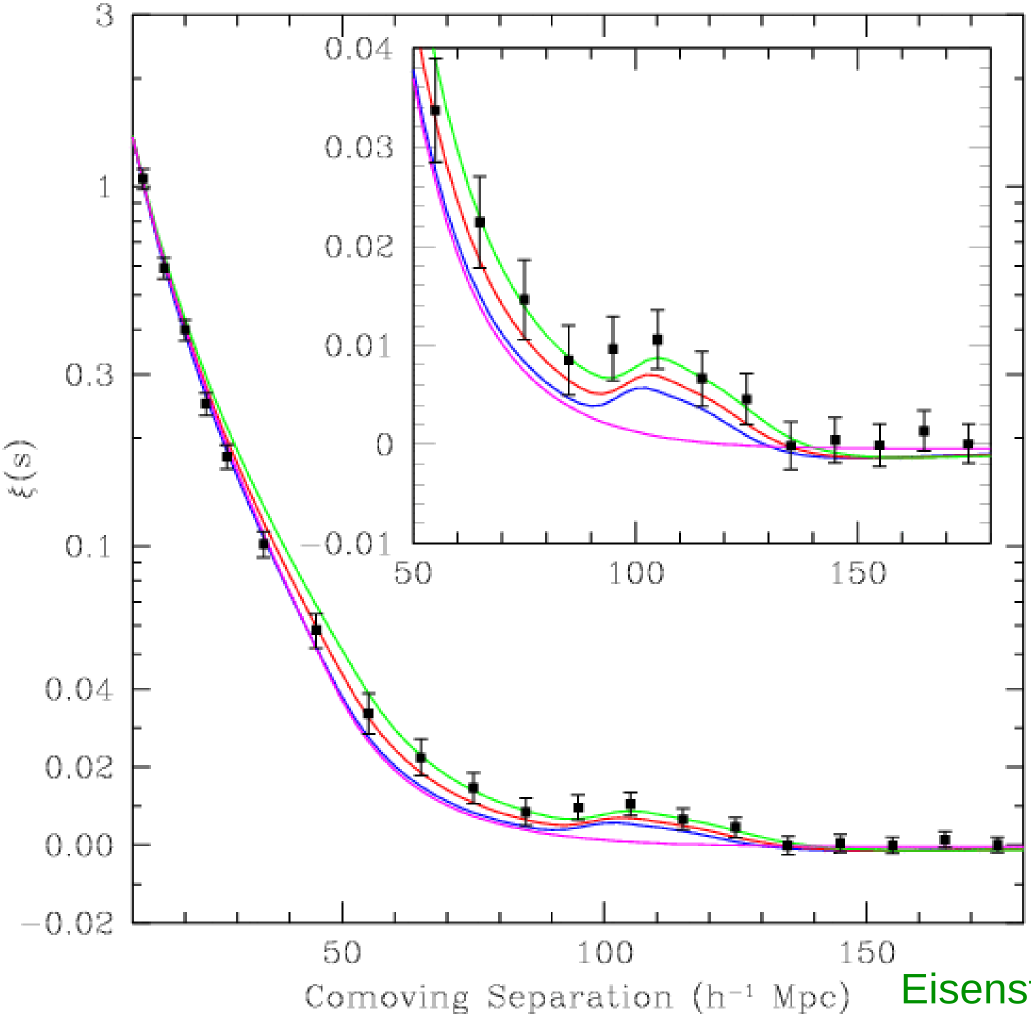

$$\xi(r) = \langle \delta(\vec{r}_1)\delta(\vec{r}_2)\rangle, \delta(\vec{r}) = \frac{\rho(\vec{r}) - \bar{\rho}}{\bar{\rho}}$$

or

$$dP_{12} = \bar{\rho}^2\left[1 + \xi(r)\right]dV_1 dV_2, r = \left|\vec{r}_1 - \vec{r}_2\right|$$

3.5-□ detection of BAO at $\langle z \rangle = 0.35$ (confirmed by 2DF and SDSS photometric survey at about 2.5 □, ανδ τηεν βψ μανψ οτηερσ)

$h = H_0$ / (100 km s^{-1} Mpc^{-1}) ~ 0.7

Eisenstein et al. 2005

Probing Dark Energy with BAO

- A standard ruler provides a measurement of the angular distance as a function of redshift:

$$\Delta\theta = \ell / d_A$$

$$d_A(z) = r(z)/(1+z)$$

$$r(z) = \int_0^z \frac{dz'}{H(z')}$$

(geometric test of dark energy)

⊗⃥ : angle subtended

l : intrinsic length

d_A : angular distance

$r(z)$: co-moving distance

- In principle, one can also put the ruler along the line of sight:

$$\ell = \Delta z / H(z)$$

⊗z : redshift subtended

Direct determination of $H(z)$, but in this case one needs to measure redshifts very precisely.

BAO Sensitivity to Dark Energy

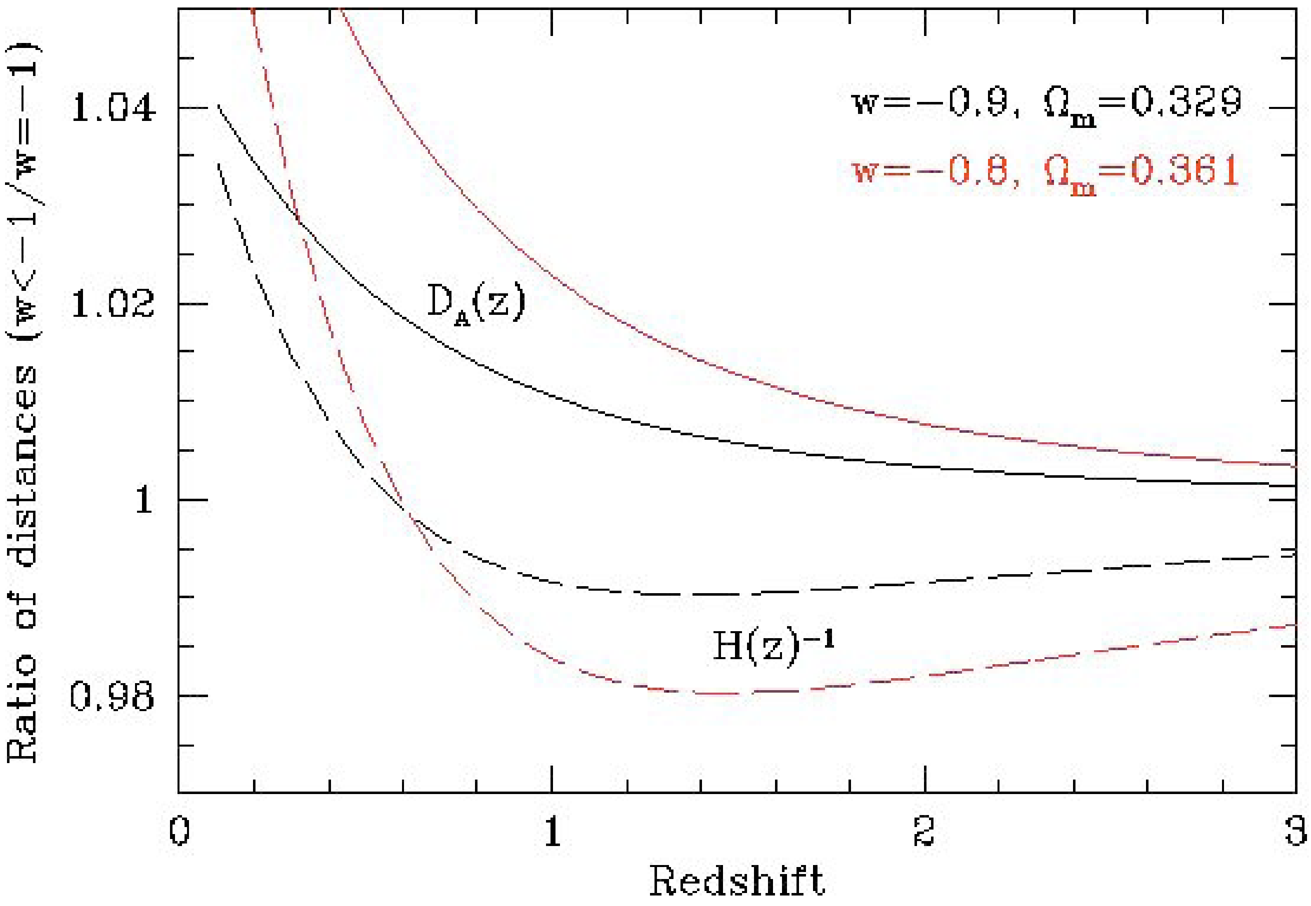

Tough measurement

Worse if one wants to measure d*w*/d*a*

BAO not as sensitive as SNe to w

Galaxy Redshift Surveys

- Galaxy redshift surveys are used to measure the 3D clustering structure of matter: only need position and *z*, no flux, no shape.
- There can be several sources of systematic errors:
  - Light from galaxies is a “biased” estimator of matter content
  - Non-linear physics involved in galaxy formation
  - Redshift distortions
- However, all effects tend to predominantly change the amplitude of the correlations, but not the position of the measured acoustic peak
- BAO are very insensitive to systematic errors, and in any case, they are very different from those of SNe.
- But small effect only visible at large scales leads to huge surveys.

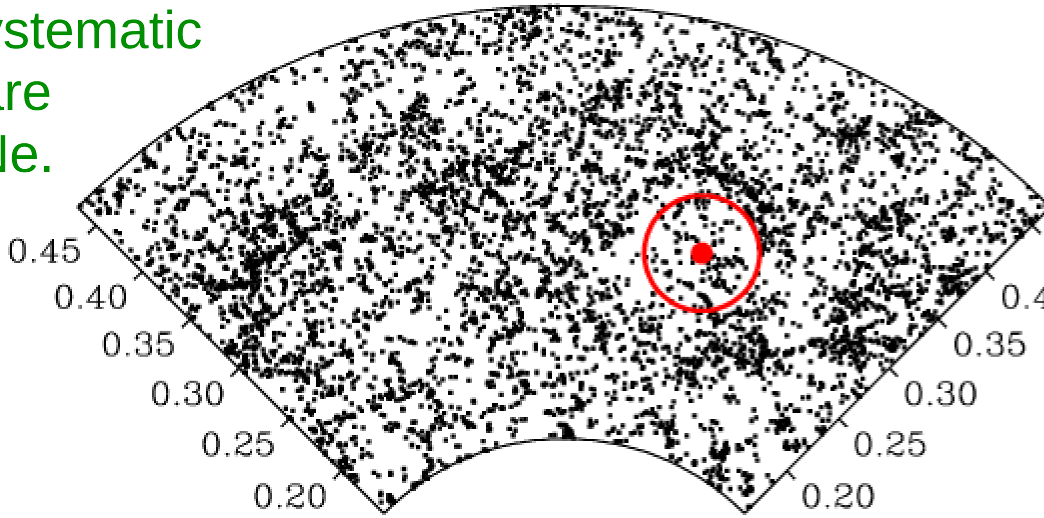

Galaxy Survey Strategy

- Statistical errors on galaxy-galaxy correlation functions are determined by “sample variance” and “Poisson (shot) noise”.

  - Sample variance: how many independent samples of the relevant scale (150 Mpc)^3 one has → volume

  - Poisson noise: how many galaxies included in each sample → density

$$\frac{\Delta P(k)}{P(k)} \propto \frac{1}{\sqrt{V}}\left(1 + \frac{1}{nP(k)}\right)$$

P(*k*): power spectrum
Fourier transform of ⌊(*r*)

n: galaxy density

- Given a fixed number of galaxies (in a spectroscopic survey), the optimal choice for measuring the correlation function is an intermediate density:

$n > 10^{-4}$ h^3 Mpc^{-3} at low redshift; somewhat higher at high redshift

Which Galaxies?

- Many surveys concentrate on "Large Red Galaxies": old elliptical galaxies, which are very bright and have a characteristic spectrum with a prominent break at 4000Å → easy to measure redshift (spectrum or photometric)

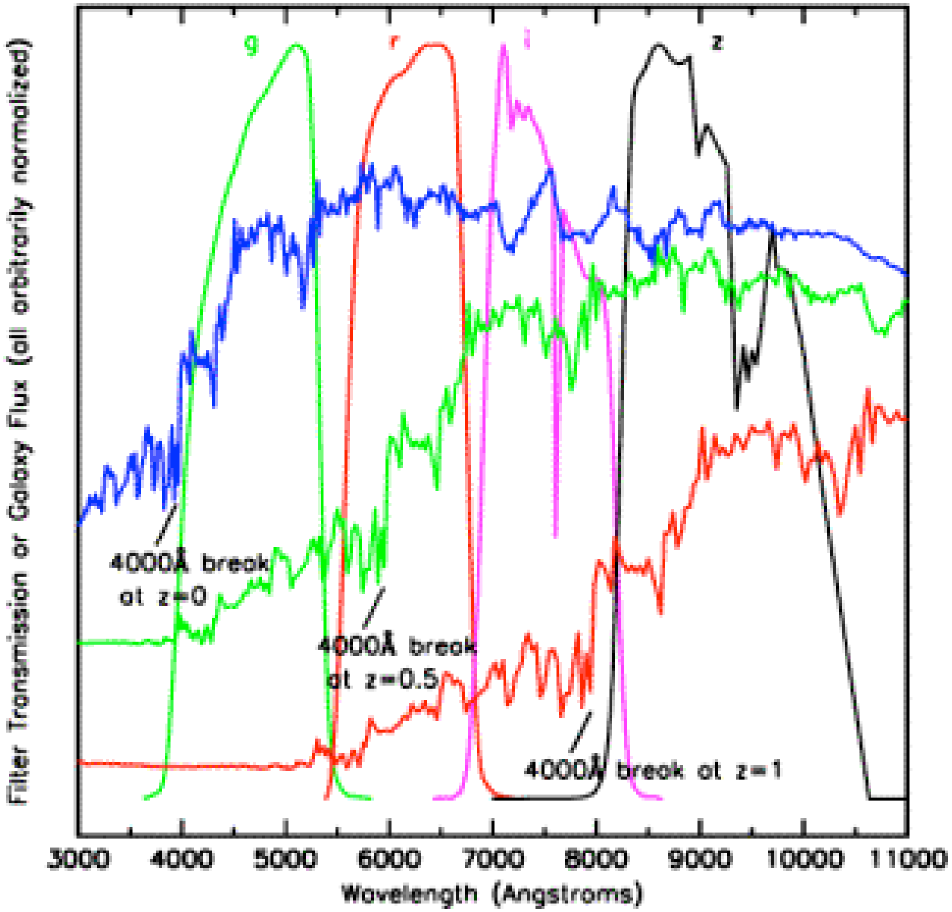

Cosmological Results from BAO

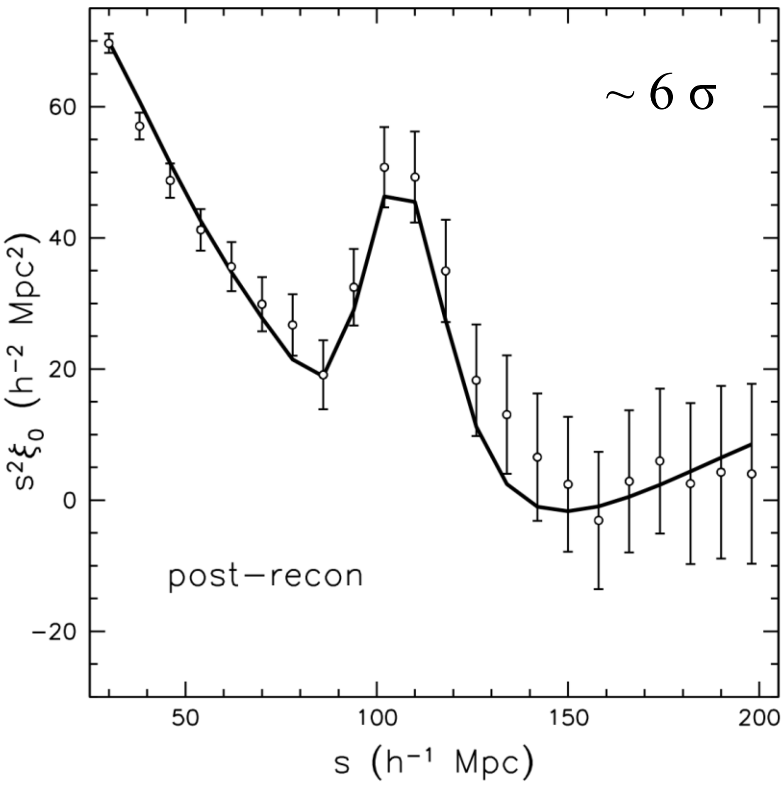

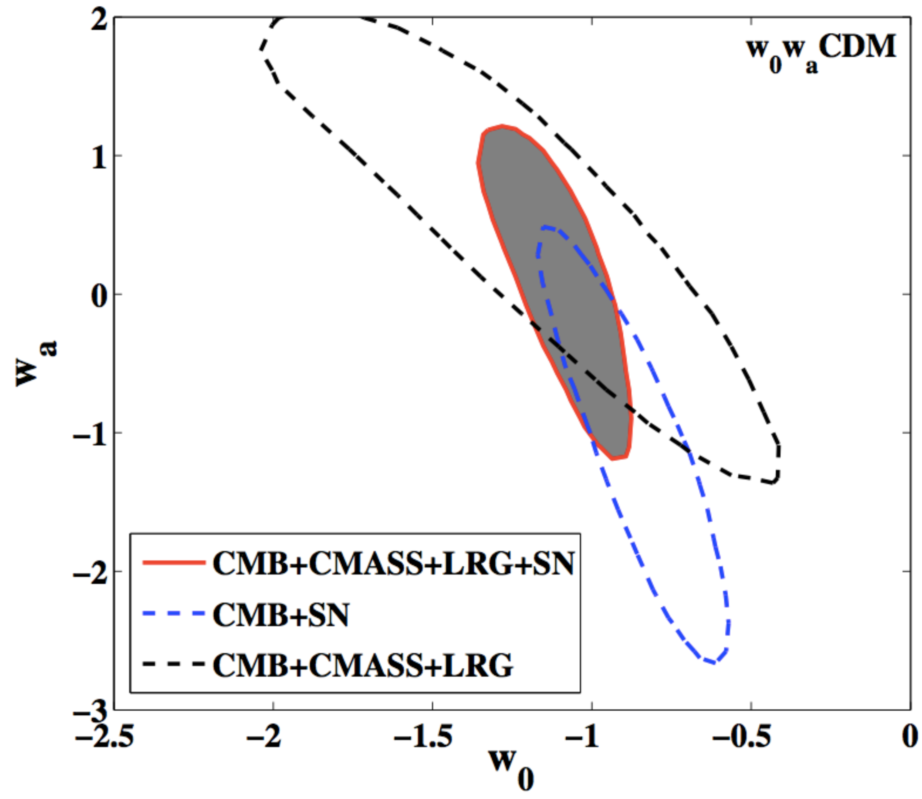

Anderson et al. (BOSS) 2013

$w(z) = w_0 + (1\text{-}a)\, w_a$

$w_a \equiv -\,(dw\,/\,da)_0$

Summary: BAO

- The BAO scale was observed in 2005-2007 at the 2.5-3.5 level in two surveys using three techniques.
- It provides very important constraints on Dark Energy properties (orthogonal to SNe).
- Statistics is crucial. Haven't reached systematics limit yet.
- Explosion of BAO surveys:
  - Photo-z from ground: Pan-STARRS, DES, LSST, PAU
  - Spectroscopy from ground: BOSS, DESI, Sumire
  - Spectroscopy from space: Euclid

Expect a lot more insight on the nature of Dark Energy from BAO studies

Weak Gravitational Lensing

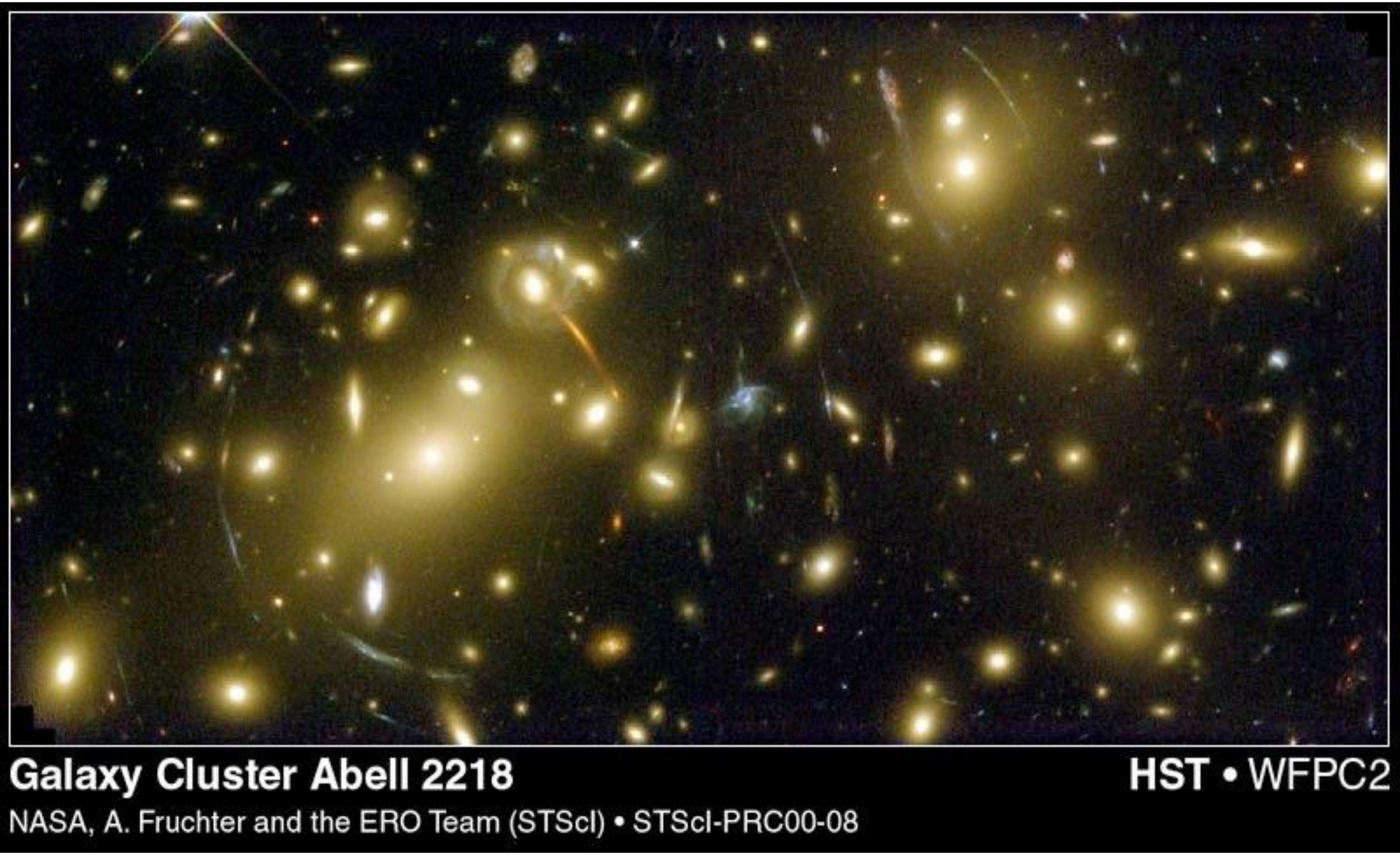

Weak Gravitational Lensing

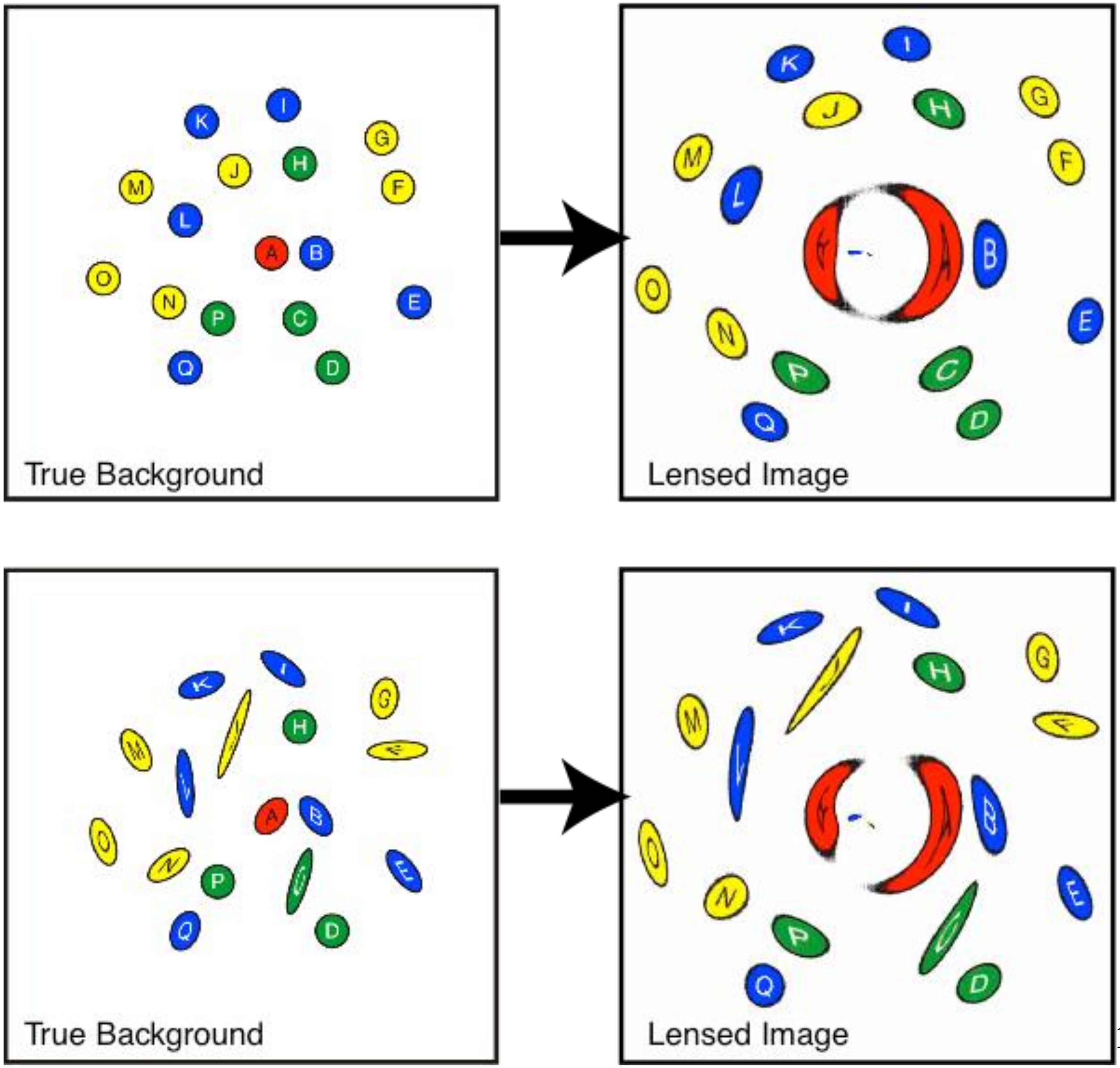

Weak Gravitational Lensing

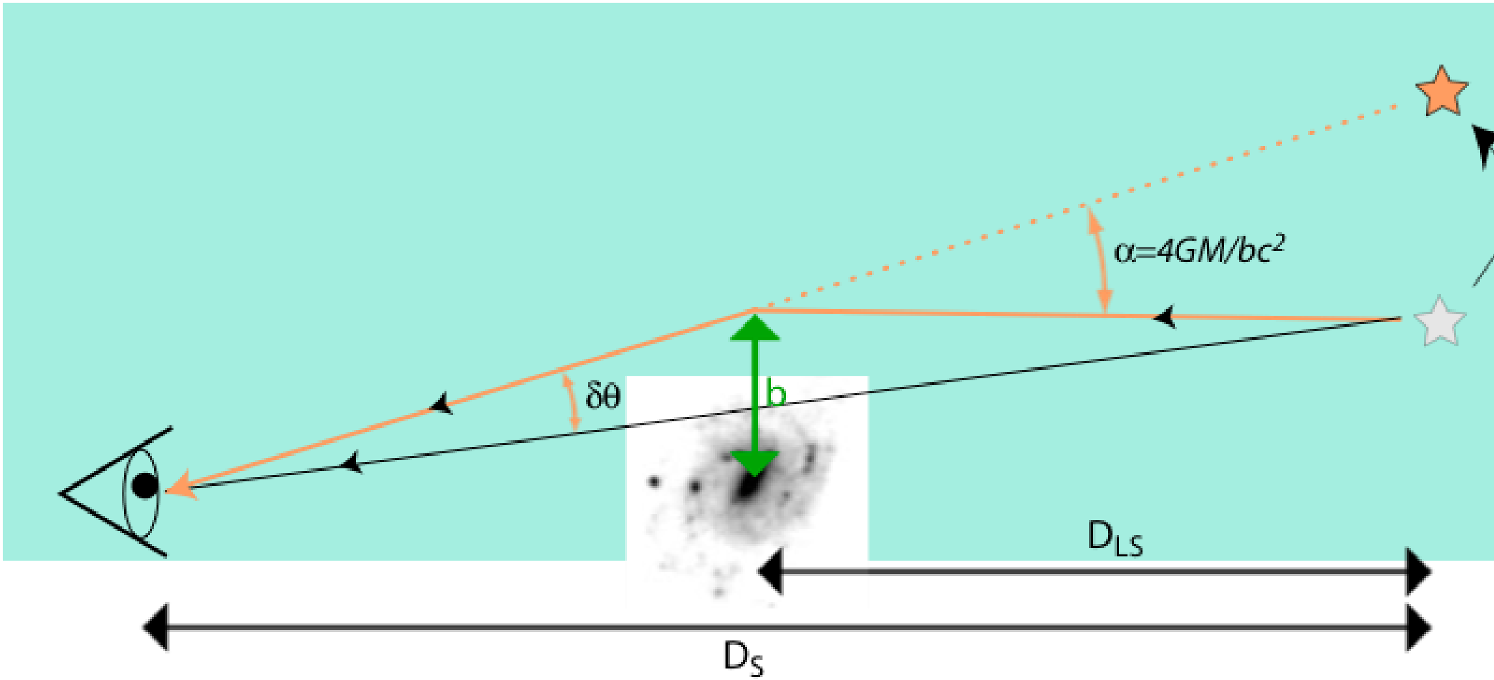

$$\delta\theta = \frac{4GM}{bc^2} \frac{D_{LS}}{D_S}$$

We observe this deflection angle (more precisely, gradients of the deflection angle).

Cosmology changes growth rate of mass structures in the Universe.

Cosmology changes the geometric distance factors.

Weak Gravitational Lensing

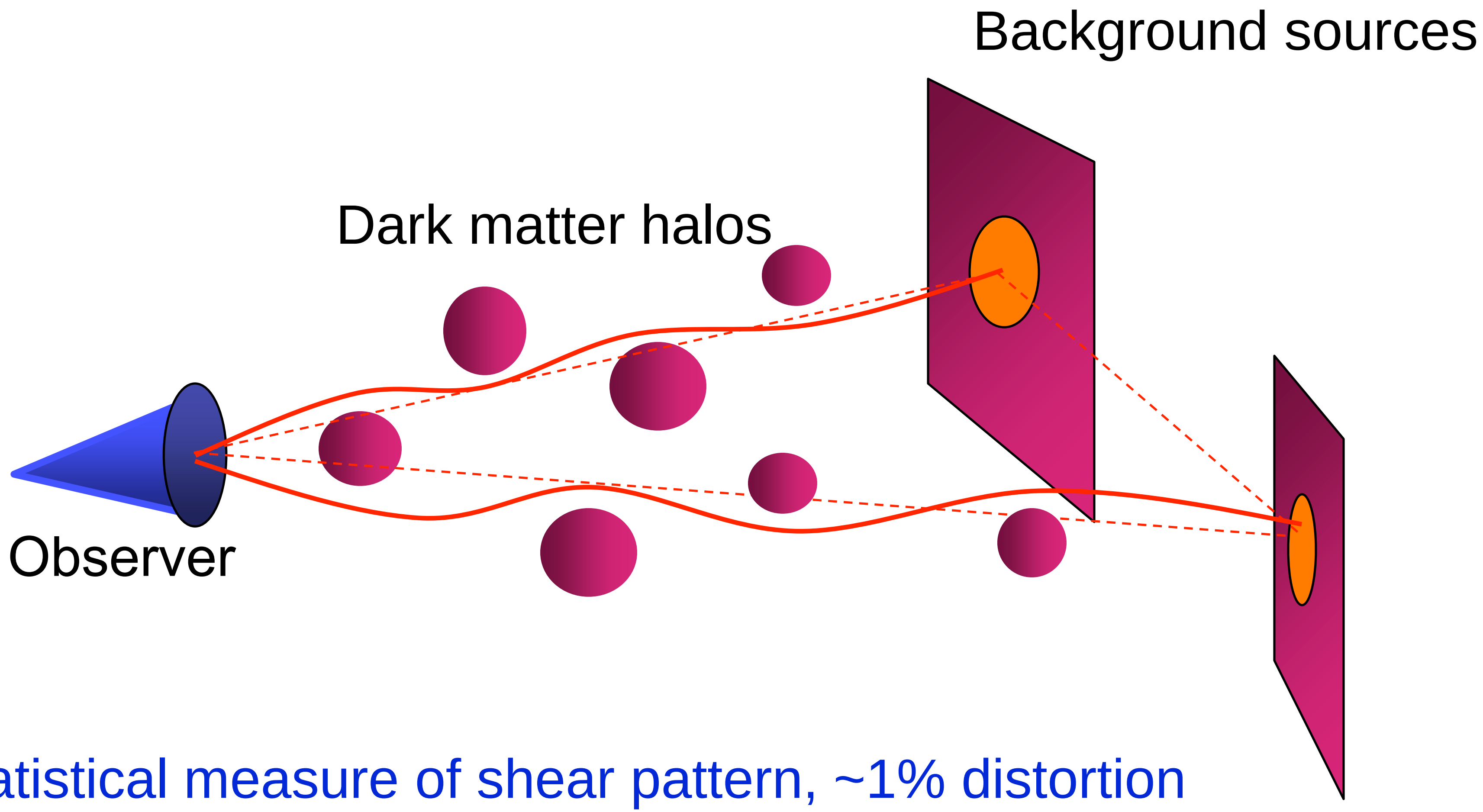

- Statistical measure of shear pattern, ~1% distortion
- Radial distances depend on *geometry* of Universe
- Foreground mass distribution depends on *growth* of structure

Weak Lensing and Dark Energy

• We can measure a power spectrum, just like CMB and BAO.

• WL can divide source galaxies into many distance slices and measure **many power spectra.** Combine them to determine the **history** of dark energy.

• WL sees non-linear, **non-Gaussian** growth and collapse of mass structures.

• WL can measure and use the relation between **visible** matter and **dark** matter.

• WL can measure the growth of Universe's size **and** growth of structure within it.

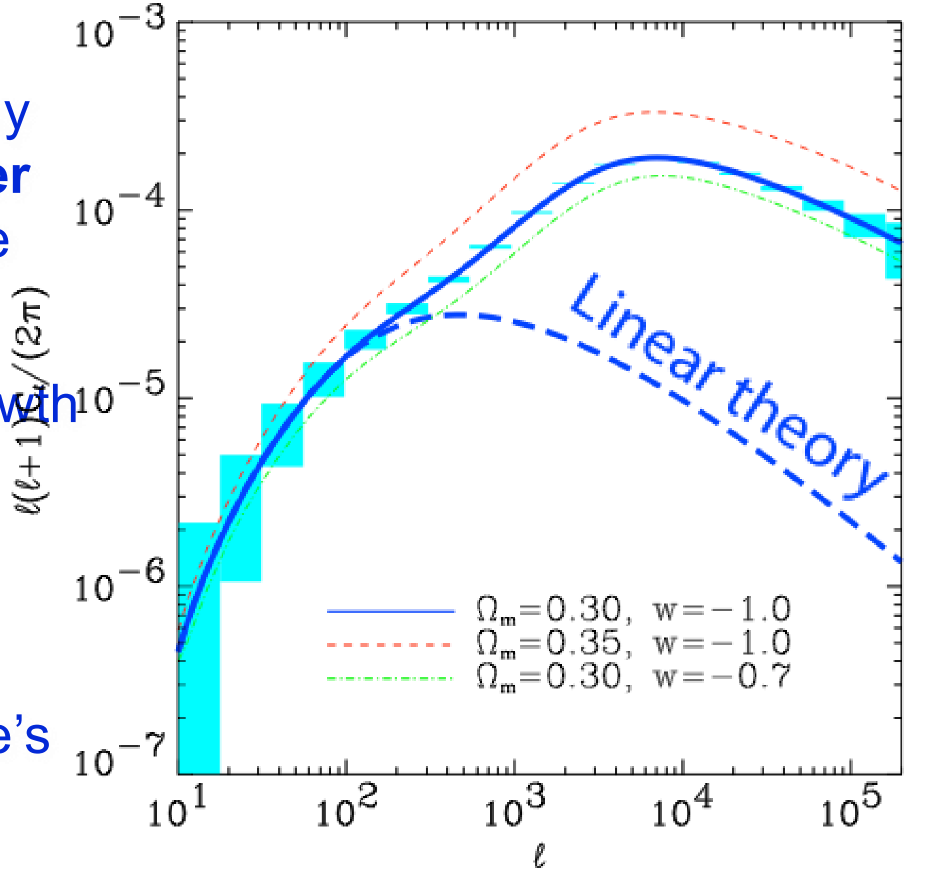

This allows us to test whether GR is correct

A Weak Lensing Survey

- Take pictures of many galaxies (ideally one billion).
- Carefully measure the shape of each one.
- Determine the mean lensing distortion to an accuracy of about 0.0001.
- Main systematic: knowledge of PSF: space much better suited for WL studies than ground-based telescopes.

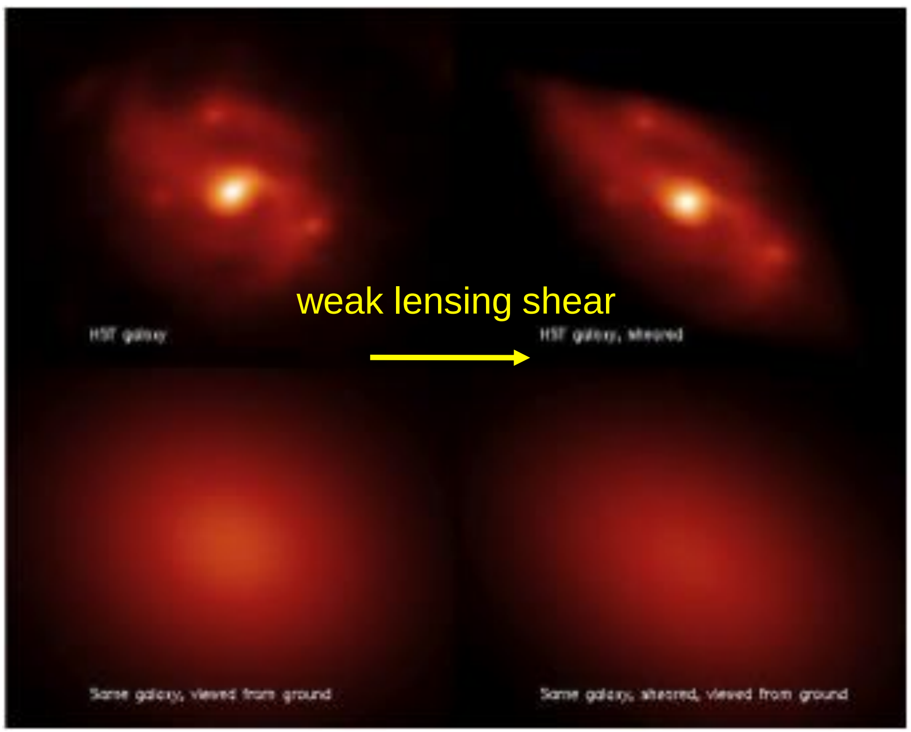

Space:

Small PSF: larger number of resolved galaxies

Stable PSF: lower systematics after calibration with stars

NIR photometry: better photo-z's

Summary: Weak Lensing

- Weak Lensing is a statistically extremely powerful dark energy probe.
- Needs large galaxy-shape surveys.
- Systematics are tough from the ground. Less so from space.
- Vigorous future program:
  - From ground: DES, KIDS, HSC, LSST
  - From space: Euclid

Weak Lensing might be the ultimate technique for determining the nature of dark energy

Galaxy Clusters

- Galaxy clusters are the largest collapsed structures.
- Their mass density function *dn / dVdM* can be predicted. It depends on DE through the growth of structure.
- The measured cluster density involves both the mass density function and the volume element, which depends on DE through geometry:

$$\frac{dn}{dzd\Omega} = \frac{dV}{dzd\Omega}\int_{M_{\rm lim}}^{\infty} dM\, \frac{dn}{dVdM}$$

$$dV / dzd\wedge = r^2(z) / H(z)$$

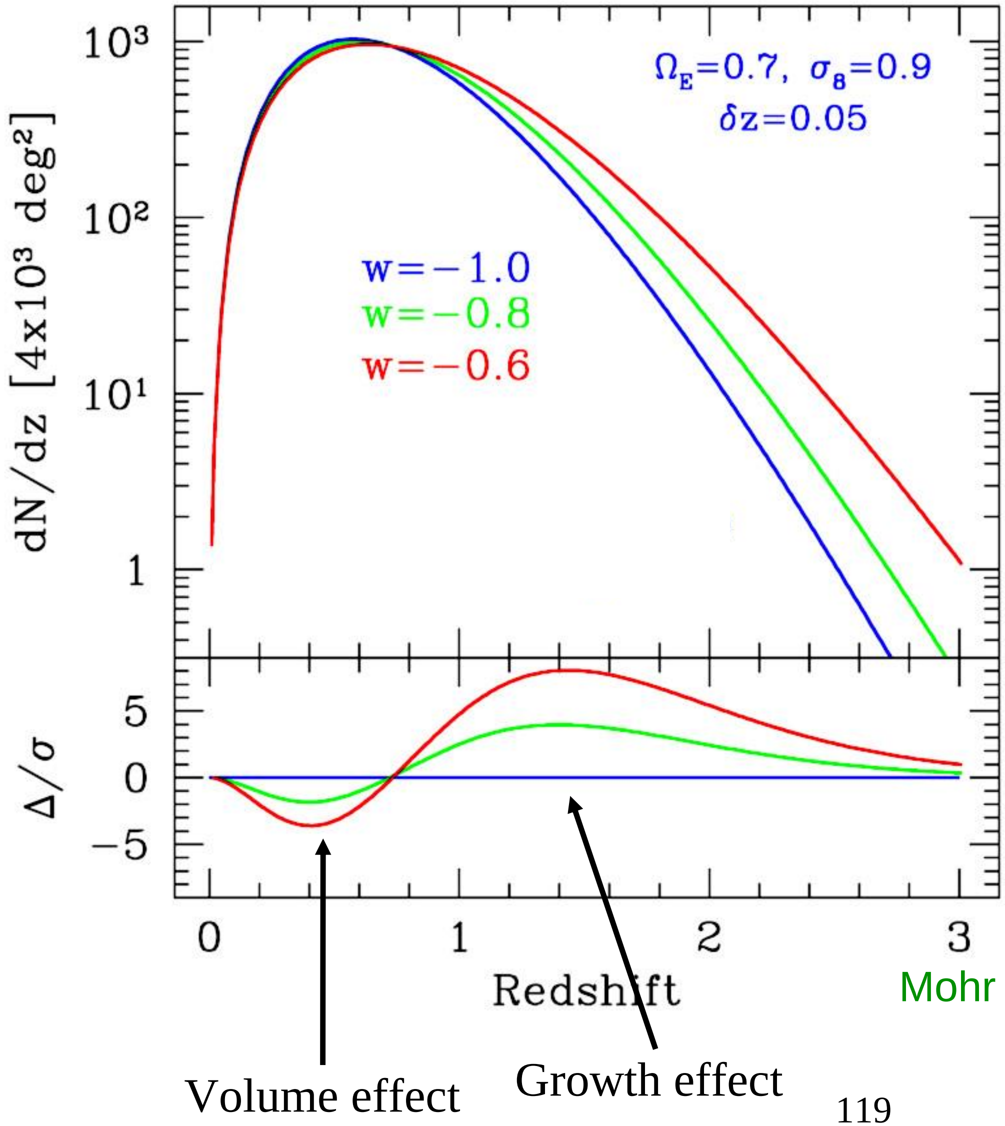

Cosmology with Galaxy Clusters: Requirements

1. Quantitative understanding of the formation of dark matter halos in an expanding universe.

2. Clean way of selecting a large number of galaxy clusters over a range of redshifts.

3. Redshift estimates for each cluster (photo-z's adequate).

4. Observables that can be used as mass estimates at all redshifts.

What is a Cluster?

Large peak in matter density:

- Dark matter clump (~75% of mass) weak lensing
- Many luminous galaxies (~2.5%: 10% of baryons)
  - BCG and red sequence
  - Additional galaxies
  - Diffuse light

  optical astronomy
- Hot gas (~22.5%: 90% of baryons)
  - Emits x-rays x-ray astronomy
  - Causes Sunyaev-Zel'dovich (SZ) decrement in CMB sub-millimeter astronomy

Cosmology with Galaxy Clusters: Systematics & Controls

1. Relationship between observable and mass is complicated: need to understand bias and resolution (dn/dM falls exponentially).
2. Sample selection function: completeness, contamination.
3. Projection effects (SZ, optical, weak lensing).
4. Photo-z calibration.

1. Self-calibration of mass-observable: clustering of clusters, shape of mass function.
2. Cross-compare identification and mass determination techniques.
3. Weak Lensing mass calibration: cluster-mass correlation function.
4. Spectroscopic training sets.

Summary: Clusters

- Galaxy cluster counting is a powerful technique that requires a multi-observable approach.
- Systematics can probably be understood with multi-probe approach.
- Large surveys just starting
- Main program: SPT + DES

Galaxy cluster studies are the most uncertain. Great potential, big challenges

The Concordance Model

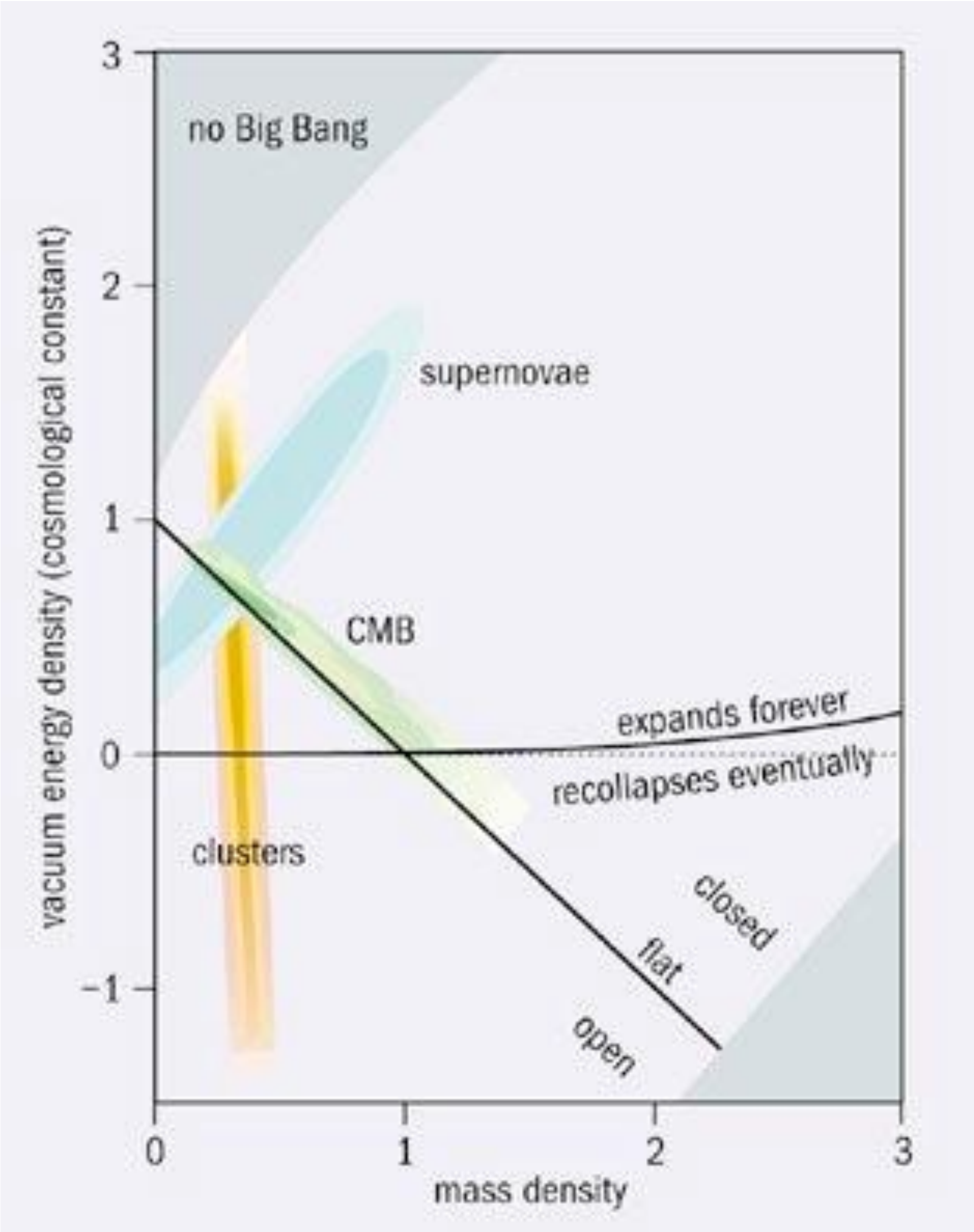

Current Situation

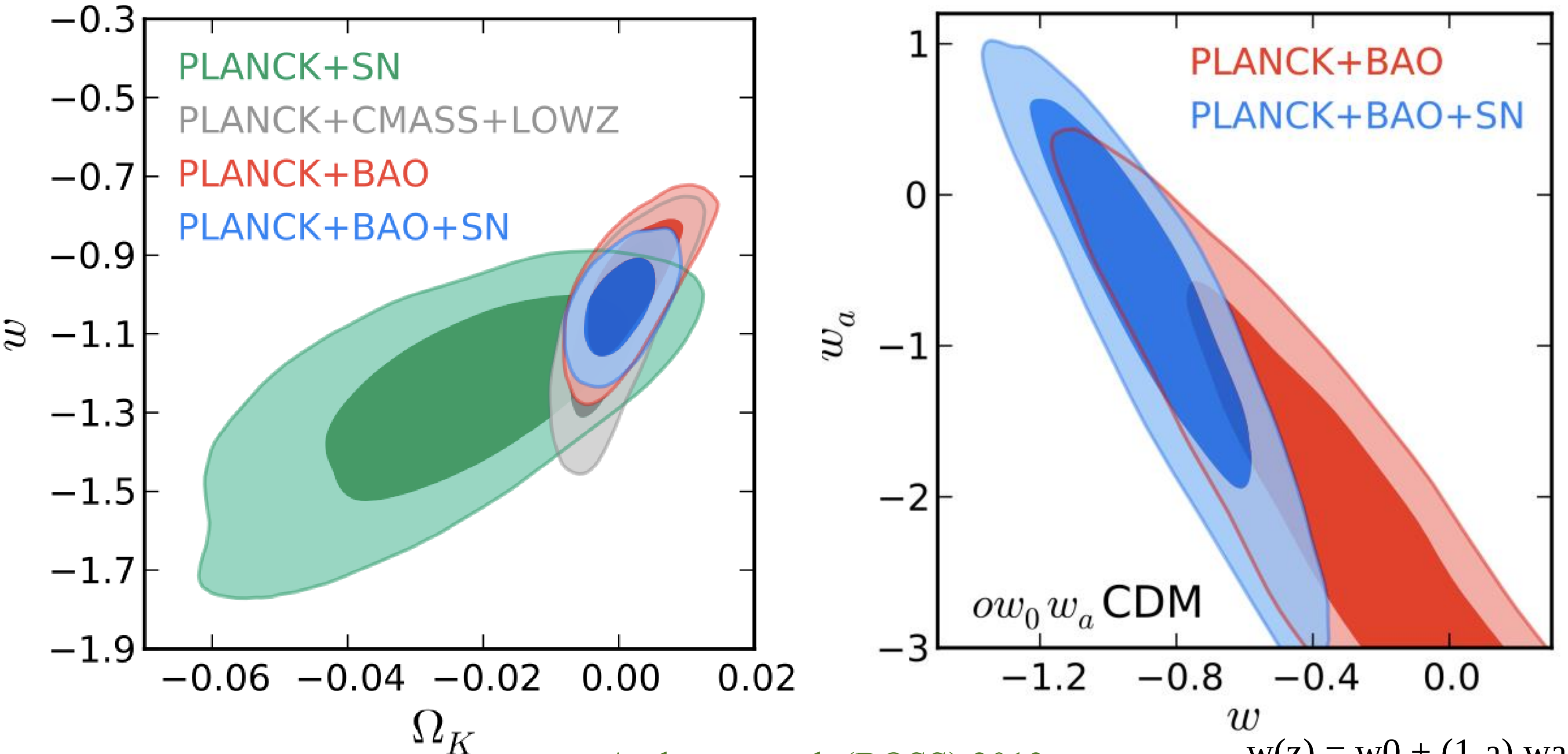

Anderson et al. (BOSS) 2013

w(z) = w0 + (1-a) wa
wa ≡ - (dw / da)0

If we assume *w* = const, data compatible with ⊄
Very little sensitivity to d*w*/d*a*

So What is the Dark Energy?

- Einstein's cosmological constant?

Data so far seems to point towards □, but see next slide

- Some dynamical field ("quintessence")?

$$\ddot{\varphi} + 3H\dot{\varphi} = -V'$$

$$\rho = \tfrac{1}{2}\dot{\varphi}^2 + V(\varphi)$$

$$P = \tfrac{1}{2}\dot{\varphi}^2 - V(\varphi)$$

Needs large fine-tuning

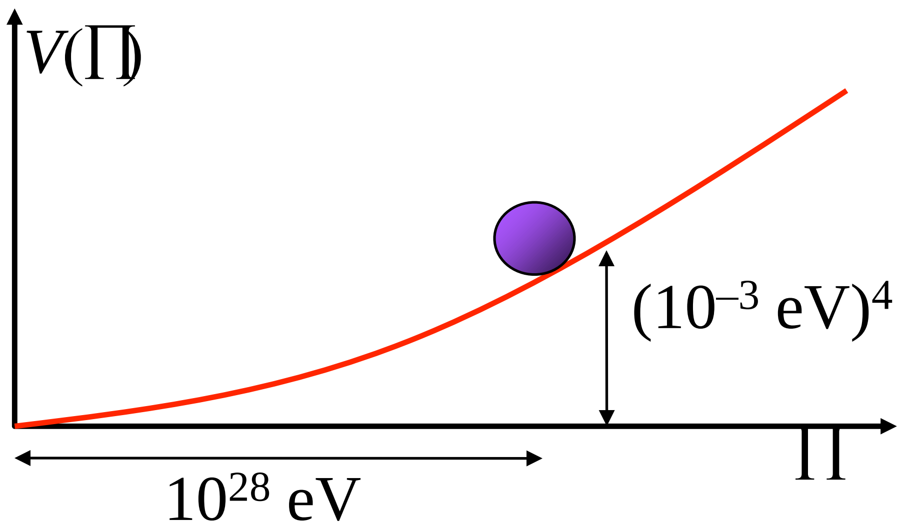

- Modifications to General Relativity?

If GR is not the right theory of gravity at large scales, then the properties of DE inferred from geometrical probes (SNe, BAO) will not, in general, coincide with the properties inferred from growth of structure probes (clusters, WL).

A Cosmological Constant?

- Data is so far compatible with dark energy being just $\not\subset$

$$w \sim -1 \pm 0.05 \qquad \text{(assuming } w = \text{constant)}$$

- However, there is no physical (microscopical) explanation for $\not\subset$. It just can be added to Einstein’s field equations:

$$R^{\lceil\{} - ½\, g^{\lceil\{} R = 8\Box G T^{\lceil\{} + \not\subset g^{\lceil\{}$$

- Since $\not\subset$ is constant in space and time, a good obvious candidate is vacuum energy. However:

$$\wedge_{\not\subset} \sim 0.7 \;\; ➔ \;\; \rangle_{\not\subset} \sim (10 \text{ meV})^4 \quad [\sim m^4_{\{} \ldots]$$

while a naïve estimate would give

$$\rangle_{\not\subset} \sim M^4_{\text{Planck}} \sim 10^{120} \times (10 \text{ meV})^4$$

- Before 1998 it was hoped that some exact symmetry would turn $\rangle_{\not\subset}$ into 0
- Now some broken symmetry is needed, leaving only one part in 10^{120}

Quite a fine-tuning problem!!!

Curent and Future Galaxy Surveys

Dark Energy Studies

- What is causing the acceleration of the expansion of the universe?
  - Einstein's cosmological constant Λ?
  - Some new dynamical field ("quintessence", Higgs-like)?
  - Modifications to General Relativity?

  } "Dark Energy"

- Dark energy effects can be studied in two main cosmological observables:
  - The history of the expansion rate of the universe: supernovae, weak lensing, baryon acoustic oscillations, galaxy-cluster counting
  - The history of the rate of the growth of structure in the universe: weak lensing, galaxy distribution (LSS), galaxy-cluster counting
- For most probes, large galaxy surveys are needed:
  - Spectroscopic: 3D (redshift), medium depth, low density, selection effects
  - Photometric: "2.5D" (photo-z), deeper, higher density, no selection effects

Spectroscopic Redshift vs. Photo-z

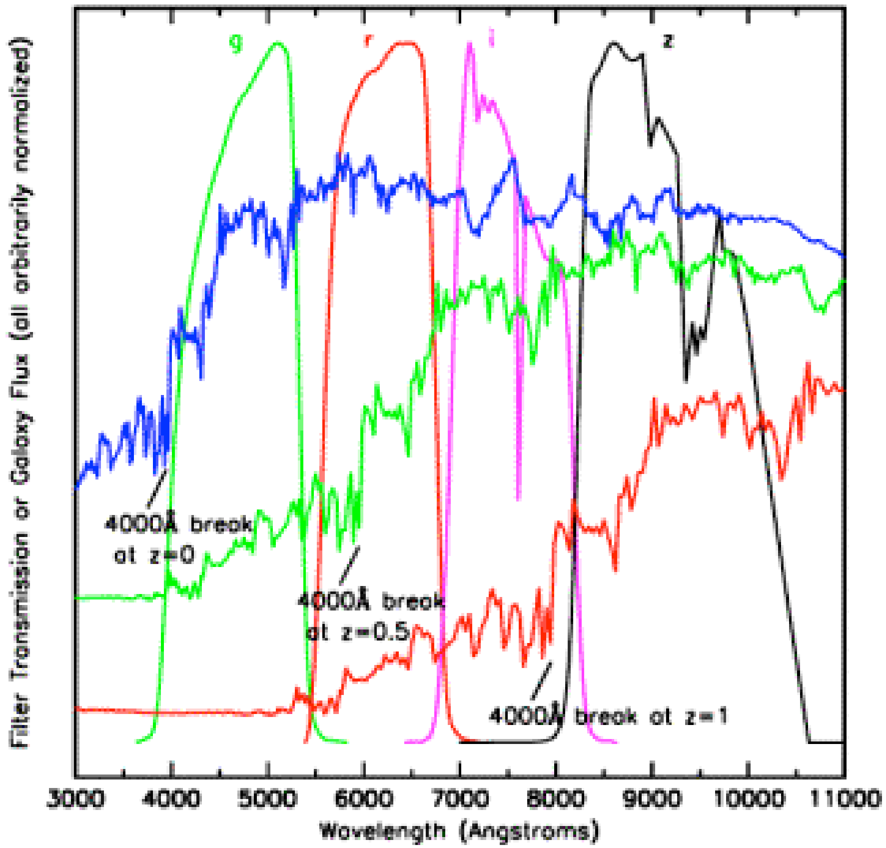

Spectroscopy: $\sigma(z)/(1+z) \quad < \quad 0.001$

Photo-z: $\sigma(z)/(1+z) \quad \sim \quad 0.05$

The Importance of Redshift Resolution

z-space, ⊗*z = 0.03(1+z)* + peculiar velocities (DES)

z-space, ⊗*z = 0.003(1+z)* + peculiar velocities (PAU)

z-space, perfect resolution + peculiar velocities (DESI)

Real space

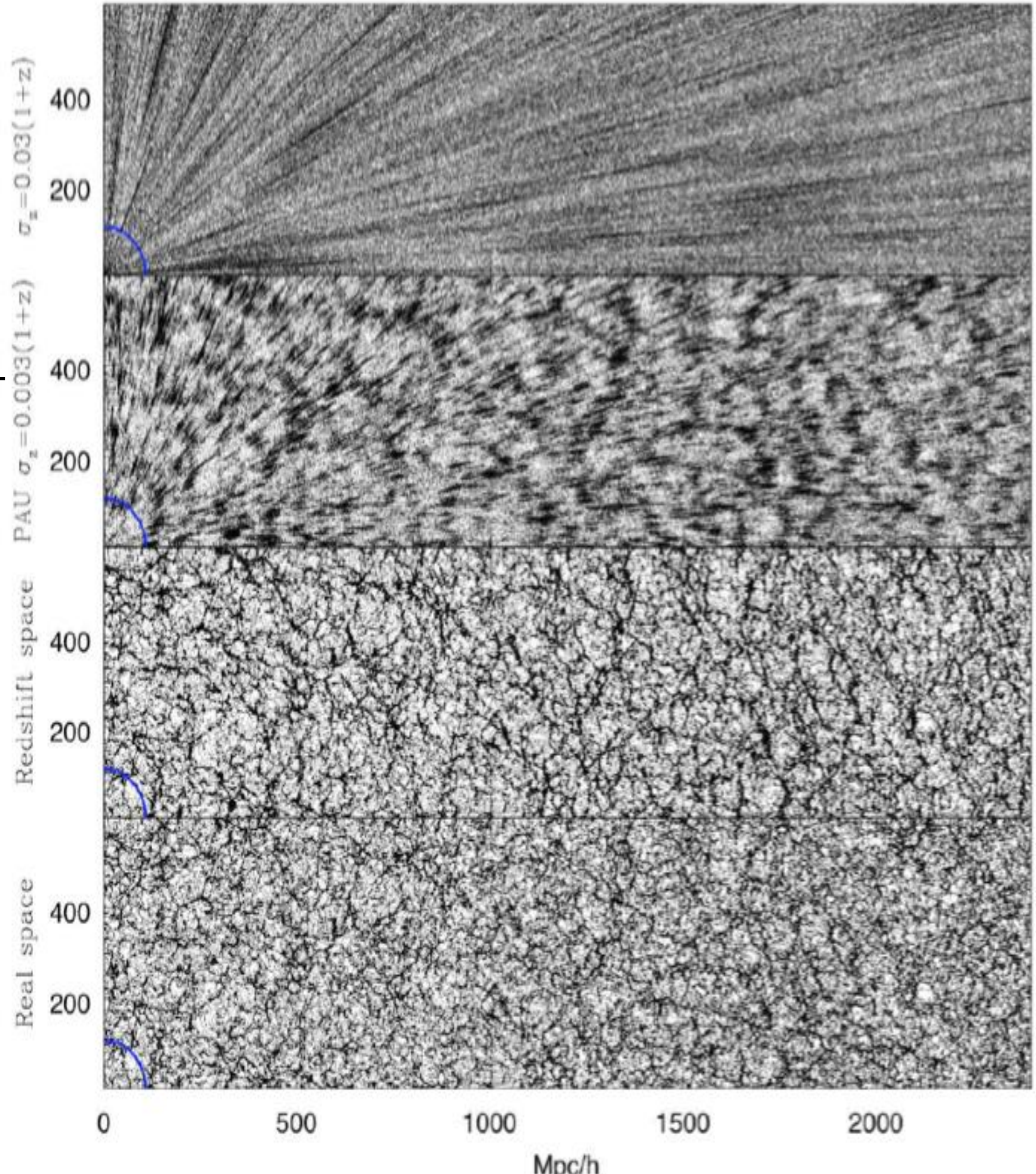

DES

DES: Dark Energy Survey

- 5000 deg^2 galaxy survey to $i_{AB} < 24$ in grizY. 300M galaxies up to $z < 1.4$. Also 4000 SNe.
- Involves groups in USA (led by FNAL), Spain, UK, Brazil, Germany, Switzerland.

2.2 deg Ø FoV

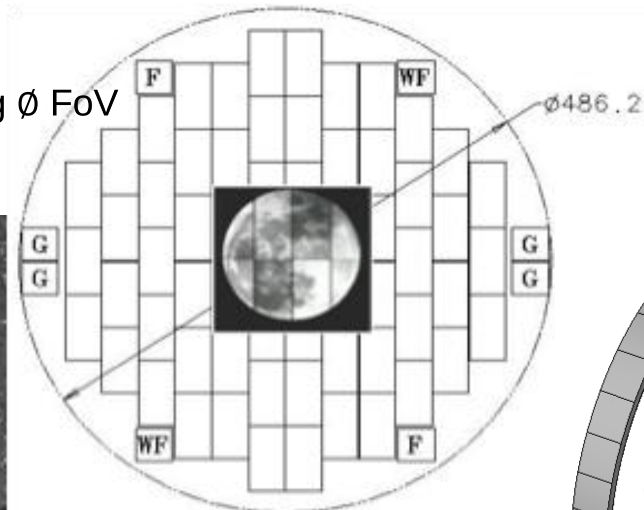

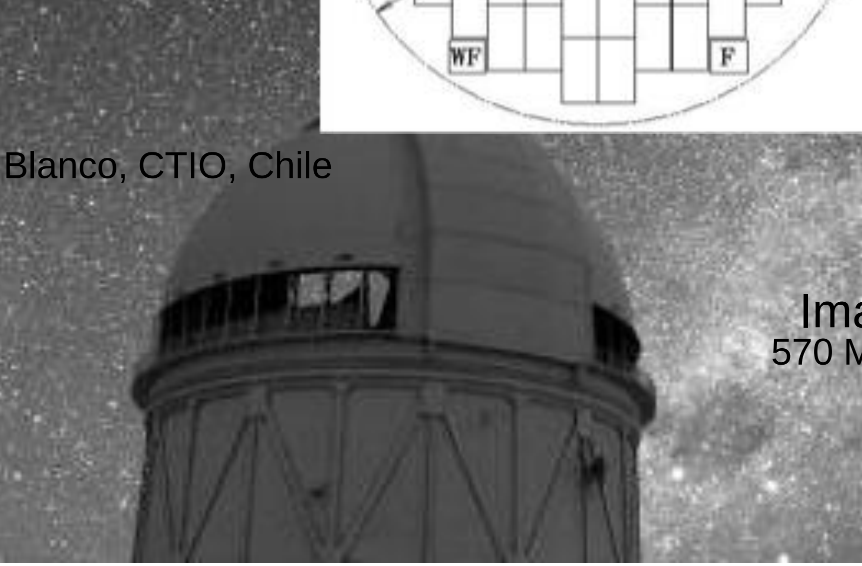

- 525 nights in 5 years
- Started on Aug 31st 2013

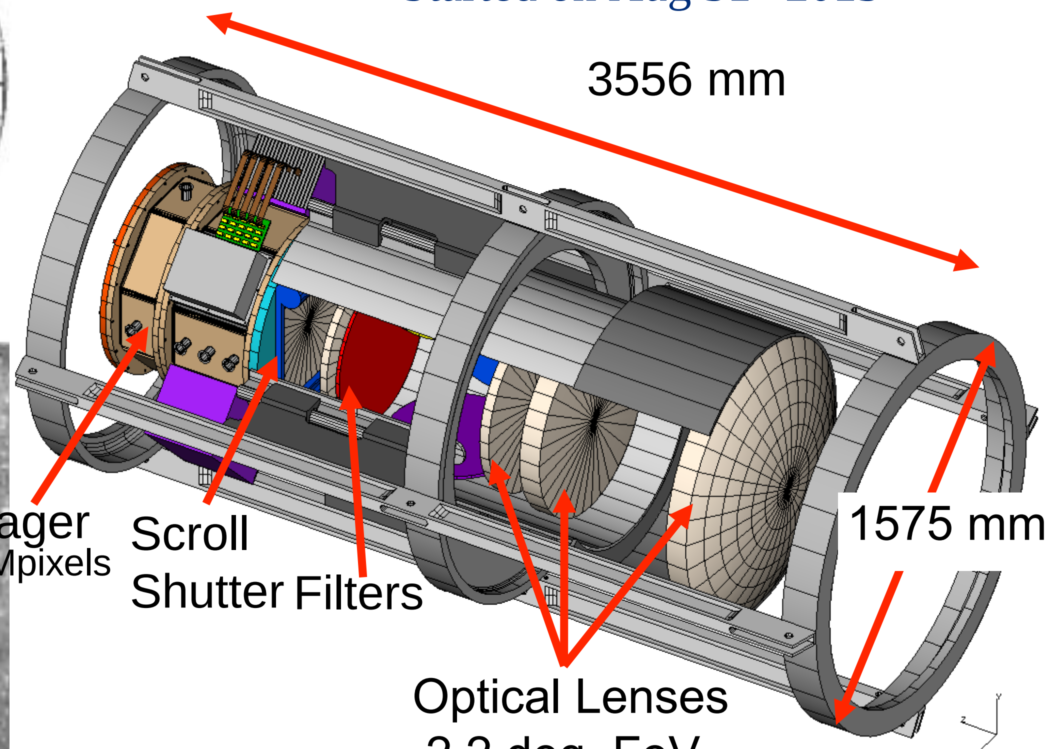

DES Science Program

DARK ENERGY SURVEY

Four Probes of Dark Energy

- Galaxy cluster counting: N(M,z)
  - Measure redshifts and masses
  - ~10,000 clusters to z>1 with M > 2×10^{14} $M_{\odot}$
- Weak lensing (shear)
  - >200 million galaxies with shape measurements to z>1
- Large-scale structure (LSS). Includes BAO
  - ~300 million galaxies to z<1.4
- Supernovae
  - ~4000 type-Ia SNe to z>1

Probes are complementary in both systematic error and cosmological-parameter degeneracies

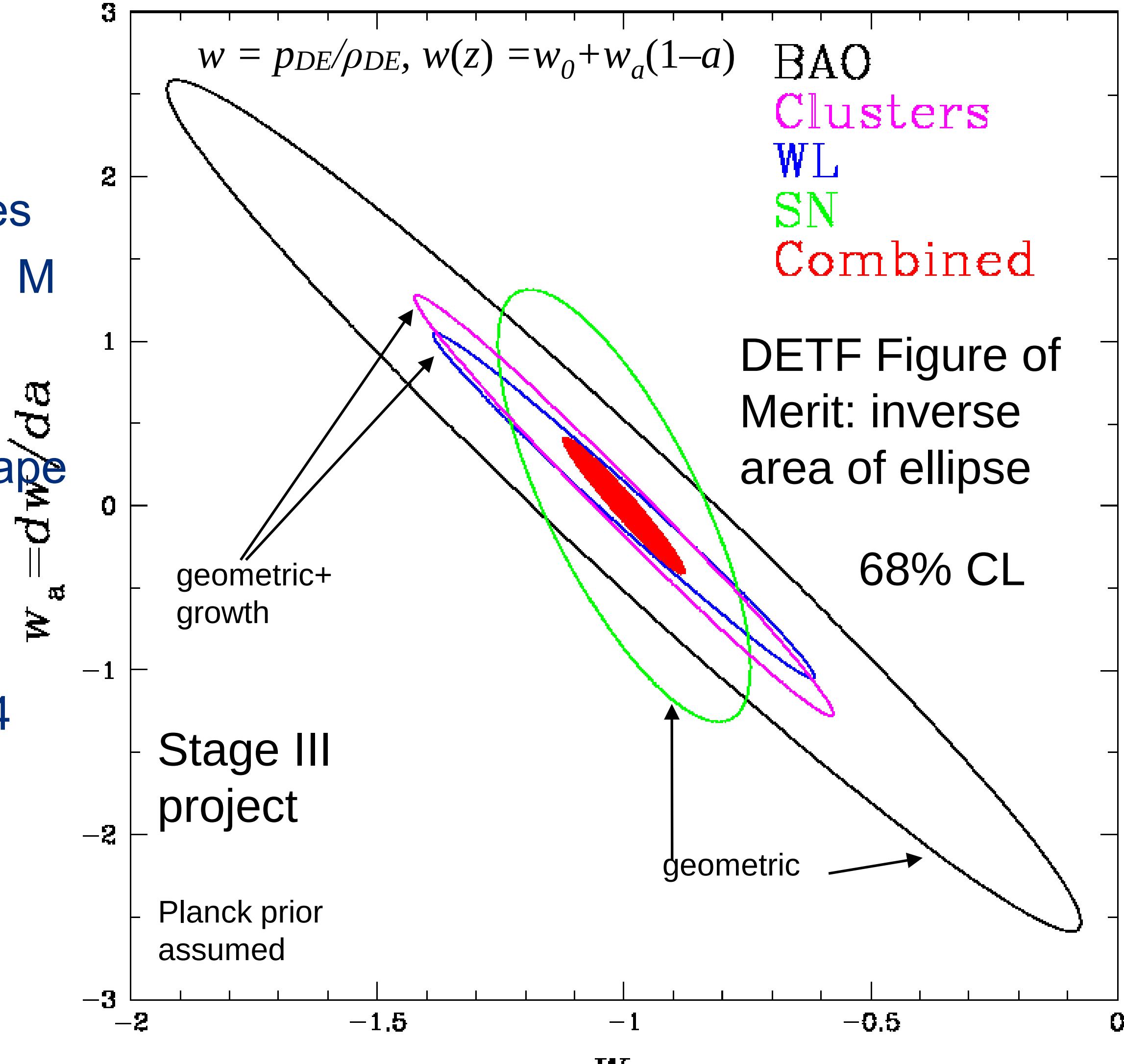

Huterer, Ma, Miquel, Weller, et al. 2007

DARK ENERGY SURVEY

The DES Collaboration

Fermilab — The Fermi National Accelerator Laboratory

Chicago — The University of Chicago

NOAO — The National Optical Astronomy Observatory

United Kingdom DES Collaboration

- UCL - University College London
- Cambridge - University of Cambridge
- Edinburgh - University of Edinburgh
- Portsmouth - University of Portsmouth
- Sussex - University of Sussex
- Nottingham - University of Nottingham

DES-Brazil Consortium

- ON - Observatorio Nacional
- CBPF - Centro Brasileiro de Pesquisas Fisicas
- UFRGS - Universidade Federal do Rio Grande do Sul

OSU — The Ohio State University

TAMU — Texas A&M University

Munich—Universitäts-Sternwarte München

- Ludwig-Maximilians Universität
- Excellence Cluster Universe

UIUC/NCSA — The University of Illinois at Urbana-Champaign

LBNL — The Lawrence Berkeley National Laboratory

Spain DES Collaboration

- IEEC/CSIC - Instituto de Ciencias del Espacio,
- IFAE - Institut de Fisica d'Altes Energies
- CIEMAT - Centro de Investigaciones Energeticas, Medioambientales y Tecnologicas

Michigan — The University of Michigan

Pennsylvania — The University of Pennsylvania

ANL — Argonne National Laboratory

Santa Cruz-SLAC-Stanford DES Consortium

- Santa Cruz - University of California Santa Cruz
- SLAC - SLAC National Accelerator Laboratory
- Stanford - Stanford University

ETH-Zuerich — Eidgenoessische Technische Hochschule Zuerich

DECam Systems

DARK ENERGY SURVEY

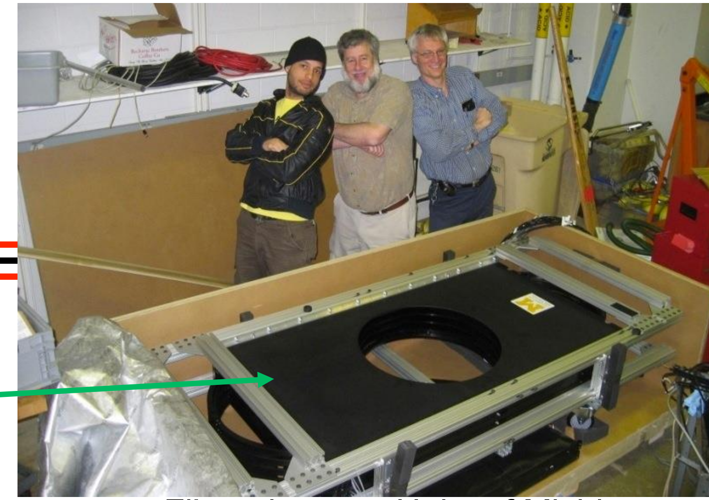

Filter changer, Univ. of Michigan

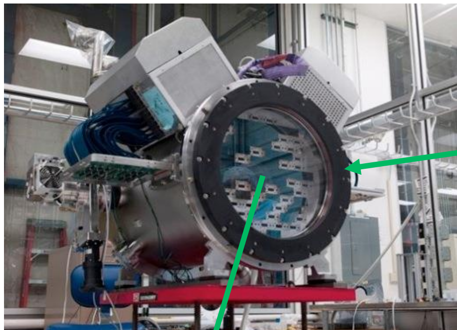

Imager, FNAL

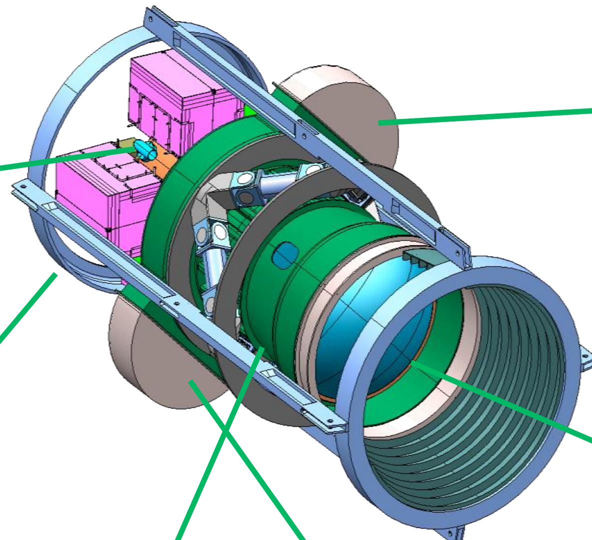

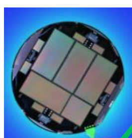

CCDs, wafers from LBL, packaged at FNAL

Barrel and cage, FNAL

Electronics, Spain and FNAL

Hexapod, Italy

Shutter, Germany

Lenses, UK

DES Optical Detectors

DARK ENERGY SURVEY

- New LBNL technology: thick back-illuminated CCD detector.
- Better red response (up to □ = 1 □m) than "thinned" CCDs devices in use at most telescopes.
- High-purity silicon has better radiation tolerance for space

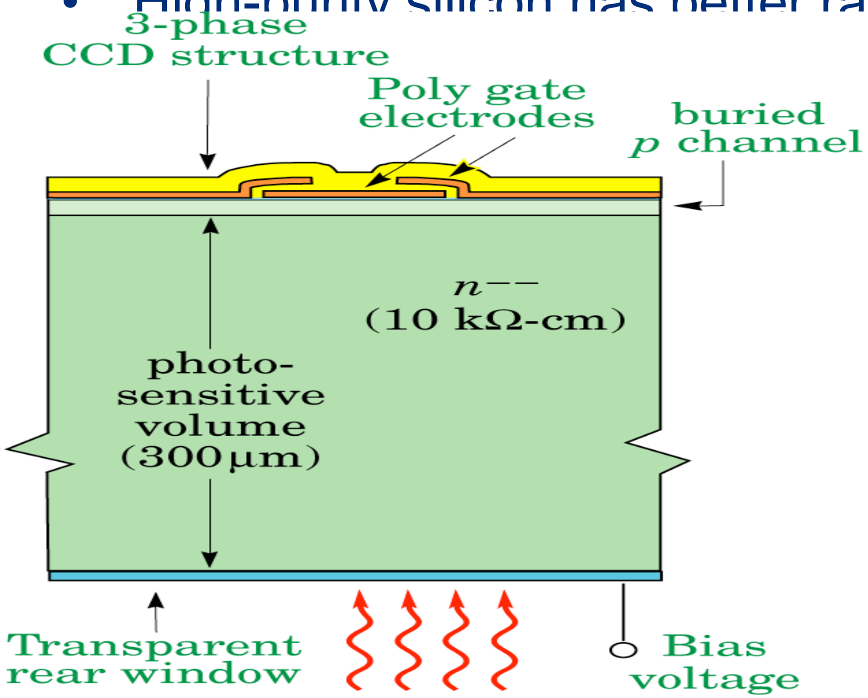

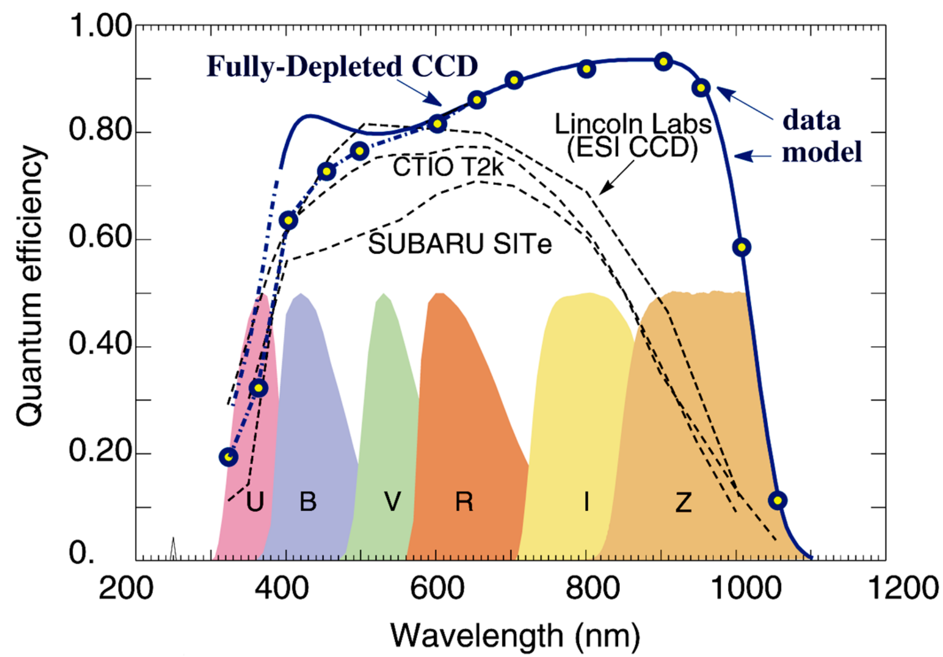

DARK ENERGY SURVEY

DECam Installation

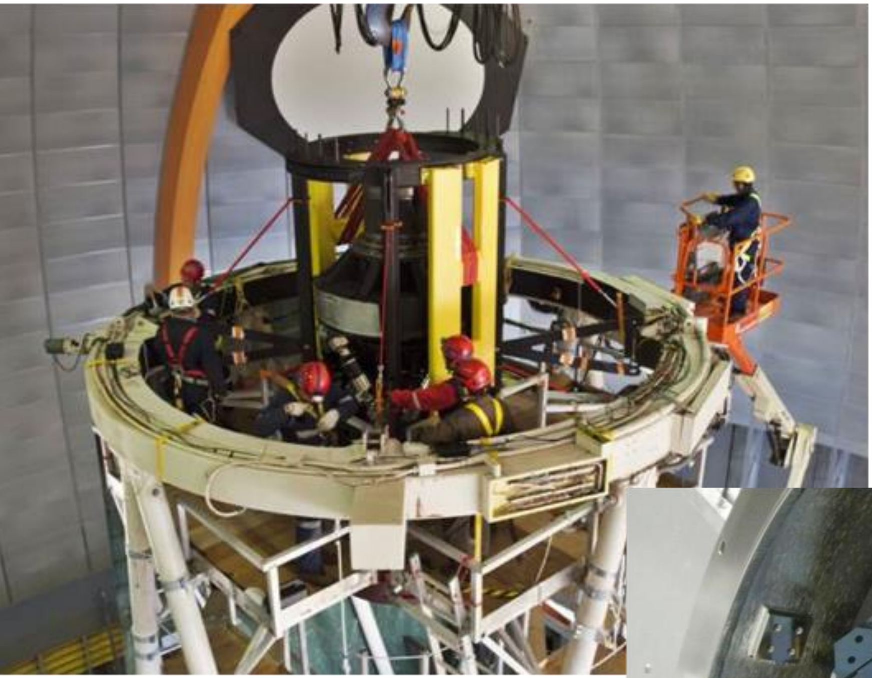

May 2012

July 2012

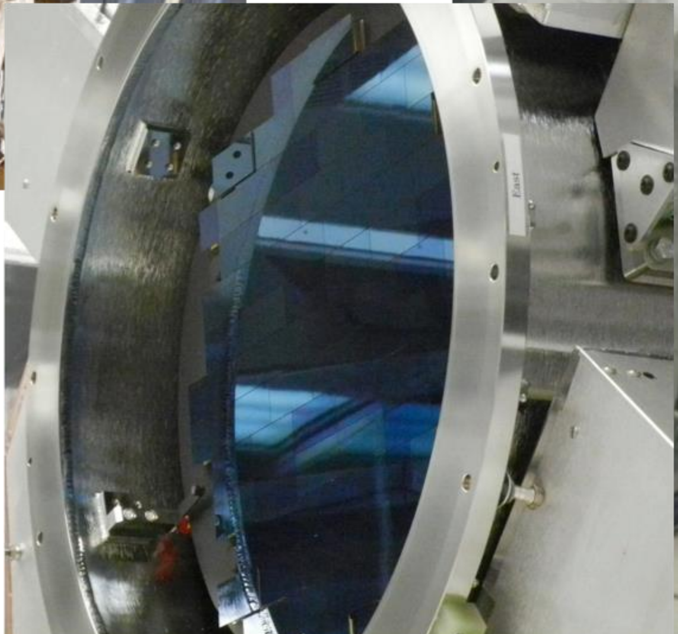

DECam on the Blanco (Sep '12)

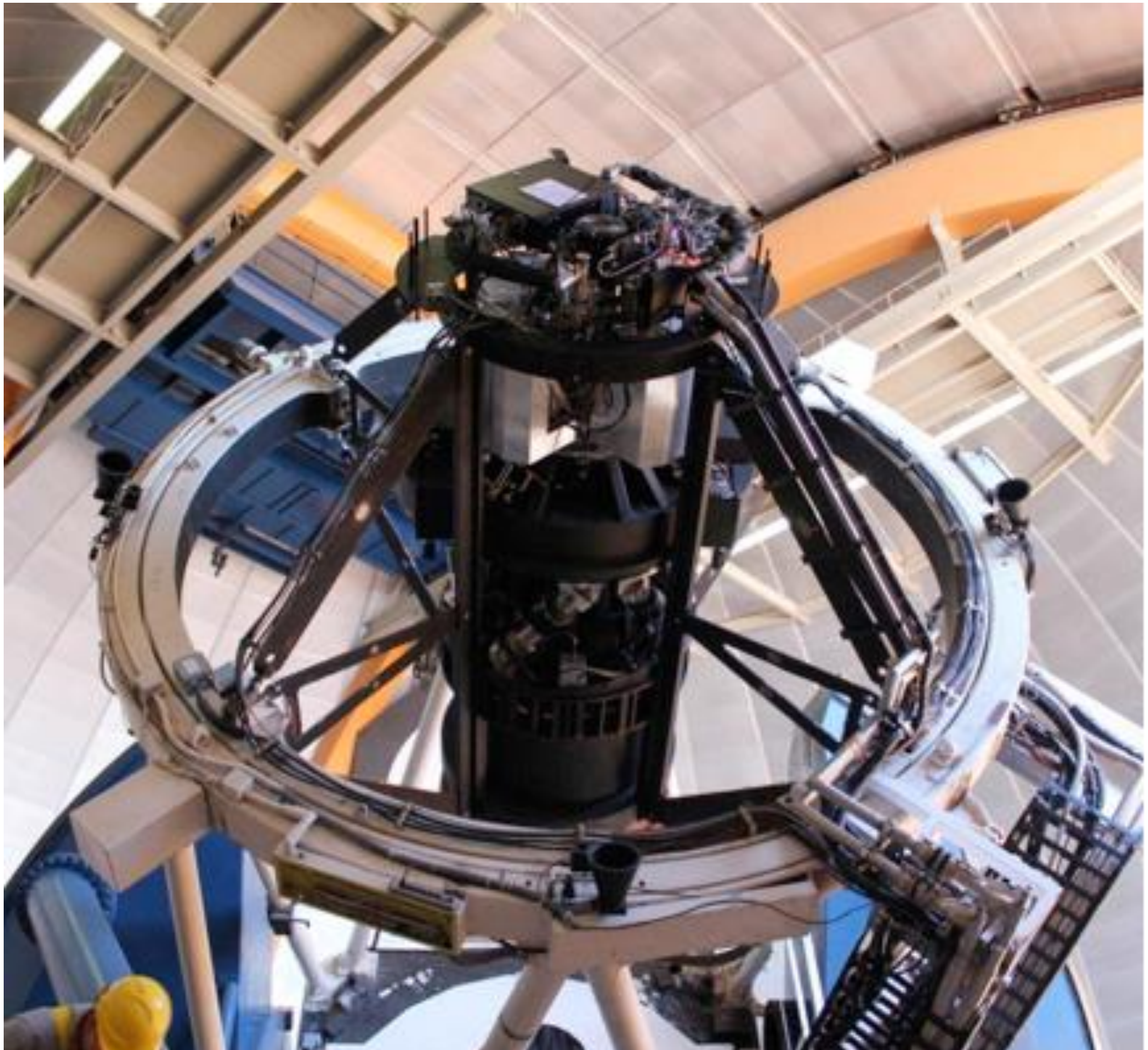

DARK ENERGY SURVEY

First DECam Image

Sep 12, 2012

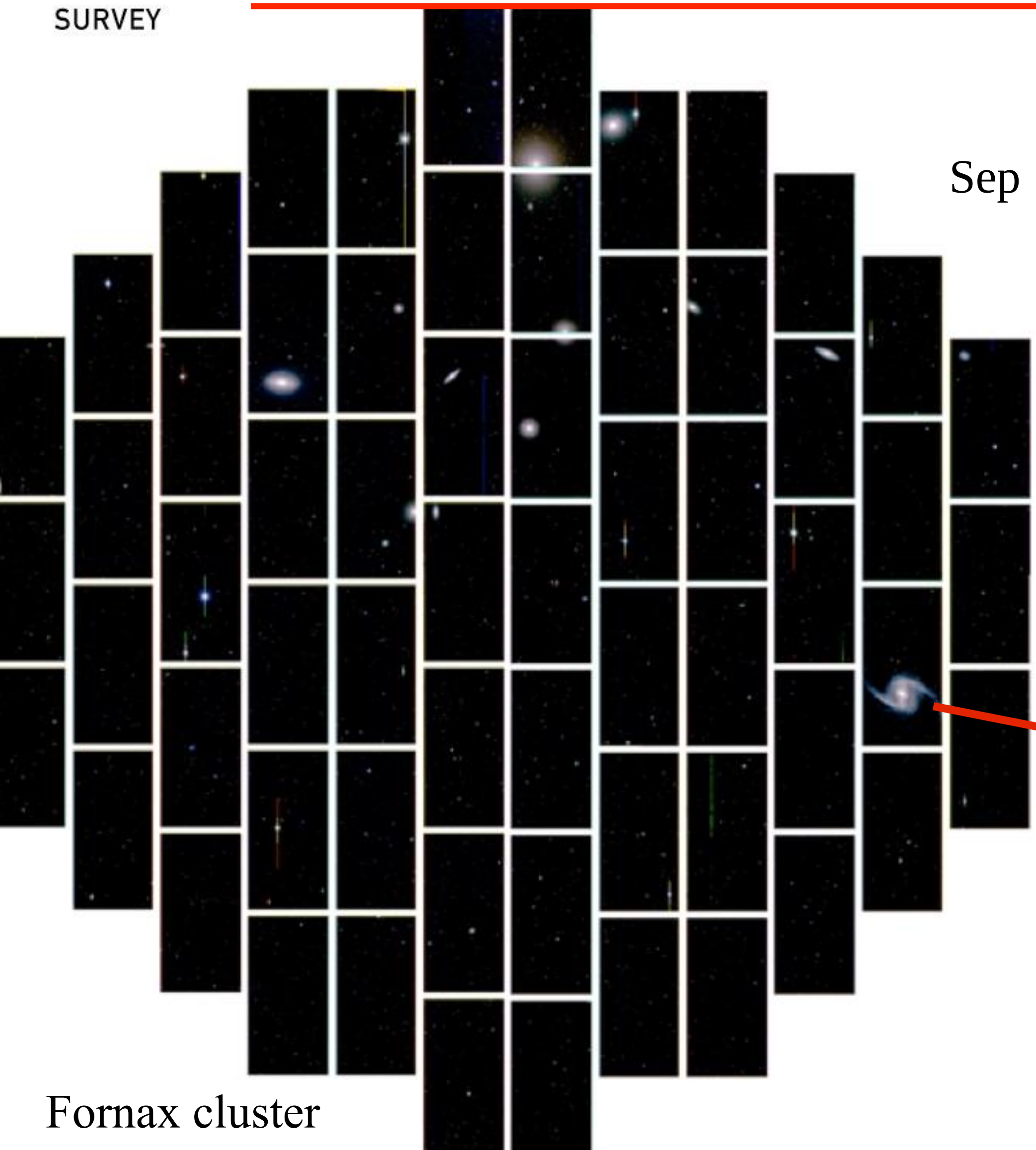

Fornax cluster

NGC 1365

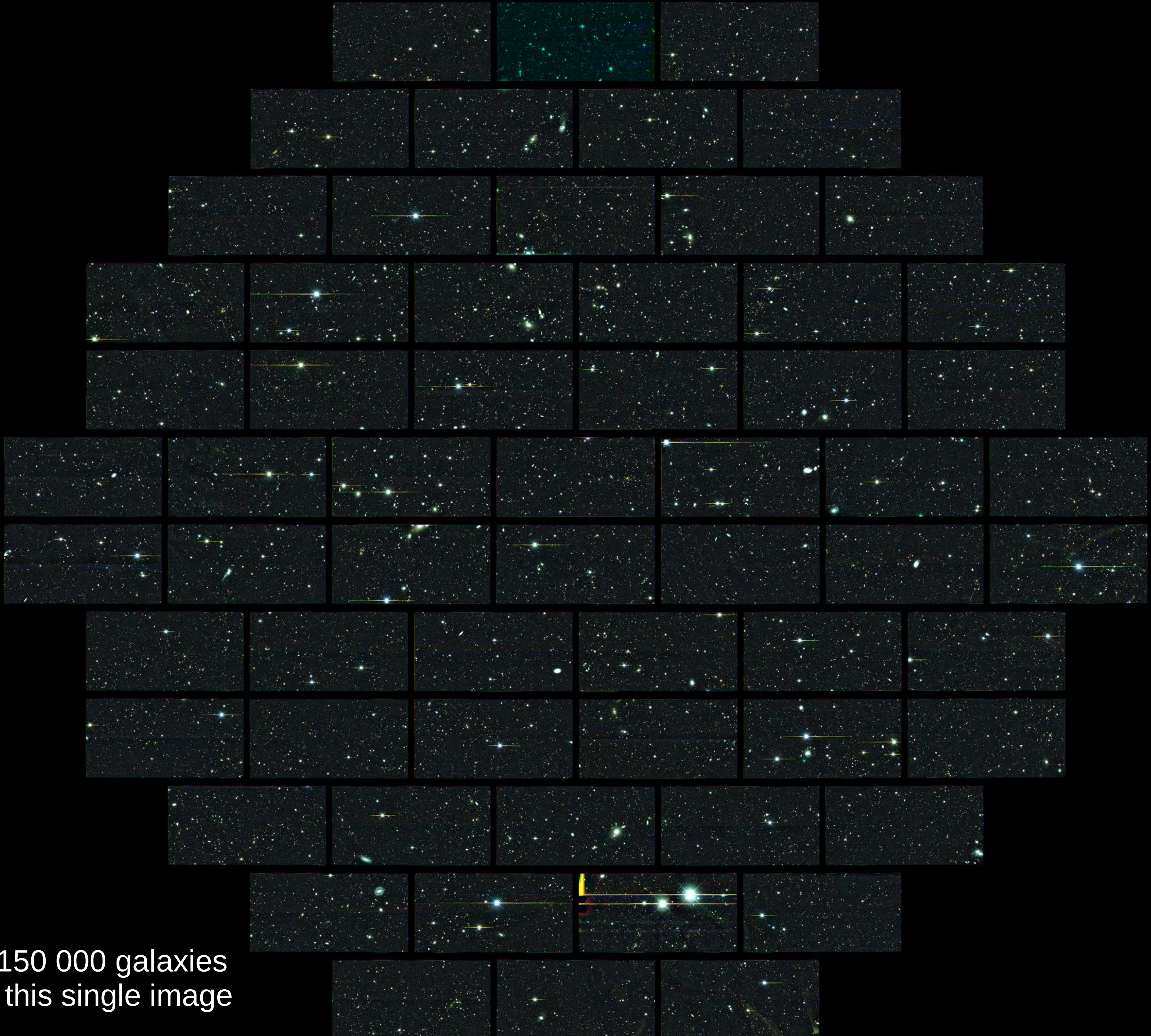

~150 000 galaxies
in this single image

DARK ENERGY
SURVEY

Measuring Galaxy Shapes

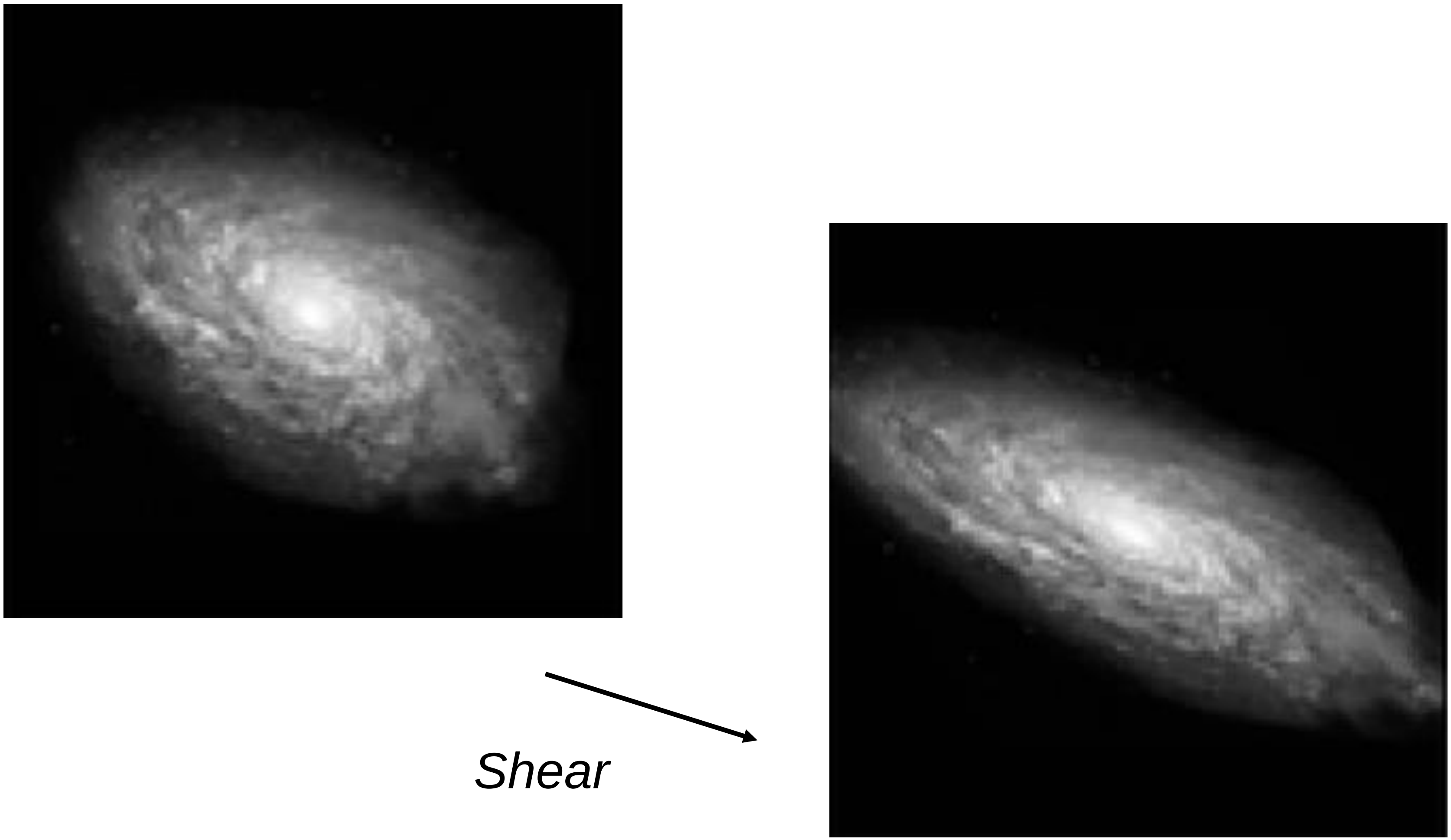

Measuring Galaxy Shapes

Shear+ PSF

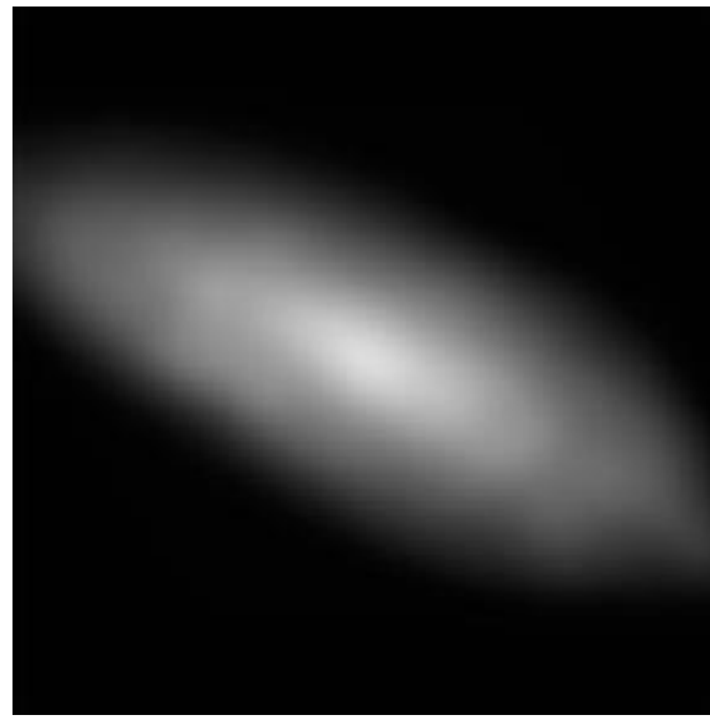

Measuring Galaxy Shapes

Shear+ PSF
+ pixelization

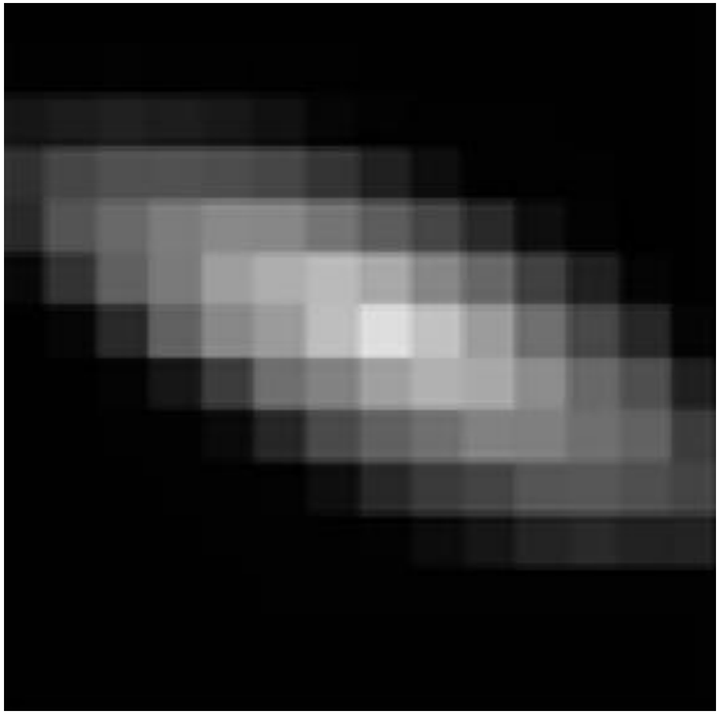

DARK ENERGY SURVEY

Measuring Galaxy Shapes

Shear+ PSF
+ pixelization
+ noise

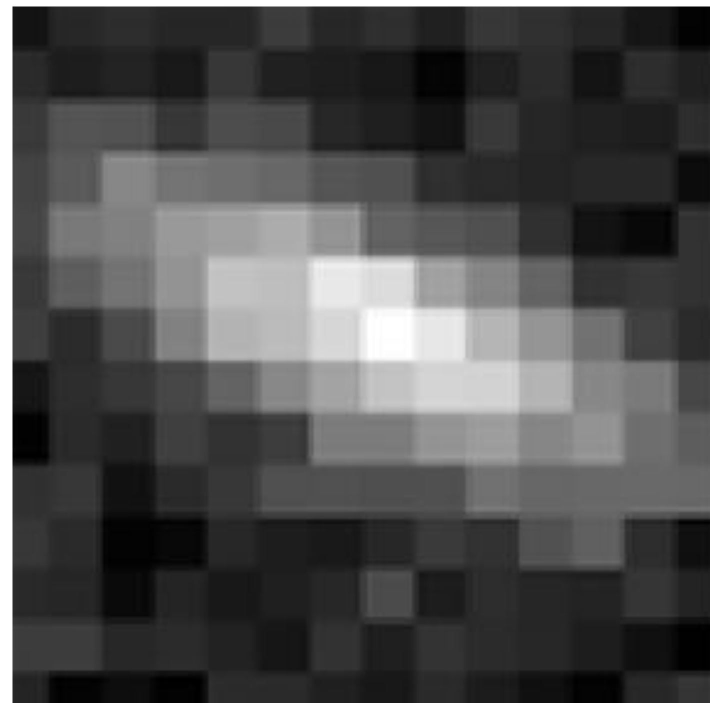

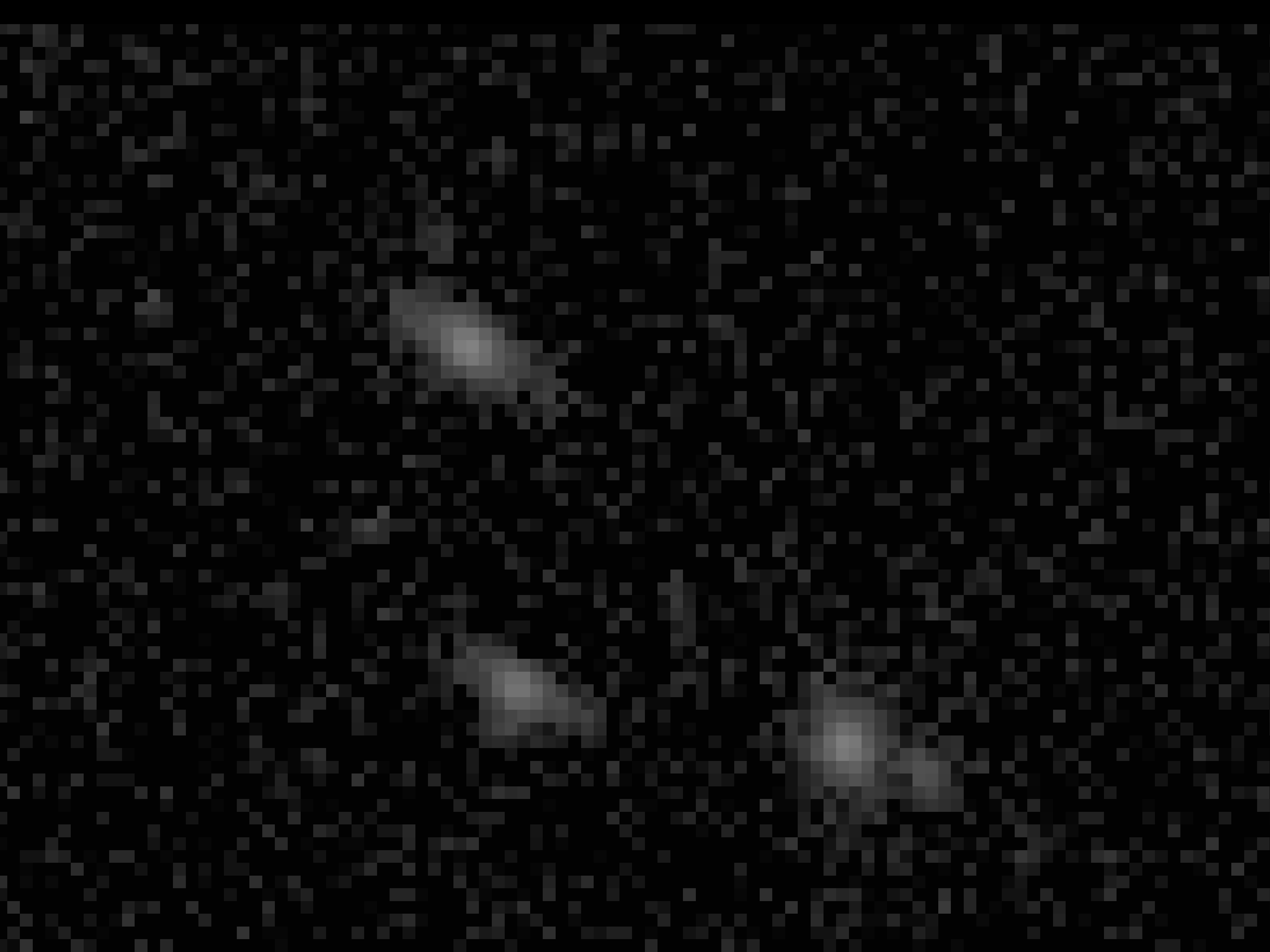

Science Verification (SV): Nov 12 - Feb 13

DARK ENERGY SURVEY

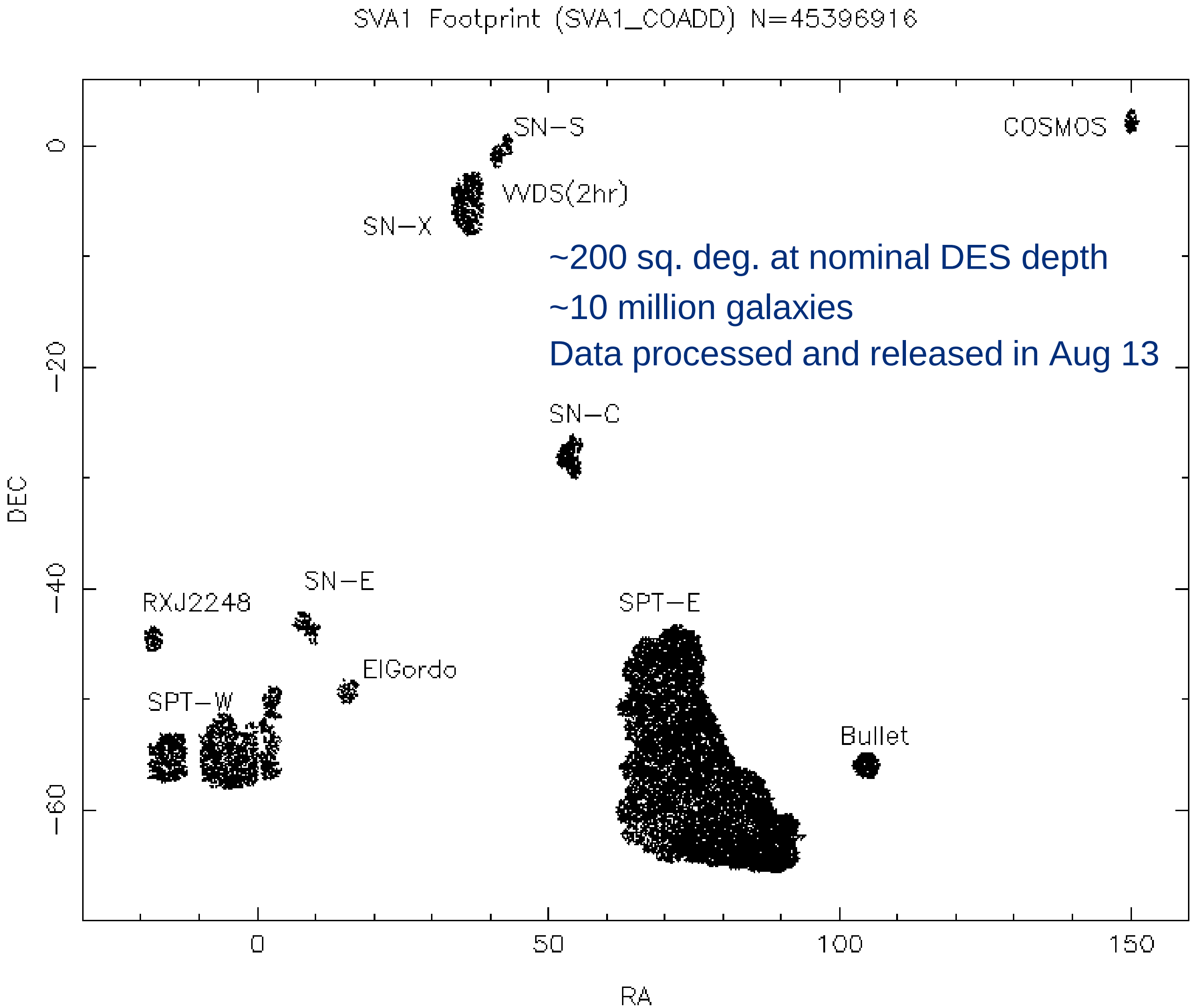

SN Observations During SV

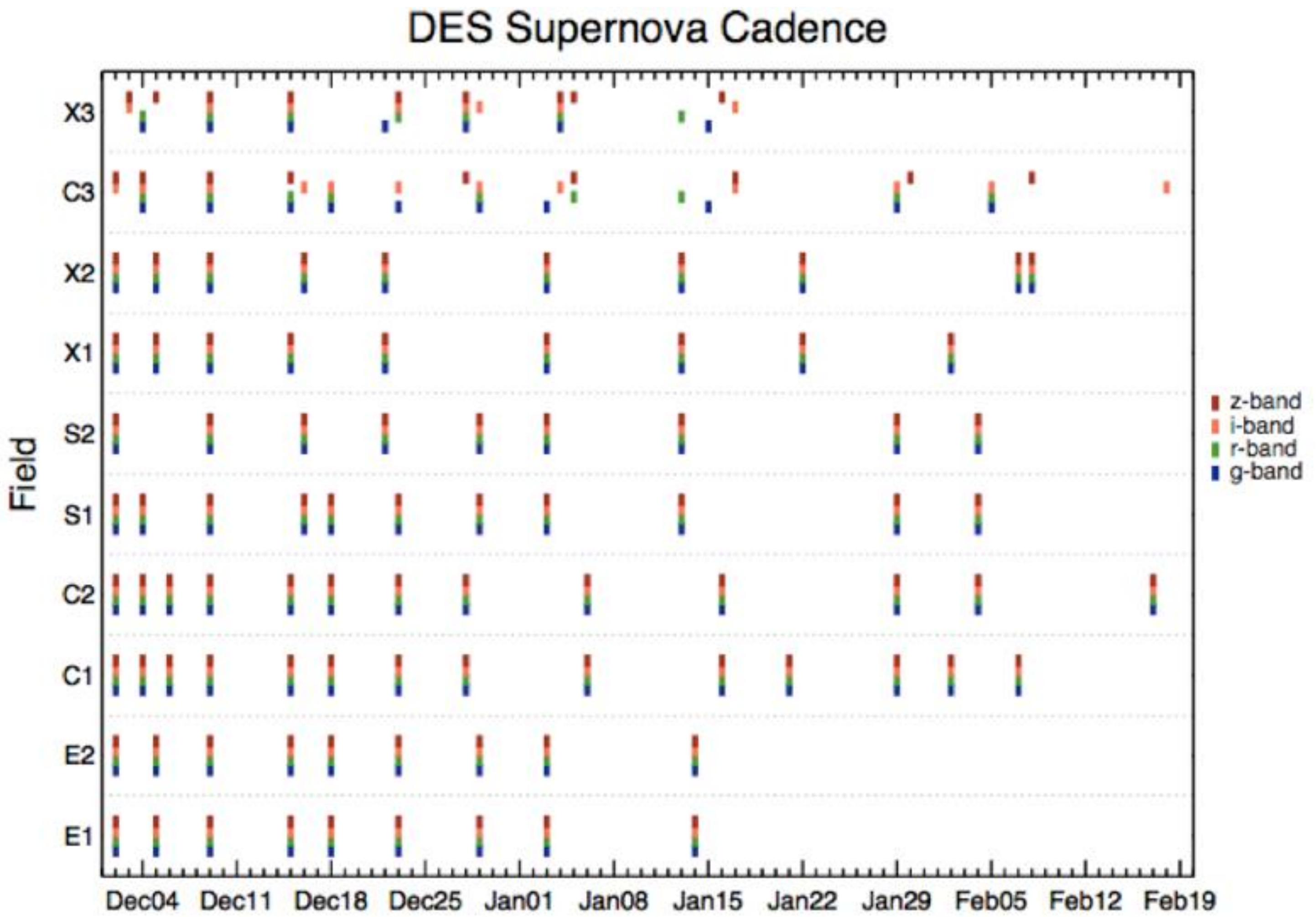

SN fields include photo-z calibration fields

SN Observations During SV

DARK ENERGY SURVEY

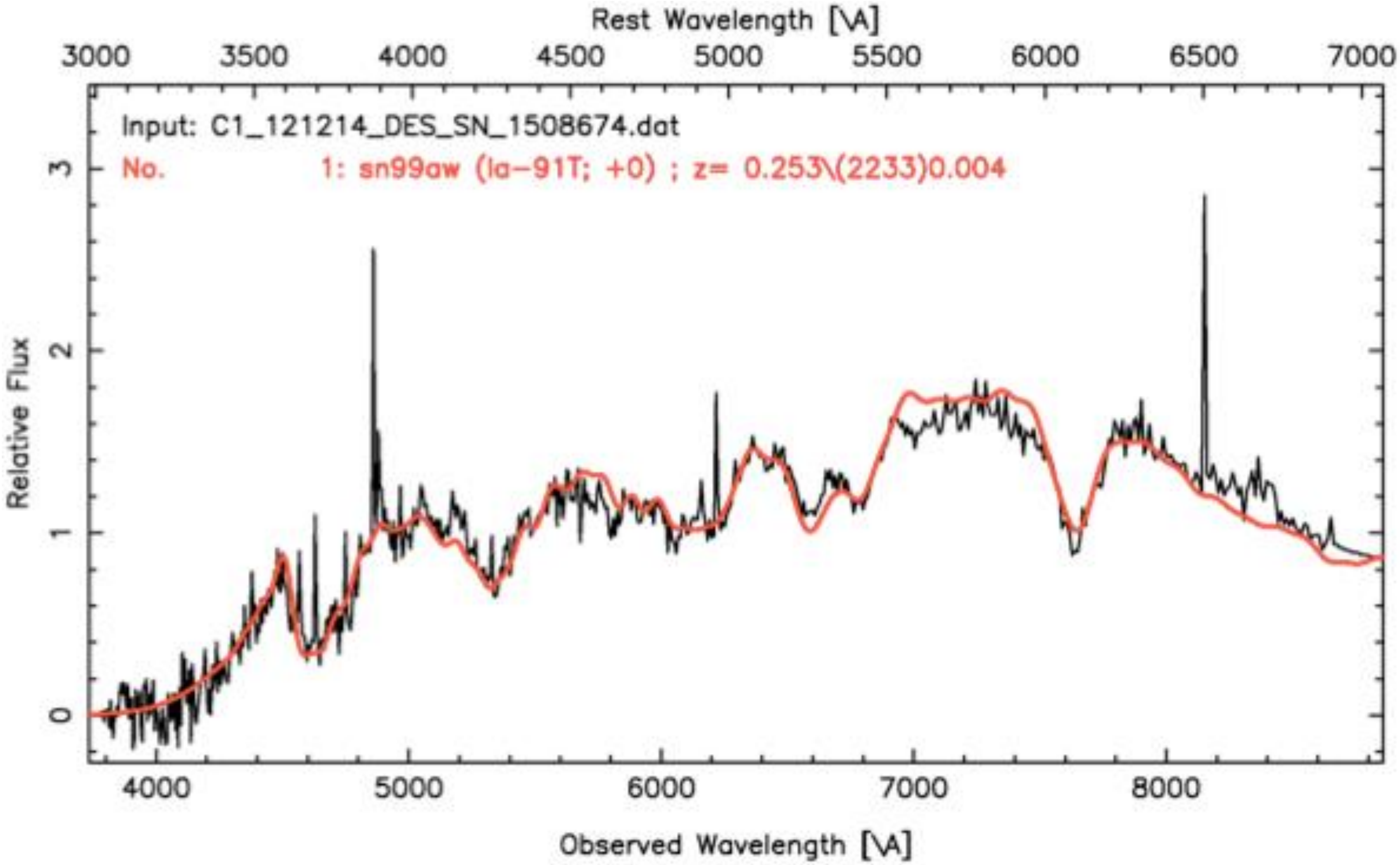

SN fields include photo-z calibration fields

First DES Paper Out on May 16th

DARK ENERGY SURVEY

P. Melchior et al. **Mass and galaxy distributions of four massive galaxy clusters from Dark Energy Survey Science Verification data**

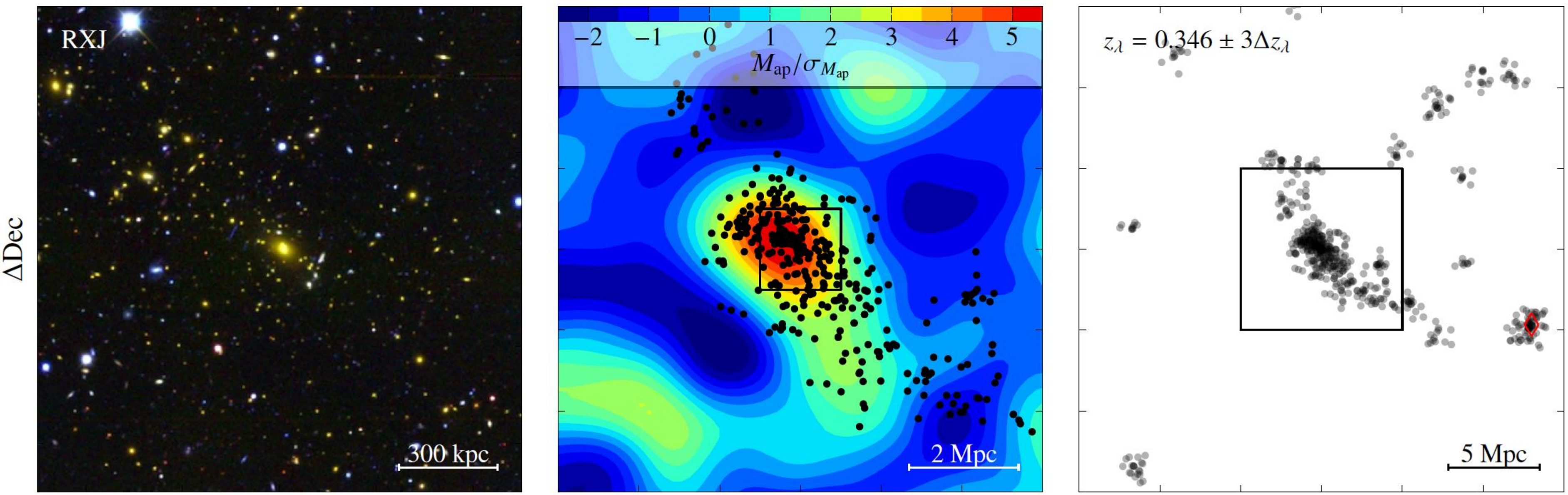

arXiv:1405.4285

First DES Paper Out on May 16th

DARK ENERGY SURVEY

P. Melchior et al. **Mass and galaxy distributions of four massive galaxy clusters from Dark Energy Survey Science Verification data**

Table 4. Weak lensing masses M_{200c} in units of $10^{14} M_{\odot}$ (with a flat prior on c_{200c}), redMaPPer richness λ and redshift estimate z_{λ}, and their statistical errors (see Section 3.2 and Section 5.1 for details). The literature mass estimates are derived from weak lensing, galaxy dynamics (D) or optical richness (R).

Cluster name	M_{200c}	λ	z_{λ}	Literature value M_{200c}
RXC J2248.7-4431	$17.6^{+4.5}_{-4.0}$	203 ± 5	0.346 ± 0.004	$22.8^{+6.6}_{-4.7}$ (Gruen et al. 2013b), 20.3 ± 6.7 (Umetsu et al. 2014), 16.6 ± 1.7 (Merten et al. 2014)
1E 0657-56	$14.2^{+10.0}_{-6.1}$	277 ± 6	0.304 ± 0.004	17.5 (Clowe et al. 2004)[i], 12.4 (Barrena et al. 2002, D)
SCSO J233227-535827	$10.0^{+3.7}_{-3.4}$	77 ± 4	0.391 ± 0.008	$11.2^{+3.0}_{-2.7}$ (Gruen et al. 2013a), $4.9 \pm 3.3 \pm 1.4$ (High et al. 2010, R)
Abell 3261	$8.6^{+8.6}_{-3.9}$	71 ± 3	0.216 ± 0.003	—

[i] We converted the measured r_{200c} from Clowe et al. (2004), which lacks an error estimate, to M_{200c} using the critical density in our adopted cosmology.

This paper proves that DES can measure galaxy shapes, even in the Science Ve

Photometric redshift analysis in the Dark Energy Survey Science Verification data

C. Sánchez[1*], M. Carrasco Kind[2], H. Lin[3], R. Miquel[1,4], F. B. Abdalla[5], A. Amara[6], M. Banerji[5], C. Bonnett[1], R. Brunner[2], D. Capozzi[7], A. Carnero[8,9], F. J. Castander[10], L. A. N. da Costa[8,9], C. Cunha[11], A. Fausti[9], D. Gerdes[12], N. Greisel[13,14], J. Gschwend[8,9], W. Hartley[6,15], S. Jouvel[5], O. Lahav[5], M. Lima[16,9], M. A. G. Maia[8,9], P. Martí[1], R. L. C. Ogando[8,9], F. Ostrovski[8,9], P. Pellegrini[8], M. M. Rau[13,14], I. Sadeh[5], S. Seitz[13,14], I. Sevilla-Noarbe[17], A. Sypniewski[12], J. de Vicente[17], T. Abbot[18], S. S. Allam[19,3], D. Atlee[20], G. Bernstein[21], J. P. Bernstein[22], E. Buckley-Geer[3], D. Burke[23,11], M. J. Childress[24,25], T. Davis[26,25], D. L. DePoy[27], A. Dey[20,28], S. Desai[29,30], H. T. Diehl[3], P. Doel[5], J. Estrada[3], A. Evrard[12,31,32], E. Fernández[1], D. Finley[3], B. Flaugher[3], E. Gaztanaga[10], K. Glazebrook[33], K. Honscheid[34], A. Kim[35], K. Kuehn[36], N. Kuropatkin[3], C. Lidman[36], M. Makler[37], J. L. Marshall[27], R. C. Nichol[7], A. Roodman[23,11], E. Sánchez[17], B. X. Santiago[38,9], M. Sako[21], R. Scalzo[24], R. C. Smith[18], M. E. C. Swanson[39], G. Tarle[12], D. Thomas[7,40], D. L. Tucker[3], S. A. Uddin[33,25], F. Valdés[20], A. Walker[18], F. Yuan[24,25], J. Zuntz[41]

18 June 2014

Second DES science paper

ABSTRACT

We present results from a study of the photometric redshift performance of the Dark Energy Survey (DES), using the early data from a Science Verification (SV) period of observations in late 2012 and early 2013 that provided science-quality images for almost 200 sq. deg. at the nominal depth of the survey. We assess the photometric redshift performance using about 15000 galaxies with spectroscopic redshifts available from other surveys. These galaxies are used, in different configurations, as a calibration sample, and photo-z's are obtained and studied using most of the existing photo-z codes. A weighting method in a multi-dimensional color-magnitude space is applied to the spectroscopic sample in order to evaluate the photo-z performance with sets that mimic the full DES photometric sample, which is on average significantly deeper than the calibration sample due to the limited depth of spectroscopic surveys. Empirical photo-z methods using, for instance, Artificial Neural Networks or Random Forests, yield the best performance in the tests, achieving core photo-z resolutions $\sigma_{68} \sim 0.08$. Moreover, the results from most of the codes, including template fitting methods, comfortably meet the DES requirements on photo-z performance, therefore, providing an excellent precedent for future DES data sets.

arXiv:1406.4407
(in press in MNRAS)

Photo-z Calibration Fields in DES SV

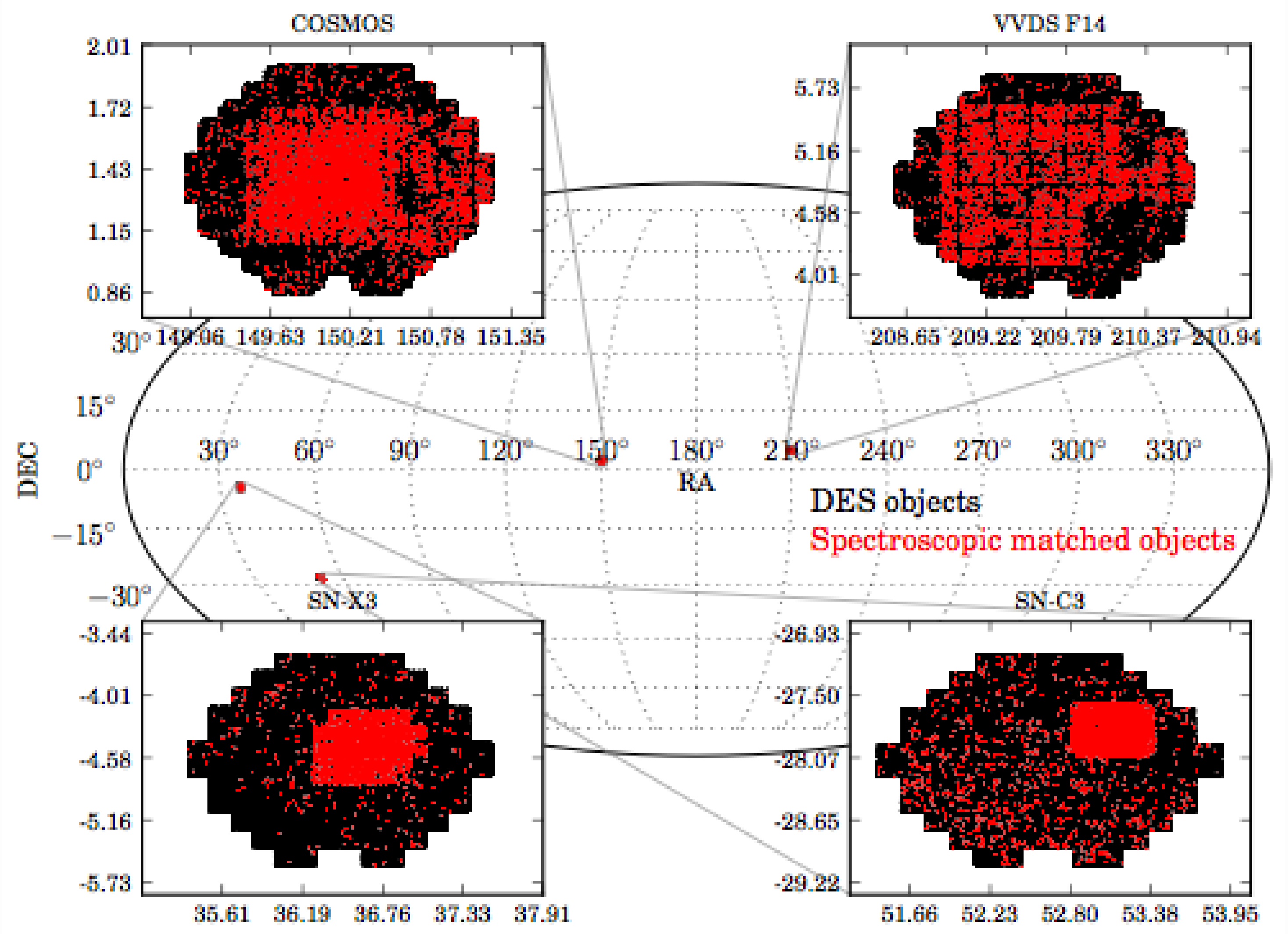

Photometry:
grizY
$18 < i_{AB} < 24$
$0 < g\text{-}r < 2$
$0 < r\text{-}i < 2$

Spectroscopy:
$0.01 < z < 1.4$
$3 \leq z\_flag < 5$
about 15600 gal

DARK ENERGY SURVEY

13 Photo-z Algorithms Have Been Tried

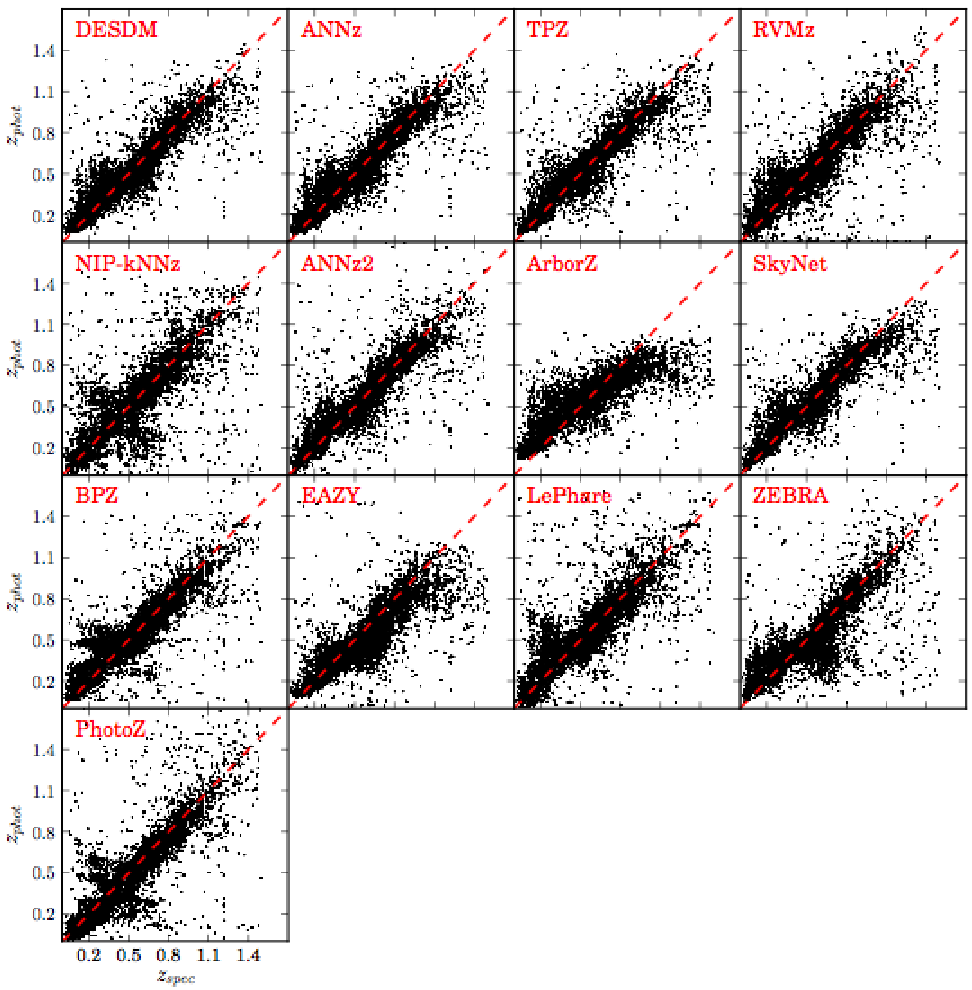

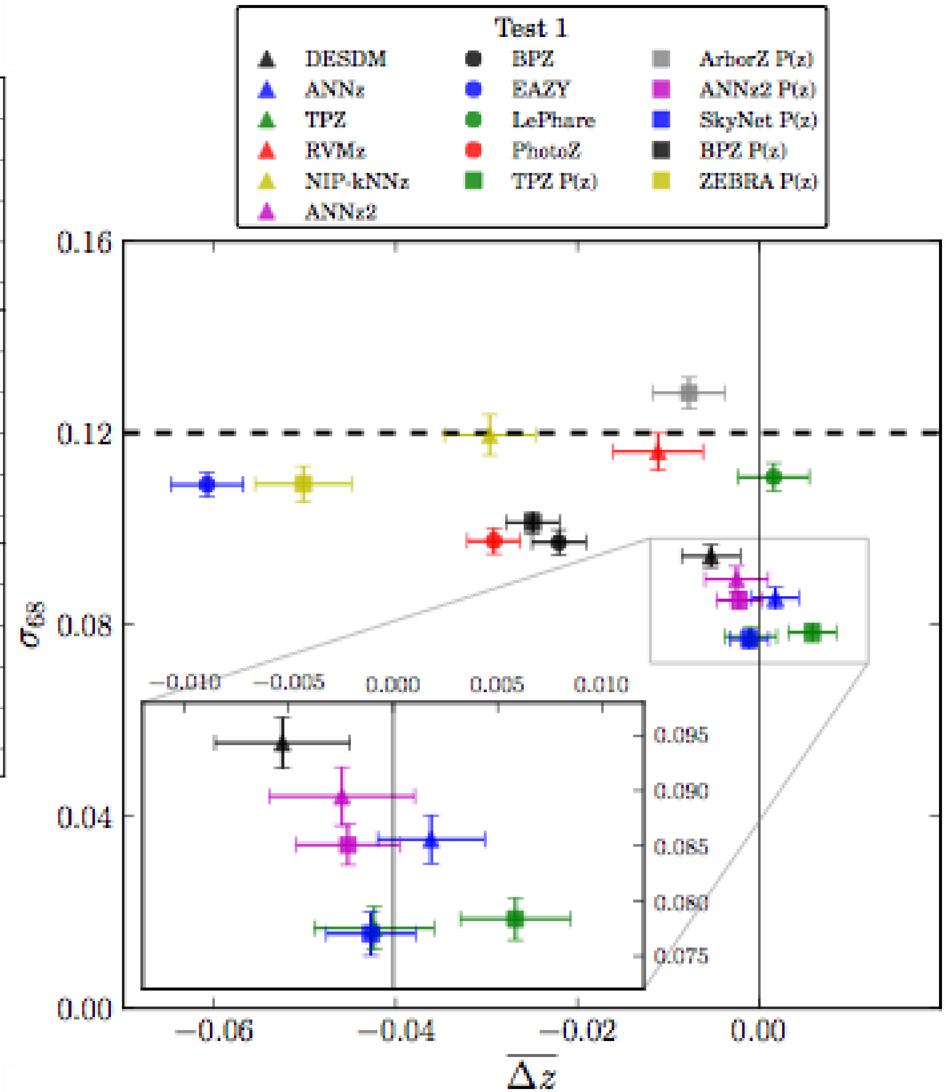

Four Algorithms Studied in More Detail

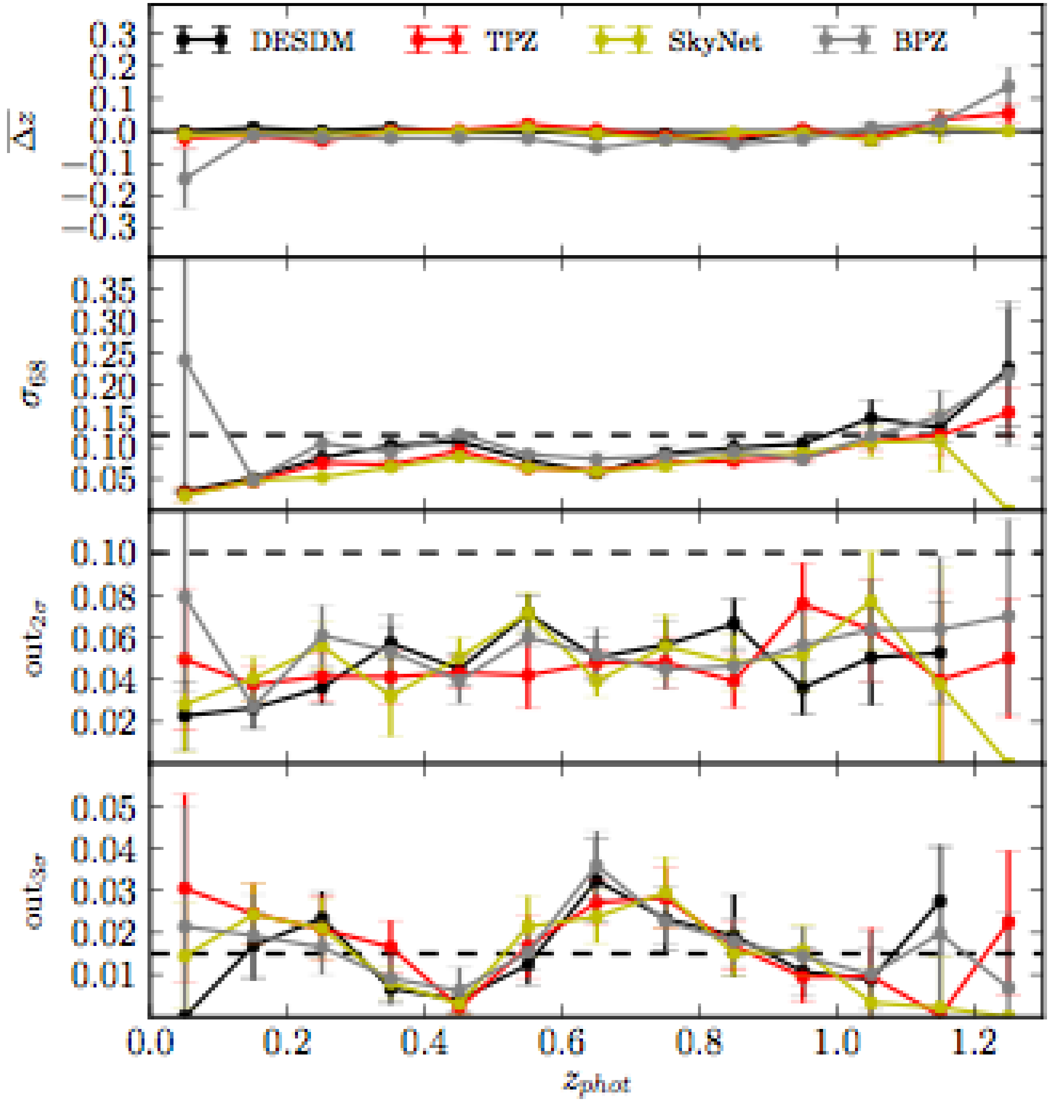

Calibrated True N(z) in Photo-z Bins

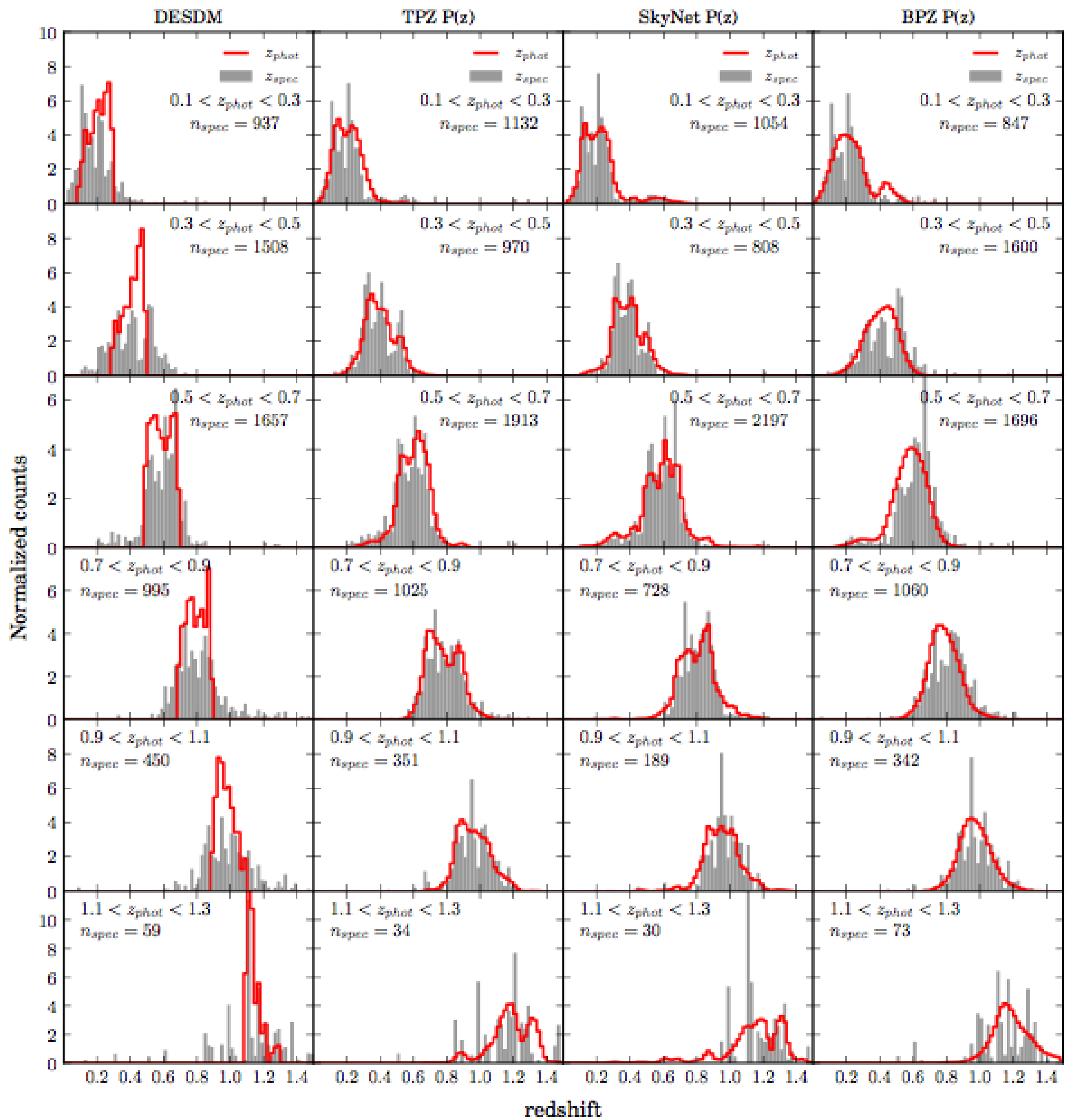

Example: DESDM Artificial Neural Net

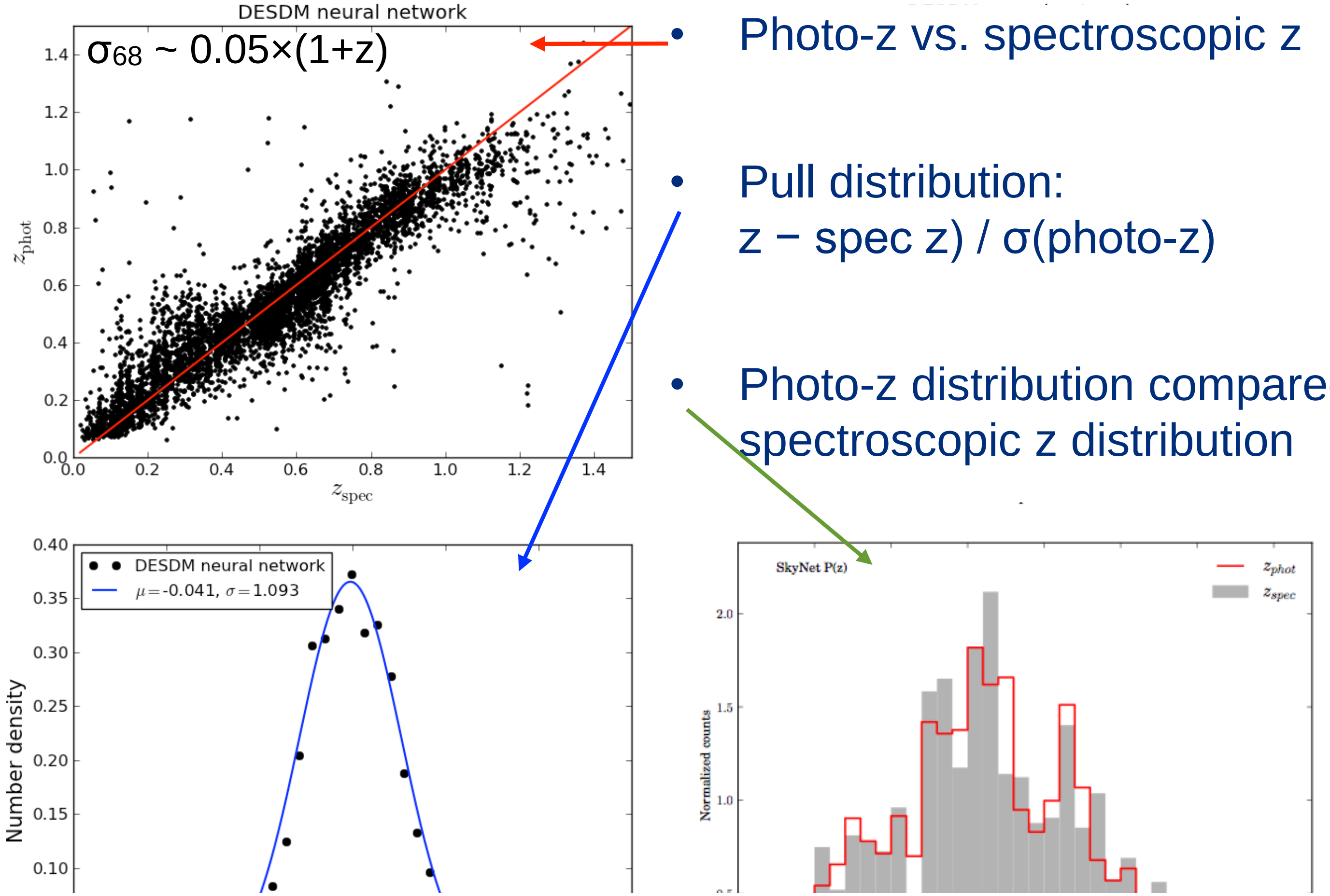

- Photo-z vs. spectroscopic z
- Pull distribution: (photo-z − spec z) / σ(photo-z)
- Photo-z distribution compared to spectroscopic z distribution

This paper proves that DES can measure colors, even in the Science Verific

Other SV Analyses in the Pipeline

Joint Optical and Near Infrared Photometry from DES and VHS ✔

Galaxy Clustering and validation against CFHTLS

DES SV Galaxies cross-correlated with CMB lensing

SPT-SZE signature of DES SV RedMaPPer clusters

Galaxy Populations within SPT Selected Clusters

DES/XCS: X-ray properties of galaxy clusters in DES SV

The Dark Energy Survey SV Shear Catalogue: Pipeline and tests

Calibrated Ultra Fast Image Simulations for the Dark Energy Survey

DES13S2cmm: The first Super-luminous Supernova from DES

The Dark Energy Survey Supernova Survey: Search Strategy and Algorithm

Wide-Field Mass Mapping with the DES SVA1 data

SV Data Analyses

DARK ENERGY SURVEY

LSS: Galaxy-galaxy correlations

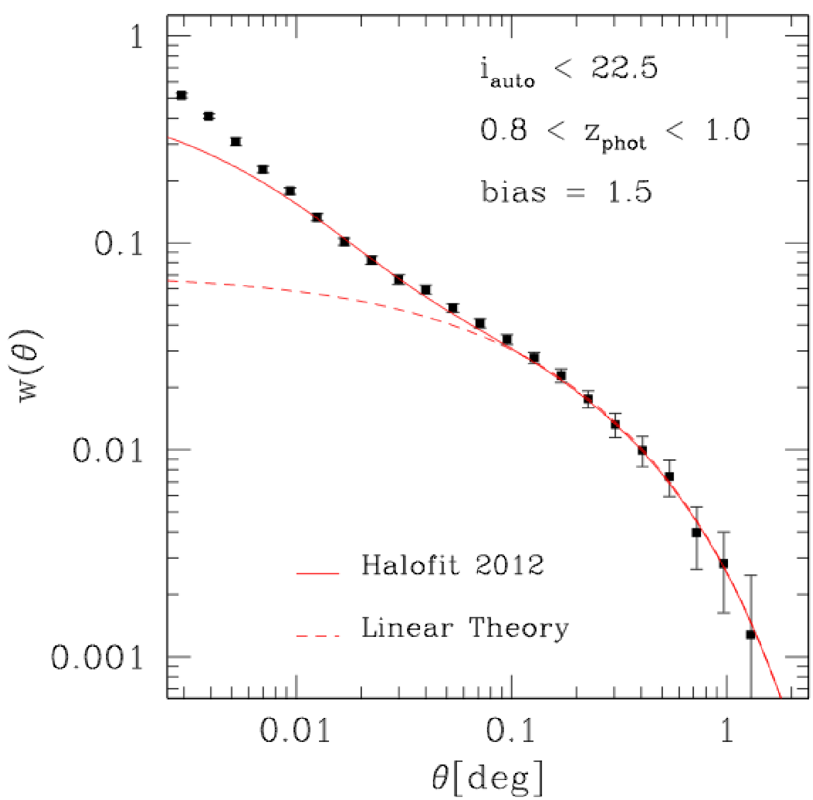

Weak lensing: Galaxy-shear correlations

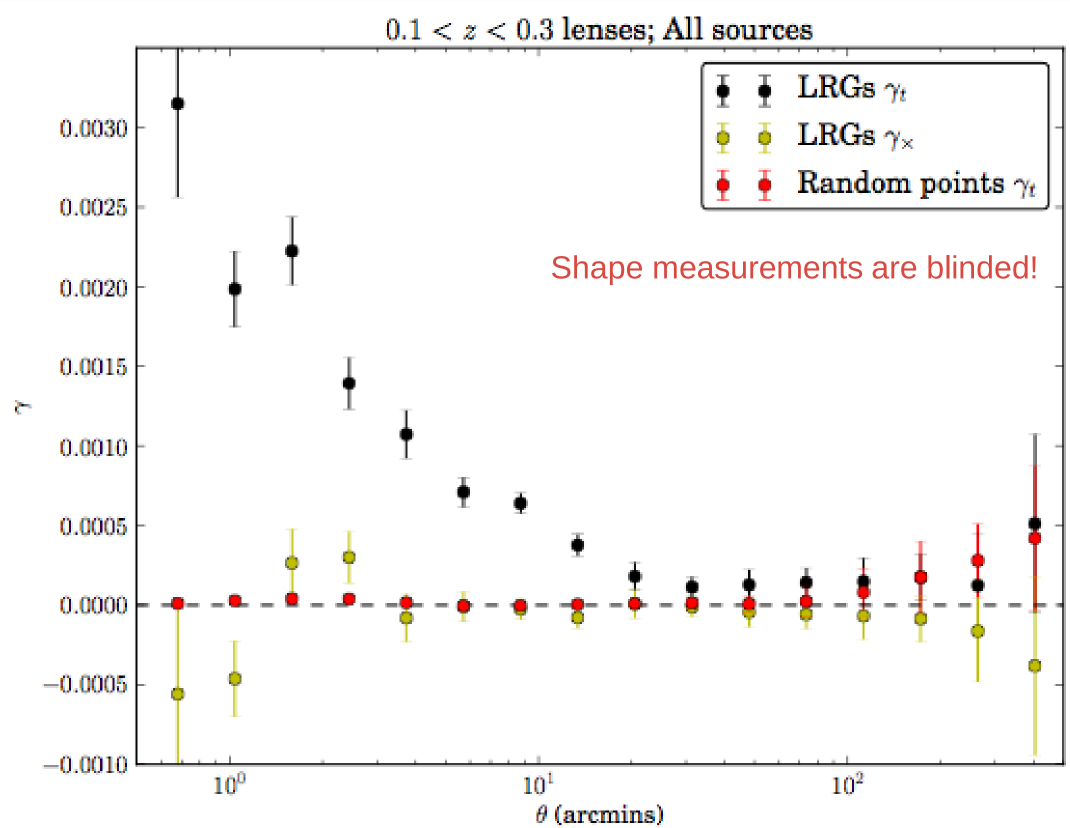

Analyses on LSS and on WL+LSS combination in DES-SV are led by DES/Spain scientists

Survey Strategy for Year 1

Year 1 of 5 (Sep '13 - Feb '14)

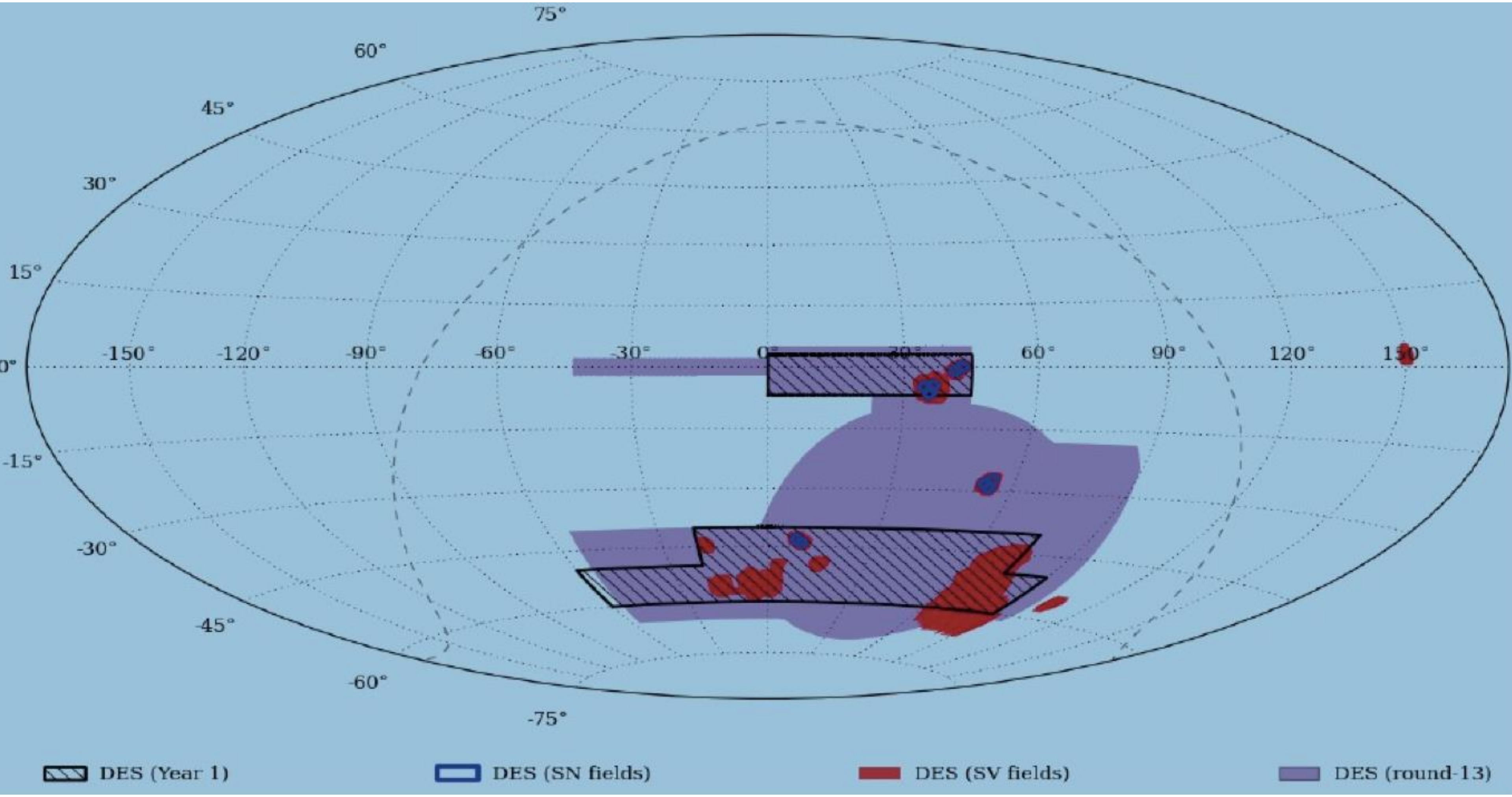

2000+ sq. deg., 4 tilings grizY + SN fields Data being processed

PSF FWHM for Y1 Data

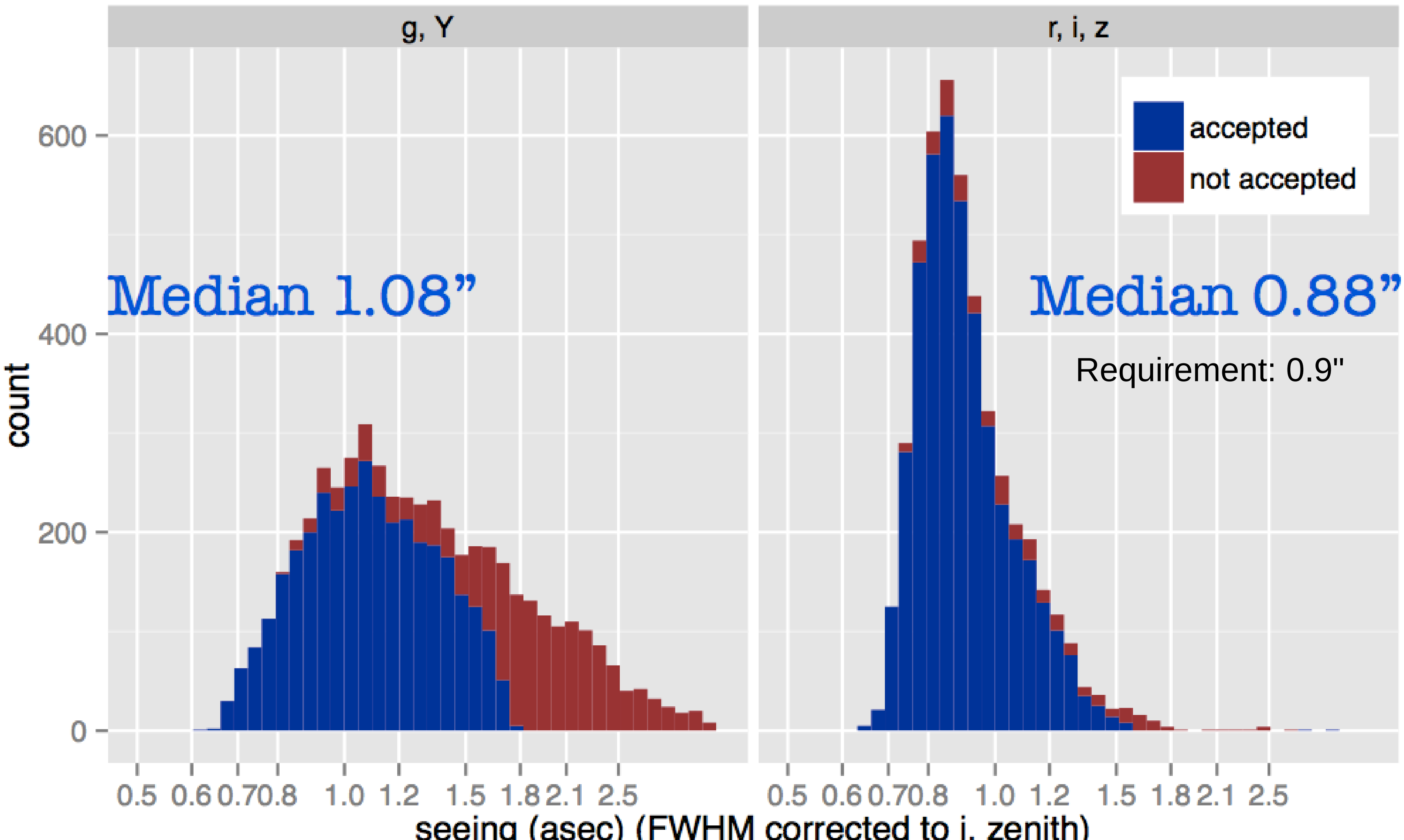

DES Summary

- DES successfully started data taking in Nov. 2012, with a Science Verification (SV) period.
- Science Verification data have enough quality to do first science with them.
- DES/Spain leading in several areas of SV analysis: calibration, photo-zs, galaxy-galaxy correlations, galaxy-galaxy lensing.
- Very fruitful collaboration between DES/Spain institutions: CIEMAT / ICE (IEEC-CSIC) / IFAE / UAM.
- DES survey started in Aug. 2013, will last till Feb. 2018.
- Looking forward to analyses with Year 1 data sample and beyond.

PAU

The PAU Survey at the WHT

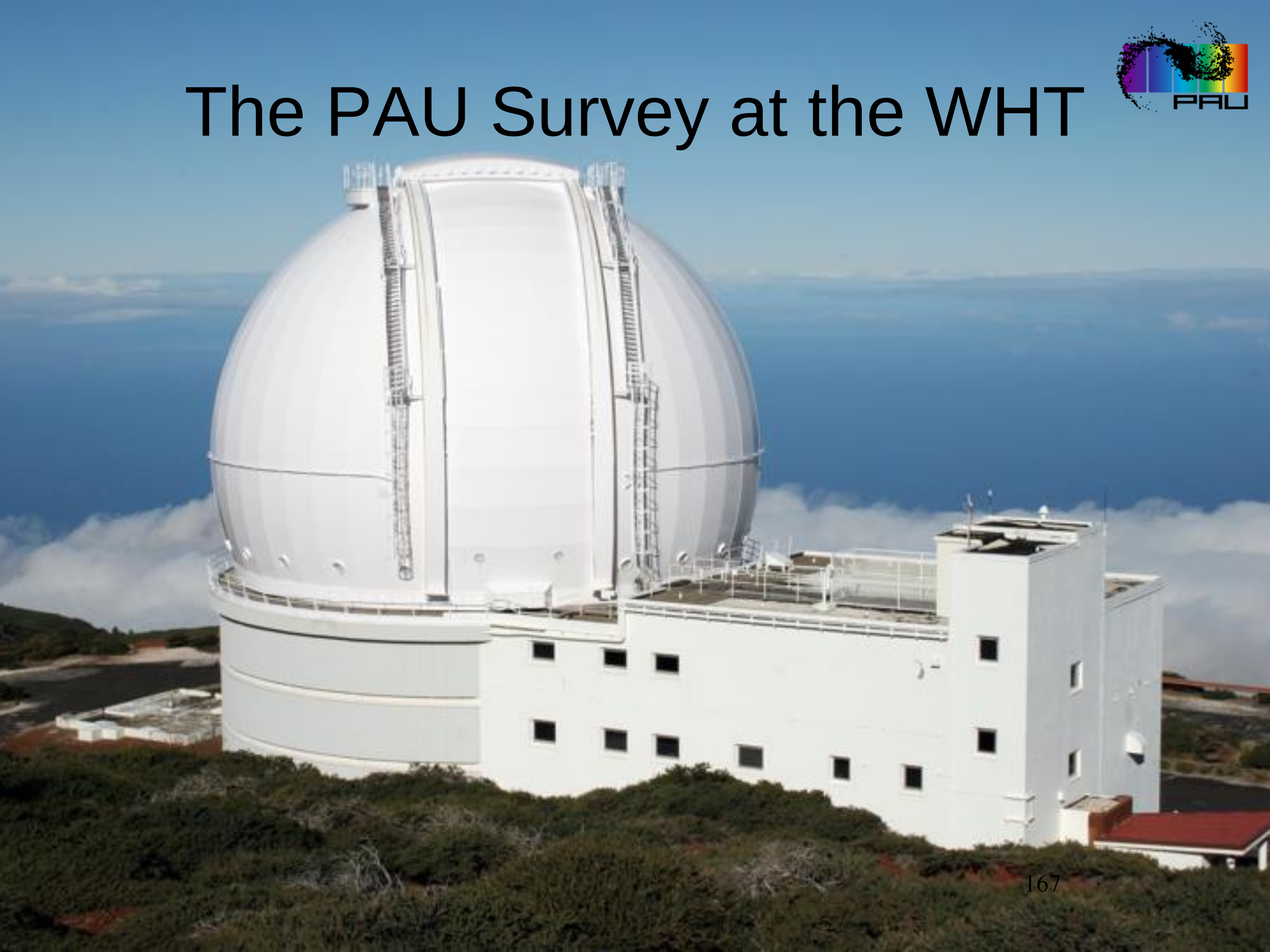

The PAU@WHT Project in a Nutshell

- New camera for WHT with **18 2k x 4k CCDs** covering 1 deg ø FoV.
- **40 100Å-wide filters** covering 4500-8600 Å in 5 movable filter trays, plus standard ugrizY filters.
- As a survey camera, it can cover **~2 deg^2 per night in all filters**.
- It can provide low-resolution spectra ($\Delta\lambda/\lambda \sim 2\%$, or $R \sim 50$) for >**30000 galaxies**, 5000 stars, 1000 quasars, 10 galaxy clusters, **per night**.
- Expected galaxy redshift resolution **$\sigma(z) \sim 0.003\times(1+z)$**.
- Plan: **100-night survey** in 4 years.

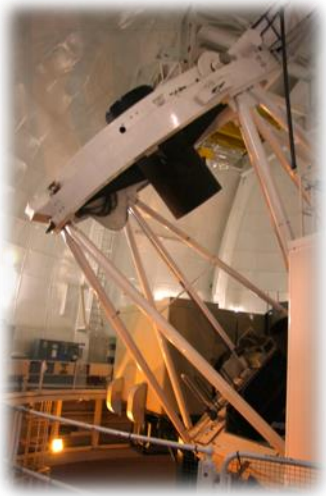

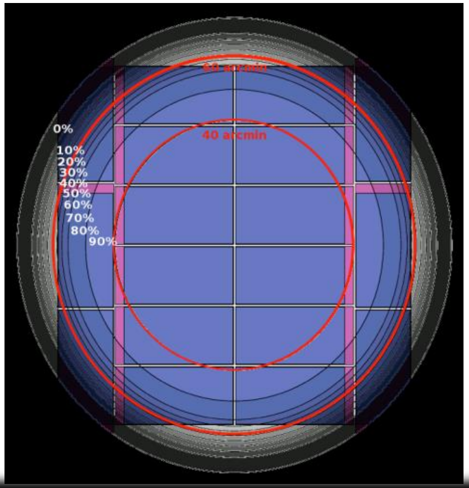

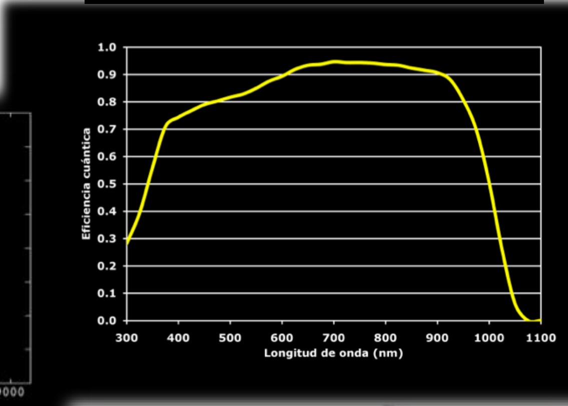

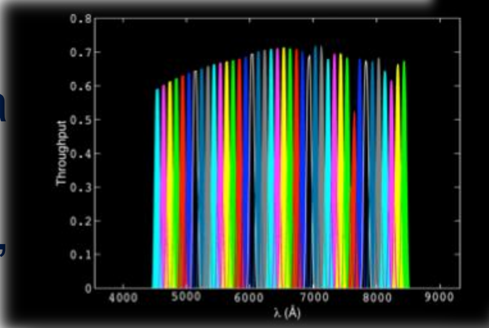

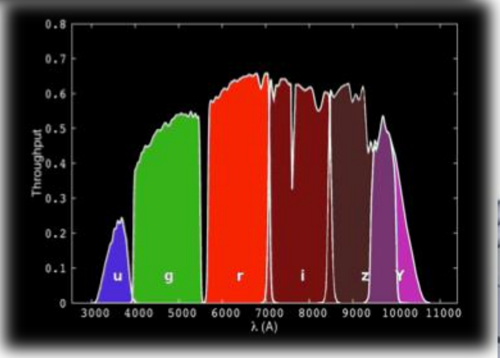

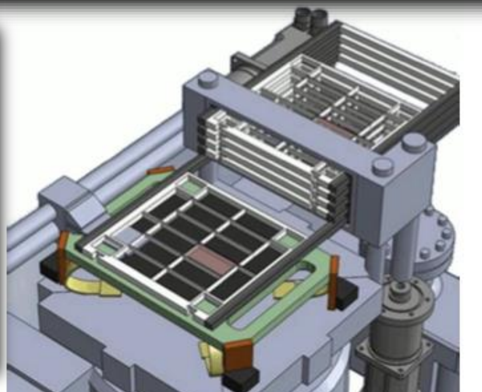

PAU@WHT Personnel

PI : E. Fernández (UAB/IFAE)
Co-Is: E. Sánchez (CIEMAT), E. Gaztañaga(IEEC/CSIC), R. Miquel (IFAE/ICREA), J. García-Bellido (IFT/UAM), M. Delfino (PIC)

PAU Camera PI: F. Castander
Project Manager: C. Padilla. **Systems Engineer**: L. Cardiel
DAQ: J. de Vicente. **Mechanics**: F. Grañena. **Control**: O. Ballester. **Optics and integration**: R. Casas, J. Jiménez

PAUDM & Science PI: E. Gaztañaga
Simulations: F. Castander. **Operations**: N. Tonello. **Data Reduction**: S. Serrano. **QA & Validation**: I. Sevilla

The Survey Team

D. Alonso[4], J. Asorey[2], O. Ballester[3], A. Bauer[2], C. Bonnett[2], A. Bueno[4], J. Campa[1], L. Cardiel[3], J. Carretero[2], R. Casas[2], F. Castander[2], J. Castilla[1], M. Crocce[2], M. Delfino[5], J.F. de Vicente[1], M. Eriksen[2], S. Farrens[2], E. Fernández[3], P. Fosalba[2], J. García-Bellido[4], E. Gaztañaga[2], F. Grañena[3], A. Izard[2], J. Jiménez[2], C. López[2], L. C. López[3], F. Madrid[2], M. Maiorino[3], P. Martí[3], G. Martínez[1], R. Miquel[3], C. Neissner[5], L. Ostman[3], A. Pacheco[5], C. Padilla[3], C. Pio[3], A. Pujol[2], J. Rubio[4], E. Sánchez[1], D. Sapone[4], S. Serrano[2], I. Sevilla[1], P. Tallada[5], N. Tonello[5].

1 Ciemat — Centro de Investigaciones Energéticas, Medioambientales y Tecnológicas

2 IEEC — Institut de Ciències de l'Espai CSIC; ICE — Instituto de Ciencias del Espacio

3 IFAE — Institut de Física d'Altes Energies; UAB — Universitat Autònoma de Barcelona

4 ift — Instituto de Física Teórica UAM/CSIC

5 PIC — port d'informació científica

The Importance of Redshift Resolution

z-space, ⊗*z* = *0.03(1+z)* + peculiar velocities (DES)

z-space, □*z* = *0.003(1+z)* + peculiar velocities (PAU)

z-space, perfect resolution + peculiar velocities

Real space

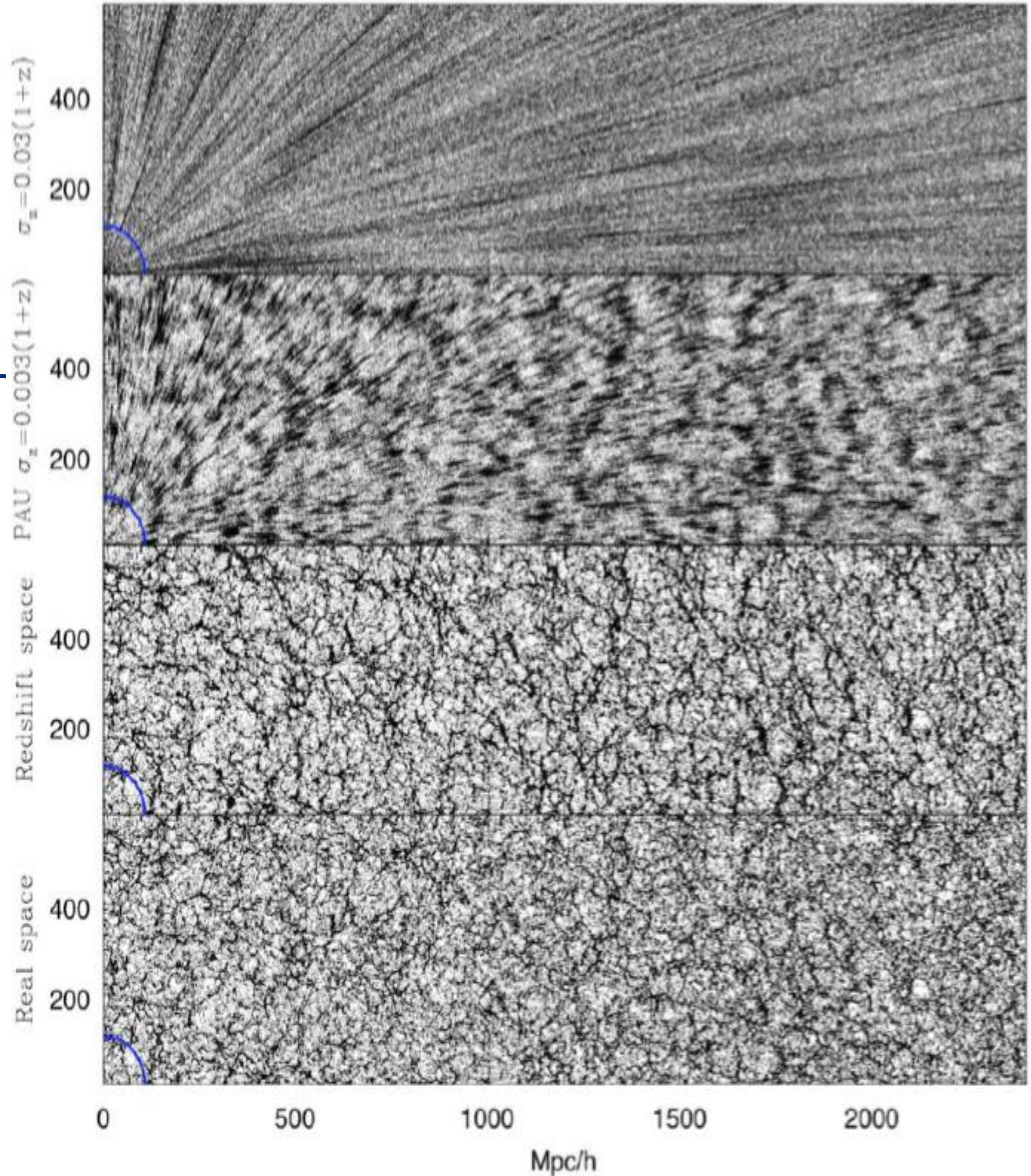

PAUCam at WHT

WHT Telescope

- Diameter: 4.2 m
- Prime focus: 11.73 m
- Focal ratio: f/2.8
- FoV: 1 deg Ø, 40’ unvignetted
- Scale: 17.58’’/mm ⇔ 0.26”/pixel

PAUCam will be mounted at the prime focus:

Strong limitation in the weight: **max. 235 kg**.

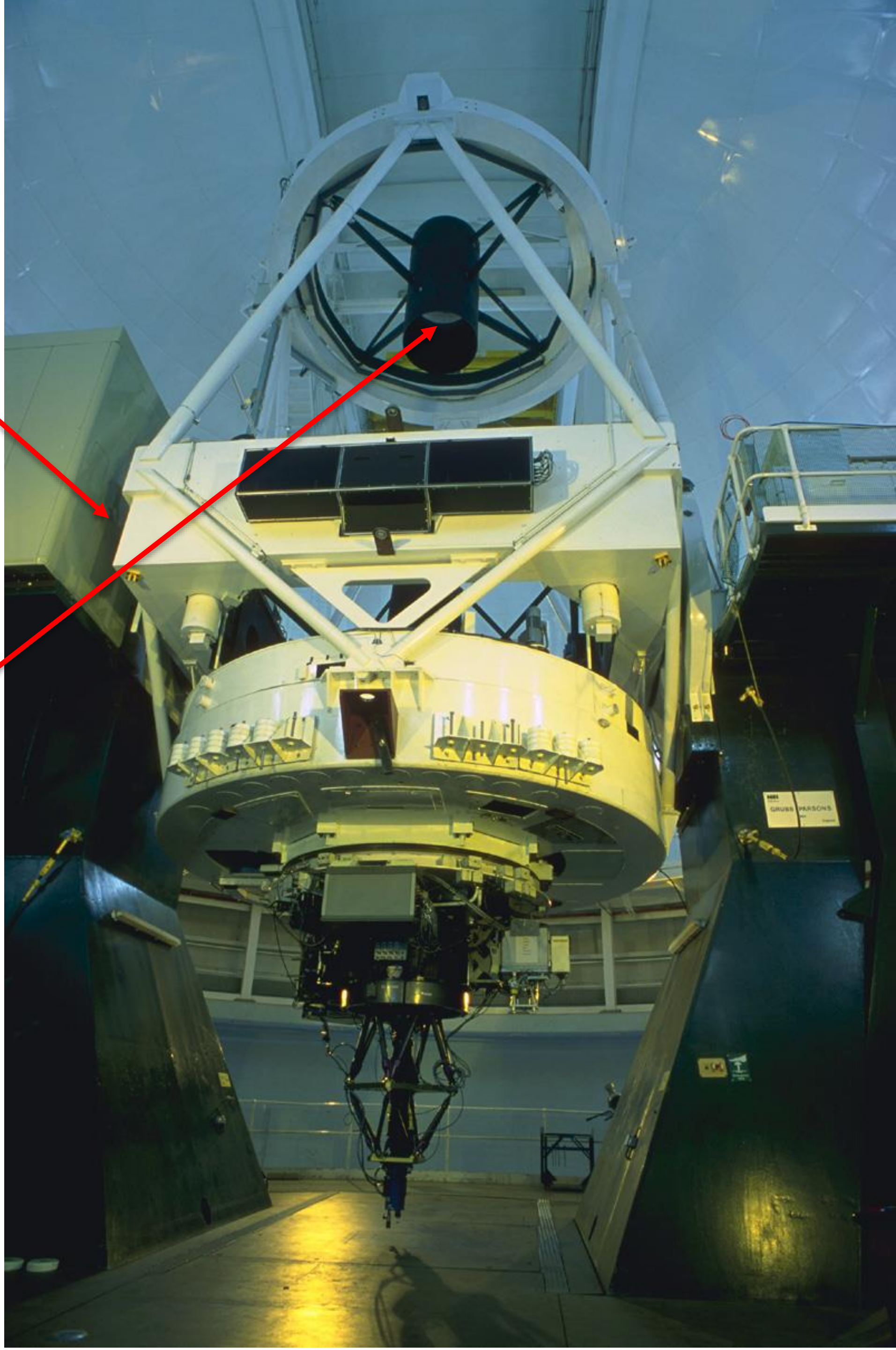

PAUCam

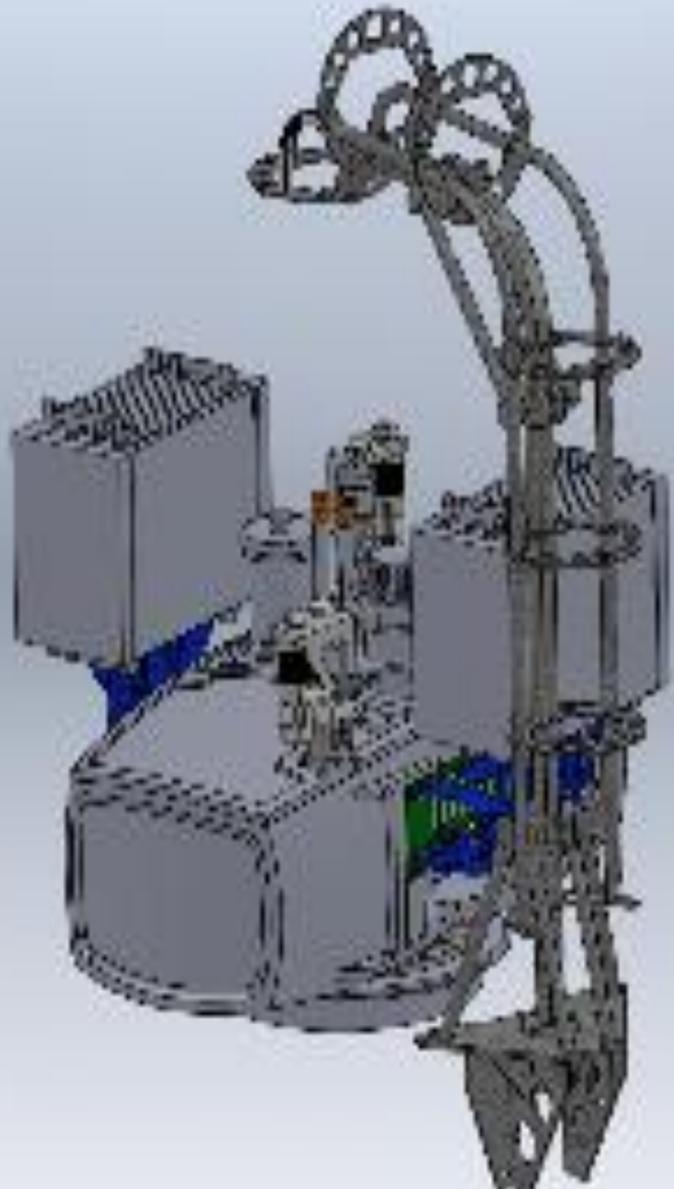

Body of camera made of carbon fiber, shaped to minimize wall thickness

PAUCam Detectors

Hamamatsu new CCDs:

- 18 4k x 2k 15 µm pixels
- Excellent sensitivity across the entire wavelength range from 0.3 to over 1 µm.
- 20 delivered and characterized at CIEMAT and IFAE

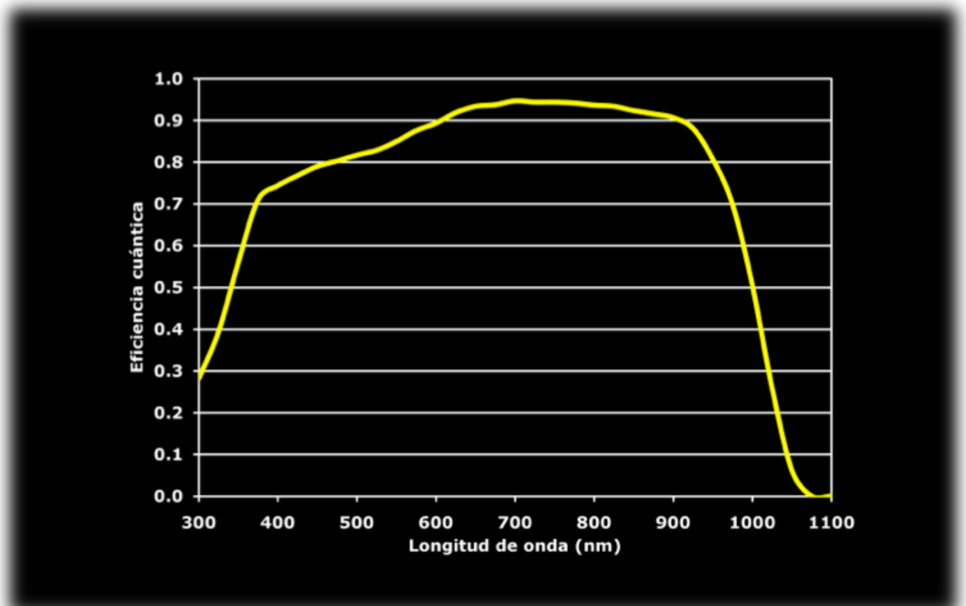

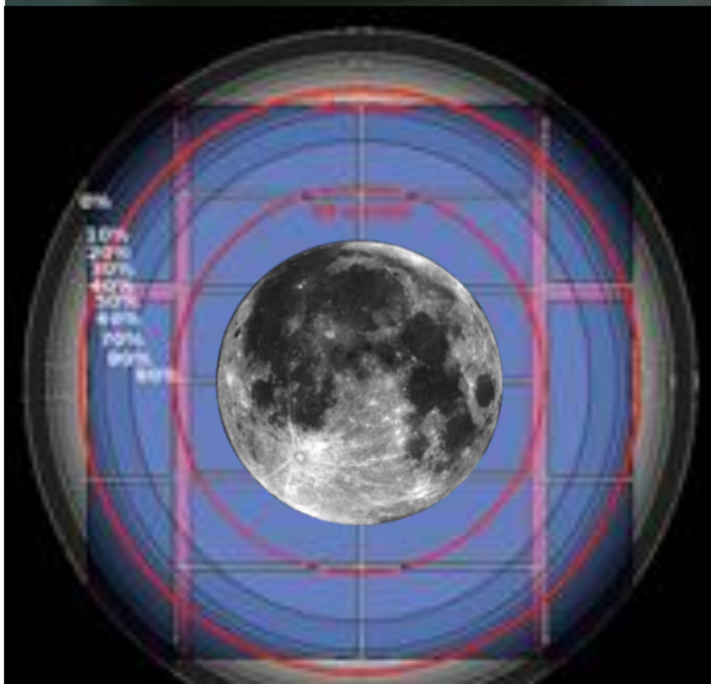

PAUCam Filter System

- 40 narrow-band filters
- FWHM = 100 Å
- Spectral range: λ=4400-8500 Å
- Rectangular transmission profile

- 6 broad-band filters
- ugriZY (SDSS & DES)

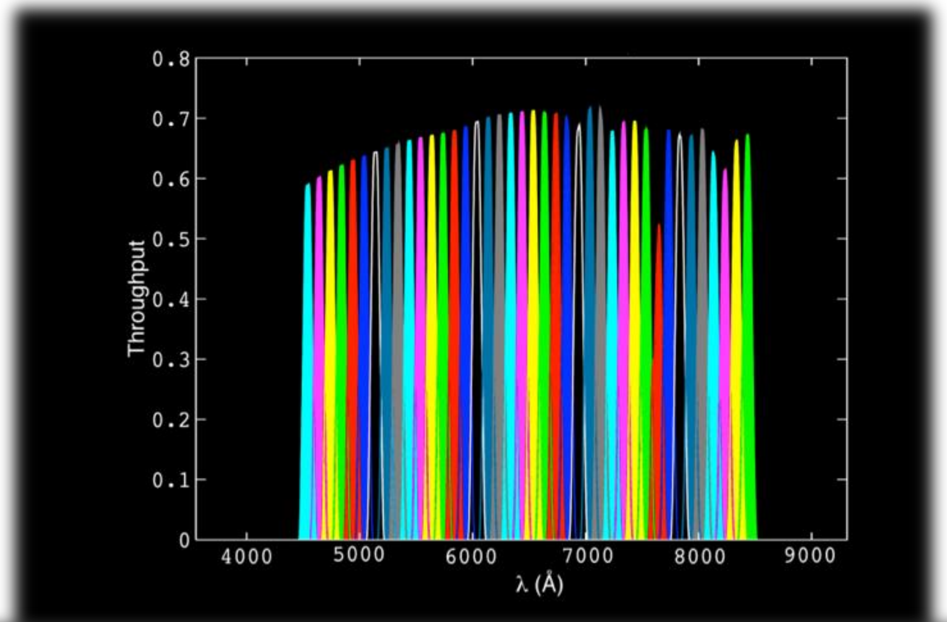

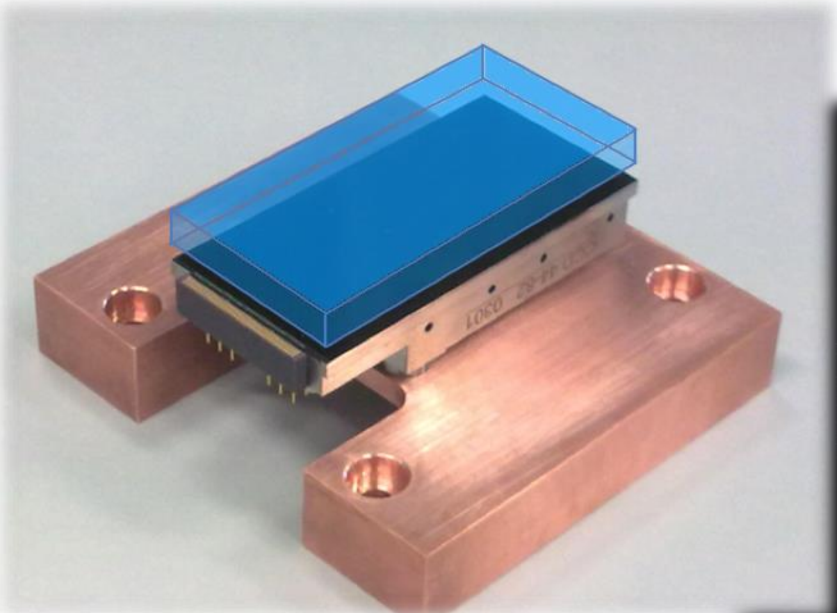

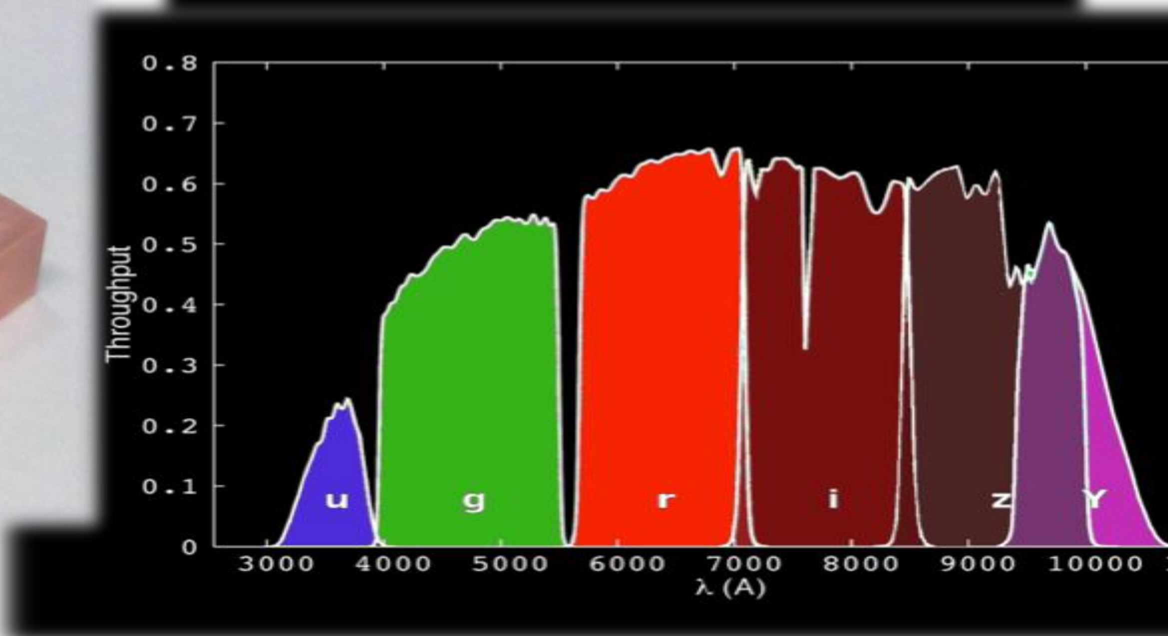

PAUCam Filter Trays

- Efficiency: filters need to be very close to sensors to avoid vignetting
- More filters than CCDs ➜ movable trays
- Jukebox-like system
- Movements in vacuum are technologically challenging

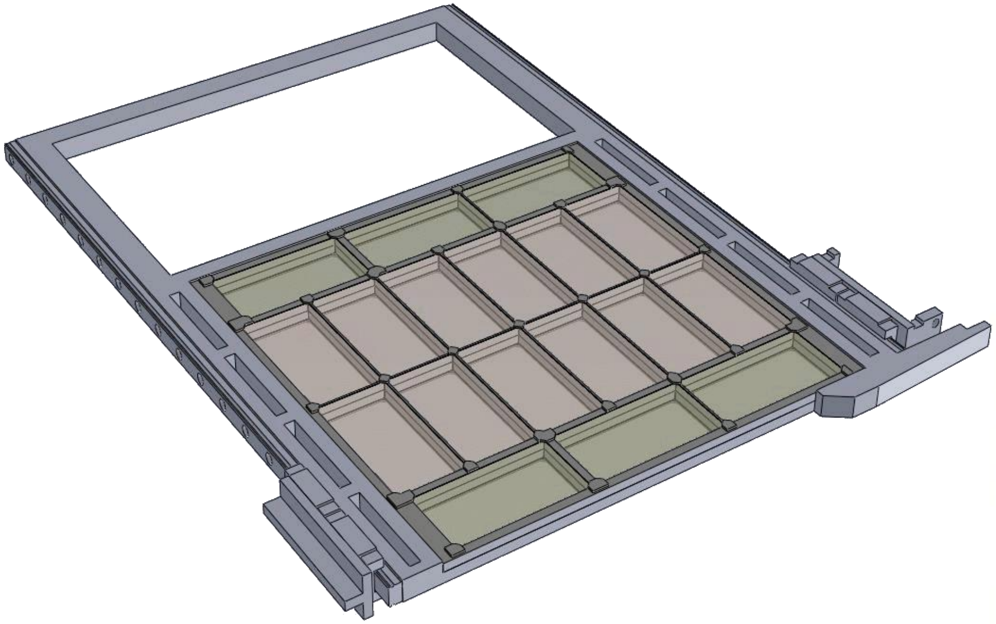

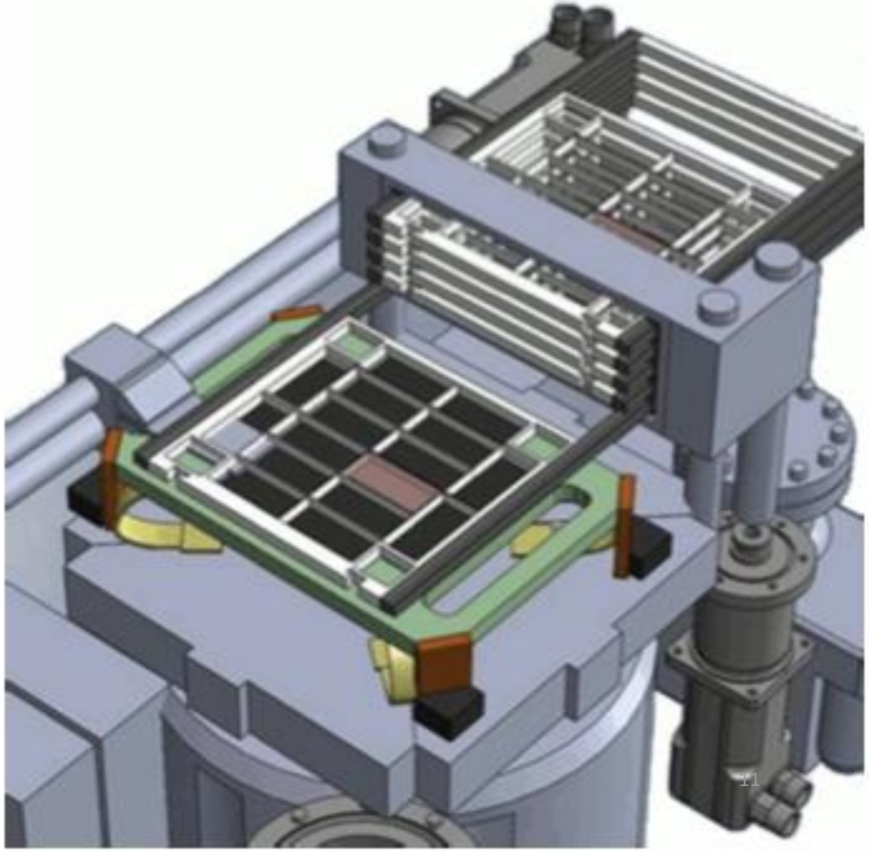

PAUCam Filter Trays

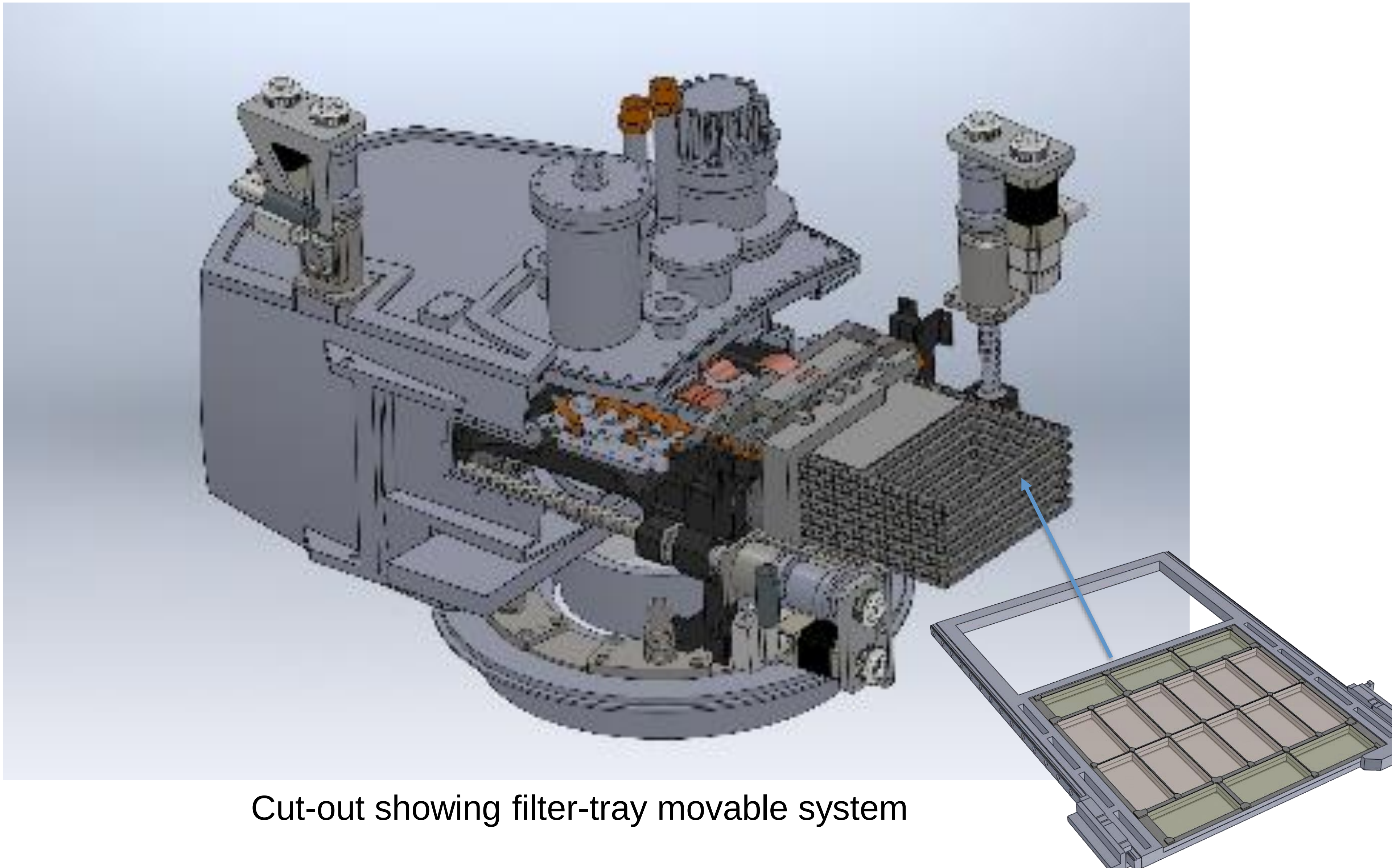

Cut-out showing filter-tray movable system

PAU Camera Construction

Cryogenics and vacuum tests on prototype

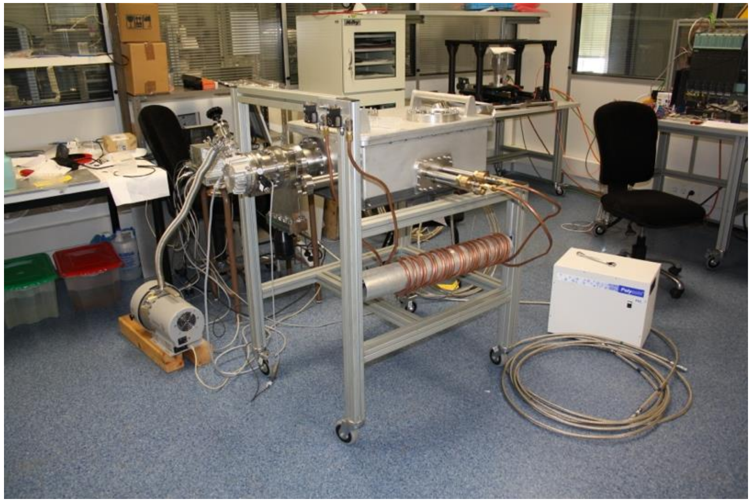

CCD test station

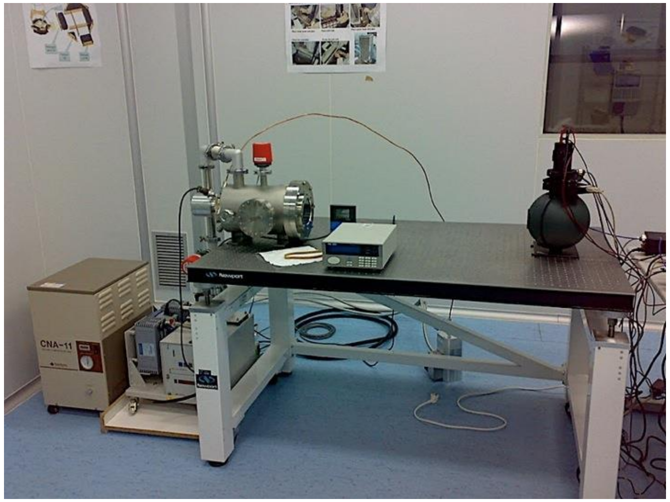

Aluminum mold of camera body

Camera body in carbon fiber

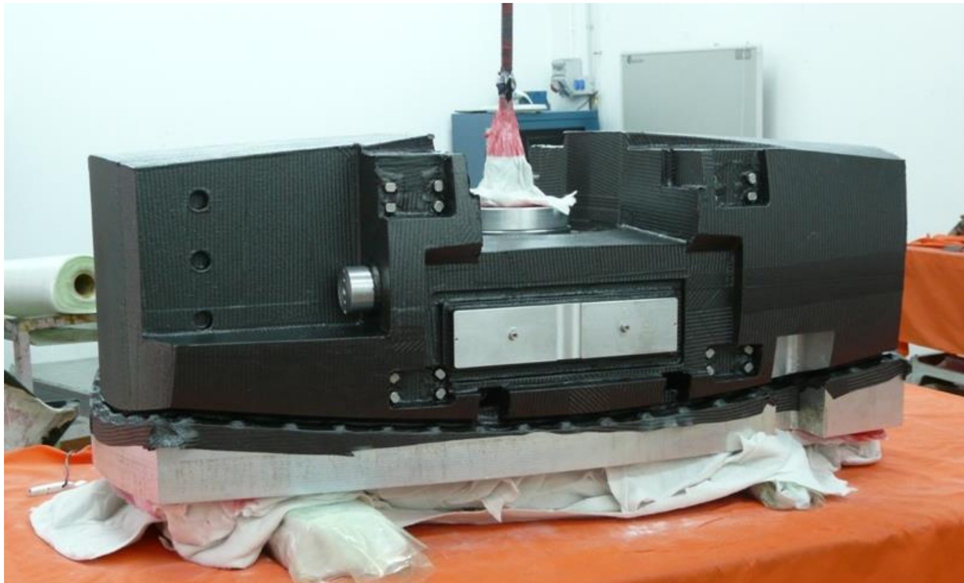

PAUCam: Measurements

Filter transmission (r-band)

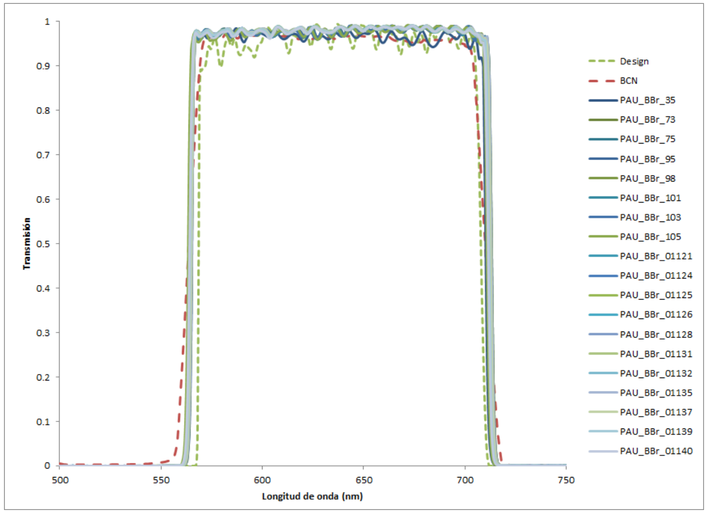

CCD image (30 min dark)

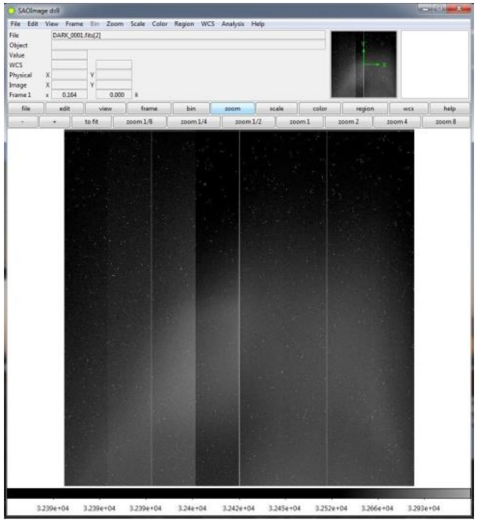

CCD noise reading 2 CCDs

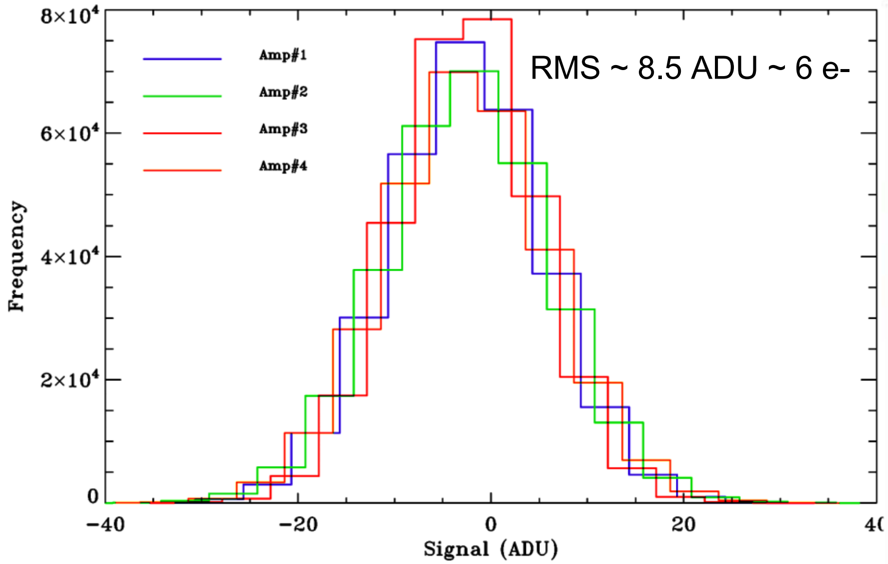

CCD QE

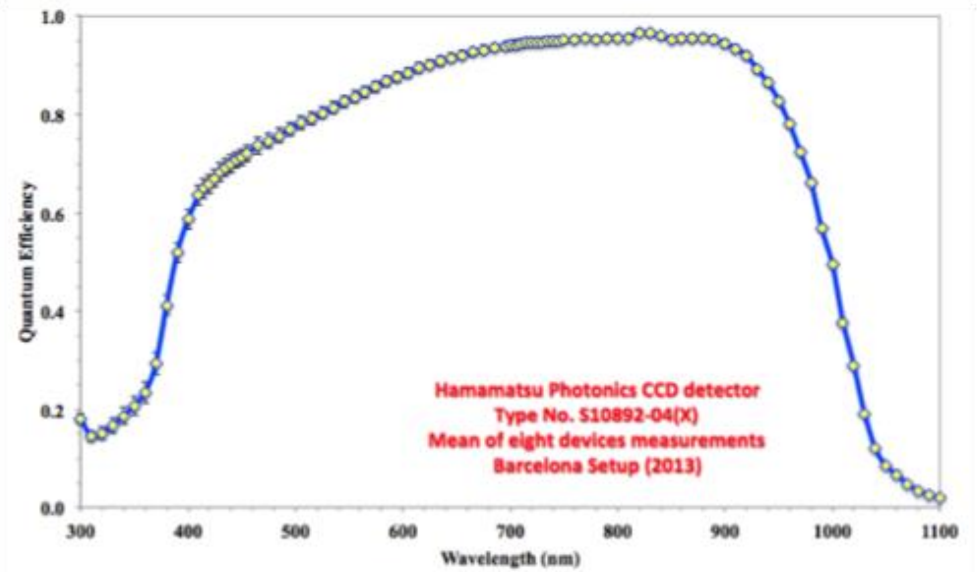

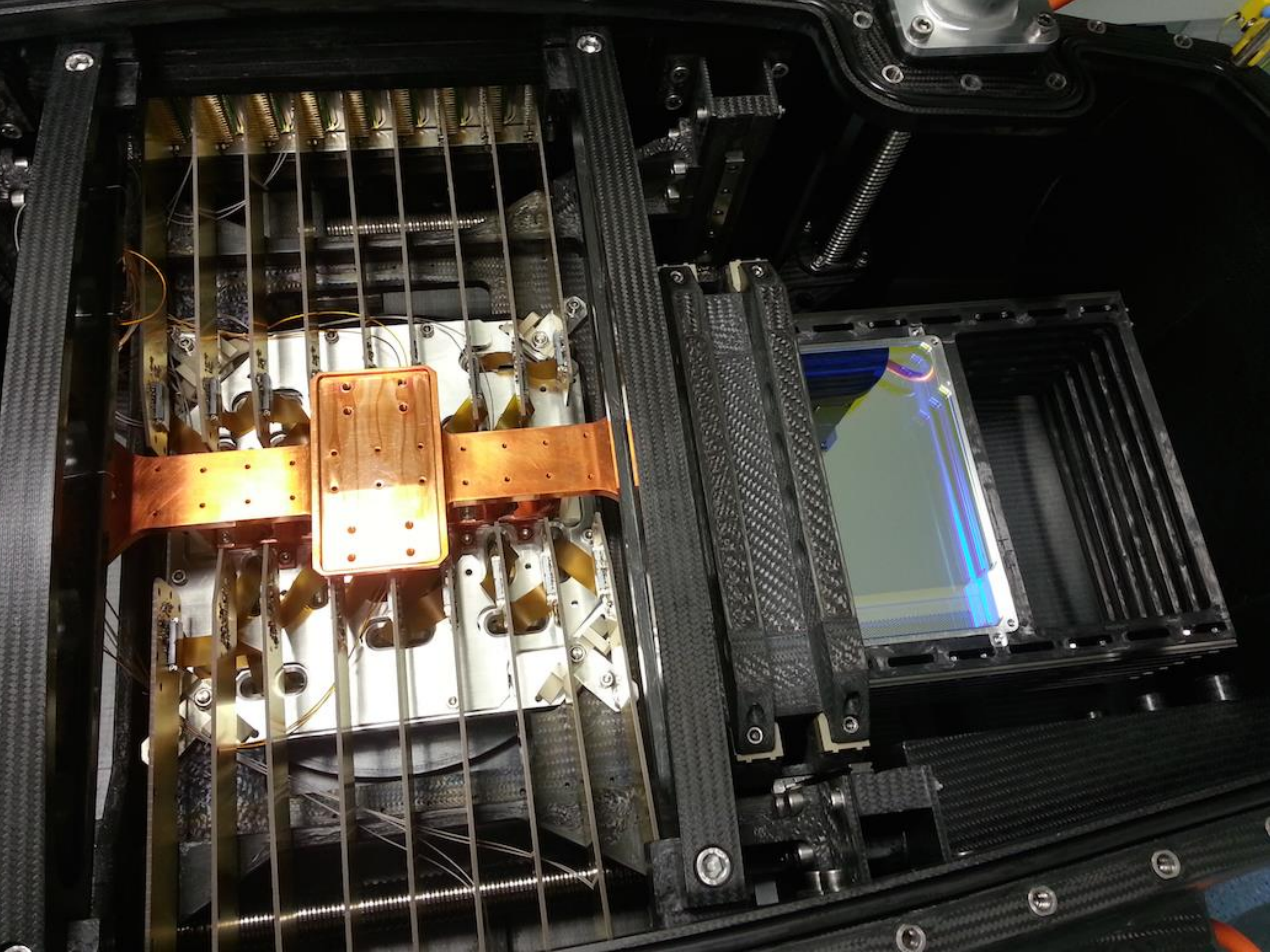

PAU Camera: Details

Shutter

Entrance window

18 CCDs in the focal plane

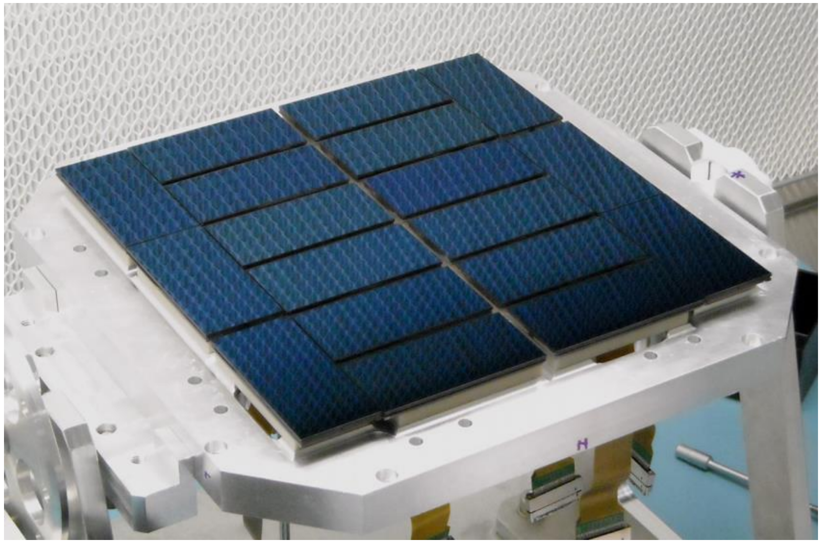

r-band filter

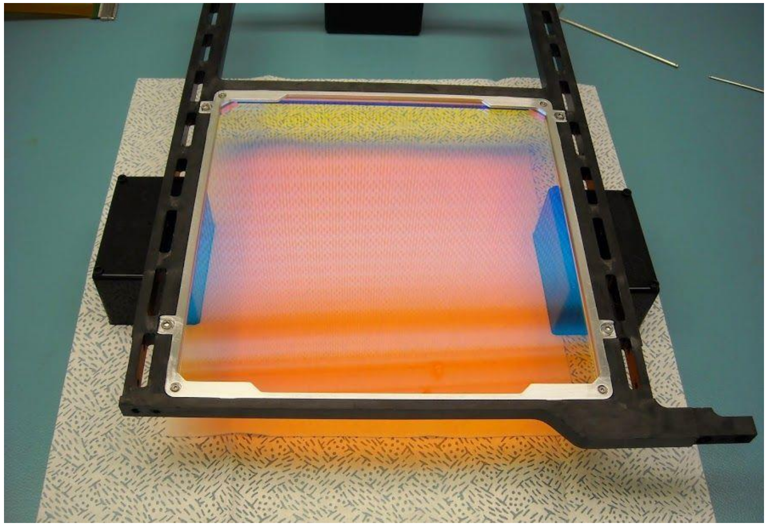

PAU Camera

Full camera

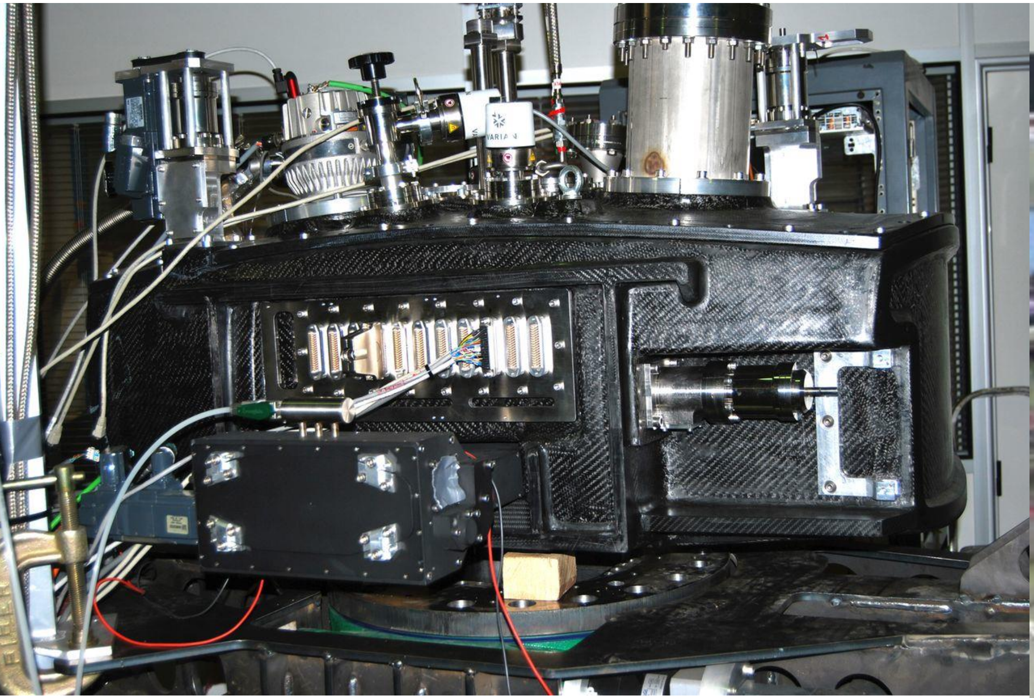

Telescope simulator

PAUCam Control System

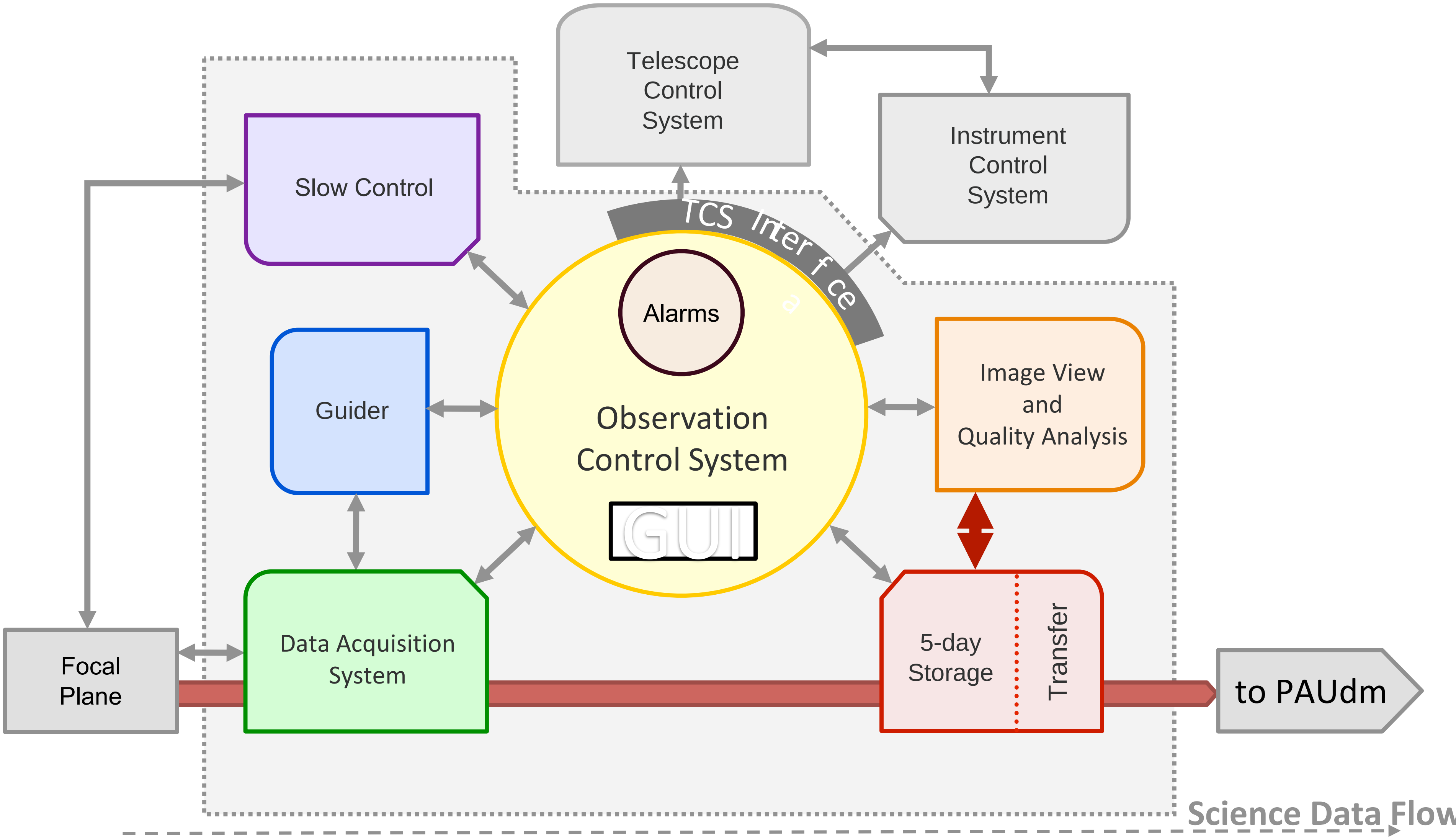

One computer already installed at the WHT. Tests of interface are already taking place.

Data Management System

PAUdm Working Packages

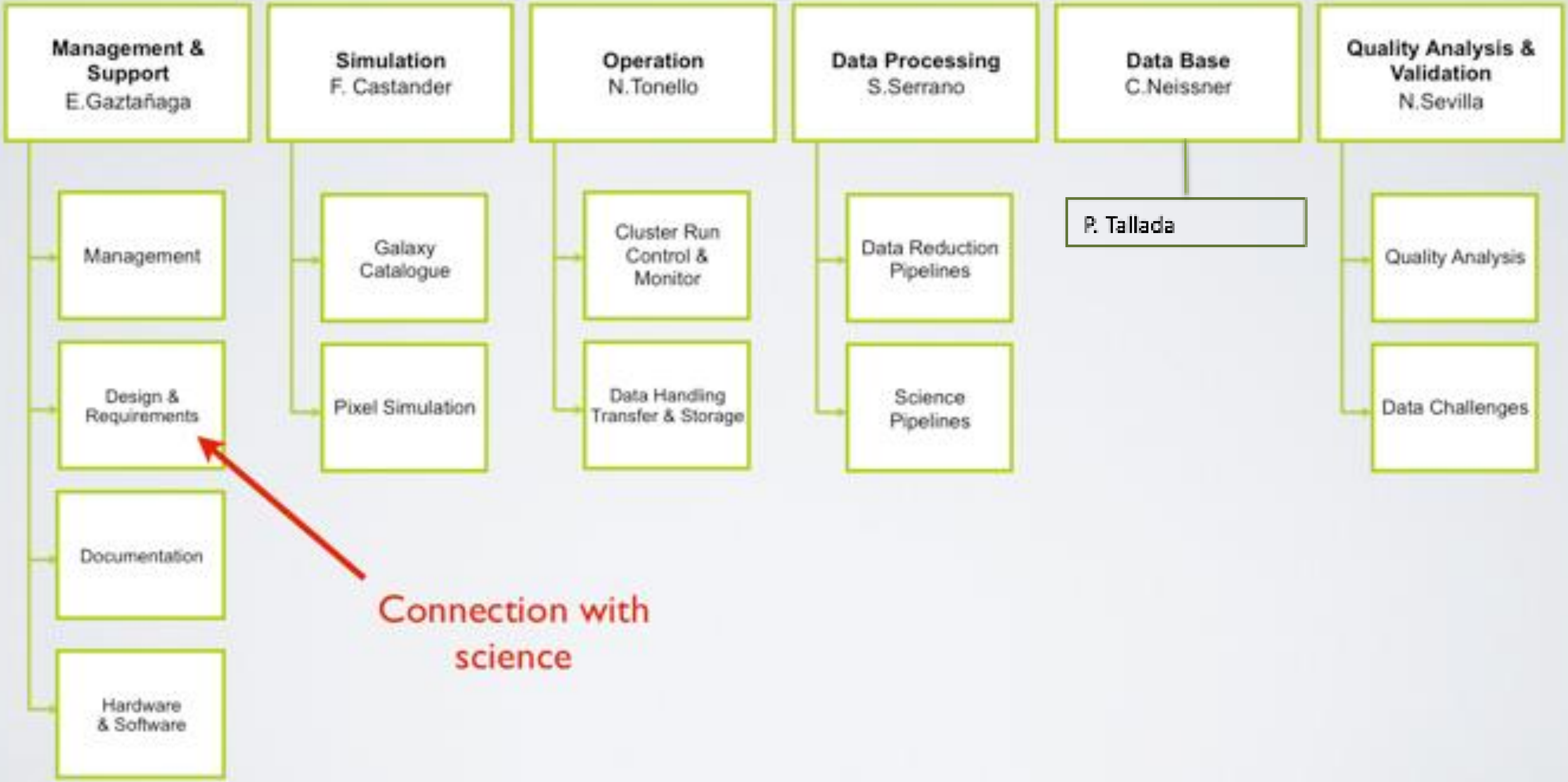

Pipelines

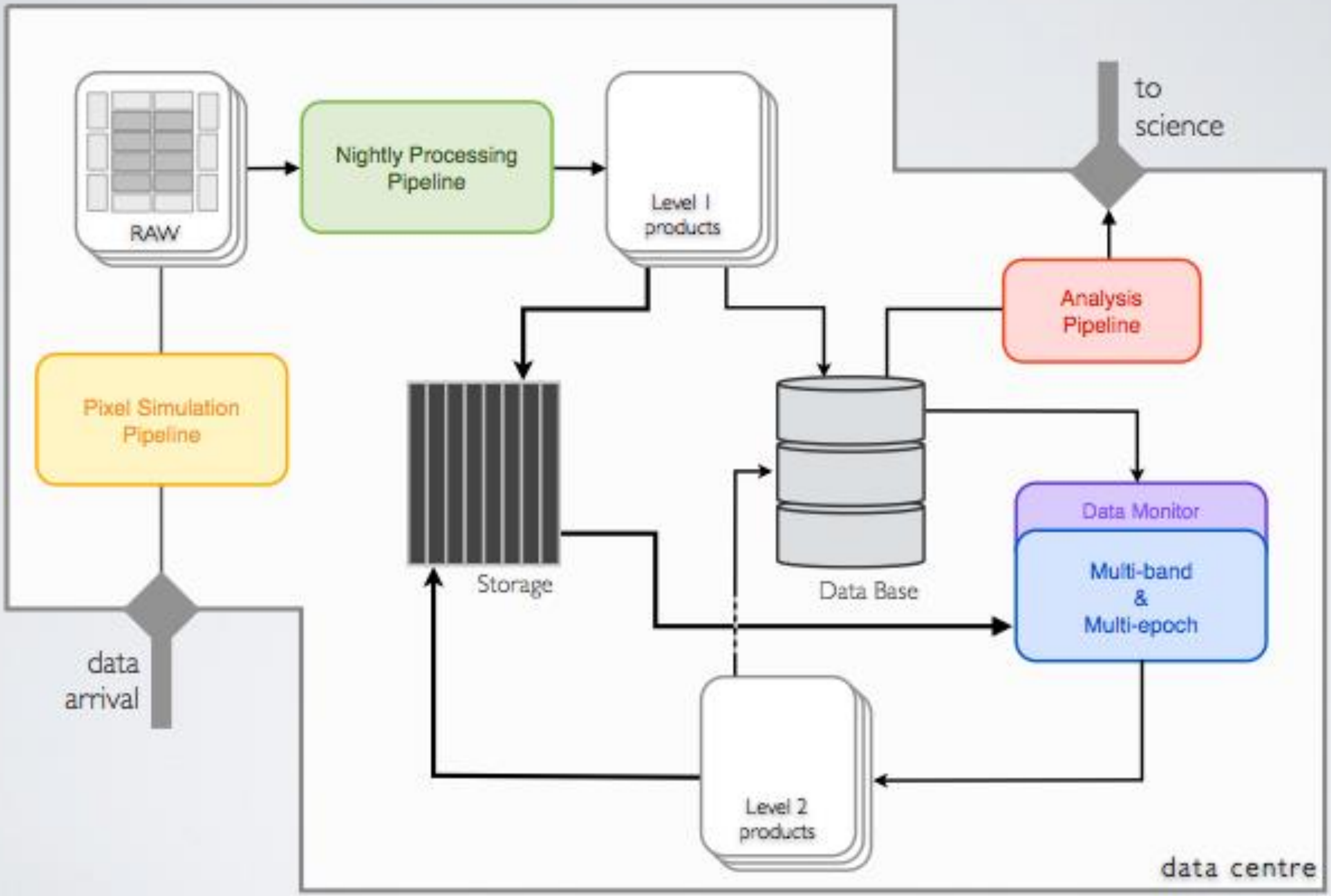
RAW
Nightly Processing Pipeline
Level 1 products
to science
Analysis Pipeline
Pixel Simulation Pipeline
Storage
Data Base
Data Monitor
Multi-band & Multi-epoch
data arrival
Level 2 products
data centre

PAUCam Simulations

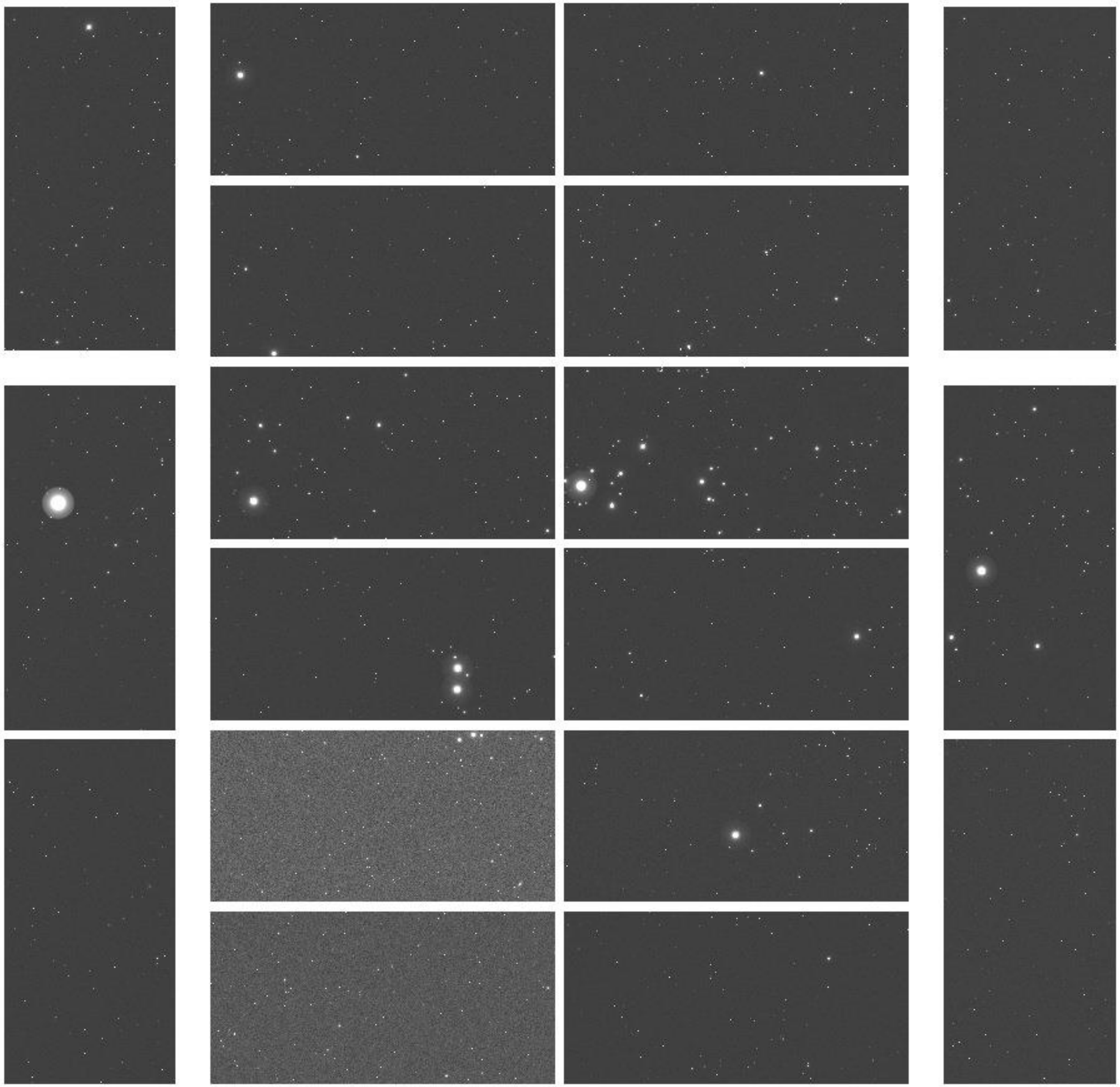

PAU Filter Transmissions

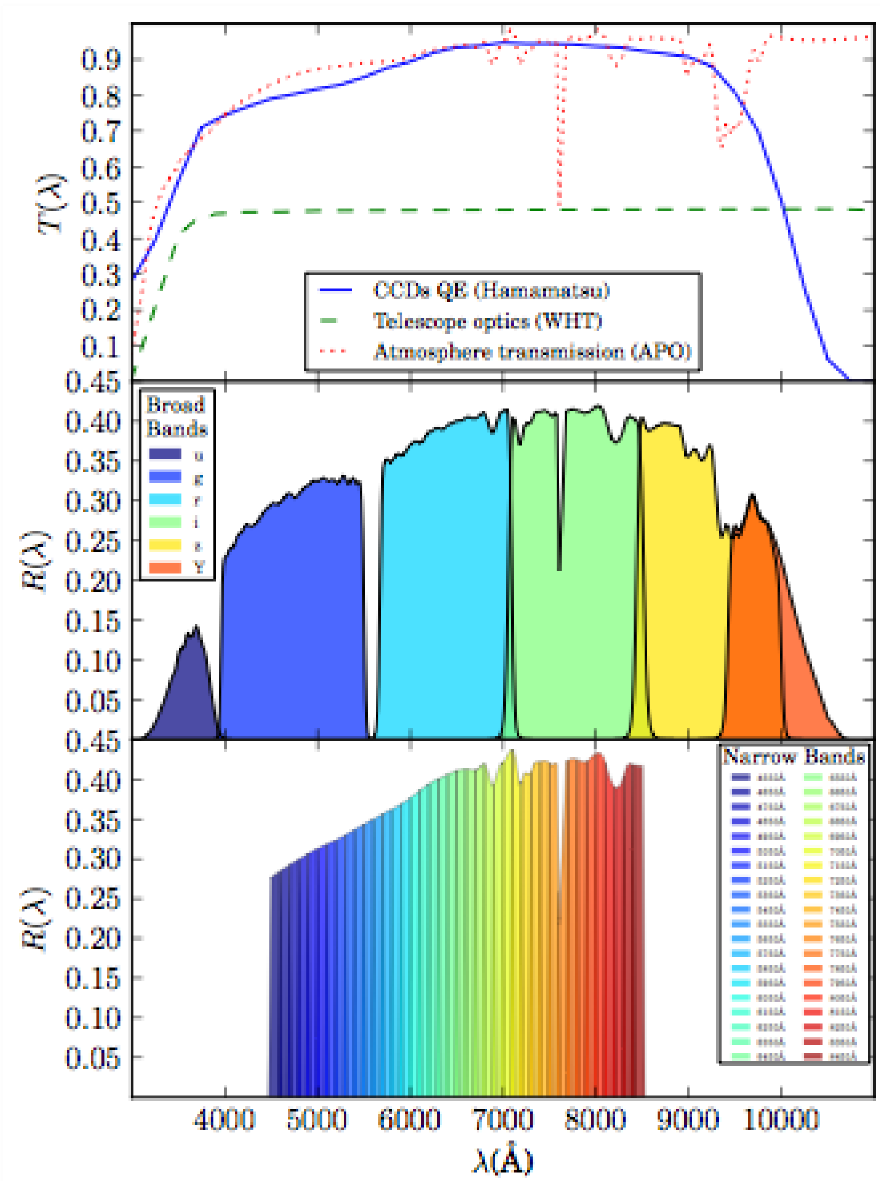

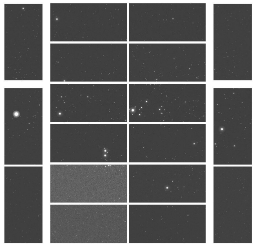

PAU Survey Strategy

- Use 8 central CCDs to define the survey footprint, use the other CCDs to increase S/N.
- Each central CCDs covers the whole survey area twice.
- 5 filters trays with 8 NB central filters.
- Broad bands reach ~1.4 magnitudes deeper than narrow bands.
- Detect objects in the broad bands, and then get flux in the narrow bands.
- Push to low signal to noise.
- Surveying capability: sample 2 deg^2 / night to i_{AB} < 22.5 mag in all NBs and i_{AB} < 23.7 in all BBs ➜ >30000 galaxies / night
- Exposure times depend on tray: ~90 s for bluest, ~150 s for reddest.
- No selection effects.

PAU Limiting Magnitudes

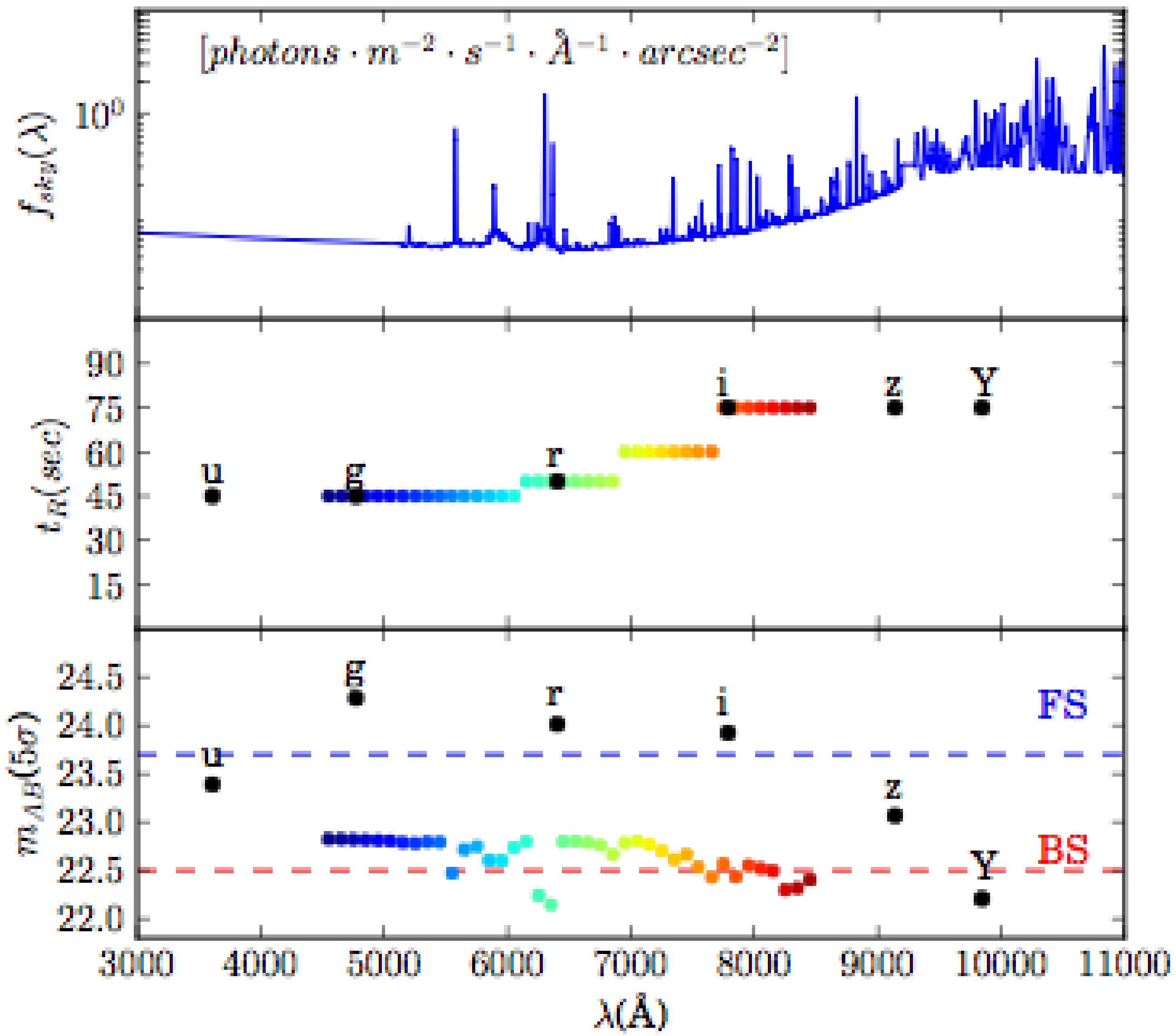

PAU Photo-z Performance ($i_{AB} < 22.5$)

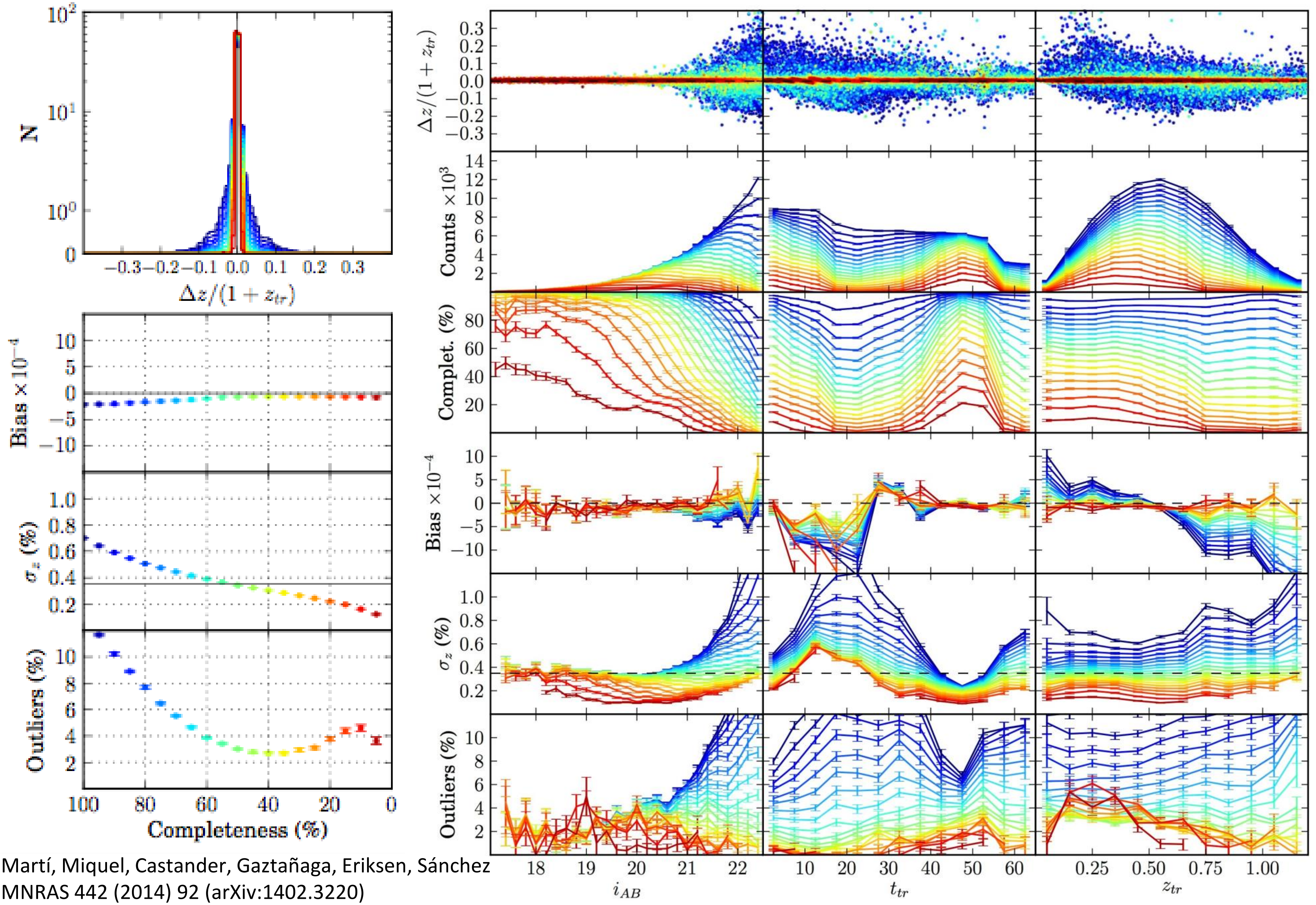

Martí, Miquel, Castander, Gaztañaga, Eriksen, Sánchez
MNRAS 442 (2014) 92 (arXiv:1402.3220)

PAU Photo-z Performance (22.5< i_{AB} < 23.7)

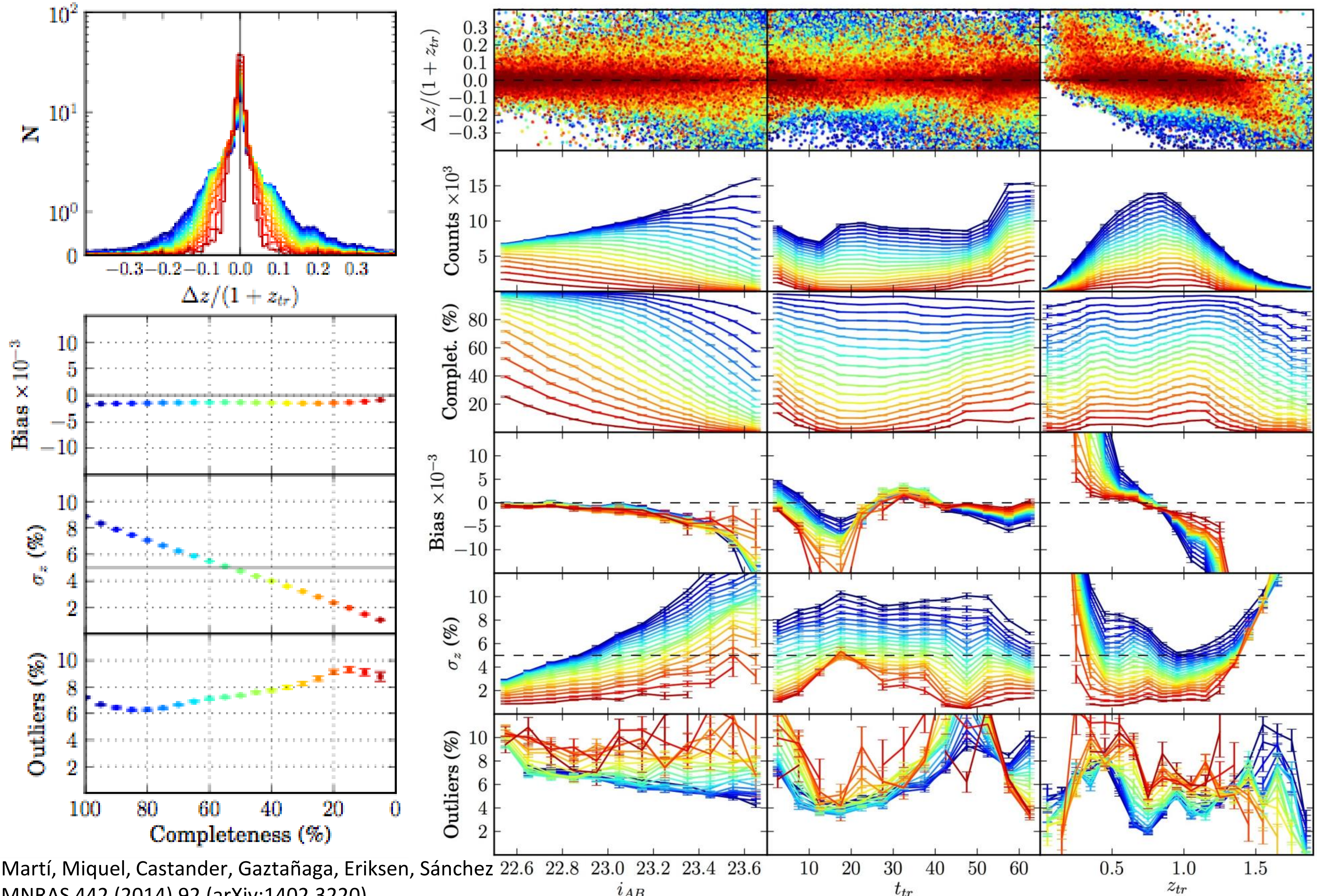

Martí, Miquel, Castander, Gaztañaga, Eriksen, Sánchez
MNRAS 442 (2014) 92 (arXiv:1402.3220)

PAU Science

- Survey strategy produces two samples:
  - “Spectroscopic” sample: excellent photo-z’s with NB filters to $i_{AB} < 22.5$
  - “Photometric” sample: medium photo-z’s with BB filters to $i_{AB} < 23.7$
- Science case depends on amount of time available
- Current science case, assuming 100 nights (200 deg^2):
  - Use bright sample for redshift-space distortions (typical of spectroscopic surveys)
  - Use faint sample for weak lensing magnification and/or shear (typical of imaging surveys)
  - Exploit the gains of cross-correlating both samples on the same area

Gaztañaga et al. 2012, MNRAS 422 2904 (astro-ph/1109.4852)

PAU Survey Samples

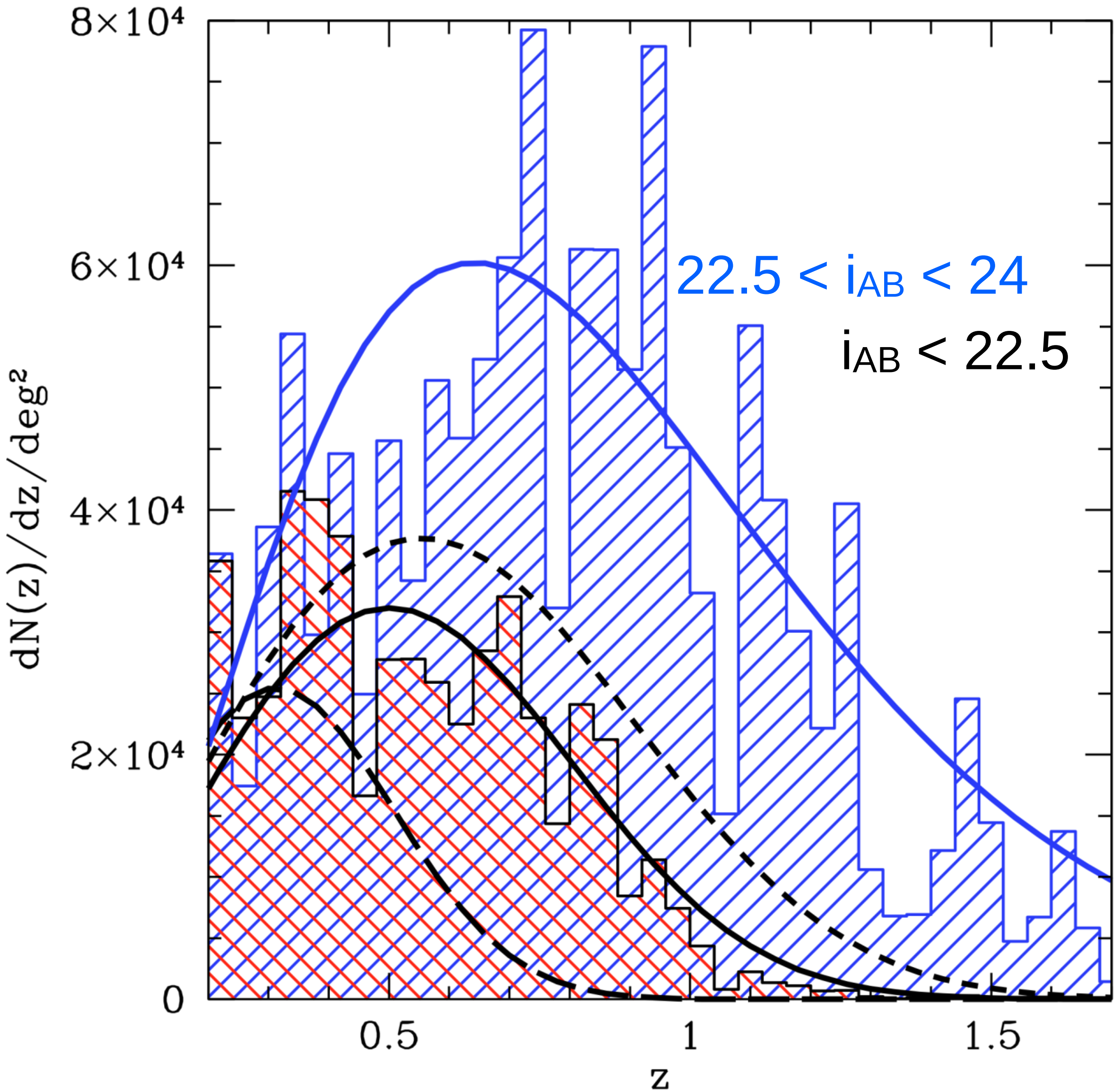

PAU's Primary Science Drivers (I)

- Redshift-space distortions (RSD):
  - Peculiar velocities of galaxies trace the matter density fields.
  - Anisotropies in the galaxy 2-point correlation function measure the growth of structure at a given redshift: probe of dark energy.
  - Relevant scales are ~10 Mpc/h, well matched to PAU's z precision.

$\sigma_z = 0.000 \times (1+z)$ $\sigma_z = 0.003 \times (1+z)$

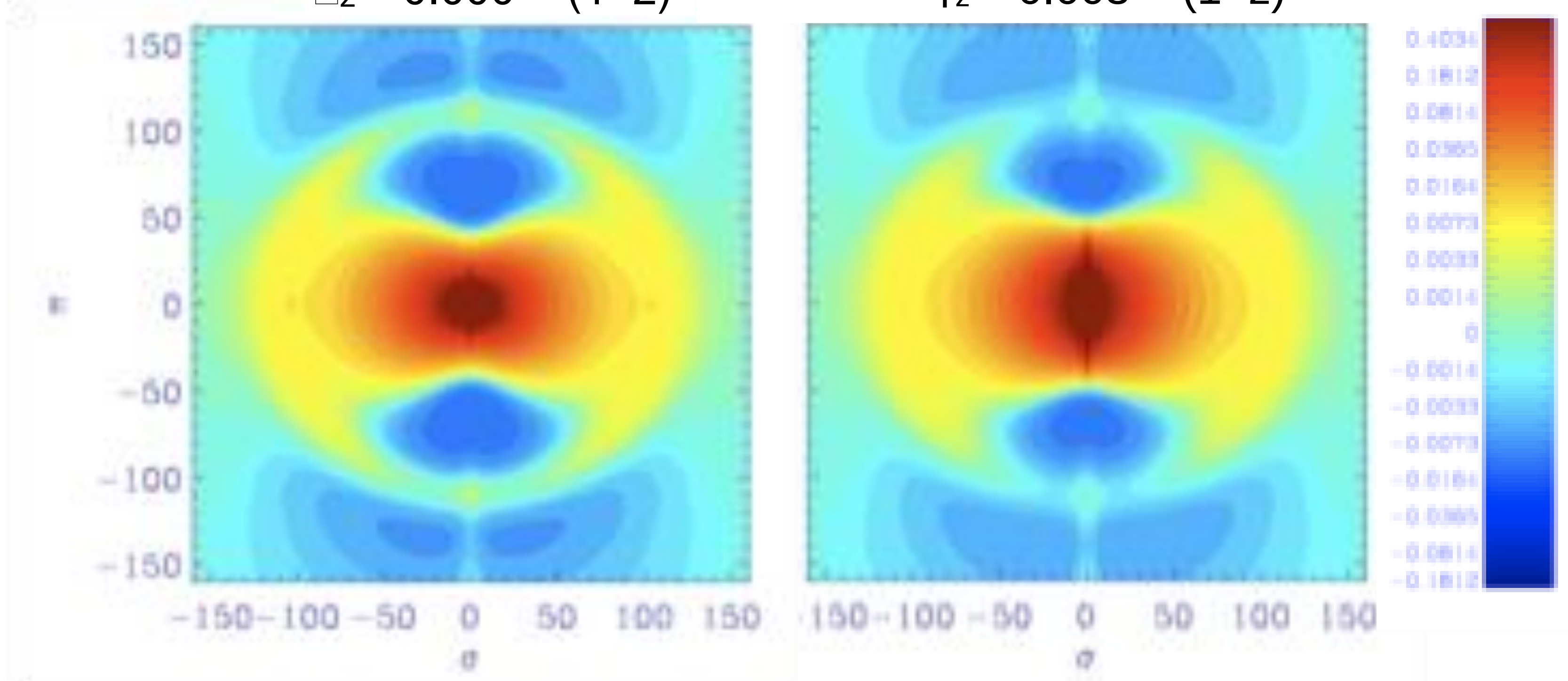

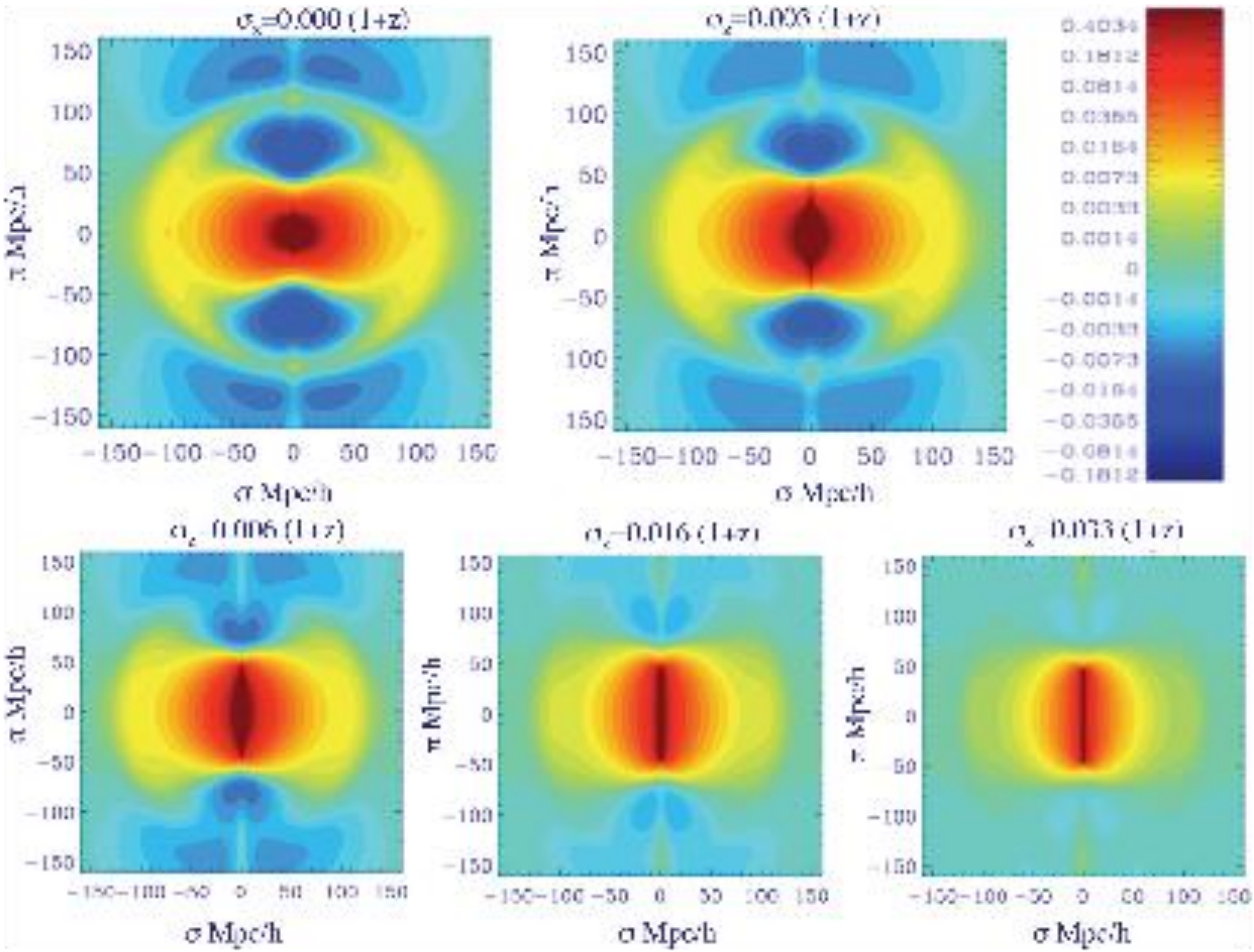
σz=0.000 (1+z)
σz=0.003 (1+z)
σz=0.006 (1+z)
σz=0.016 (1+z)
σz=0.033 (1+z)
π Mpc/h
σ Mpc/h
0.4034
0.1812
0.0814
0.0365
0.0164
0.0073
0.0033
0.0014
0
-0.0014
-0.0033
-0.0073
-0.0164
-0.0365
-0.0814
-0.1812

PAU’s Primary Science Drivers (II)

- Lensing magnification (MAG):
  - Gravitational lensing affects the measured galaxy number density.
  - Main observable is the cross-correlation between galaxies in different redshift bins as a function of angular separation.
  - Very precise photo-z’s allow PAUCam to perform **cross-correlations between well-defined narrow redshift bins.**

- Combination of RSD and MAG includes:
  - 3D galaxy clustering, which is degenerate with galaxy bias.
  - Weak lensing magnification, which is unbiased.
  - Redshift-space distortions, which also measure bias, and growth.
  - Probes dark energy through both growth of structure and geometry.

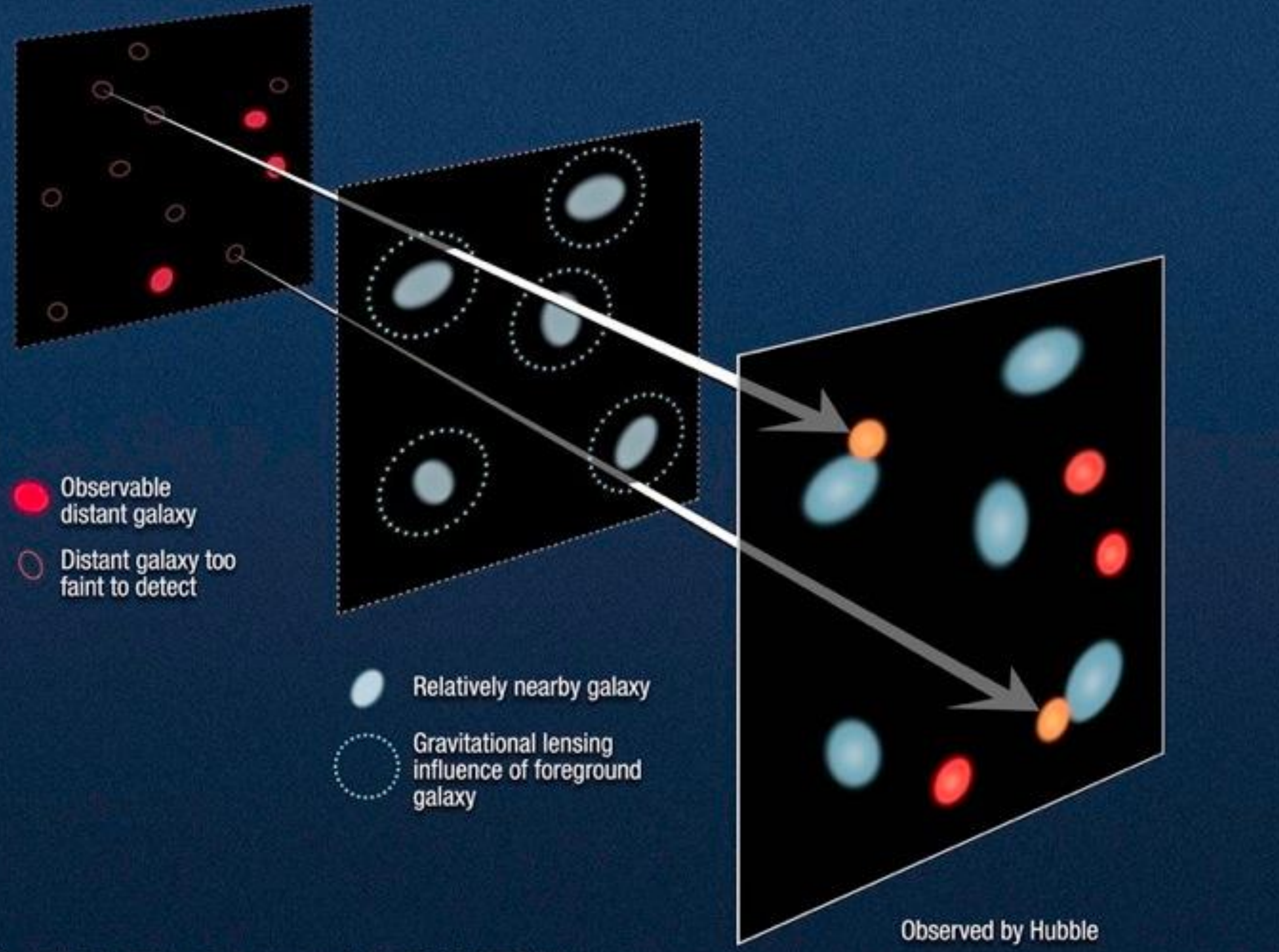

Credit: NASA, ESA, Z. Levay and A. Field (STScI)

PAU Survey Science Reach

- The combination of RSD and MAG in the same data set is very powerful in breaking degeneracies between cosmological parameters ➔ a unique advantage of PAU.

- **Figures of merit** with free Ω_m, Ω_{DE}, h, σ_8, Ω_b, w_0, w_a, γ, n_s, 4 bias parameters.

$$FoM_{w\gamma} = \sqrt{\frac{1}{\det\left[F^{-1}\right]_{w\gamma}}}$$

$$f = \frac{d\log D}{d\log a} = \Omega_m^{\gamma}(z)$$

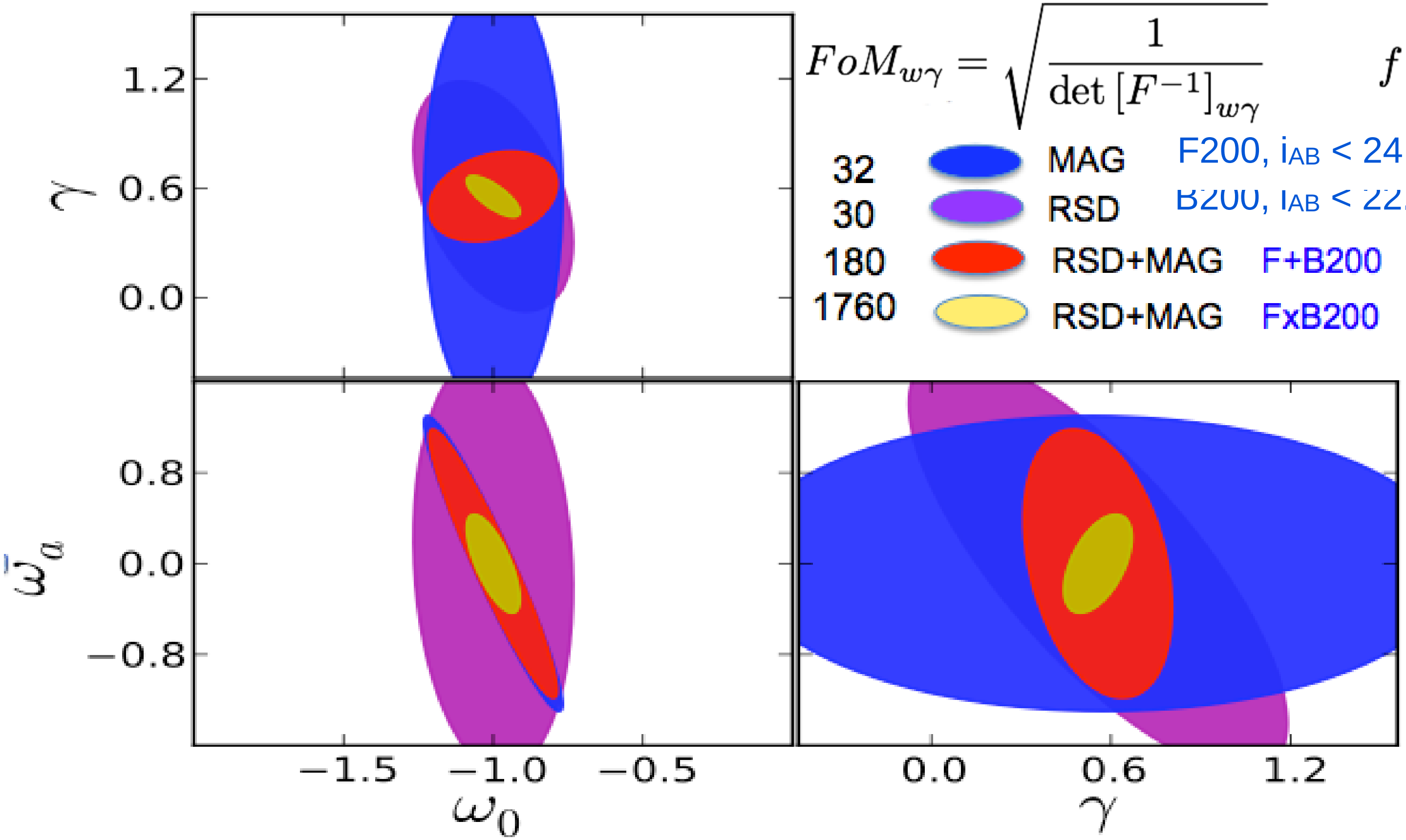

(including Planck and stage-II SNe priors)

E. Gaztañaga, M. Eriksen, M. Crocce, F. Castander, P. Fosalba, P. Martí, R. Miquel, A. Cabré, MNRAS 422 (2012) 2904

Other Science

- **Intrinsic alignment of galaxies (main systematic for future weak-lensing surveys, e.g. Euclid)**
- **Photo-z calibration of future photometric surveys (DES, HSC, LSST, Euclid)**
- Large Scale Structure, including BAO
- Galaxy clusters
- Galaxy evolution
- Quasars and the Lyα forest
- Multiply imaged gravitational lenses
- High redshift galaxies
- Low surface brightness galaxies
- Intergalactic dust
- Halo stars
- Local group stars
- Brown dwarfs and cool stars
- Exoplanets
- ....

PAU Conclusions

PAUCam is essentially completed, with many tests being done.

First commissioning in Fall 2014.

Regular data taking expected in 2015.

PAUCam will be the most powerful imaging instrument at the Roque de los Muchachos

DESI

The Dark Energy Spectroscopic Instrument (DESI)

Spectroscopic Galaxy Surveys

Instrument	Telescope	No. Gal.	Sq. Deg.	z max	Leader
SDSS	APO 2.5	85K LRGs	7600	0.6	USA
Wiggle-Z	AAT 3.9	239K	1000	0.7	Australia
Now BOSS	APO 2.5	1.4M LRGs + QSOs	10000	0.7	USA
HETDEX	HET 9.2	1M	420	3.0	USA
eBOSS	APO 2.5	600K	7500	1.0	CH / Fr / US (J.-P. Kneib)
DESI	Mayall 4	25M + QSOs	14000	1.7 (3.5 with QSOs)	USA
SuMIRe PFS	Subaru 8.2	4M	1400	2.4	Japan
4MOST	VISTA 4.1	??	15000	1.5	ESO
Euclid	Space 1.2	50M	15000	2.0	ESA

DESI: Dark Energy Spectroscopic Instrument

- Scale up BOSS to a massively parallel fiber-fed spectrometer at a 4-meter telescope.
- Stage-IV BAO and power spectrum, built upon BOSS
- Broad range of target classes: LRGs, ELGs, QSOs, Ly-α QSOs
- Broad redshift range: $0.2 < z < 3.5$
- Sky area: ~14,000 sq. deg.
- Number of redshifts: ~25 M
- Medium resolution spectroscopy, R ~ 3000 - 5000
- Spectroscopy from blue to NIR
- Automated fiber system: $N_{fiber} \sim 5000$

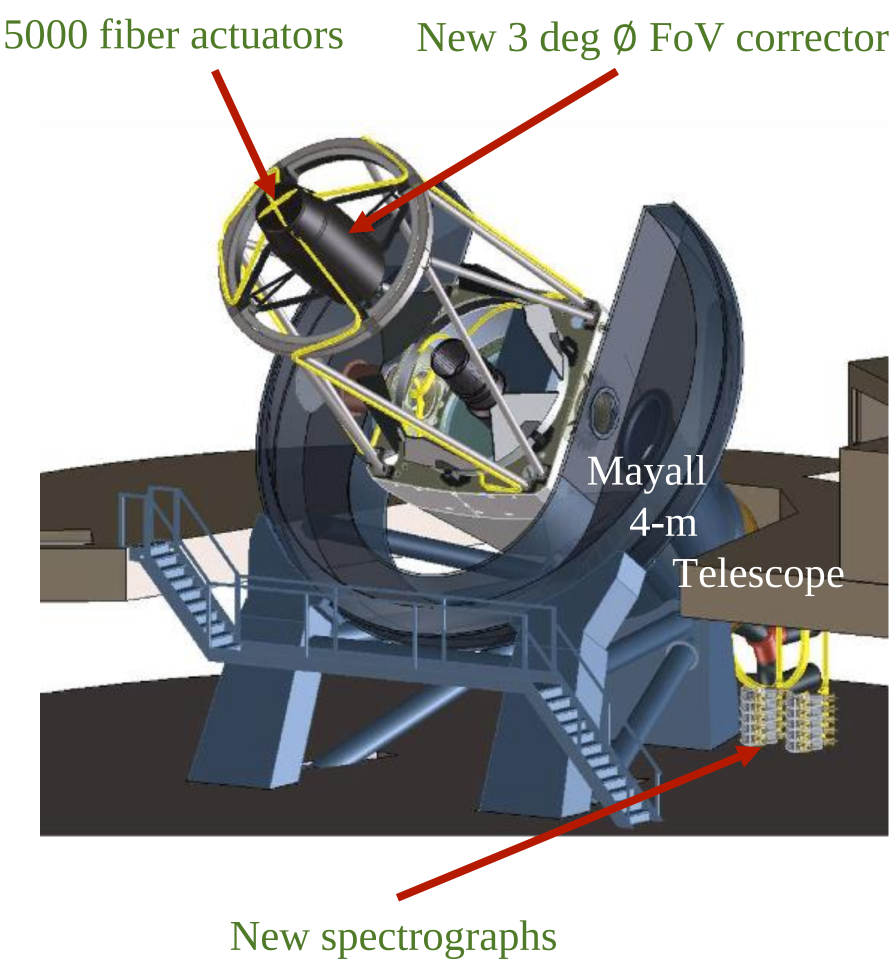

Requesting ~100% of dark time for 3 - 5 years

What is the DESI survey?

SDSS ~2h^{-3}Gpc^3 ➡ BOSS ~6h^{-3}Gpc^3 ➡ DESI 50h^{-3}Gpc^3

Four target classes spanning redshifts z=0 ➔ 3.5

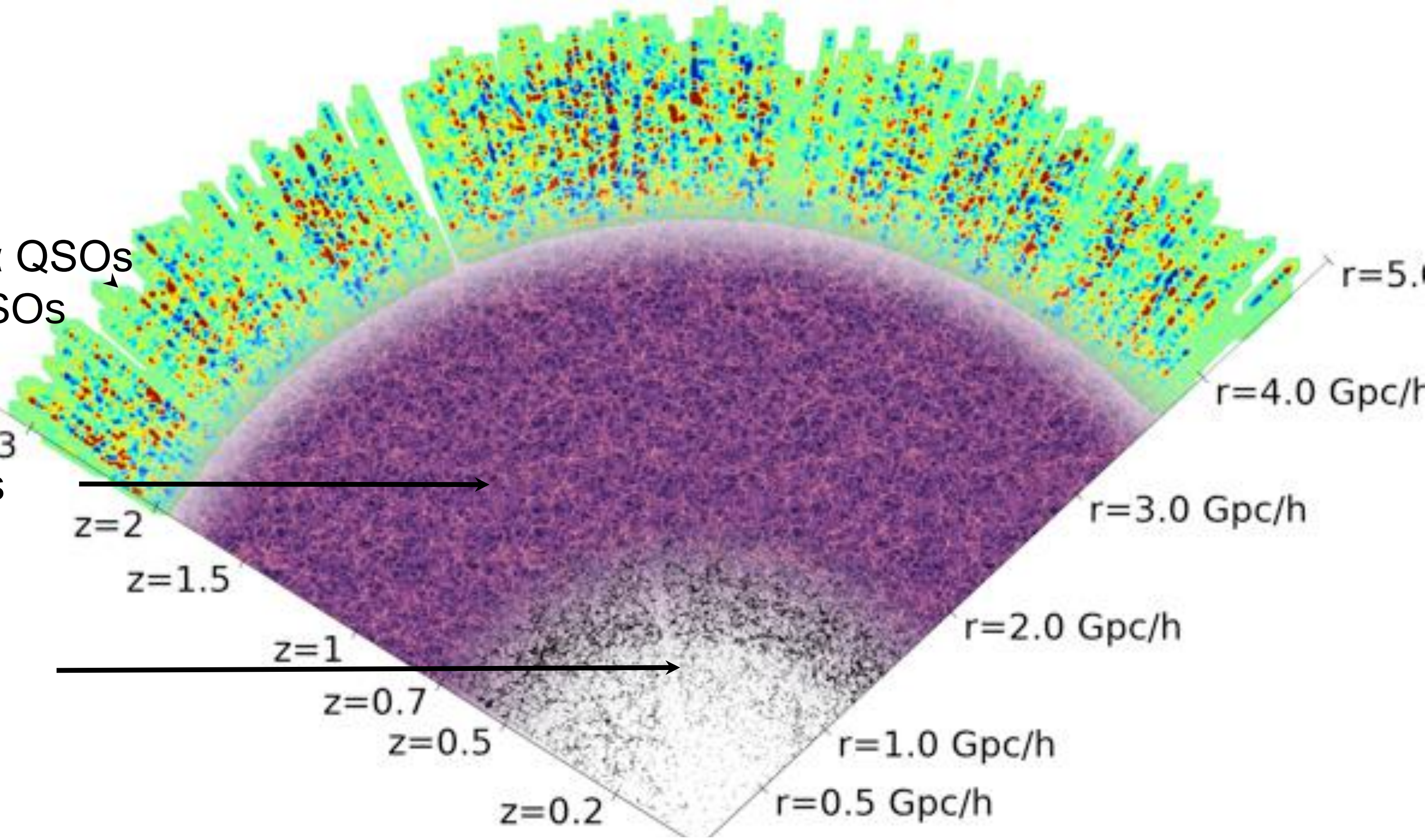

LRG Targets

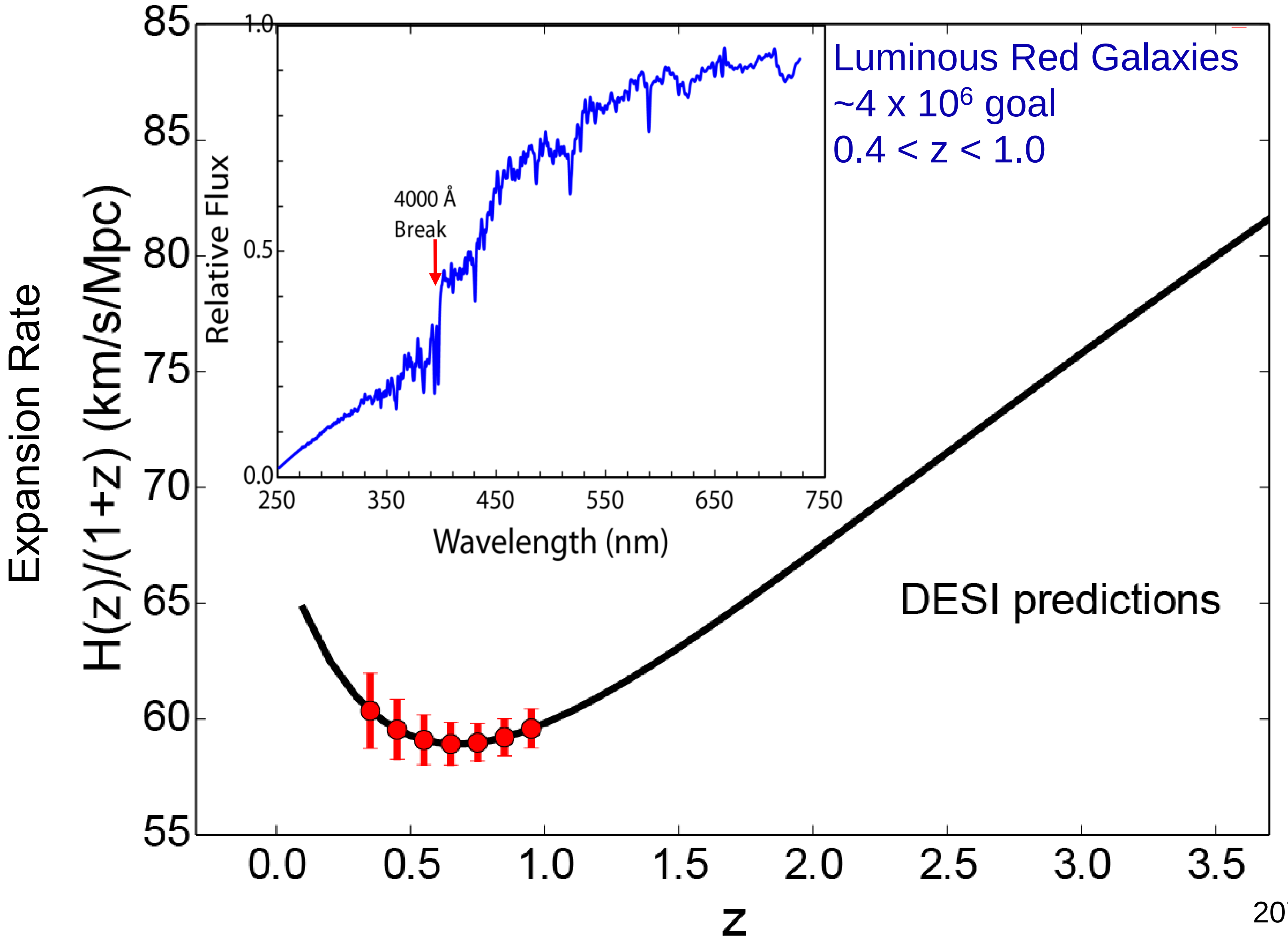
85
85
80
75
70
65
60
55
Expansion Rate
H(z)/(1+z) (km/s/Mpc)
0.0
0.5
1.0
1.5
2.0
2.5
3.0
3.5
z
DESI predictions
1.0
0.5
0.0
Relative Flux
250
350
450
550
650
750
Wavelength (nm)
4000 Å
Break
Luminous Red Galaxies
~4 x 10^6 goal
0.4 < z < 1.0

ELG Targets

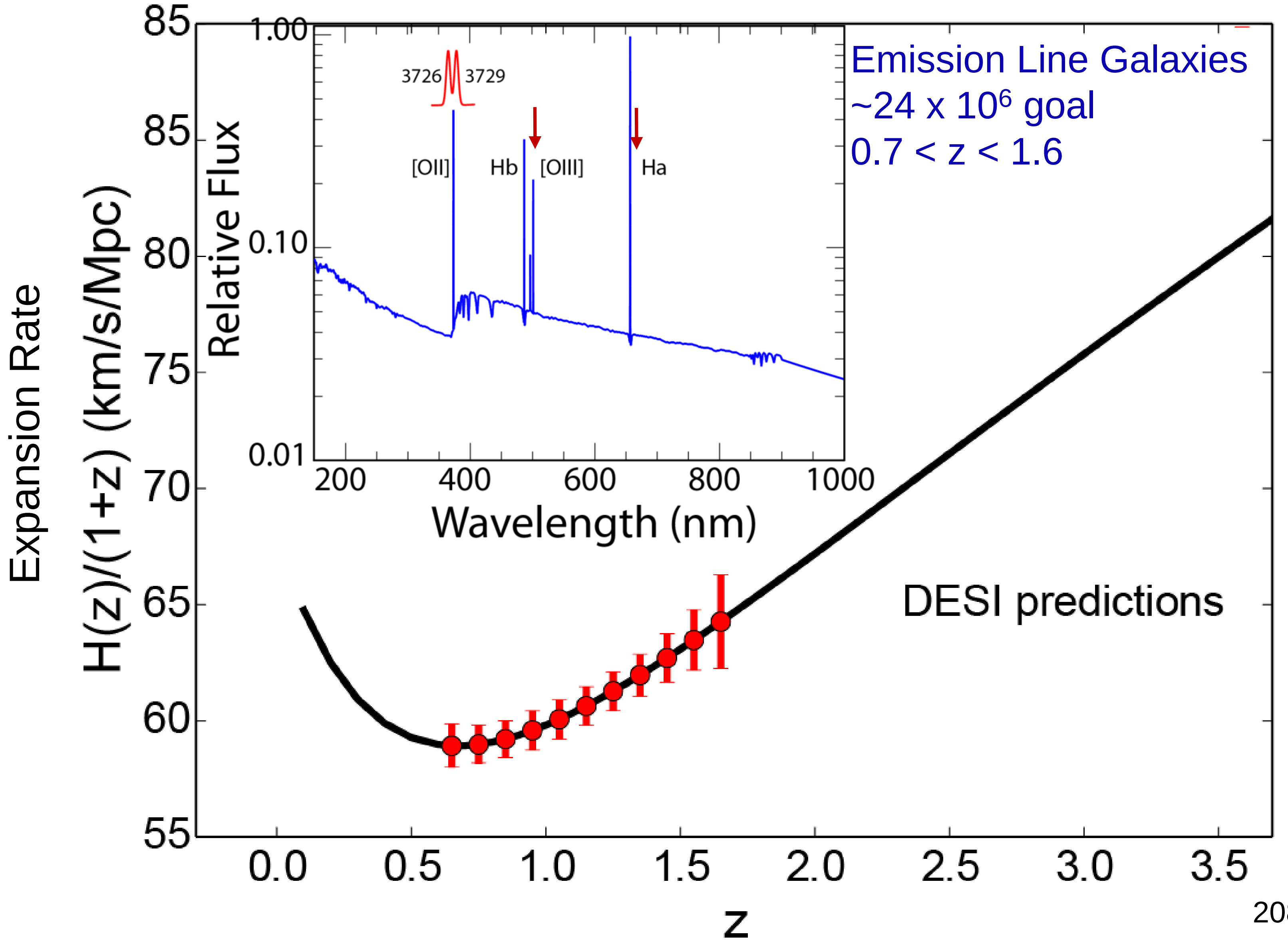

Emission Line Galaxies
~24 x 10^6 goal
0.7 < z < 1.6
3726
3729
[OII]
Hb
[OIII]
Ha
Relative Flux
1.00
0.10
0.01
200
400
600
800
1000
Wavelength (nm)
Expansion Rate
H(z)/(1+z) (km/s/Mpc)
85
80
75
70
65
60
55
0.0
0.5
1.0
1.5
2.0
2.5
3.0
3.5
z
DESI predictions

QSO Targets

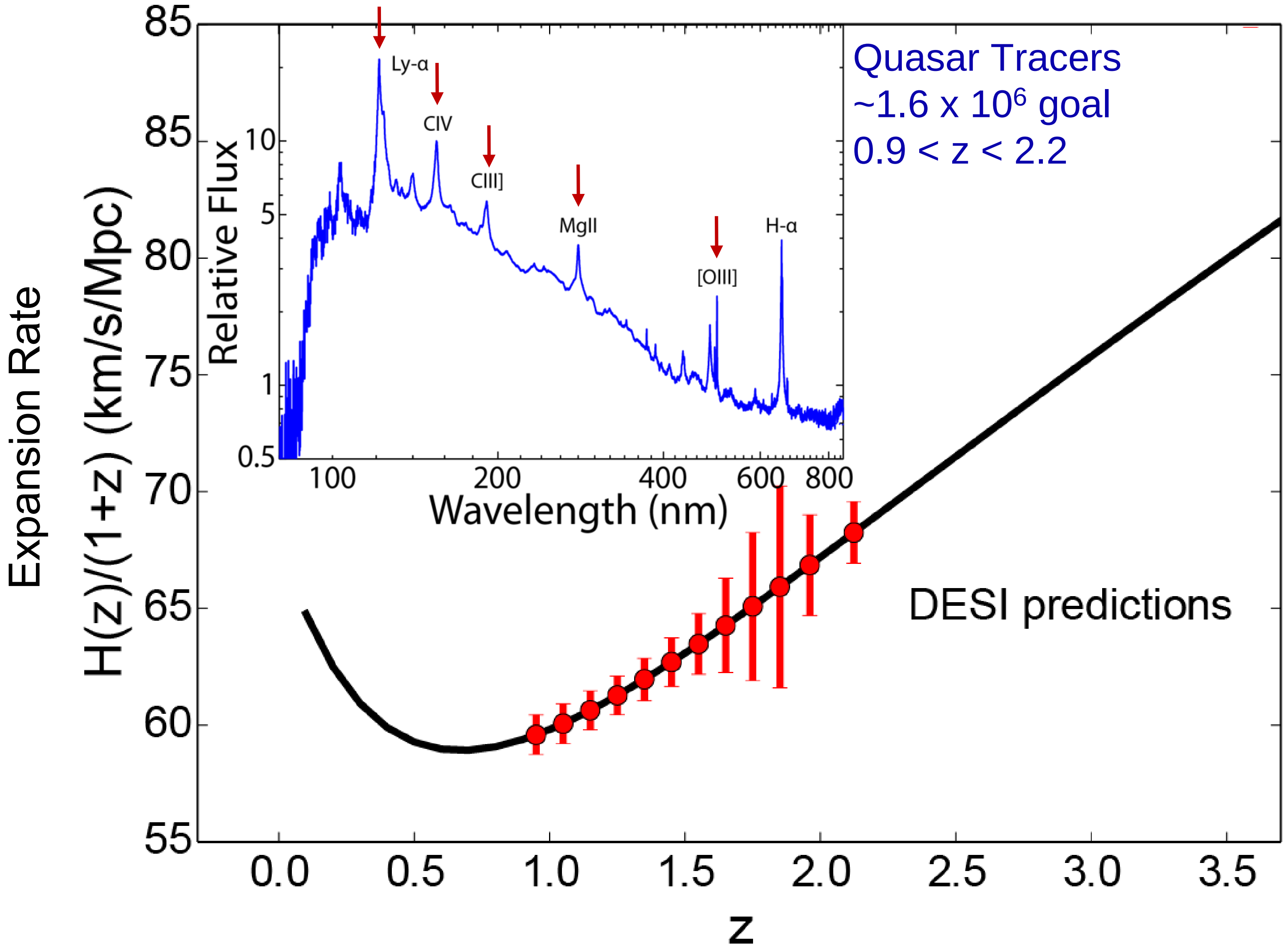
Quasar Tracers
~1.6 x 10^6 goal
0.9 < z < 2.2
DESI predictions
Expansion Rate
H(z)/(1+z) (km/s/Mpc)
z
Ly-α
CIV
CIII]
MgII
[OIII]
H-α
Relative Flux
Wavelength (nm)

Ly-α Forest QSO Targets

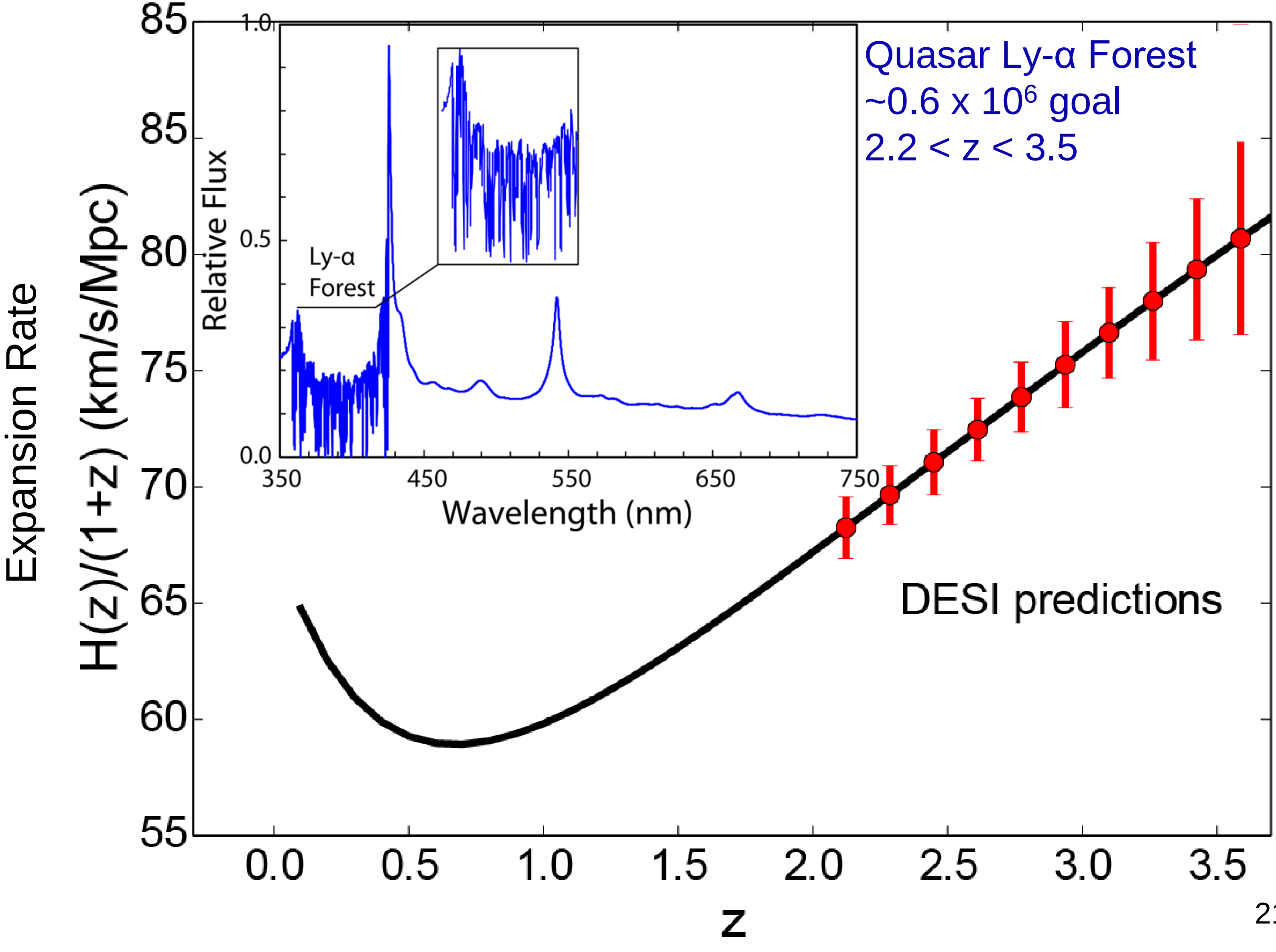

DESI on the Hubble Diagram

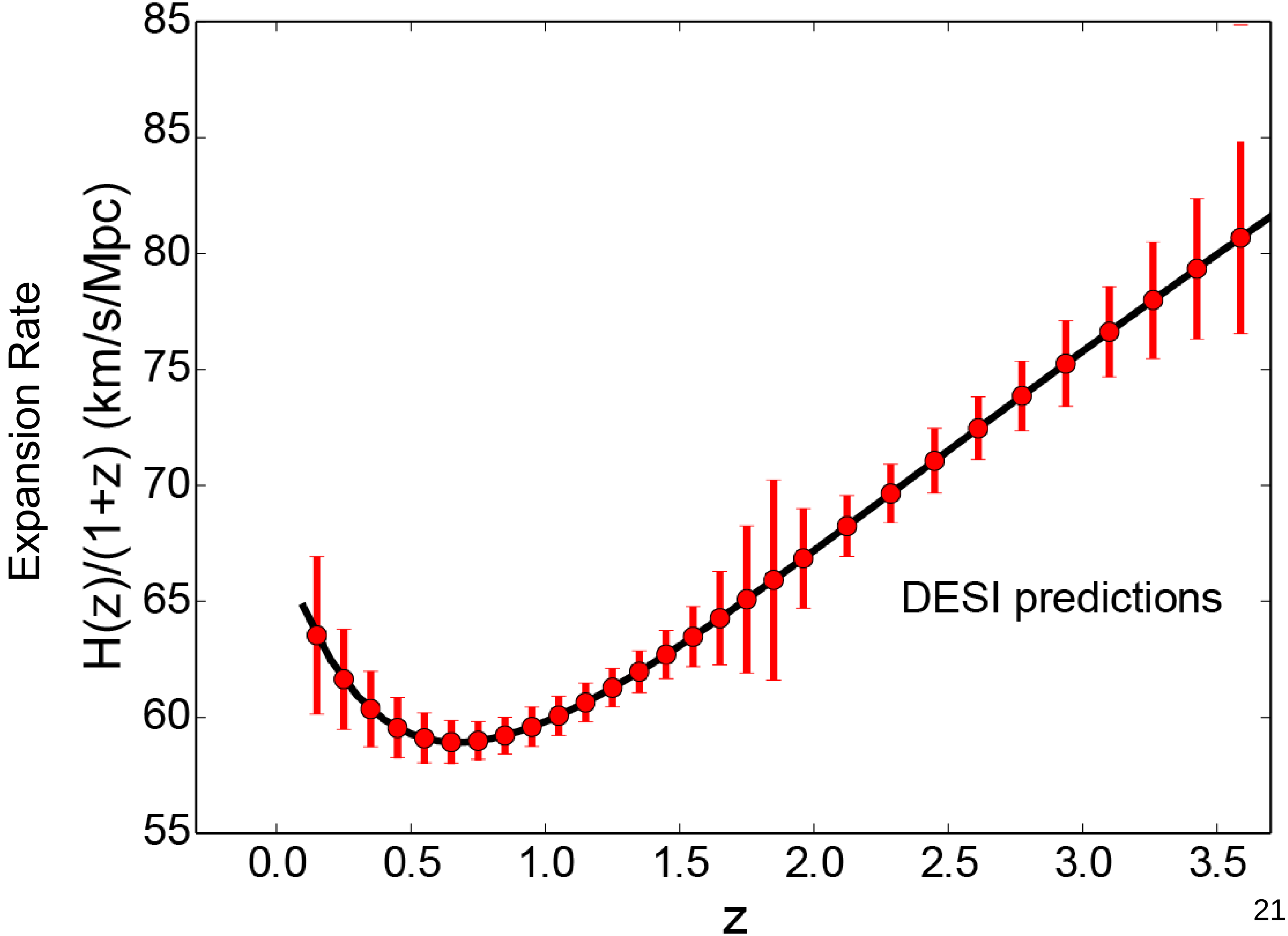

DESI Broad Science Goals

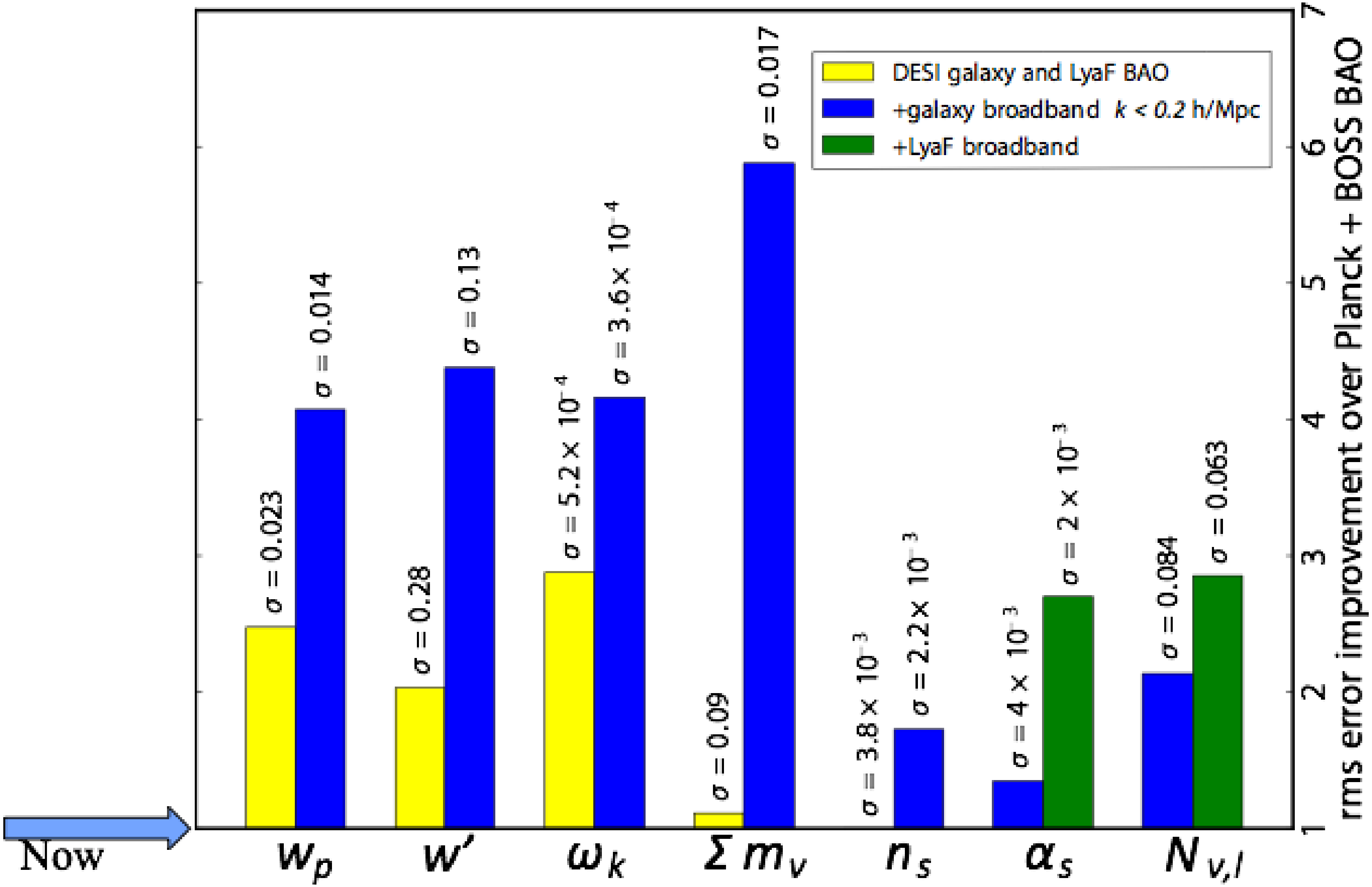

P. McDonald (LBNL)

Comparison With Other Surveys

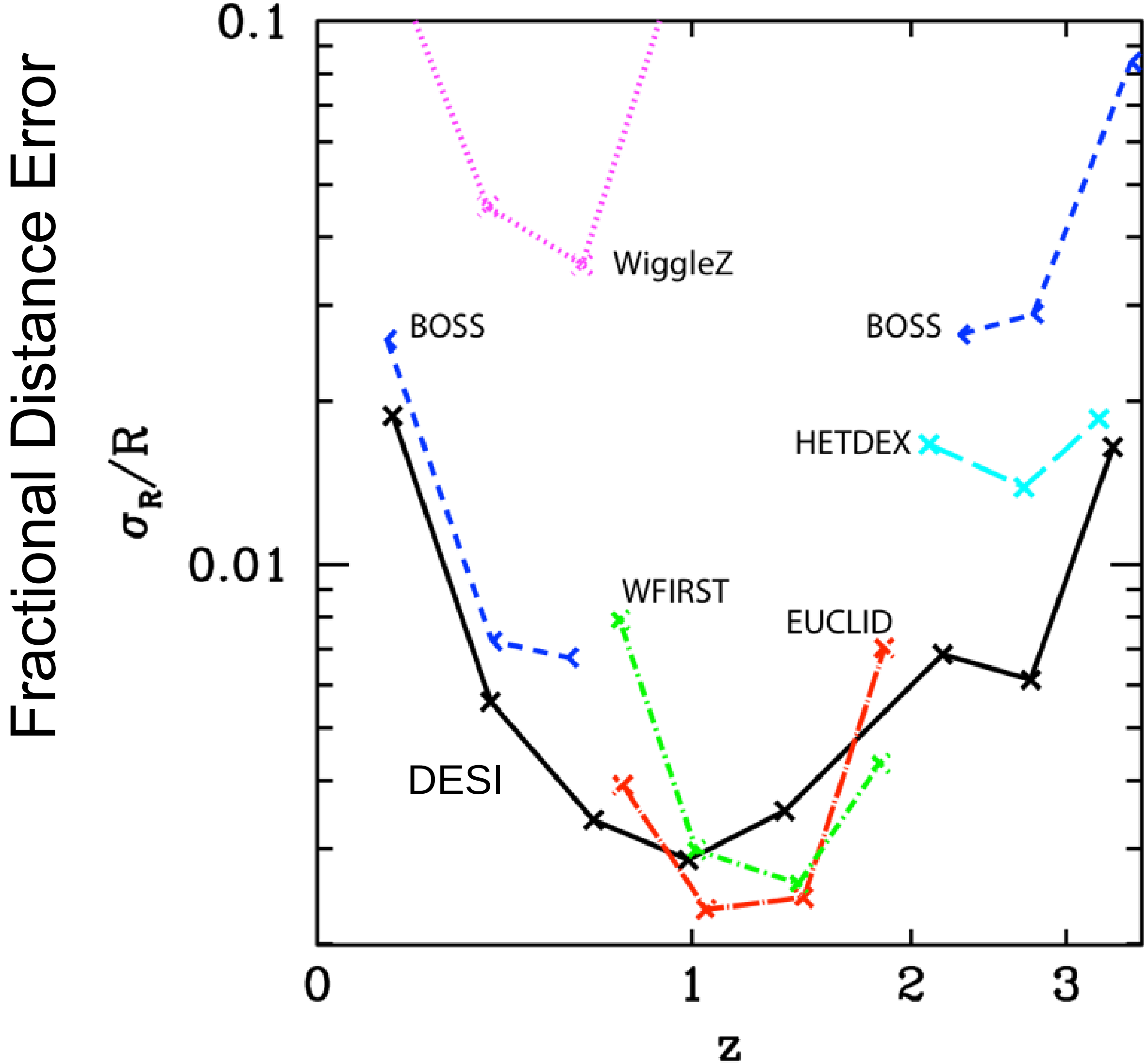

Institutions Interested in DESI (Jul 2013)

- AAO
- Argonne
- Brazil
- Brookhaven
- Carnegie Mellon Univ.
- Durham
- EPFL
- ETH Zurich
- FNAL
- Harvard
- IAA et al.
- Kansas
- KASI
- LAM/CPPM
- Mexico
- NOAO
- New York Univ.
- Portsmouth
- Saclay
- SJTU
- SLAC
- IFAE/ICE/CIEMAT/UAM
- Texas A&M
- The Ohio State Univ.
- Univ. College London
- UC Berkeley
- UC Irvine
- UC Santa Cruz
- U. Edinburgh
- U. Michigan
- U. Pittsburgh
- U. Utah
- USTC
- Yale

DESI Current Schedule

DESI notional timeline

- Oct 2018: Commissioning / pilot observations
- April 2019: Survey starts
- April 2020: 1st data set defined
- Nov 2020: BAO results on 1st year data
- Nov 2022: BAO results with 60% of data, surpasses science requirements

Milestone	Milestone Title	Schedule Date
CD-0	Approve Mission Need	09/30/12 (A)
CD-1*	Approve Alternative Selection and Cost Range	Q4 FY 2014
CD-2	Approve Performance Baseline	Q2 FY 2015
CD-3a	Approve Start of Construction (Long Lead Procurements)	Q2 FY 2015
CD3-3b	Approve Start of Construction	Q4 FY 2015
CD-4	Approve Project Completion	Q4 FY 2019

*Conceptual Design Review: Passed on September 11, 2014

IFAE/ICE/CIEMAT/UAM Contributions

- Design, production and test of 10+2 Guiding, Focusing and Alignment (GFA) units (IFAE, CIEMAT, ICE). ✔
- Software for guiding (ICE). ✔
- Imaging of ~5000 sq. deg. in the *z* band using PAUCam for targeting purposes (All). Under discussion
- Provision of large galaxy simulations tailored to DESI's needs (ICE, CIEMAT, UAM). Proposed

GFA Unit

- It is the only imaging component of DESI
- 10 (+2 spare) identical cameras: one CCD + mechanical packaging + read-out electronics. Stand-alone system.

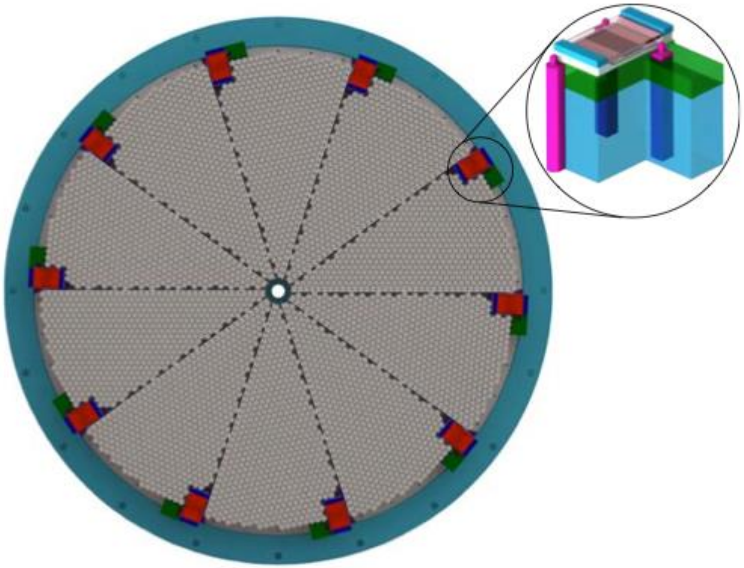

Figure 4.36: The DESI focal plane with GFA sensors shown in red. The inset is a detail of the packaging concept. The CCD is the rectangular object on the top. The rectangular boxes are volumes for some of the control electronics. The three towers contain mechanical survey balls and point illuminators for the Fiber View Camera.

GFA Unit

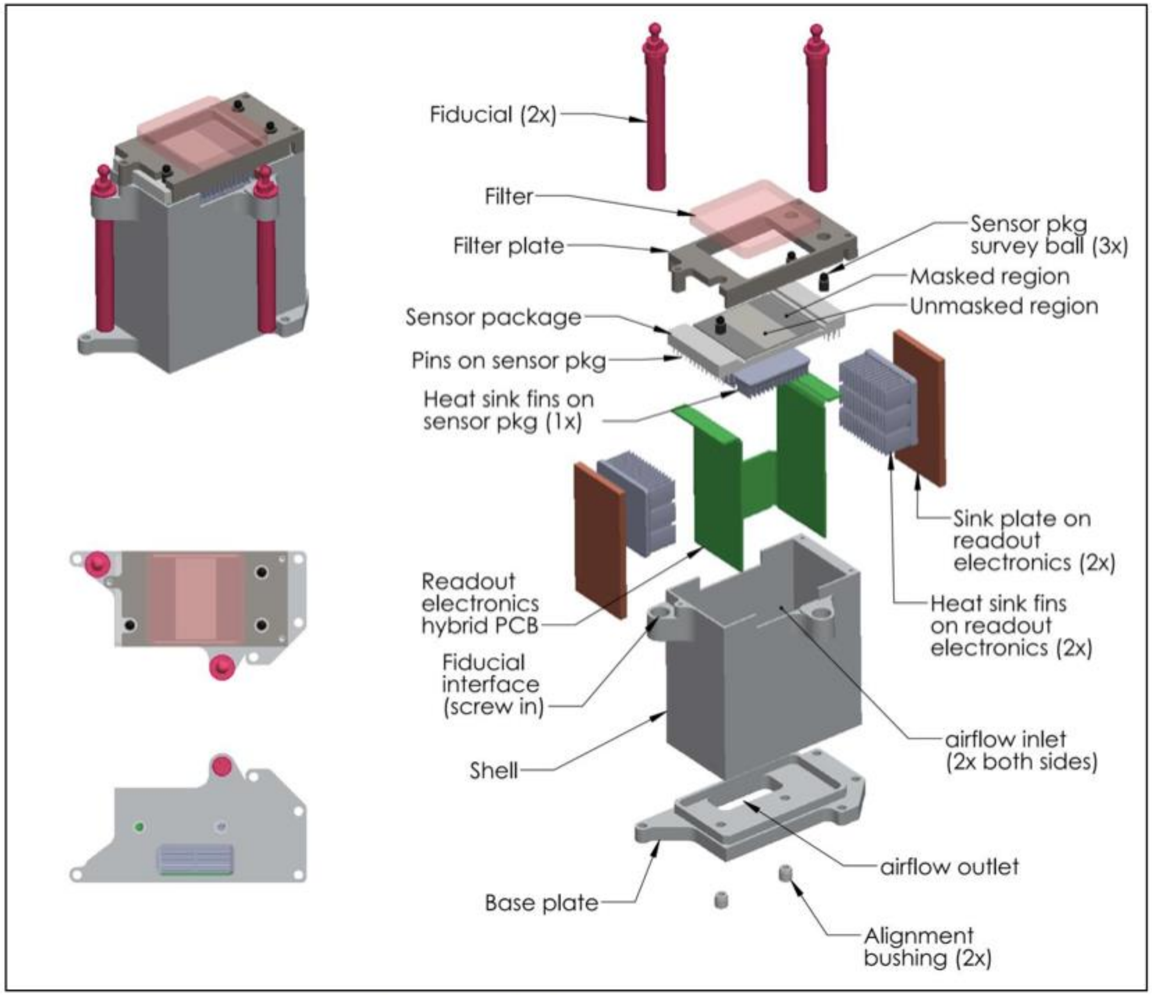

Figure 4. Exploded view of GFA unit conceptual design.

DESI Summary

- DESI will be a Stage-IV dark energy project, prior and complementary to Euclid. Very exciting science:
    - Dark Energy
    - Inflation
    - Neutrino mass, including hierarchy
- Expect to operate for 5 years starting in 2019
- Possible very interesting synergies with the PAU survey.

Summary

—Cosmology has blossomed into a quantitative science in the last two decades

—The CMB is a magnificent tool to study the early Universe

—In 1998, the discovery of the accelerated expansion of the Universe changed completely our understanding of the Universe and its components.

—Ten years on, the quest to understand what causes the acceleration continues with many galaxy surveys.

↓

A (the?) most pressing problem in fundamental science

—**Cosmology has already become part of "Particle Physics"**